

# CHAPTER ONE

## INTRODUCTION

### 1.1 Background of the Study

One of the stratigraphic units of the Southern Benue Trough delineated mainly by biostratigraphy is the Eze-Aku Shale (Simpson, 1955; Reyment, 1965). All lithologies including shales, limestones and sandstones, siltstone of Turonian age were considered as one formation contrary to the stratigraphic rules (Murphy and Salvador, 1999) which emphasizes lithologic distinctiveness as main criteria for defining a formation.

Murat (1972) rightly referred to this lithologically very heterogenous formation as a “Group” comprising more than one “Formation”. Whiteman (1982) identified the Amasiri Sandstone, Konshisha River “Group”, Nkalagu Limestone as formations of the Group. Ojoh (1992) also identified Ezillo Formation within the Eze-Aku Group. Nwajide (2013) split the Eze-Aku Shale into five formations while Igwe and Okoro (2016) on the eastern limb of the Abakaliki Anticlinorium, split the Eze-Aku Group into two component formations - the late Cenomanian-early Turonian Eze-Aku Shale (transgressive phase) and the middle-late Turonian Amasiri Sandstone (regressive phase). Ekweozor and Unomah (1990) were the first to report the presence of outcropping rocks that they believed were oil shales at Lokpanta and surrounding villages. Umeji (2007) described these shales in Lokpanta Junction (km 164 along Enugu-Port Harcourt expressway) as calcareous dark grey shales alternating with grey siltstones and fine sandstones. These authors identified these formations but failed to define type sections, a necessary criterion, for definition of any lithostratigraphic unit.

Moreover, the presence of several lithologies such as sandstones, siltstones, shales and limestones, unfortunately led to varying conflicting and misleading interpretations for the Eze-Aku Group. Thus, this study focuses on evaluating the stratigraphy, sedimentology and gas shale potential of the calcareous and carbonaceous shales of the Eze-Aku Group so as to accurately establish its status as a formation and interpret the paleodepositional environments, paleogeography and the gas shale potentials.

## **1.2 Statement of the Problem**

The carbonaceous rock of the Eze-Aku Group (Ekweozor and Unomah, 1990) has not been properly described and defined lithostratigraphically. It appears to have some distinct characteristics from the Eze-Aku Shale of Reyment (1965). One of the reason for this study is to properly define, describe and laterally trace the carbonaceous rock across the basin and to ascertain its stratigraphic status.

Moreover, the depositional environment, paleogeography and paleoceanography of the calcareous and carbonaceous rocks needs to be re-evaluated because of the review of the stratigraphy of the Eze-Aku Group. There is also the need to evaluate the source rock properties and gas shale potential of these rocks because of the keen interest in the search for hydrocarbons in the inland sedimentary basins of Nigeria and surge in production of shale gas in the world.

## **1.3 Aim and Objectives of the Study**

The aim of this study is to review the stratigraphy, sedimentology and gas shale potential of parts of the Eze–Aku Group, Abakaliki Anticlinorium, Southern Benue Trough.

The objectiveness of the study are:

1. To characterize the rocks and interpret the depositional environment of the stratigraphic unit.
2. To establish the elemental and oxide compositions of the rocks.
3. To carry out biostratigraphic study of the rocks for interpreting the age of the succession.
4. To construct the paleodepositional, paleobathymetry and paleogeographic models for the succession.
5. To evaluate the source rock properties as well as the gas shale potential of the rocks.
6. To produce a geologic map of the study area

#### **1.4 Scope of the Study**

The scope of this research includes the following:

1. The revision of the stratigraphy of the Eze-Aku Shale with respect to its component lithostratigraphic units in the study area.
2. The reconstruction of paleodepositional, paleogeographic and paleobathymetric models of the carbonaceous rocks using sedimentologic and inorganic geochemical studies.
3. The evaluation of source rock properties and gas shale potential of the carbonaceous rocks using organic geochemical studies.

## **1.5 Significance of the Study**

The significance of this study are as follows:

- a) To refine further the stratigraphy of the Eze-Aku Group.
- b) This will provide a more detailed geologic framework for economic/mineral evaluation and environmental studies.
- c) It will provide more detailed scientific information on the paleodepositional environment and paleogeographic conditions during the deposition of the carbonaceous rocks.
- d) It will provide information on gas shale potential of this stratigraphic unit in the Benue Trough.

## **1.6 Location of Study Area**

The area of study is bounded by Latitudes  $5^{\circ}55'$  and  $6^{\circ}20'N$  and Longitudes  $7^{\circ}25'$  and  $7^{\circ}50'E$  (Figure 1.1). The area extent is approximately  $2,151.4\text{km}^2$ . The area situates within the Abakaliki Anticlinorium, in the Southern Benue Trough.

The major access route to the area is the Enugu- Port Harcourt Expressway, which runs from the north to the south in the western part. Other secondary and minor roads in the area helped to map the area (Figure 1.1).



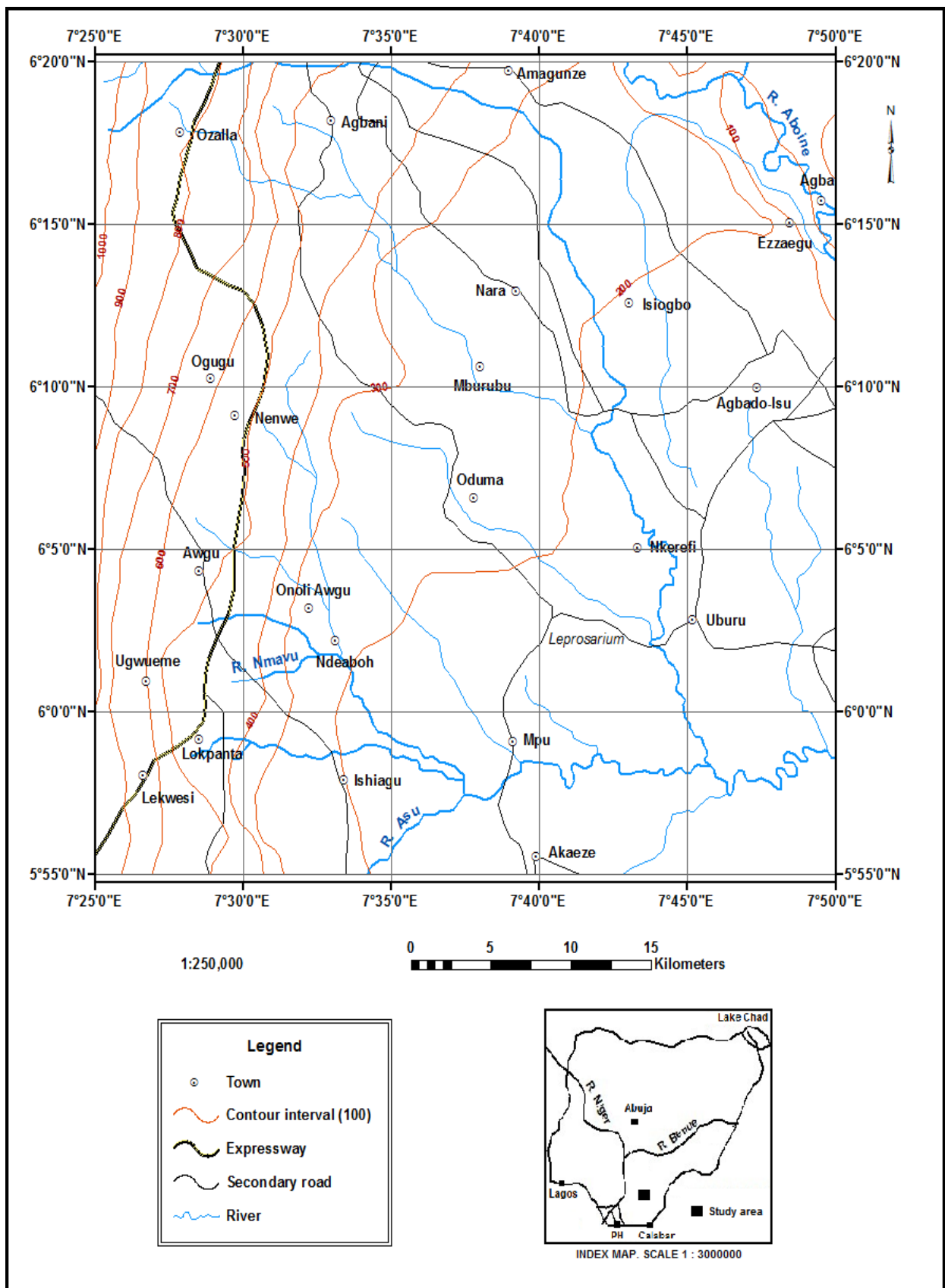


Figure 1.1: Location, Accessibility and topography map of the study

## **1.7 Topography**

The study area has an undulating topography ranging from gently sloping lowlands to slightly steep highland. The regional geomorphic feature that has shaped the landscape is the Enugu Cuesta. Weathering, mass wasting, and quarrying are factors, which have caused appreciable changes in geomorphic processes and features within the study area.

The highest topographic points reach up to 1000m and the lowest at about 100m above sea level (see Figure 1.1). Local variations in the intensity of temperature, moisture, altitude/slope, soil/rock exposure, lithology (Egboka, 1993) have sharpened the present land surface giving it an undulating pattern.

## **1.8 Climate**

The study area is located within the tropical rain forest zone of Nigeria with a derived savannah (Iloeje, 1981; Reifsnnyder and Darnhofer, 1989 and Sanni, 2007). It has a tropical savannah climate (Sanni, 2007). The tropical savannah, tropical wet and dry climates are extensive in area and covers most of western to central Nigeria beginning from the tropical rain forest climate boundary in southern Nigeria to central part of Nigeria.

The tropical savannah climate exhibits a well-marked rainy season and a dry season with a single peak known as the summer maximum due to its distance from the equator. Temperatures are above 18 °C (64 °F) throughout the year. It is characterized by two main seasons; rainy (wet) and dry seasons. The rainy season lasts between the months of April and October while the dry season lasts from the months of November to March. Rainfall is brought by the moist equatorial maritime air mass from the Gulf of Guinea with prevailing

winds from the south-west (Inyang, 1978). The average annual rainfall is about 1750mm (Inyang, 1978).

The rainy season is often characterized by heavy downpour accompanied by thunderstorms, heavy flooding, soil leaching, extensive sheet wash, groundwater infiltration and percolation (Egboka and Okpoko, 1984). The dry season is characterized by the dusty dry harmattan wind. This lowers the temperature appreciably in the months of December to January with associated excessive evaporation, low relative humidity (20%), low rainfall and general dryness (Egboka, 1993 and Nimako, 2008). In addition, a short spell of dry season is usually felt in August commonly called “The August break”. Figure 1.2 shows the climatic map of the study area.

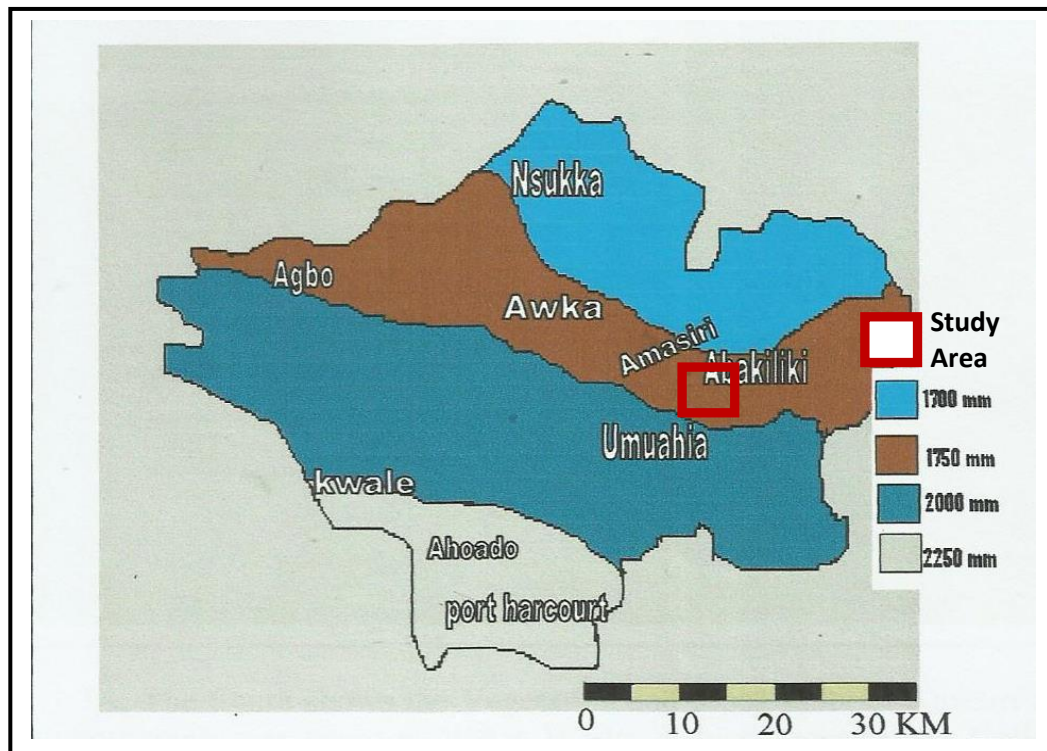


Figure 1.2: Map of Southeastern Nigeria showing climatic condition with respect to annual rainfall of the study area (modified from Inyang, 1978)

## 1.9 Vegetation

Vegetation within the study area is generally enhanced and promoted by the high annual rainfall and humidity (Iloeje, 1981). It belongs to tropical rain forest zone with a derived savannah belt of Nigeria (Iloeje, 1981; Reifsnyder and Darnhofer, 1989 and Sanni, 2007). This ensures adequate moisture supply and promotes perennial tree growth and thick undergrowth. The trees have luxuriant foliage with the presence of climbers and epiphytes forming complex tangles. Trees such as *Robinia Pseudoacacia* (the locust bean tree), Bamboo and Elephant grass are common in the study area.

However, as a result of man's interference with the original plant cover, the tropical rainforest vegetation is disappearing in many parts of the study area giving rise to derived savannah vegetation of shrub-land and bushes (Egboka, 1993 and Umenweke, 1996). These authors described the present vegetation as an imposed one. The vegetation cover also varies depending on the topsoil and lithology, as well as topography and drainage pattern (Egboka, 1993). Figure 1.3 shows the map of Nigeria with its natural vegetation belts.

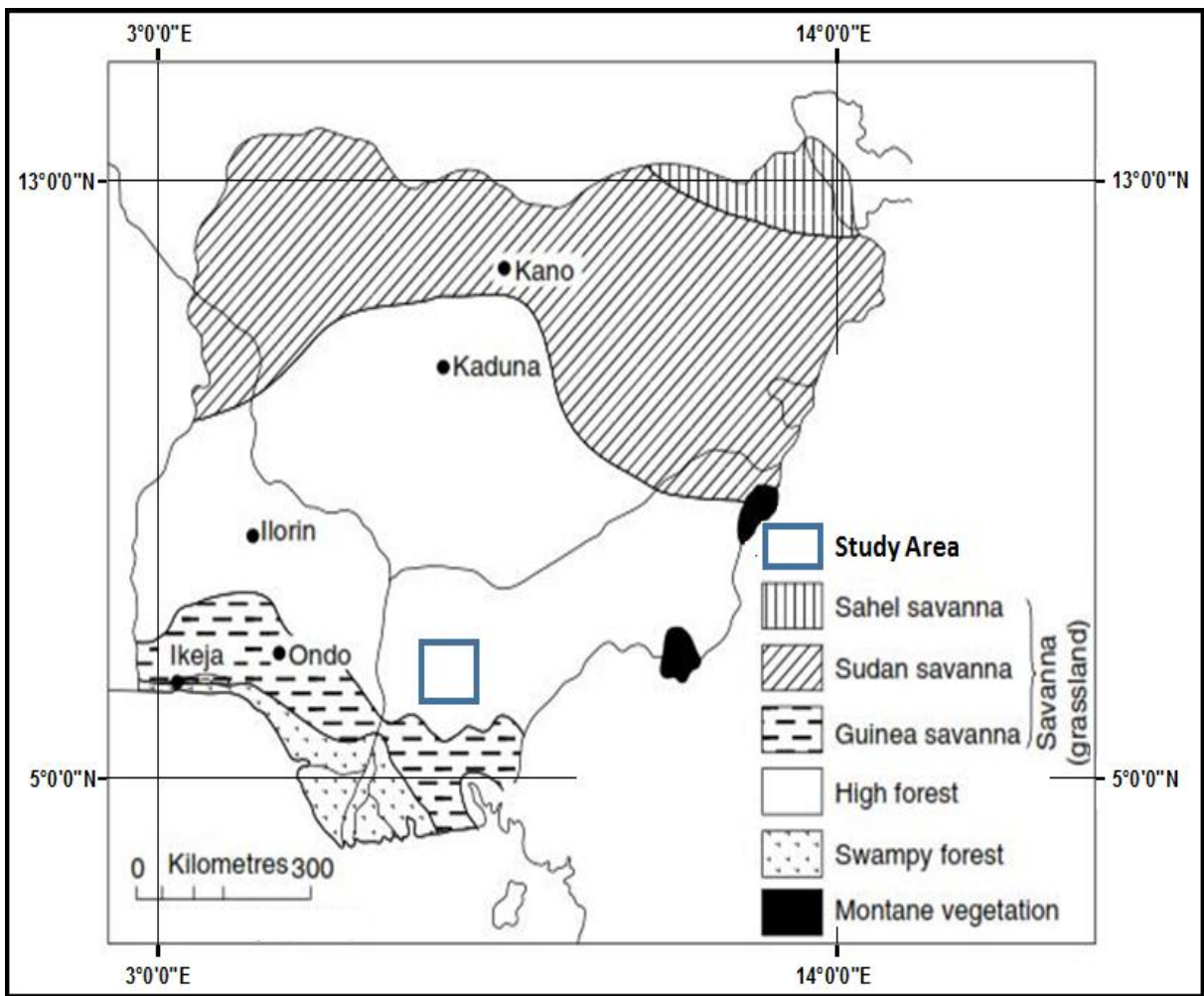


Figure 1.3: Map of Nigeria showing the vegetation belts (modified from Iloeje, 1981)

## 1.10 Drainage

The study area falls within the Cross River drainage basin. The river systems that drain the area include the River Asu, River Mmavuvu, River Abio, River Aboine (Ebonyi) and their tributaries. These rivers empty themselves into the River Cross, which is far south-east of the study area. The drainage pattern of the rivers varies from dendritic to trellis. Figure 1.4 is the drainage map of the study area.

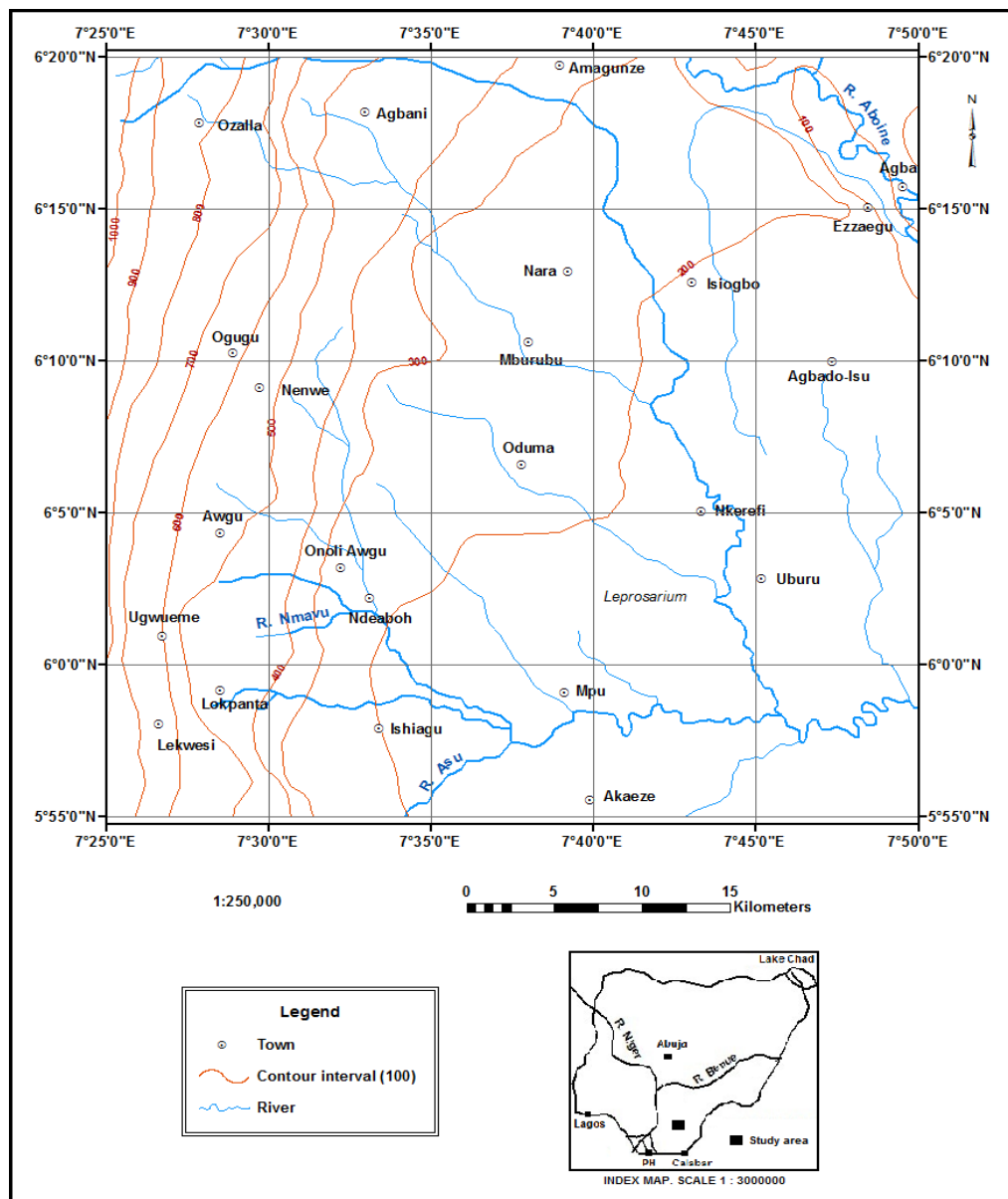


Figure 1.4: Drainage Map of study area.

# CHAPTER TWO

## LITERATURE REVIEW

### 2.1 Regional Tectonic Setting and Structural Framework

An adequate interpretation of the geology and history of the Benue Trough requires a proper understanding of its regional tectonic framework. The origin, tectonic evolution, and the stratigraphy of the Benue Trough has been discussed by several authors (Reyment, 1965; Wright, 1968, 1989; Grant, 1971; Burke *et al.*, 1972; Murat, 1972; Petters, 1978; Olade, 1975, 1979; Ajakaiye, 1981; Benkhelil and Guiraud, 1980; Benkhelil, 1982, 1986, 1989; Benkhelil and Robineau, 1983; Hoque and Nwajide, 1984; Sheideggar and Ajakaiye, 1985; Maurin *et al.*, 1986; Amajor, 1985, 1987; Ojoh, 1990; Reijers, 1996; Odedede, 2011).

Sheideggar and Ajakaiye (1985) considered the Benue Trough a continuation of a sinistral shear fracture zone crossing the Mid Atlantic Ridge with its counterpart in Brazil. Wright (1968; 1989) considered the trough as a sediment-filled rift of tensional origin. Burke *et al.* (1970) and Grant (1971) on their part, considered the Trough a “failed” arm of a triple plate margin. Burke *et al.* (1970) went further to propose an aulacogen model which refers to the Benue Trough as the failed arm of a triple RRR (Rift – Rift – Rift) Junction which evolved by mantle upwelling, crustal stretching and the separation of the West African and South American continental plates. The gravity profile across the Benue Trough which is remarkably similar to that of the Red Sea and the presence of igneous intrusions of alkaline genetic class (Obiora, 2002) seem to support the aulacogen model. Though this model seems to be very popular, it failed to account for the Santonian compressive phase in the evolution of the Benue Trough (Burke *et al.*, 1970).

Benkhelil (1982, 1989) in his studies proposed a model in which transcurrent movements were considered to be the basic tectonic mechanism in the formation and subsequent evolution of the Benue Trough. The strike-slip faulting along a pre-determined zone of northeast-southwest trend, played a major role in the tectonic evolution of the Benue Trough. (Benkhelil and Robineau, 1983).

Generally, the Benue Trough is believed to be the failed third arm of the rifts originating from the early Cretaceous rifting of the African basement, following the splitting of the Gondwanaland supercontinent and the subsequent drifting apart of the African and the South American plates during the Jurassic period (Murat, 1972; Hoque and Nwajide, 1984; Reijers, 1996). The trough forms a regional structure which is exposed from the northern frame of the Anambra Basin and runs northeastwards for about 1000km to the southern fringe of the Chad Basin (Reijers, 1996). Following the evolution of the Benue Trough, differences in the rate of subsidence and adjustment of the graben and horst fault blocks gave rise to a complex of basins, which include: (1) The Gongola Basin (2) The Yola rift and Mamfe arms (3) The Benue Trough (4) The Abakaliki Anticlinorium (5) The Afikpo Synclinorium, and (6) The Calabar Flank (Ikang Trough, Ituk High, Calabar Hinge Line) (Hoque and Nwajide, 1984) (Figure 2.1).

The ages of the basin-fills in the Benue Trough generally decreases southwards from Pre-Albian to Coniacian (Amajor, 1987) while sediment thicknesses increase southwards (Reijers, 1996). The Benue Trough is better subdivided into the Northern, the Central, and the Southern Benue Trough for effective description based on tectonic, geographical and stratigraphic features (Nwajide, 2013).



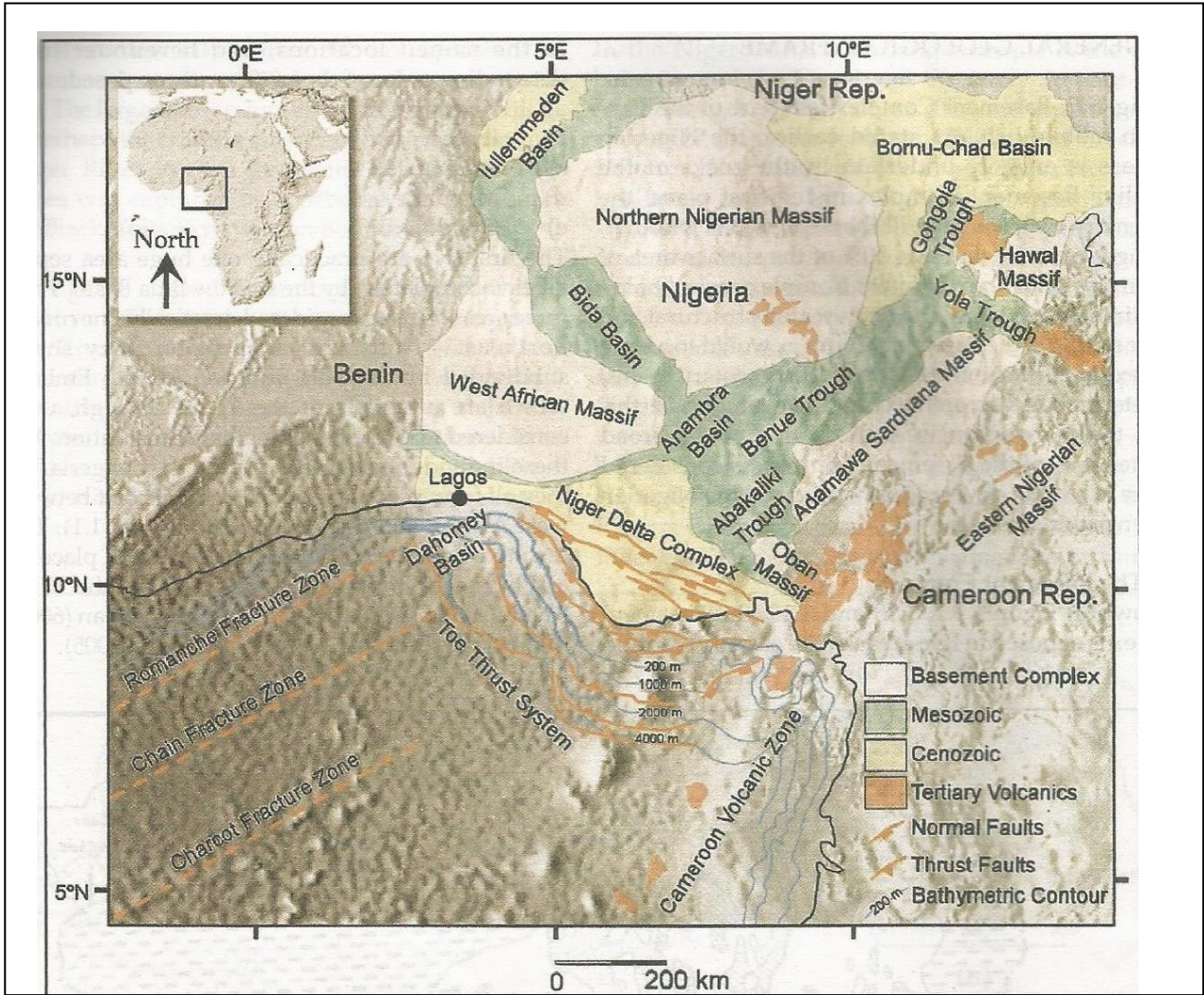


Figure 2.1: Map of Nigeria showing various geological features- Areas of basement exposure, Sedimentary basins, Tertiary volcanism, as well as some local and regional tectonic lineaments. (after Corredor *et al.*, 2005)

The Gongola Basin and the Yola Rift make up the Northern Benue Trough. The Central Benue Trough is the linear part of the basin and includes the Benue Basin, while the Abakaliki Anticlinorium, the Mamfe Rift, the Afikpo Synclinorium, and the Calabar Flank make up the Southern Benue Trough (Hoque and Nwajide, 1984; Benkhelil, 1989; Nwajide and Reijers, 1996).

The tectonic and basin development process of the Trough can be summarized into five phases:

1. An Early Cretaceous rift phase with the deposition of intracontinental arkosic sandstones and shales of fluviatile and lacustrine origin (Bima, Mamfe, Ogoja and Awi Formations), which rest unconformably on the Basement Complex rocks (Uzuakpunwa, 1974; Olade, 1975, 1979; Hoque, 1984).
2. Late Cretaceous phase of rapid subsidence and initiation of marine transgression in all rift segments, characterized by submarine gravity flows with megaslumps and turbidites (Ojoh, 1990).
3. Prolonged shelf and deep basin deposition especially in the southern Trough under predominantly oxygen deficient bottom water conditions (Hoque, 1984).
4. Tectonism, involving deformation and magmatism and the formation of lead – zinc deposits from circulating hot brines (Benkhelil, 1989).
5. Late Cretaceous post – deformation subsidence with westward displacement of depocenters, e.g. the Anambra Platform, where extensive coal forming swamps developed (Hoque, 1984).

Figure 2.2 shows the tectonic map of southern Nigeria from Albian to Eocene times. This work will provide the paleogeographic map of the Cenomanian – Turonian age of the Late

Cretaceous period in the Southern Benue Trough. It will also attempt to reconstruct Paleocceanographic conditons (Paleoredox, paleotemperature and paleosalinity) of Southern Benue Trough during this age.

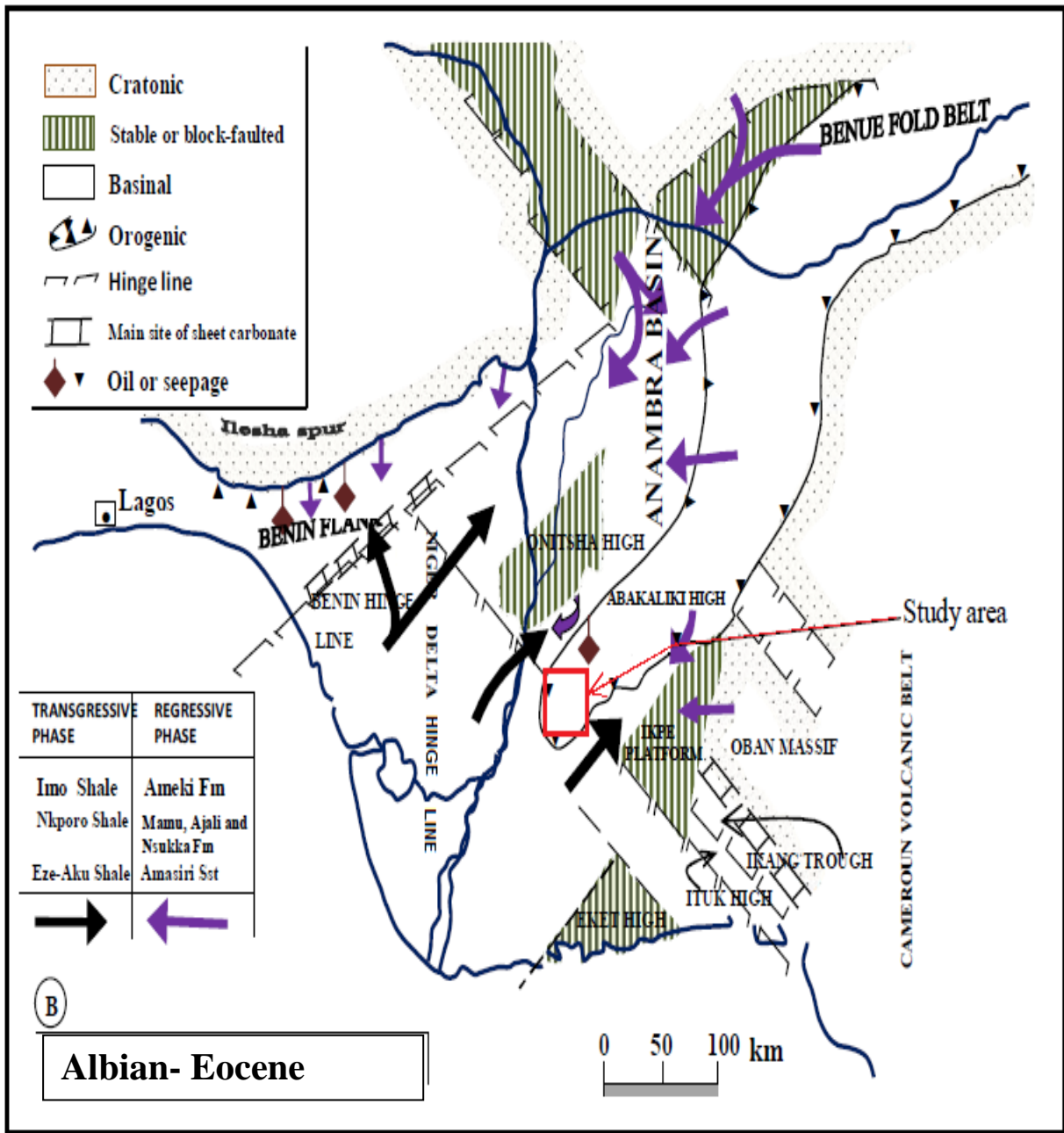


Figure 2.2: Tectonic Map of Southern Nigeria from Albian to Eocene (modified from Murat. 1972)

## **2.2 Regional Stratigraphic Setting**

The stratigraphy of the southern Nigeria sedimentary basins is controlled by three tectono – sedimentary cycles (Murat, 1972; Whiteman, 1982; Hoque and Nwajide, 1984). The first cycle started with the opening of the Southern Benue Trough during the Jurassic to Aptian times. Sediments in the trough were deposited from Aptian to the Coniacian in environments believed to vary from continental to shallow marine. Ojoh (1990) and Okoro and Igwe (2014) noted the presence of deep marine turbidites and megaslumps in some places. Nwachukwu (1972) noted a minor break in sedimentation during the Cenomanian.

In the second cycle, over 2,000 m of sediments were eroded from the Abakaliki Anticlinorium, and deposited in the post-rift subsiding depression of the Anambra Basin from the Late Campanian to the Danian (Murat, 1972). The overall thickness of the sediments deposited was reported to be over 4,000 m (Hoque and Nwajide, 1984).

The third sedimentary cycle started after the filling up of the Anambra Basin and subsequent lateral shift of the depocenter southwards into the modern Niger Delta from the late Paleocene to Recent (Murat, 1972).

Sedimentation in the trough started during the Aptian to early Albian (Late-early Cretaceous) with the deposition of the intracontinental arkosic sandstones of fluvial and lacustrine origin. The Bima Sandstone and Mamfe Formation in the northern and southern Benue Trough respectively represent this event in geologic history. Two cycles of transgressions and regressions followed this, from the middle Albian to the Coniacian, and filled the southern part of the trough with mudrocks, sandstone and limestones with an estimated thickness of about 3,500m (Murat, 1972; Hoque, 1977, 1984; Olade, 1975, 1978). These

sediments belong to the Albian Asu River Group, Cenomanian Odukpani Group, Turonian Eze-Aku Group, and the Coniacian Awgu Formation.

The Santonian transpressional movements, folded, fractured and uplifted the Aptian to Coniacian sediments to form the Abakaliki Anticlinorium (Grant, 1971; Murat, 1972; Whiteman, 1982). The Eze-Aku Group occupies both flanks of the Anticlinorium while the Asu River Group is at the core and overlies the Oban and Bamenda massifs in southern Benue Trough (Figure 2.3). A SE to NW polarity relative to the axial fracture system resulted in the subsidence of the Ikpe Platform and the Anambra Platform, east and west of the Abakaliki Anticlinorium respectively (Benkhelil, 1987; Reijers, 1996).

### **2.3 The Sedimentology and Fill of the Southern Benue Trough**

The sedimentary rocks distribution in the Southern Benue Trough is shown on the geologic map (Figure 2.3). Table 2.1 shows the stratigraphic framework for early Cretaceous to Tertiary strata in southeastern Nigeria. The earliest workers to give an account of the stratigraphy of the Benue Trough were Falconer (1911), Wilson and Bain (1928), Tattam (1944), McConnell (1949), Farrington (1952) and Simpson (1955). Shell BP (1957) produced the Geological maps on the scale of 1:250,000 after a reconnaissance mapping of the sedimentary basins.

The study area is part of the western flank of the Abakaliki Anticlinorium. This area is underlain by sediments of the Asu River Group, the Eze.Aku Group, Awgu Shale and post rift succession of Nkporo Group, Mamu, Ajali and Nsukka formations (Figure 2.3).



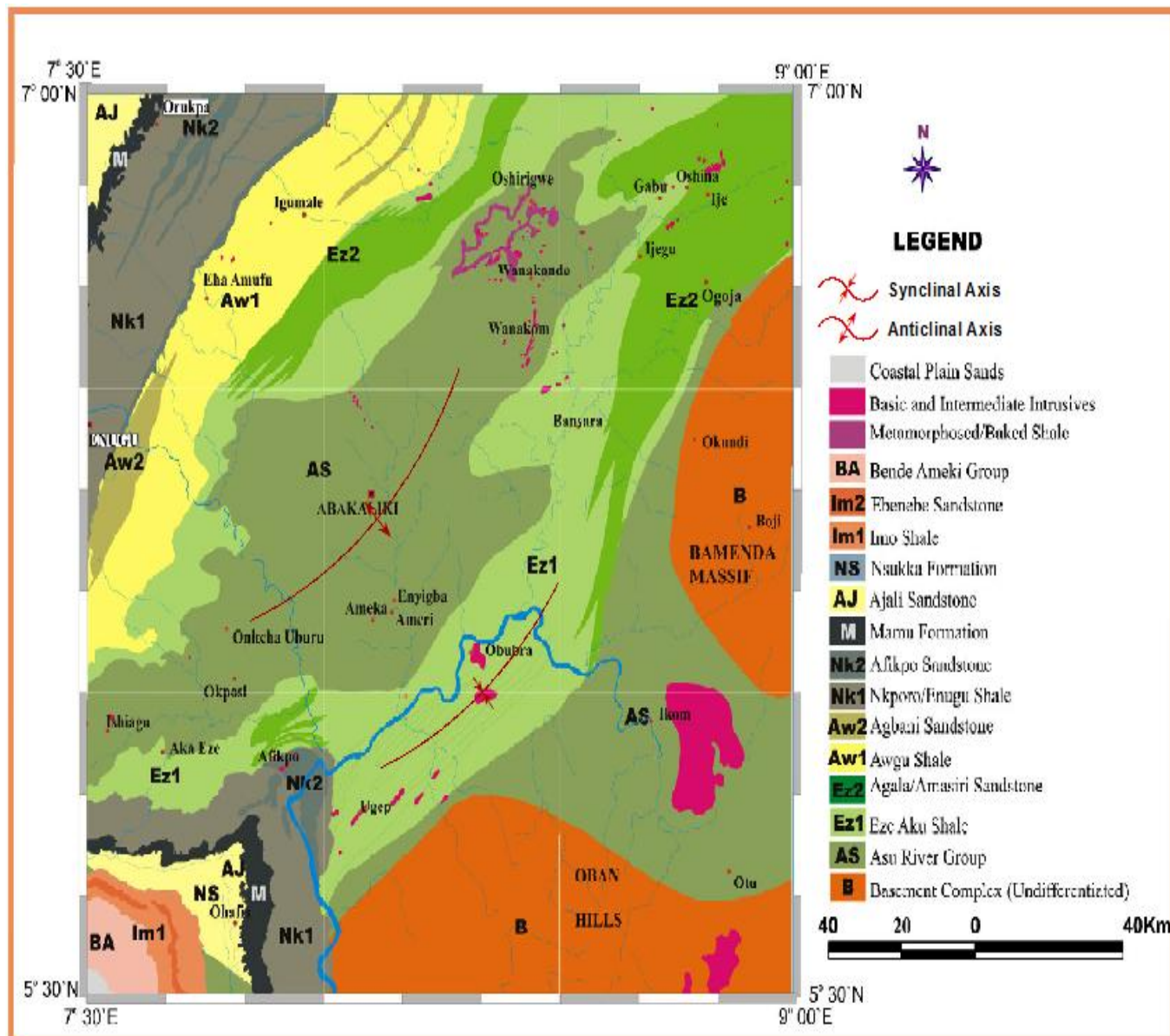



Figure 2.3: Regional Geologic Map of Southern Benue Trough (modified from Oha *et al.*, 2016)

Table 2.1: Stratigraphic Framework for Early Cretaceous-Tertiary Strata in Southeastern Nigeria (modified from Nwajide, 1990)

<b>AGE (M.Y)</b>	<b>AGE</b>	<b>ABAKALIKI BASIN/ANAMBRABASIN/NIGER DELTA BASIN</b>
30	Oligocene	Ogwashi -Asaba Formation
54.9	Eocene	Ameki/Nanka Formation
65	Paleocene	Imo Formation
		Nsukka Formation
73	Maastrichtian	Ajali Formation Mamu Formation
83	Campanian	Nkporo Group/ Owelli Sandstone/ Enugu Shale
	Santonian	
87.5	Coniacian	Agbani Sandstone/ Awgu Shale
88.5	Turonian	Eze Aku Group
93	Cenomanian	
100	Albian	Asu River Group
119	Aptian Barremian Hauterivian	U n - n a m e d Units
	Precambrian	Basement Complex

### **2.3.1 The Asu River Group**

The Asu River Group is the basal lithostratigraphic unit of the Abakaliki Anticlinorium. It consists of poorly bedded, olive brown, sandy shales with fine-grained micaceous sandstones, micaceous mudstones, and sandy limestone lenses (Reyment, 1965; Cratchley and Jones, 1965; Whiteman, 1982; Kogbe, 1989). Coarse to very coarse arkosic sandstones and conglomerates of the Mamfe Formation and Awi Formation of the Group unconformably overlie the Basement Complex rocks.

The sediments are strongly folded and are associated with extensive magmatism, which resulted in the intrusion of diorites and dolerites in Abakaliki, Wonikande, Ugep, Amasiri, and Ishiagu areas. The fold axis trends NE – SW with fractures filled with lead – zinc mineralization in the Abakaliki and Ishiagu areas. The Group is mainly restricted to the southern and Central Benue Trough, and includes such units as the Abakaliki Shale, Yandev Limestone, Mamfe Formation, Awi Formation, Mfamosing Limestone (Reyment, 1965; Whiteman, 1982; Ramanathan and Nair, 1984; Umeji, 2000, Nwajide, 2013). The Asu River Group is dated Middle – Late Albian and is believed to have been deposited as shallow – deep marine deposits during the middle Albian transgression based on diagnostic ammonite fauna (Reyment, 1965). The thickness ranges from 1500 m to 1800 m (Cratchley and Jones, 1965).

### **2.3.2 The Eze-Aku Group**

The Eze-Aku Group has been variously studied (Simpson, 1955; Reyment, 1965; Murat, 1972; Fayose and De Klasz, 1976; Arua and Rao, 1978; Petters, 1978, 1980; Banerjee, 1981; Umeji, 1984; Whiteman, 1982; Petters and Ekweozor, 1982; Agagu, 1985; Amajor, 1985,



1987, 1992; Orajaka and Umenwaliri, 1989; Ojoh, 1990; 1992; Ekweozor, 2001, 2004, 2005; Nyong, 2009; Ede, 2009; Ojo *et al.*, 2010; Ehinola, 2010; Okoro and Igwe, 2014).

Simpson (1955) and Reyment (1965) delineated the lithostratigraphic and biostratigraphic units using lithology and fossil content of the rocks. Reyment (1965) identified a type locality for the Eze-Aku Shale at Eze-Aku River in Aka-Eze, Southeastern Nigeria. It unconformably overlies the Asu River Group. The sediments were deposited during the extensive marine transgression at the beginning of the Turonian when the sea invaded the Benue Trough from the Gulf of Guinea (Reyment, 1965; Kogbe, 1989). The Eze-Aku Shale consists of calcareous shales, sandstones, and thin sandy or shelly limestones and calcareous fine to medium-grained sandstones (Reyment, 1965). Occasionally, thick sandstone or limestone units alternate with the calcareous shales. The Eze-Aku Shale was elevated in lithostratigraphically to a group by Murat (1972) without identifying the component Formations.

Whiteman (1982) identified the Eze-Aku Shale, the Amasiri Sandstone, the Konshisha River Sandstone, the Agila Sandstone, the Makurdi Sandstone, and the Nkalagu Limestone as formational units of the Eze-Aku Group. Using such diagnostic ammonites as *Vascoceras globosan*, *Neoptychites telingaeformis*, and *Eotissotia simplex*, Reyment (1965) dated the Eze-Aku Shale as early Turonian. Other fossils in the Eze-Aku Group include *vascocerastids*, pelecypods, gastropods, echinoids, decapod, and plant fragments (Reyment, 1965). Ojoh (1990) and Umeji (2007) dated the lower part of the Group as Cenomanian – Turonian based on palynomorph evidence. The shales and limestones are also rich in foraminiferas, ostracods, and fish teeth (Ojo *et al.*, 2010; Ehinola, 2010).

The environments of deposition of the Eze-Aku Group have been very controversial, in terms of what portion of the shallow marine deposited it (Simpson, 1955; Reyment, 1965; Petters,

1978, 1980; Banerjee, 1980, 1981; Whiteman, 1982; Petters and Ekweozor, 1982; Amajor, 1985 and Ekweozor, 2001, 2004, 2005). Some workers (Murat, 1972; Nwachukwu, 1972; Olade, 1975; Petters, 1978; Agagu and Adighije, 1983; Zaborski, 1987) have reconstructed the paleogeography of the Southern Benue Trough. There is still need for further studies to refine the depositional environment and paleogeography.

The environment of deposition and paleogeography is important in evaluating the economic potentials of any basin. Therefore the evaluation of the gas shale potential of the Eze-Aku Group in particular and the Southern Benue Trough in general can only be done, if the sedimentologic characteristics of the shales are studied.

Arua and Rao (1978) studied the biostratigraphy of the limestone of the Eze-Aku Group exposed at the Nkalagu Limestone quarry, and proposed a Turonian age based on the ammonite contents. Fayose and de Klasz (1976) proposed Lower Turonian age while Petters (1978, 1980) advocated a Late Turonian to Coniacian age based on foraminiferal content. Ojo *et al.* (2010) and Ehinola (2010) studied the biostratigraphy of the Lokpanta Oil shale of Ekweozor and Unomah (1990), and proposed a Turonian age for it. Ojoh (1992) interpreted the black shale facies of the Eze-Aku Group as Lower Turonian in age on the basis of ammonite content. He used the presence of abundant planktonic foraminifera ooze made up essentially of *Heterohelix globulosa* to infer pelagic water conditions for the shaly units of the Group.

Ekweozor and Unomah (1990) reported the presence of carbonaceous rocks, which they called oil shale at Lokpanta and surrounding villages. Ekweozor (2001) described the rocks as a distinct facies of the Eze-Aku Shale that should be given a formational status. Umeji (2007)

briefly described these rocks as calcareous dark grey shales, siltstones and fine sandstones. This work is to ascertain its lithostratigraphic status of the carbonaceous rocks within the stratigraphic framework of the Southern Benue Trough.

### **2.3.3 The Awgu Formation**

The Awgu Formation conformably overlies the Eze-Aku Group in the western flank or limb of the Abakaliki Anticlinorium, but is absent in the eastern flank/limb, possibly due to erosion or non-deposition (Agagu *et al.*, 1985). The Formation was deposited during the end of the Turonian transgressive cycle, and comprises bluish – grey shales with occasional intercalations of shelly limestones, and sandstones. The thickness of the Awgu Formation is estimated to be about 900 m (Benkhelil, 1986). It is dated Coniacian – early Santonian based on ammonite contents (Reyment, 1965). The ammonites include *Tissotia latelobata*, and *Tissotia awguensis*. *Pelecypods*, *Inoceramus schloenbachi*, and *Inoceramus lubatiae* were also recovered from the Formation (Reyment, 1965). The Agbani Sandstone and the Ogugu Formation (Agagu *et al.*, 1985) are the sandstone units of the Formation (Reyment, 1965; Agagu *et al.*, 1985).

### **2.3.4 The Nkporo Group**

The Nkporo Group is the oldest lithostratigraphic unit of the Anambra Basin and unconformably overlies the sediments of the Benue Trough. Component formations of the Group are the Nkporo Shale, Enugu Shale, Lafia Sandstone, Owelli Sandstone, Afikpo Sandstone and Otobi Sandstone.

The Nkporo Shale consists of dark grey shales with thin layers of sandstones and limestone (Kogbe, 1989b). The Enugu shale consists of black carbonaceous shales interbedded with thin layers of sandstone and siltstone with abundant plant debris deposited in a coastal swamp environment. Lafia Sandstone consists of white to grey, crossbedded, fine to coarse, poorly sorted, feldspathic sandstone, succeeded by white to brown clay, and bright red, friable ferruginous sandstone, capped by laterite (Nwajide, 2013). The fluviatile Owelli Sandstone consists of fine to coarse, pebbly, poorly sorted, texturally immature, compositionally mature cross-bedded sandstones (Agumanu, 1993). In the subsurface, it also consists of dark grey, micaceous, pyritic, calcareous shales. Afikpo Sandstone is made up of pebbly sandstone, siltstone and shales. Otobi Sandstone consists of alternations of siltstone and sandstone with lenticular laminations common.

### **2.3.5 The Coal Measures**

The Coal Measures represent an extensive Maastrichtian interval and reveal a period of non-marine alternating with shallow marine sedimentation in the Anambra Basin. In the Maastrichtian stage a period of regression led to the deposition of the paralic Mamu Formation consisting of shales, heterolith sandstone and coals (Lower coal measures). This Formation is the major stratigraphic unit that forms the lower part of the Enugu Cuesta (Riegers, 1996 and Nwajide, 2013). It consists of alternations of sandstones, siltstones, mudstones, coal seams and rare shales (with concretionary siderite and marcasite) (Nwajide, 2103).

The Nsukka Formation overlies the Ajali Formation. It is the Upper Coal Measures. The type area of the Nsukka Formation is the territory around the Nsukka municipality and northwards,

with well developed exposures of the Formation found in Udi, Oji and Awgu areas of Enugu State (Nwajide, 2013). The type section of the Formation is the Nkalagu village water point, about 6km west of Ibagwa Aka town, a suburban community northwest of Nsukka town. It consists of lignite seam, carbonaceous siltstones, cross-bedded and bioturbated sandstones (Nwajide, 2013).

### **2.3.6 Ajali Formation**

The Ajali sandstone Formation lies conformably on the Mamu Formation. It forms the middle part of the Enugu Cuesta. It consists of characteristically friable largely medium grained poorly to moderately sorted crossbedded sandstones with presence of clayey fractions. It also consists of isolated well-rounded pebbles, and sand, silt and clay heteroliths. It marks the height of the regression, which ended the Nkporo depositional cycle (Riegers, 1996 and Nwajide, 2013).

## **2.4 Gas Shale Potential**

The hydrocarbon potential of the inland basins has been studied by various authors (Obaje *et al.*, 1999; Mode, 2002; Obaje *et al.*, 2004; Ekweozor, 2005; Nwajide, 2005; Onuoha, 2005; Wipf and Party, 2006; Akande *et al.*, 2007; Akande *et al.*, 2011; Anyiam and Onuoha., 2014; Okeke *et al.*, 2014; Madukwe, 2014 and Abubakar, 2014). In the Southern Benue Trough, the Cretaceous formations contain oil and gas prone organic matter, which are marginally mature to mature (Obaje *et al.*, 2004, Akande *et al.*, 2007; Akande *et al.*, 2011; Anyiam and Onuoha, 2014). The Campanian and Maastrichtian formations also contain oil and gas prone organic matter but immature to marginally mature (Obaje *et al.*, 2004; Ekweozor, 2005; Akande *et al.*, 2007; Okeke *et al.*, 2014 and Abubakar, 2014).

Oil shale, belongs to the group of sapropel fuels (Ots, 2007); organic-rich fine-grained sedimentary rock containing kerogen (a solid mixture of organic chemical compounds) from which the liquid hydrocarbons, called shale oil is derived. Oil shales are not "geological nor geochemically distinctive rocks but rather an 'economic' term" (Hutton, 1994). The deposits of oil shale have given rise to expectations of yielding at least 40 litres of shale oil per tonne of oil shale, using the Fischer Assay (Dyni, 2006; Altun *et al.*, 2006). Oil shale is found in many places worldwide. An oil shale deposit of high economic value has been found and corresponds to the Turonian Eze-Aku Shale in Lokpanta near Okigwe, in Abia State, Nigeria (Ekweozor and Unomah, 1990). An initial appraisal of the economic potential of the fossil fuel deposit by pyrolysis (modified Fischer Assay) indicates an average oil-yield of more than 42 litre tonne<sup>-1</sup>, which is the lower acceptable threshold for economic exploitation and this deposit remains unexploited (Ekweozor and Unomah, 1990).

Gas shale studies have not been carried out in Nigeria. This work forms an initial attempt at evaluating the gas shale potential of any formation in Nigeria. However, elsewhere in Europe and USA, gas shale reservoir studies have identified shale gas plays (Banikowski and Hand, 1987; Dyni, 2003; Hill *et al.*, 2004; Frantz *et al.*, 2005; Shute, 2007; Sumi, 2008; Durhan, 2008; Mayhood, 2008; Hust, 2008; Wickstrom *et al.*, 2008; Ernst and Young, 2011; Kuuskra *et al.*, 2011; North Rose Full Bright, 2013; EIA, 2011). Cretaceous shale gas plays such as Marcellus Shale and Barnett Shale have been prolific, with an estimates of 300 – 350 scf and 60-100 scf of gas per ton of shale respectively (Bullin and Krouskop, 2008). The environmental implications and its management which are the main concerns in the exploitation of gas and oil shale have been studied and recommendations made by various authors (Sumi, 2008; Lechtenböhmer *et al.*, 2011; North Rose Full Bright, 2013; EIA, 2011).

# CHAPTER THREE

## Materials and Methods

### 3.1 Materials

The materials used during the fieldwork include global positioning System (GPS). Measuring tape, Masking tape, Digital camera, Hand lens, Geologic hammer, Pickaxe, Brunton compass, Sampling bags, Field notebook, Cutlass.

The materials employed for the various laboratory studies/methods are as follows:

#### Atomic Absorption Spectrometry Method

- |                                |                           |
|--------------------------------|---------------------------|
| 1) 1g of air dried rock sample | 2) 250ml conical flask    |
| 3) distilled water             | 4) 100ml volumetric flask |
| 5) Polypropylene               | 6) Perchloric acid-1      |
| 7) Nitric acid-2               | 8) Sulphuric acid-2       |

#### X-Ray Fluorescence Method

- |   |  |
|---|--|
| 1) 5.0g of dry rock sample  | 2) Tema vibrating mill                 |
| 3) Flux (X-ray Flux-Type 66:34% (66.0% Lithium Tetraborate: 34% Lithium metaborate) |  |
| 4) Pre-set furnace  | 5) Epsilon 5 Panalytical model machine |

### **XRay Diffraction Method**

- 1) Empyrean diffractometer DY 674 (2010)
- 2) Xpert Highscore Plus
- 3) ICDD PDF 2 (2010) database

### **Petrographic Method**

- 1) Vapour phase bath
- 2) Epoxy
- 3) Glass slide
- 4) Carbonate stain of Alizarin Red-S
- 5) Potassium ferricyanide
- 6) Cover slip

### **Palynologic Method**

- 1) 36% Hydrochloric acid
- 2) 40% Hydrofluoric acid\
- 3) 70% Nitric acid
- 4) 2% Potassium Hydroxide solution
- 5) Zinc Chloride (S.G. 1.9)
- 6) ultrasonic radiation
- 7) Safranin-o
- 8) Olympus-CH2 binocular microscope

### **Rock Eval Pyrolysis**

- 1) 200mg Pre-Cleaned Sample
- 2) 10 % HCl
- 3) Delsi-Nermag Rock Eval II Plus Toc Module
- 4) Pestle and Mortar
- 5) Flame Ionization Detector (FID)
- 6) Thermal Conductivity Detector (TCD)



### **3.2 Field Method**

This involved geologic mapping and lithological description of rock exposures to provide the necessary data for lithofacies identification and paleoenvironmental interpretations. The rock descriptions relied on their lithological attributes such as lithology, composition, attitude of the beds, sedimentary structures and fossil contents. The stratigraphic units within the study area were identified. The carbonaceous unit within the Eze-Aku Group was traced laterally along its strike direction in the study area. The exposures were systematically logged. Their sedimentary features were also noted. The lithofacies recognized were then grouped into a Lithifacies association.

Fresh ten (10) representative samples were collected from the Lokpanta Junction, 164km along Enugu-Port Harcourt expressway (Latitude 05° 59' 39" N, Longitude 07° 27' 35.2"E; 100.00m above sea level), River Nmavu channel (Latitude 06° 01' 6.2" N, Longitude 07° 30' 30.9"E; 65.00m above sea level) and Ezzaegu Area (Under the Ezzaegu –Agba bridge, Latitude 06° 05' 20" N, Longitude 07°49' 25"E; 85.00m above sea level) for laboratory analyses (Figure 3.1). Global Positioning System (GPS) device was used to georeference outcrop locations and their topographic elevation. 500 grams of calcareous shale and marlstone samples were collected at a depth of about 1m to get fresh samples at the three exposures from the top, middle and top of each of them. All the ten (10) shale samples were immediately stored in zip lock polyethylene bag and preserved at room temperature. The Lokpanta Junction samples were labelled EXLK, while the River Nmavu channel samples were labelled LK, and Ezzaegu area samples were EZZ. The locations and lithologies were plotted on the topographic map to produce a geologic map.

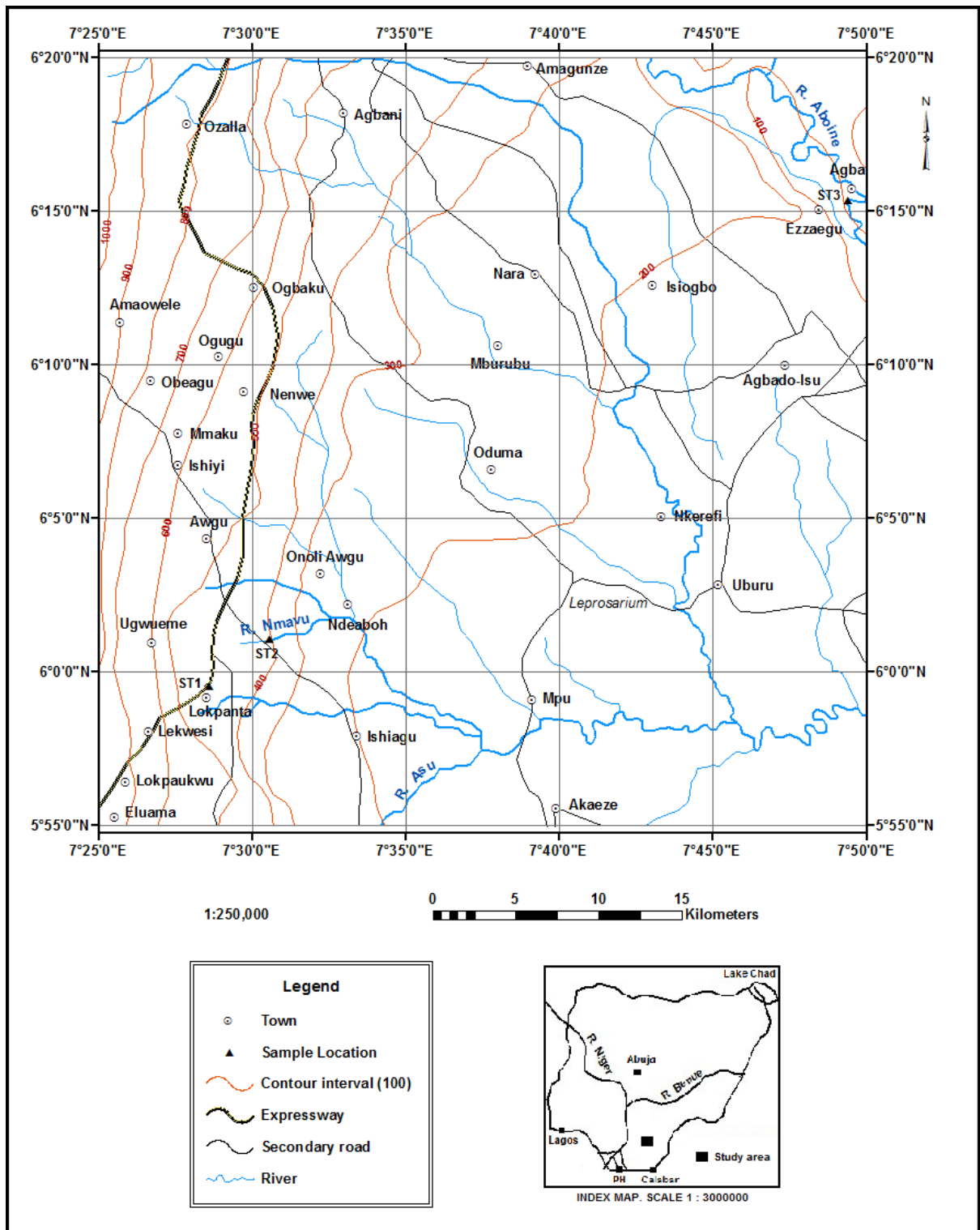


Figure 3.1: Map of the Study area showing the sample locations

### **3.3 Laboratory Techniques**

Laboratory techniques applied in the AAS method, XRF method, XRD method, petrographic method, palynological method and Rock-Eval pyrolysis method are explained below.

#### **3.3.1 Atomic Absorption Spectroscopy (AAS) Method**

This is a spectroanalytical procedure for the quantitative determination of chemical elements using the absorption of optical radiation (light) by free atoms in the gaseous state.

The technique was used for determining the concentration of a particular element (the analyte) in the samples collected. AAS can be used to determine over 70 different elements in solution or directly in solid samples used in geologic and other scientific research.

Ten (10) representative rock samples were analysed. The samples were first prepared for analysis following the digestion procedure. This was done using the hot plate, 250ml Pyrex conical flask acid washed and rinsed with distilled water, and 100ml volumetric flask polypropylene as the apparatus. The reagents used were Perchloric acid-1, Nitric acid-2, and Sulphuric acid-2.

1g of air-dried rock sample passed through (2mm sieve) with foil paper was weighed accurately and transferred to a 250ml conical flask. A measured volume of well-mixed acid, Perchloric acid nitric acid, and Sulphuric acid in the ratio 1:2:2 was then transferred into the flask containing the soil sample in the fume hood and heated to about (15-20 min) in the hot plate until a white fume was observed. The digestion was then stopped and cooled, after which a 20 ml of distilled water was added and boiled to bring the metal into solution. This

was further allowed to cool and filtered through Whatman 42 filter paper in a 100ml volumetric flask and made to mark with distilled water, and then finally transferred to 100ml plastic can for AAS analysis.

The heavy metal analysis was done using the Perkin-Elmer Analyst 100. The AAS System was powered on and the element Hollow-Cathode lamp placed in lamp holder. The system was then allowed to warm up for about 30mins. The operating conditions were set as follows;

- a) Manual Zero mode and Auto Zero Button was set out
- b) The selection knob on the machine was turned and the voltage is adjusted from 250 - 350 Volts.
- c) Wavelength was set to obtain a maximum energy reading and optimized by adjusting the vertical/horizontal lamp mount control.
- d) The Acetylene: Air ratio was ensured to be 1:8 i.e. 5Psi: 40 psi before the flow of air and acetylene was turned on.
- e) The distilled water was ignited and aspirated for about 5mins to warm up the system and afterwards checked to see if it is still close to Zero ( $\pm 0.005$ )
- f) The Nebulizer was adjusted when necessary to get a stable maximum signal and the wavelength checked to get a maximum signal.

For the Calibration and Sample Analysis, a five-point calibration standard was made and the system calibrated. The analysis began by aspirating the sample blank, zero the energy, and then aspirating the standards and samples recording the ABS (Absorbance). The standards and blank intensities throughout the analysis were checked.

The results were quantified by plotting a calibration curve and obtaining a regression equation. The ABS (Absorbance) was used to calculate the concentration of the analyte from the regression equation.

Metal concentration in rock sample-mg/kg = (A x B)/Z sample

Where A= Concentration of metal in digested solution.

B= Final volume of digested solution (dilution factor)

Z= sample weighed.

### **3.3.2 X-Ray Fluorescence (XRF) Method**

Ten (10) representative rock samples were analysed using X-Ray Fluorescence method. They were reduced to less than 63microns using a Tema vibrating mill. The agate mortar in the mill crushes the samples before sieving them to pass through 63 microns.

Beads used for the major elemental analysis expressed in oxide weight percent were prepared first by drying the sample powder in an oven at 110<sup>0</sup>C for 24 hours to remove moisture in the rock powder. About 5.0g of dry rock sample powder was weighed in a silica crucible and then ignited in the furnace at 1000<sup>0</sup>C for 2 to 3 hours for the calcinations of impurities in the rock powder. The samples were then removed from the furnace and allowed to cool to room temperature in desiccators. Each ignited rock powder was then weighed again to determine the weight of calcinated impurities which were H<sub>2</sub>O, H<sub>2</sub>O<sup>+</sup> and CO<sub>2</sub>. 1.0g of the stored ignited rock powder was weighed and exactly 5 times of flux (X-ray Flux-Type 66:34% (66.0% Lithium Tetraborate: 34% Lithium metaborate) was added to lower the vitrification temperature of the rock powder. The weighted mixture was mixed properly in a platform dish and ignited in the pre-set furnace (Eggon 2 Automatic fuse bead maker) at 1500<sup>0</sup> C for 10

minutes to form glass bead. Each glass bead was labeled and slotted into the computerized XRF (Epsilon 5 Panalytical model) for major elemental analysis.

Trace elemental analysis was carried out using compressed powder pellets. These pellets were prepared by weighing 3.0g of oven dried powder samples and 3.0g flux (cellulose-powder) added as a binder and dispersive agent, and shaking in small plastic containers for 12 minutes. The well mixed mixture was then compressed by applying pressure of  $1,500\text{kgm}^{-2}$  using both manual and electronic compressors. The pellets were placed in the computer-programmed XRF and the conditions for trace elemental analysis set to give the result in elemental. Also, corrections were done to convert these trace elements in ppm to elemental oxides of those trace elements.

### **3.3.3 XRD (X-Ray Diffraction) Method**

The diffractometer used for this analysis was the Empyrean diffractometer DY 674 (2010) with copper anode material manufactured by Panalytical, Holland. It works with a combination of other components like the water chiller, which cools the x-ray tube and maintains a uniform temperature. There is also the compressed air that helps in opening and closing of the cabinet door.

The goniometer forms the central part of the Empyrean diffraction system. It contains the basic axes in X-ray diffractometry: the omega and  $2\theta$  axes. The X-ray tube, incident beam optics, the sample stage and the diffracted beam optics including the detector are mounted on specific positions on the goniometer. The goniometer is set up in vertical mode and can be configured for theta-theta and alpha-1 diffraction geometries. The goniometer radius is

240mm. The diffractometer consists of three basic elements: an X-ray tube, a sample holder, and an X-ray detector.

The software used:

- 1) Data collector which connects the XRD machine with the work station.
- 2) Xpert Highscore Plus which is used to analyse and interpret the data to produce the resulting diffractogramme.
- 3) ICDD PDF 2 (2010) database for easy searching and matching of the diffractogramme to identify the minerals and compounds.

Five (5) representative rock samples were finely ground, homogenized, and sieved to pass through the 75 microns. A representative portion of the powdered sample is then prepared using the sample preparation block and compressed in the flat sample holder to create a flat, smooth surface that was later mounted on the sample stage in the XRD cabinet.

The sample is analysed using the reflection-transmission spinner stage using the theta-theta settings. Two-theta starting position is 0.00483 and ends at 75.000 with a  $2\theta$  step of 0.026  $^\circ$  at 3.57 seconds per step. Tube current was 40mA and the tension was 45VA. Fixed Divergent Slit size of  $1^\circ$  is used and the goniometer radius is 240mm.

The intensity of diffracted X-rays is continuously recorded as the sample and detector rotate through their respective angles. A peak in intensity occurs when the mineral contains lattice plane with  $\delta$ -spacings appropriate to diffract x-ray at that value of  $\theta$ . Although, each peak consists of two separate reflections ( $K\alpha_1$ ,  $K\alpha_2$ ), at small values of  $2\theta$  the peak locations overlap with  $K\alpha_2$  appearing as a hump on the side of  $K\alpha_1$ . Greater separation occurs at higher values of

$\theta$ . Typically, these combined peaks are treated as one. The  $2\lambda$  position of the diffraction peak is typically measured as the centre of the peak at 80% peak height.

Results are commonly presented as peaks positions at  $2\theta$  and X-ray counts (intensity) in the form of a table or an x-y plot. Intensity ( $I$ ) is either reported as peak height intensity, that intensity above background, or as integrated intensity, the area under the peak. The relative intensity is recorded as the ratio of the peak intensity to that of the most intense peak (*relative intensity*-  $I/I_1 \times 100$ ).

The  $d$ -spacing of each peak is then obtained by solution of the Bragg equation for the appropriate value of  $\lambda$ . Once all  $d$ -spacings have been determined, automated search/match routines compare the  $d$ s of the unknown materials. Each mineral has a unique set of  $d$ -spacings and due to this, the matching of these  $d$ -spacings provides an identification of the unknown sample. A systematic procedure is used by ordering the  $d$ -spacings in terms of their intensity beginning with the most intense peak. Files of  $d$ -spacings for hundreds of thousands of inorganic compounds are available from the International Centre for Diffraction Data as the powder Diffraction File. The peaks obtained from analyses were matched with the minerals from ICDD database which is attached to the software of the machine.

### **3.3.4 Petrographic Method**

This method estimates pore size distribution, grain size, sorting, porosity, mineral abundances, fabric, rock classification, types of porosity varieties and abundances. Ten (10) thin sections were prepared from fresh rock samples, mainly the marlstones.

The following procedures were adopted in preparing the slides:



- 1) Samples were cleaned in a vapor phase bath to remove solvable excess residual hydrocarbon.
- 2) The samples were then impregnated with blue epoxy to identify porosity and preserve the textures. They were then polished and mounted onto a glass slide.
- 3) The samples on the slides were then ground down to a thickness of 30 microns and stained with a combined carbonate stain of Alizarin Red-S (for calcite) and potassium ferricyanide (for ferroan carbonate identification).
- 4) The cover slip was glued on the polished surfaces. The prepared thin sections were examined petrographically using a petrographic microscope.

### **3.3.5 Palynological Method**

The condition and identification of those particles, organic and inorganic, give the palynologist clues to the life, the environment, and energy conditions that produced them.

Ten (10) representative rock samples from the calcareous shales and marlstones under investigation were processed for palynological analysis. 10g of each of the samples was subjected to standard chemical treatment for concentration of acid insoluble microfossils. Adequate precautions were taken to achieve maximum recovery of miospores. An outline of the sample digestion procedure adopted is presented below:

- a. Dissolution of Carbonates using 36% Hydrochloric acid;

- b. Dissolution of Silica and Silicates using 40% Hydrofluoric acid;
- c. Removal of aliquot quantity of samples residue utilized for the fourth step used for kerogen (palynodebris) studies;
- d. Oxidation of organic material using 70% Nitric acid;
- e. Dissolution of humic acids (amorphite) using 2% Potassium Hydroxide solution and to improving staining quality;
- f. Separation of the mineral components if any, by the action of Zinc Chloride (S.G. 1.9);
- g. Deflocculation of residue with ultrasonic radiation; and
- h. Staining with Safranin-o to provide sufficient contrast for observation and photography;

Recovered residue were stored in vials, later diluted to a consistent concentration, and used for making slides mounts for kerogen and palynomorph assemblage studies. Two slides were prepared for each sample for kerogen studies. Four slides were prepared from each sample for palynomorph studies.

The slides were systematically studied using the Olympus-CH2 binocular microscope. Identification of palynomorphs was attempted for as many forms as possible. Photomicrographs were taken using Polyvar microscope with 35mm camera attachment.

The strategies adopted for the analysis included:

1. Counts of palynomorphs were made per slide. Counts were taken from three or four slides for samples with low palynomorph concentrations so as to reach target.
2. All slides were traversed to check for the presence of stratigraphic marker species encountered.
3. All unidentifiable or poorly preserved palynomorphs were noted but excluded in computing pollen sum and percentage composition.
4. All discordant palynomorphs were noted but excluded in the total count and calculation of palynomorph sum.
5. Ancillary palynomorphs like chitinous foraminifera tests lining, fungal elements, Algae (*Botryococcus*, *Pediastrum*, *Chomotriletes*, *Tasmanites*) were noted but excluded in the computation of pollen sum and percentages.

### **3.3.6 Rock Eval Pyrolysis**

Rock Eval pyrolysis was done using the Delsi-Nermag Rock Eval II Plus TOC module. Samples analysed on the Rock Eval are usually subsampled from the previously crushed and freeze-dried rock samples in the coulometer.

Ten (10) representative rock samples were initially cleaned by seeping in 100% dichloromethane followed by decanting of the solvent after shaking until the rocks were clean. The samples were dried, then washed under running tap water and then dried again in an oven at pre-set temperature of 30<sup>0</sup>C.

Total Organic Carbon (TOC) analysis was performed by means of the LECO C<sub>S1</sub>25 Carbon

Analyzer according to the following procedure:

- a) About 200 mg of the pre-cleaned sample was crushed and accurately weighed into clean LECO crucibles.
- b) The sample was de-mineralised by hot 10 % HCl and washed repeatedly with distilled water.
- c) After drying at 60<sup>0</sup>C, the sample was automatically introduced into the furnace for combustion and measurement of the organic carbon content.

Pyrolysis was performed by means of the Delsi-Nermag Rock Eval II Plus TOC module as follows:

- 1) Each pre-cleaned lot of shale was crushed with pestle and mortar and weighed accurately (100mg 40pprox.) into the sample holder.
- 2) All the sample holders were then transferred into prenumbered slots in the sample carousel.
- 3) A commercial standard rock sample was then similarly weighed into other sample holders and slotted into the carousel after every 10 (ten) rock samples.
- 4) Thereafter, the carousel was placed in its appropriate location in the instrument and the analysis START programme was activated. The instrument operated automatically until the last sample in the carousel was analysed.
- 5) The process involved the transfer of each sample into the furnace where it was heated initially at 300<sup>0</sup>C for three minutes in an atmosphere of helium to release the free hydrocarbons (s<sub>1</sub>).

- 6) Pyrolysis of the bound hydrocarbons to give the  $s_2$  peak followed immediately as the oven temperature was ramped up rapidly to  $550^{\circ}\text{C}$  at the rate of  $25^{\circ}\text{C}/\text{min}$ . Both the  $s_1$  and  $s_2$  hydrocarbon peaks were measured using a flame ionization detector (FID).
- 7) A splitting arrangement permitted the measurement of the  $s_3$  peak (carbon dioxide) by means of a thermal conductivity detector (TCD). The instrument automatically recorded the temperature corresponding to the maximum of the  $s_2$  peak, i.e.  $T_{\text{max}}$ . An in-built computer processed the raw data to afford the values corresponding to the respective Rock-Eval indices.

Above, I have outlined the various methods utilized in the course of this study. The strictest adherence to safety standards was followed as the various analyses performed. Table 3.1 shows the standards for interpretation; the subject matters of interest to this study, the methodology employed and their respective references.

Table 3.1: Standards for Interpretations

S/N	Subject Matter	Methodology	Reference
1.	Environment of deposition (Paleoredox conditions)	Ni/Co	Jones and Manning (1994)
		V/Cr	Dill et al. (1988)
		V/(V+Ni)	Hatch and Laventhal (1992)
		Palynomacerals	Whitaker et al., 1992 and Batten, 1996 )
2.	Tectonic Setting	SiO <sub>2</sub> vs. K <sub>2</sub> O/ Na <sub>2</sub> O	Roser and Korsch, 1986
		K <sub>2</sub> O/ Na <sub>2</sub> O vs SiO <sub>2</sub> /Al <sub>2</sub> O <sub>3</sub>	Roser and Korsch, 1986
		Al <sub>2</sub> O <sub>3</sub> / SiO <sub>2</sub> vs Fe <sub>2</sub> O <sub>3</sub> +MgO	Bhatia, 1983
		Fe <sub>2</sub> O <sub>3</sub> +MgO vsTiO <sub>2</sub>	Bhatia, 1983
3.	Provenance/Paleoclimatology	Al <sub>2</sub> O <sub>3</sub> /K <sub>2</sub> O	Aplin,1993
		Al <sub>2</sub> O <sub>3</sub> /TiO <sub>2</sub>	Maslov et al., 2003
		K <sub>2</sub> O vs Rb	Floyd and Leveridge, 1987
		Al <sub>2</sub> O <sub>3</sub> vs TiO <sub>2</sub>	Amajor, 1987
		correlation and element enrichment of Cr and Ni	Floyd and Leveridge, 1987
4.	Mineralogy/ Maturity/ (Weathering and Diagenesis)	Plot of Weathering index	Kronberg and Nesbitt, 1981
		Chemical Index of Alteration	Nesbitt and Young, 1984
		Mineralogical Index of Alteration	Voicu et al. (1997)
5.	Source rock evaluation/shale gas potential	Modified Van Krevelen (Plot of HI against OI)	Peters, 1986
		Plot of s <sub>2</sub> against TOC	Langford and Blanc-Valleron, 1990)
		Plot of PI against T <sub>max</sub> (°C)	Peters, 1986
		Plot of HI against T <sub>max</sub> (°C)	Gorin and Feist-Burkhardt, 1990)
6.	Paleoproductivity	Cd and Ba enrichment	Middleburg and Comans, (1991); van Capellen and Ingall, (1994)
		Correlation of Cd and Ba content	
7.	Paleosalinity	Sr enrichment	Degens et al., 1957; Degens, 1958; Tourtelot, 1964 and Hossein et al., 2012
		Sr/Ba enrichment	Hossein et al., 2012)
		Ga depletion	Degens et al., 1957; Degens, 1958; Tourtelot, 1964)
		Al <sub>2</sub> O <sub>3</sub> vs TiO <sub>2</sub> crossplot	Hossein et al., 2012

# CHAPTER FOUR

## RESULTS AND DISCUSSION

### 4.1 Results

#### 4.1.1 Lithostratigraphy

Regional mapping of the study area revealed six (6) lithostratigraphic units (Figure 4.1). The basal lithostratigraphic unit in the study comprises of predominantly hard, poorly bedded light grey to light brown shales with subordinate occasionally sandy, splintery metamorphosed mudstone, localized occurrences of light grey to white sandstones, siltstones and limestone interbeds. Lenses of sandstones, siltstones and limestones are highly fractured. This represents the Abakaliki Shale of the Asu River Group. Its estimated mean thickness is about 200 m and lateral extent is about 25 km (Reyment, 1965; Nwajide, 2013).

This lithostratigraphic unit is overlain by the Eze-Aku Group comprising hard grey marlstones, dark grey and black shales, siltstones, sandstones and limestones. The alternating/rhythmic sequence of hard grey platy marlstones and dark grey to black papery calcareous shales have been designated as the Lokpanta Shale. Casts and moulds of *Inoceramus labiatus* and depauperate ammonites are the only biogenic structures that occur in this rock. The Lokpanta Shale has been traced from Lokpanta in the southern part of the study area up to Ezzaegu area with outcrops under the Ebonyi River Bridge in the northeast part (Figure 4.1). Shales and marlstones with similar characteristics have been described at the Calabar Flank (Nyong, 1995). These rocks are very carbonaceous and lack bioturbations. Its estimated mean thickness is about 150 m and lateral extent is about 35 km.

Overlying this shale is the mainstream Eze-Aku Shale, which consist hard flaggy grey to black shales, limestones and siltstones. This stratigraphic unit was described at Akaeze, in the Eze-Aku River channel by Reyment (1965). Its estimated average thickness is about 100 m and lateral extent is about 15 km (Reyment, 1965; Nwajide, 2013; Igwe and Okoro, 2016).

The Amasiri Sandstone facies outcrops at Ugwunwanne hills, north of Lokpanta area and east of Amagunze area. It consists of heteroliths, crossbedded sandstones and pebbly coarse-medium to fine grained, poorly sorted sandstones. The sandstones are profusely bioturbated. It is the topmost unit of the Eze-Aku Group in the study area. Its type locality is Amasiri in the Afikpo Synclinorium located in eastern flank of the Abakaliki Anticlinorium where Amasiri Sandstone has been described extensively. The reason the outcroppings of the Amasiri Sandstone is seen on both flanks of the Abakaliki Anticlinorium is because it was deposited horizontally on the underlying formations before the Santonian event which folded the then Abakaliki Basin. Its estimated average thickness is about 200 m and lateral extent is 3 km (Nwajide, 2013).

This Formation is overlain by grey shales with occasional intercalations of fine grained, pale yellow, calcareous sandstones and shelly limestones of the Awgu Group. It outcrops in Awgu, Onoli-Awgu, Ugwueme, Nara, Agbani areas. Its estimated mean thickness is about 15 m and lateral extent is 5 km (Reyment, 1965; Nwajide, 2013).

The topmost lithostratigraphic unit consist of dark grey to black shales with occasional thin beds of sandy shales and sandstones belonging to the Nkporo Group. It outcrops in Ogugu, Amaowele, Ogbaku, Obeagu, Mmaku, Nenwe and Ishiyi areas where it laterally changes facies to the Owelli Sandstone. Its estimated average thickness is about 20 m and lateral extent is 5 km (Reyment, 1965; Nwajide, 2013).



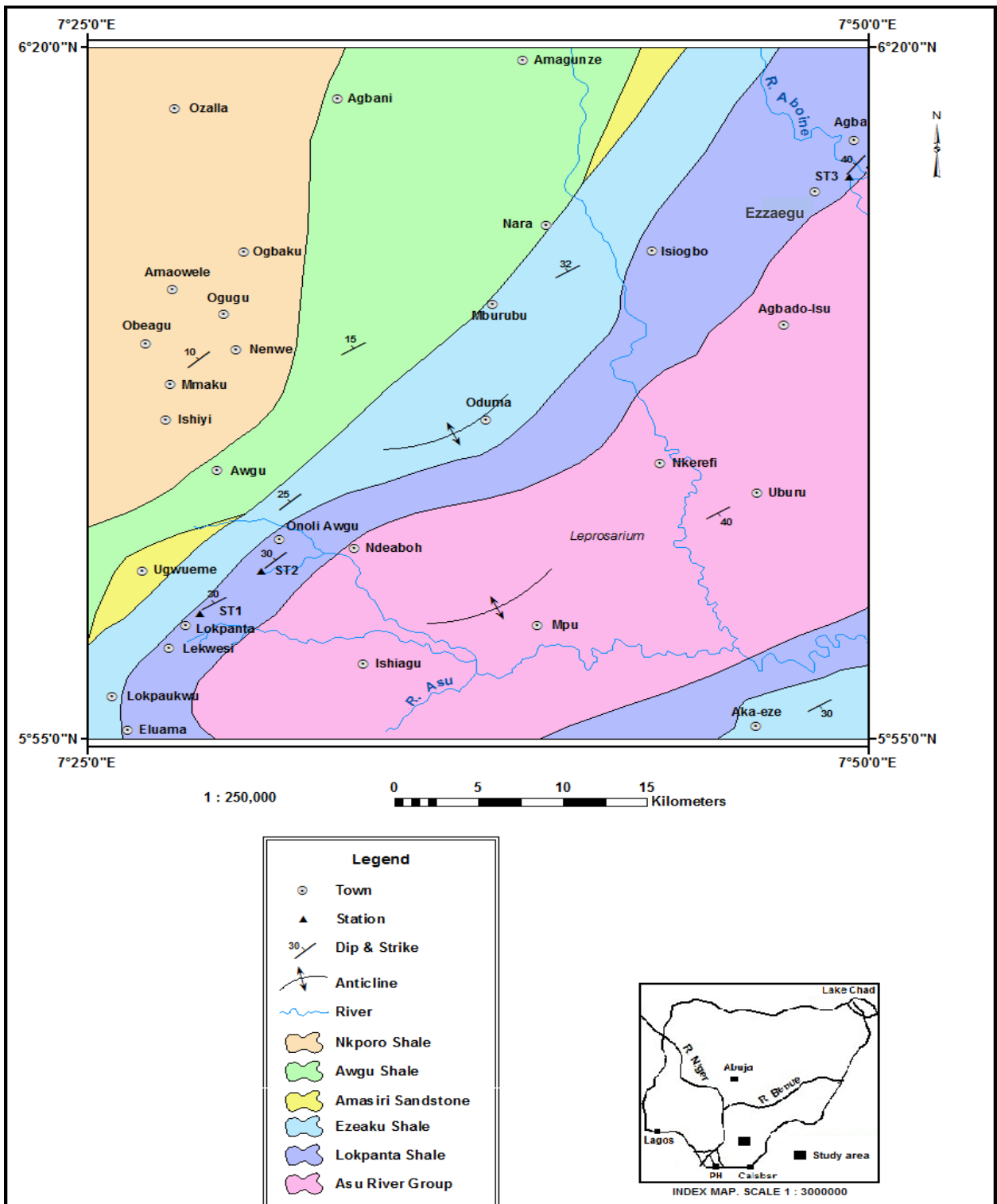


Figure 4.1: Geologic map of study area showing the stratigraphic and geographic position of the Lokpanta Shale in the Abakaliki Anticlinorium

#### 4.1.2 The New Formation

Six lithostratigraphic units were mapped in the study area - the Asu River Group, Lokpanta Shale, Eze-Aku Group, Amasiri Sandstone, Awgu Group and Nkporo Group (see Figure 4.1).

The unit of interest in this study is the Eze-Aku Group. Murat (1972) used the term, Eze-Aku Shale Group for this lithostratigraphic unit. He recognized the variability in lithologic character of the lithostratigraphic unit. Nwajide (2013) discussed the upgraded lithostratigraphic status from “Formation” (Simpson, 1955 and Reyment, 1965) to “Group” recognizing dark grey- black shale with siltstone and limestone interbeds as formations while the sandstone lithofacies of Amasiri, Konsisha River and Igumale represent other formations in the Group.

Ekweozor and Unomah (1990) reported the presence of carbonaceous rocks within the Eze-Aku Group, around Lokpanta and surrounding villages. Ekweozor (2001 and 2005) proposed that this carbonaceous rock should be recognized as a distinct Formation of the Eze-Aku Group. He proposed Lokpanta as the type locality for this new Formation. Exposures of this rock also occur in the Nmavu River channel in Onoli-Awgu.

The definition of a “formation” should be on the basis of a type section. The formation should show lithologic homogeneity or uniform variability, mappability on the scale of at least 1:25,000; and must be traceable laterally for a reason extent (Nichols, 2009).

The Lokpanta Shale exposures show good lithologic homogeneity throughout the area of study and may be correlatable with the Ezillo Formation of Ojoh (1992). The lithology is made up of interbedded dark grey to black calcareous shales and light grey marlstones. Macrofossils are absent except for depauperate ammonites and *Inoceramus*

*labiatus*. The rock unit is traceable laterally and mappable within the study area and beyond (see Figure 4.1). The Abakaliki Shale of the Asu River Group which represents the basal lithostratigraphic in the study area has been described and established by Simpson (1955) and Reyment (1965) with its type locality around the Abakaliki Town. This extensive basal brown to light grey mottled shales represents the lower boundary stratotype of this lithostratigraphic unit. The lower boundary stratotype has a thickness of 200 m and extends laterally for over 25km. Its upper boundary is marked by the presence of flaggy grey shales and siltstones with large ammonites, pelecypods and plant fragments occurring in places. The rocks are bioturbated. The upper boundary represents the Eze-Aku Shale of Reyment (1965) with type locality at Eze-Aku River in Akaeze. The upper boundary stratotype has a thickness of 100 m and extends laterally for over 15 km.

The Lokpanta Shale is obviously different from the Eze-Aku Shale (Simpson, 1955; Reyment, 1965). The Eze-Aku Shale comprises of grey flaggy shales and siltstones, rich in *vascoceratids*, pelecypods, echinoids, fish teeth, decapods and plant fragments. The main differences between these carbonaceous rocks and the Eze-Aku Shale are lithologic (rhythmic nature of the dark grey calcareous shales and light grey marlstones as opposed to the flaggy shales and siltstones interbeds of the Eze-Aku Shale), and fossil content/biogenic activities (lack of bioturbation and macrofossils except casts and moulds of depauperate ammonites and the bivalve, *Inoceramus labiatus* in contrast to the presence of bioturbation and macrofossils such as larger ammonites, *vascoceratids*, pelecypods, echinoids, fish teeth, decapods and plant fragments). This carbonaceous rock is the basal lithostratigraphic unit of the Eze-Aku Group in the study area.

The proposed name for the new lithostratigraphic unit is the **Lokpanta Shale** based on the geographic feature where the stratotype occurs.

Three formations of the Eze-Aku Group have been recognized in the study area: the extensive basal predominantly dark grey to black calcareous shaly unit of interbedded dark grey to black calcareous shale and light grey platy marlstone facies representing the Lokpanta Shale, the predominantly shaly unit representing the Eze-Aku Shale and the tidally influenced cross-bedded, clay filled sandstone facies representing the Amasiri Sandstone (Figure 4.2). Figure 4.2 is a composite section for the Eze-Aku Group in the Abakaliki Anticlinorium. The estimated thicknesses of the stratigraphic units were obtained from actual field studies and literature. The geologic mapping also revealed a sandstone Formation of the Eze-Aku Group. The outcropping section exposed in the northeast trending Ugwunwanne ridge, and Amagunze area. The influence of the Santonian tectonism is evident on the steeply dipping nature of the channel fills and erosional surfaces. This represents the Amasiri Sandstone, reaching a thickness of 200 m and extends laterally about 3 km.

The Lokpanta Shale comprises of interbedded dark grey to black calcareous shales and light grey platy marlstones (Figure 4.3). The fossils encountered in the Formation during field studies are the moulds and casts of the bivalve, *Inoceramus labiatus* and depauperate ammonites. Sideritic/pyritic concretions are the chemical structures in the Formation. This unit outcrops prominently at the Lokpanta Junction, Nmavu River and Agba/Ezzaegu areas, with a cumulative thickness of 150m and a lateral extent of about 35km. Other areas where the unit outcrops include Lekwesi, Lokpaukwu and Isiogbo. The stratotype (Figure 4.3) is described along the Nmavu River channel where it is prominently exposed



The Formation has been dated by both Amoke (2009) and this present study as being Cenomanian- Turonian in age. The lower boundary of the formation is identified at the outskirts of Ishiagu (Latitude 6°01' 8''N and Longitude 7°30'49.9''E) where interbedded dark grey to black calcareous shales and light grey platy marlstones is underlain by hard grey to olive green and brown shales (Abakaliki Shale) while the upper boundary consists of dark grey shales which is overlain by grey flaggy shales and siltstones of the Eze-Aku Shale in the Lokpanta area (Latitude 5°58' 15''N and Longitude 7°28'10.2''E). There was no proper exposure of the Eze-Aku Shale. It is represented partially by a covered section in the composite section. The type locality for the Lokpanta Shale is the Nmavu River channel (Onoli-Awgu) 3km along the Onoli-Awgu/Ishiagu road from its intersection at the Port Harcourt-Enugu Expressway. The stratotype of the Eze-Aku Shale is as described by Simpson (1955) and Reyment (1965) in the Eze-Aku River channel at Akaeze. The Lokpanta Shale unconformably overlies the Abakaliki Shale (Asu River Group) and conformably underlies the Eze-Aku Shale.



Figure 4.3: Calcareous shales and marlstones at the type locality along the Nmavu River, Onoli-Awgu

## 4.2 Eze-Aku Group

The Eze-Aku Group in the study area consists of three lithostratigraphic units. These are the Lokpanta Shale, Eze-Aku Shale and Amasiri Sandstone.

The Eze-Aku Shale consists of siltstones with interbedded lenses of oolitic crossbedded and coquinoid limestones, hard flaggy grey micaceous shales with gypsum efflorescent needles and bioclastic limestones. The biogenic structures, which occur in the Formation, include juvenile and adult gastropods, articulated pelecypods, adult ammonites and casts of *Inoceramids*. The Formation shows evidence of bioturbation.

The Lokpanta Shale is the basal lithostratigraphic unit of this group. It consists of the repetitive alternation of dark grey to black papery calcareous shales and light grey platy to flaggy marlstones. The dominant lithology is shale. The unit is devoid of bioturbation and body fossils. Casts and moulds of *Inoceramus labiatus* and stunted ammonites are the sole biogenic structures. The physical structures, which occur in this unit, are thin laminations. Its chemical structures are the sideritic/pyritic ellipsoidal and spheroidal concretions.

The Amasiri Sandstone is made up of clayey, friable, medium to coarse sandstones. It exposes a coarsening upwards succession of clayey, flaser bedded; bioturbated fine to medium-grained sandstone interbedded with mudstone at the base, and cross bedded coarse grained sandstone at the top. The entire exposure is profusely channeled with over twenty channels encountered in the 0.03km<sup>2</sup> area of the exposure. The sedimentary structures of the Formation include parallel laminations, flaser bedding, cross stratification, convolute bedding, vertical burrows (*Skolithos* ichnofacies- *Paleophycus* and *Ophiomorpha* ichnogenera).



### 4.3 Description Of Selected Outcrop Sections Of The Lokpanta Shale

#### 4.3.1 Lokpanta Junction Section

The rock exposures at the Lokpanta Junction, 164 km on the Enugu – Port Harcourt Expressway occurs on both sides of the road for a distance of about 500 m. A total thickness of 25.80 m of section consisting of alternations of dark grey shales and light grey marlstones was logged (Figure 4.4). The rocks are generally calcareous. The marlstones show very thin laminations of mm-scale. They exhibit platy fissility. The shales display fissility with laminae ranging from 0.50mm to 1.00mm. Spheroidal or oval shaped sideritic concretions are common in the shales and marlstones (Figure 4.5a). The predominant lithology is the shale with thicknesses ranging from 0.20 to 10.00 m. Thickness of the marlstones range from 0.02 to 0.30 m. Macrofossils are absent but impressions or casts of *Inoceramus labiatus* occur in the shales and marlstones (Figure 4.5b). The composite lithologic log of the section is shown in Figure 4.6.



Figure 4.4: Vertical section at the Lokpanta Junction along the Enugu-Port Harcourt Expressway

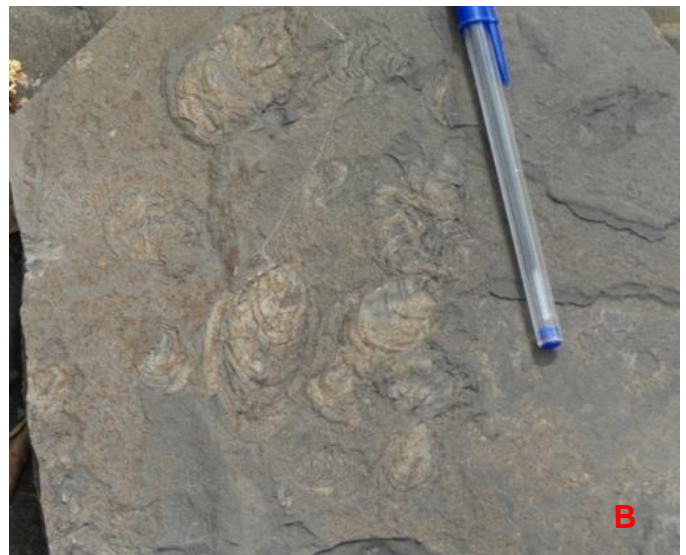


Figure 4.5a and b: Spheroidal concretion and Cast of *Inoceramus labiatus* on the calcareous shales at the Lokpanta Junction along the Enugu-Port Harcourt Expressway

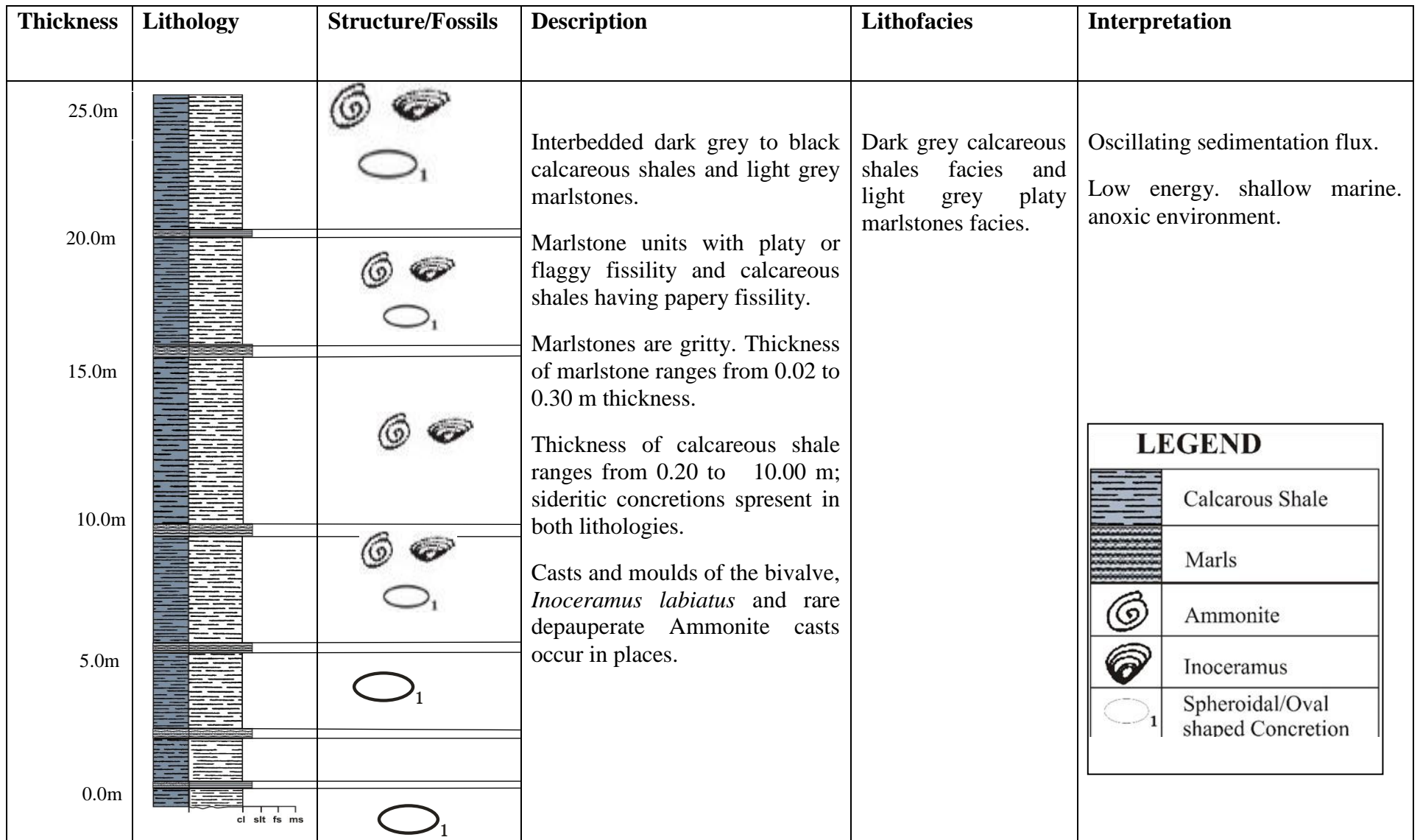


Figure 4.6: Composite lithologic log of Lokpanta Junction

### 4.3.2 River Nmavu Section

Along the River Nmavu channel about 3.00-4.00 km on the way to Ishiagu from the Enugu – Port Harcourt Expressway at Onoli-Awgu (Ishiagu Junction), dark grey shales and marlstones are exposed. The rocks exhibit rhythmic alternation of dark grey to black calcareous shales and light grey marlstones. A total thickness of 106.80 m of exposed rock consisting of interbeddings of calcareous shales and marlstones was logged. The exposures were logged in segments, from OT 1 to OT 8.

#### **Outcrop (OT 1)**

This segment of the section lies unconformably on a mottled light grey silty shale. The contact is represented by a paleosol horizon thought to be the top of Abakaliki Shale of the Asu River Group. The succession comprises of interbedded dark grey calcareous shale and light grey marlstone beds which are well indurated. Mineral composition of the rocks is dominated by clay and calcite. The bedding planes are sharp and planar. The marlstone beds exhibit platy and flaggy fissility while the calcareous shale beds show papery fissility. There is absence of bioturbation and macrofossils, but casts and moulds of the bivalve *Inoceramus labiatus* are common. The chemical structures common are the sideritic and pyritic concretions; which are spheroidal and ellipsoidal in morphology (Figure 4.7). The total thickness of this segment is 7.50m (Figure 4.8).





Figure: 4.7: Interbedded calcareous shale and marlstone exposures of OT 1 segment

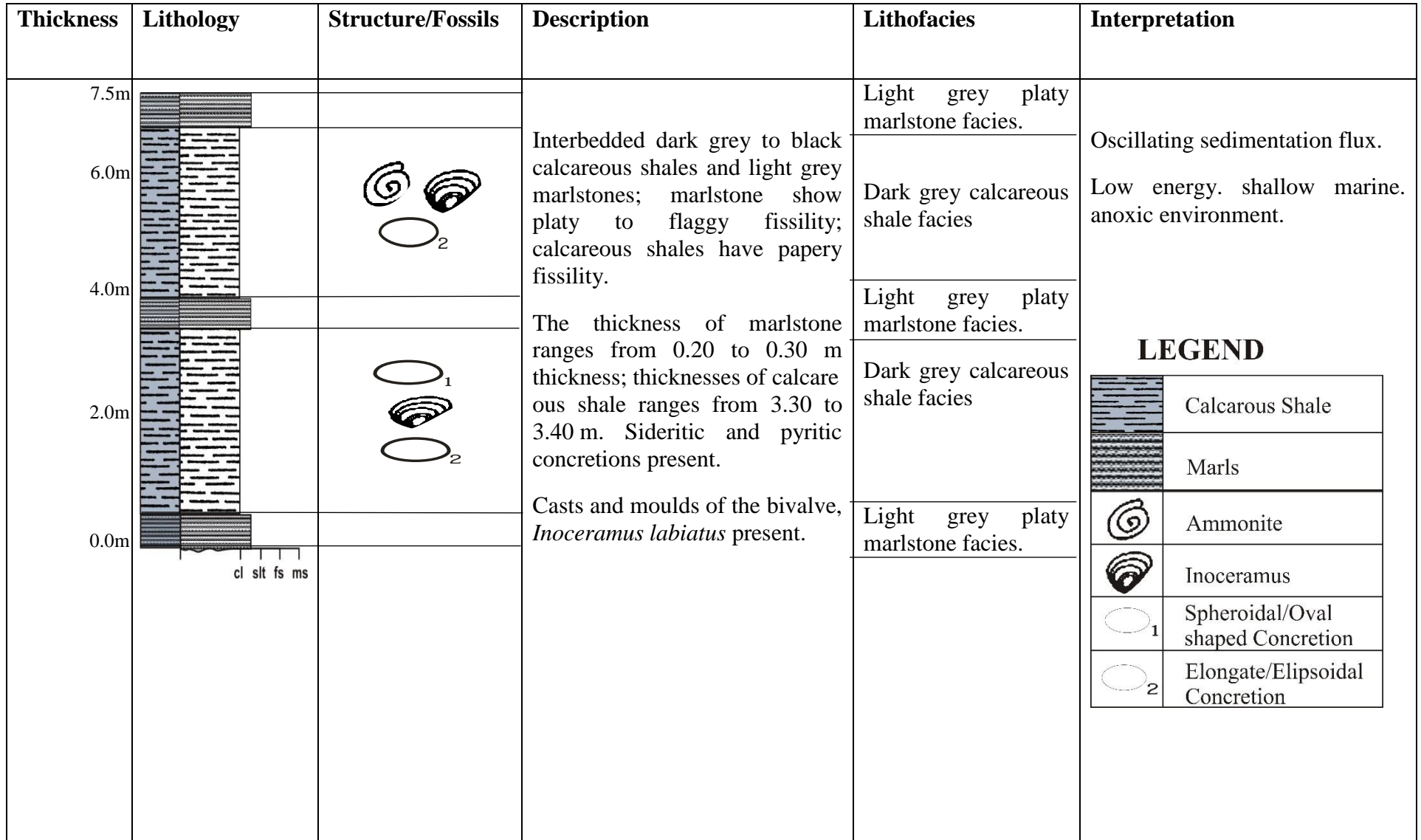


Figure 4.8: Lithologic log of OT 1 Section along Nmavu River channel

## Outcrop (OT 2)

This segment is located 125.00 m upstream from Outcrop OT 1 outcrop along the Nmavu River channel. It is indurated dark grey calcareous shale interbedded with light grey marlstones. The successive beds have sharp contacts. Clay, calcite and quartz are the mineral contents. The rocks are thinly laminated and fissile with the marlstone displaying thicker laminae while the shales show papery fissility (Figure 4.9). Casts and moulds of the bivalve, *Inoceramus labiatus*, and spheroidal and ellipsoidal sideritic concretions are common features within the rock. The logged thickness of the exposure is 1.60 m (Figure 4.10).



Figure 4.9: Marl and Shale unit showing good fissility

Thickness	Lithology	Structure/Fossils	Description	Lithofacies	Interpretation												
1.5m			Dark grey to black calcareous shales, clayey with papery fissility.	Dark grey calcareous shale facies	<p>Low energy. shallow marine. anoxic environment.</p> <p><b>LEGEND</b></p> <table border="1"> <tr> <td></td> <td>Calcareous Shale</td> </tr> <tr> <td></td> <td>Marls</td> </tr> <tr> <td></td> <td>Ammonite</td> </tr> <tr> <td></td> <td>Inoceramus</td> </tr> <tr> <td></td> <td>Spheroidal/Oval shaped Concretion</td> </tr> <tr> <td></td> <td>Elongate/Ellipsoidal Concretion</td> </tr> </table>		Calcareous Shale		Marls		Ammonite		Inoceramus		Spheroidal/Oval shaped Concretion		Elongate/Ellipsoidal Concretion
			Calcareous Shale														
			Marls														
	Ammonite																
	Inoceramus																
	Spheroidal/Oval shaped Concretion																
	Elongate/Ellipsoidal Concretion																
1.0m	Marlstones, silty with flaggy fissility.	Light grey platy marlstone facies															
0.5m																	
0.0m	<p>cl slit fs ms</p>		<p>The thicknesses of marlstone and shale is 0.40m and 1.60m respectively.</p> <p>Casts and moulds of the bivalve, <i>Inoceramus labiatus</i> present.</p>														

Figure 4.10: Lithologic log of OT 2 Section along Nnavu River Channel



### Outcrop (OT 3)

This is located 90.00 meters upstream from Outcrop OT 2 along the Nmavu River channel. The thickness of logged unit is 6.00m. Dark grey calcareous shale and light grey marlstones alternate with each other in rhythms of 2.80 to 3.00 m and 0.20 m respectively. The mineral composition is consistent with what have been observed previously in the other outcrops. Similar sedimentary features such as thin laminae within each bed, casts and moulds of the bivalve *Inoceramus labiatus*, spheroidal and ellipsoidal sideritic concretions occur within the rock (Figure 4.11). The lithology of the outcrop is shown in Figure 4.12.



Figure 4.11: Dark grey shales with ellipsoidal sideritic concretions

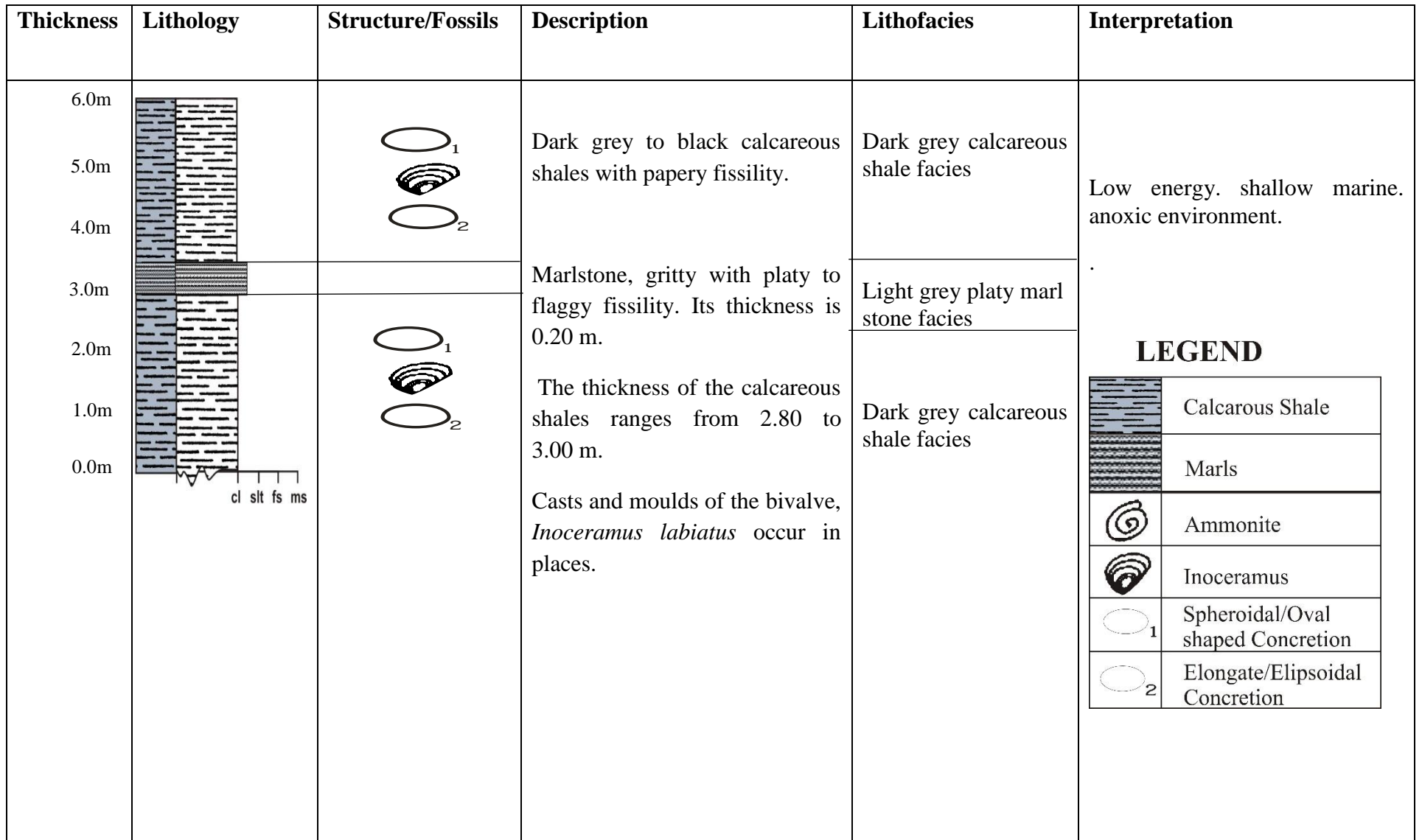


Figure 4.12: Lithologic log of OT 3 Section along Nmavu River

### **Outcrop (OT 4)**

This segment is exposed about 100 m away from Outcrop OT 3. The thickness of the exposure logged is about 4.0 m. It consists of alternating beds of dark grey calcareous shales and light grey marlstones with thicknesses ranging from 0.60 to 1.50m and 0.10 to 0.30m respectively. The composition consists of clay, quartz and calcite. The beds have sharp planar contacts. Figure 4.13 shows the dark grey shale with concretions while Figure 4.14 shows a lithologic log of the exposed section.



Figure 4.13: Dark grey shale unit with sideritic/pyritic concretions overlain by marl bed

Thickness	Lithology	Structure/Fossils	Description	Lithofacies	Interpretation
4.0m			Papery dark grey to black calcareous shales.	Dark grey calcareous shale facies	Oscillating sedimentation flux. Low energy. shallow marine. anoxic environment.
3.5m			platy light grey marlstones.	Light grey platy marlstone facies	
3.0m			The thicknesses of calcareous shale ranged from 0.60 to 1.50m.	Dark grey calcareous shale facies	
2.5m			There are sideritic and pyritic concretions		
2.0m			The thicknesses of marlstone ranged from 0.10 to 0.30m.	Light grey platy marlstone facies	
1.5m			Biogenic structures in the rock are the casts and moulds of the bivalve, <i>Inoceramus labiatus</i> .	Light grey platy marlstone facies	
1.0m					
0.5m					
0.0m					

**LEGEND**

	Calcarous Shale
	Marls
	Ammonite
	Inoceramus
	Spheroidal/Oval shaped Concretion
	Elongate/Elipsoidal Concretion

Figure 4.14: Lithologic log of OT 4 Section along Nmavu River Channel



### **Outcrop (OT 5)**

About 100m upstream from Outcrop OT 4 along the river channel a spectacular view of the rocks with full compliment of sedimentary features and structures occurs (Figure 4.15) . Its reference coordinate is Latitude  $6^{\circ} 01' 6.2''$  N and Longitude.  $7^{\circ} 30' 30.9''$  E. It is a step-like rhythmic succession of dark grey to black calcareous shale and light grey marlstones. Their mineralogical composition and texture of both rock types are consistent with those previously logged. The marlstones exhibit platy fissility while the calcareous shales display papery fissility. Casts and moulds of the bivalve *Inoceramus labiatus* and depauperate ammonite casts occur (Figures 4.16 a,b and 4.17a,b). Spheroidal and ellipsoidal sideritic concretions with diameters ranging from 3.00-8.00 cm represent chemical structures (Figure 4.18a and b). The total thickness of the logged section is about 48.90 m (Figure 4.19).



Figure 4.15: Panoramic view of outcrop OT 5

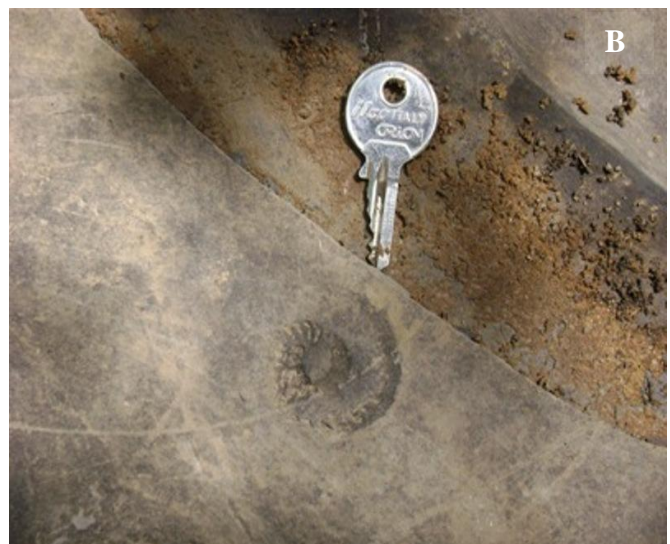


Figure 4.16 a & b: Depauperate Ammonite impression/cast and mould on the calcareous shale and marl





Figure 4.17 a & b: *Inoceramus labiatus* impressions/casts



Figures 4.18 a & b: Sideritic concretions in the calcareous shales in OT 5

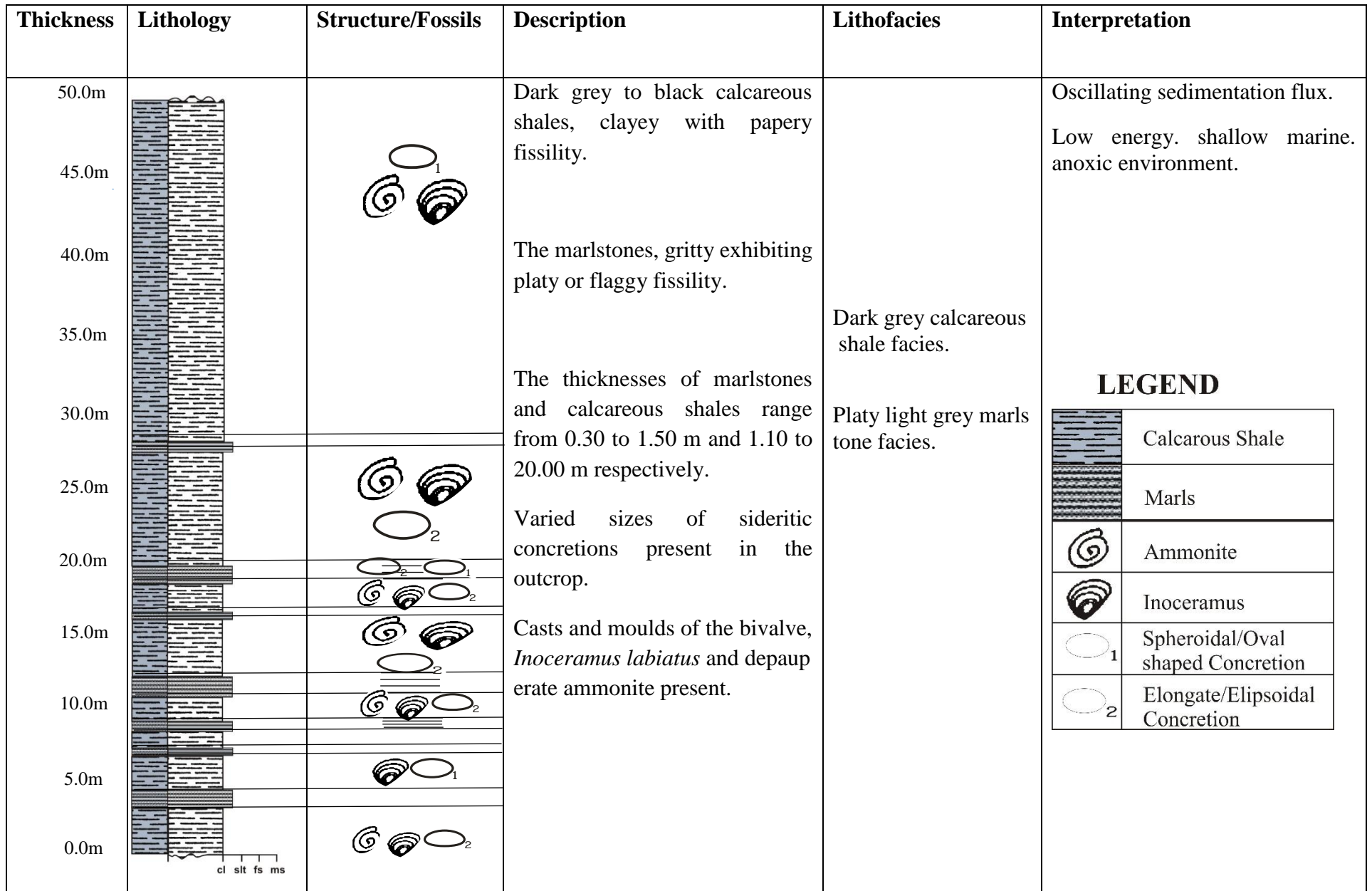


Figure 4.19: Lithologic log of OT5 Section along Nnavu River



### Outcrop 6 (OT 6)

This exposure about 200 metres upstream from Outcrop OT 5. It is a 1.5 m thick dark grey calcareous shale (Figure 4.20). The texture of the shale is consistent with previously dark grey shales. It is fissile with absence of bioturbation and macrofossils except casts and moulds of the bivalve, *Inoceramus labiatus* and depauperate ammonite. Figure 4.21 shows the logged section of the exposure.



Figure 4.20: Exposed section of outcrop OT 6 along Nmavu River Channel, Onoli-Awgu

Thickness	Lithology	Structure/Fossils	Description	Lithofacies	Interpretation								
1.5m 1.0m 0.5m 0.0m			<p>Dark grey calcareous shale with papery fissility. Sideritic/pyritic concretions.</p> <p><i>Inoceramus labiatus</i> and depauperate ammonite cast present.</p>	<p>Dark grey Calcareous shale facies</p>	<p>Low energy. shallow marine. anoxic environment.</p> <p><b>LEGEND</b></p> <table border="1"> <tr> <td></td> <td>Calcarous Shale</td> </tr> <tr> <td></td> <td>Ammonite</td> </tr> <tr> <td></td> <td>Inoceramus</td> </tr> <tr> <td></td> <td>Spheroidal/Oval shaped Concretion</td> </tr> </table>		Calcarous Shale		Ammonite		Inoceramus		Spheroidal/Oval shaped Concretion
	Calcarous Shale												
	Ammonite												
	Inoceramus												
	Spheroidal/Oval shaped Concretion												

Figure 4.21: Lithologic log of OT 6 Section along Nmavu River Channel



### **Outcrop (OT 7)**

This is located about 150 m upstream from Outcrop OT 6. It is an interbedding of dark grey calcareous shales and light grey marlstones (Figure 4.22). The marlstone beds show platy fissility while the calcareous shales show papery fissility. Casts and moulds of *Inoceramus labiatus* and diminutive ammonites occur in the rock. The total thickness of the exposed section logged is 6.00 m (Figure 4.23).



Figure 4.22: Exposed section of outcrop OT 7 along Nmavu River Channel,

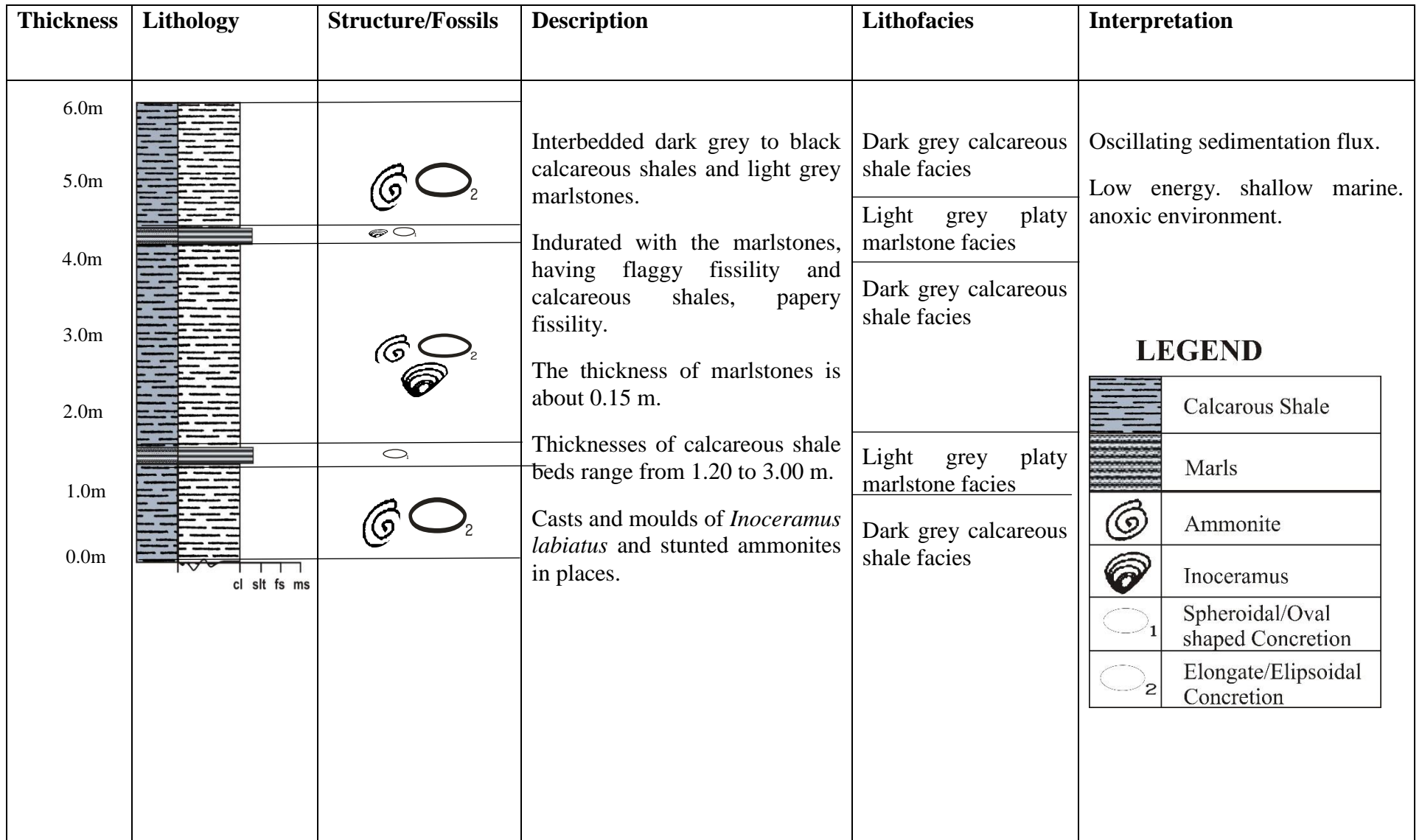


Figure 4.23: Lithologic log of OT 7 Section along Nnavu River channel



### **Outcrop (OT 8)**

The section is located beneath the culvert at 3km from Express Road on the Ishiagu road. It consists of interbedding of dark grey to black shales and light grey marlstones (Figure 4.24). The physical sedimentary structure the thin laminae which are silty, clayey and carbonaceous layers There is absence of bioturbation and macrofossils except of the *Inoceramus labiatus* and stunted ammonites occur. Spheroidal and ellipsoidal sideritic concretions or nodules are common. The diameters of these concretions vary from 3.00-8.00 cm in length. The total thickness of the exposure logged is 31.50m. Figure 4.25 is the lithologic log of the exposed section. A composite lithologic log of the entire Nmavu River section is shown in Figure 4.26.

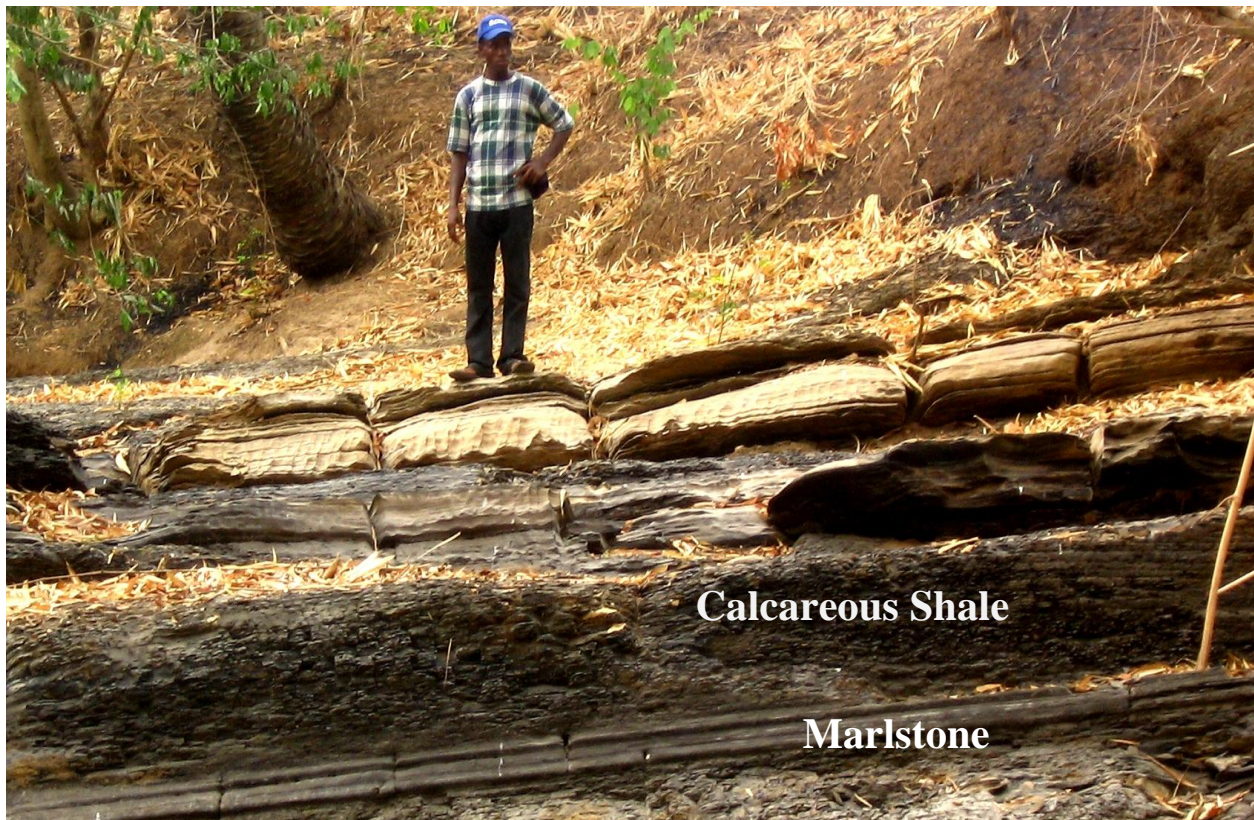


Figure 4.24: Marlstone and Calcareous shale units of OT 8

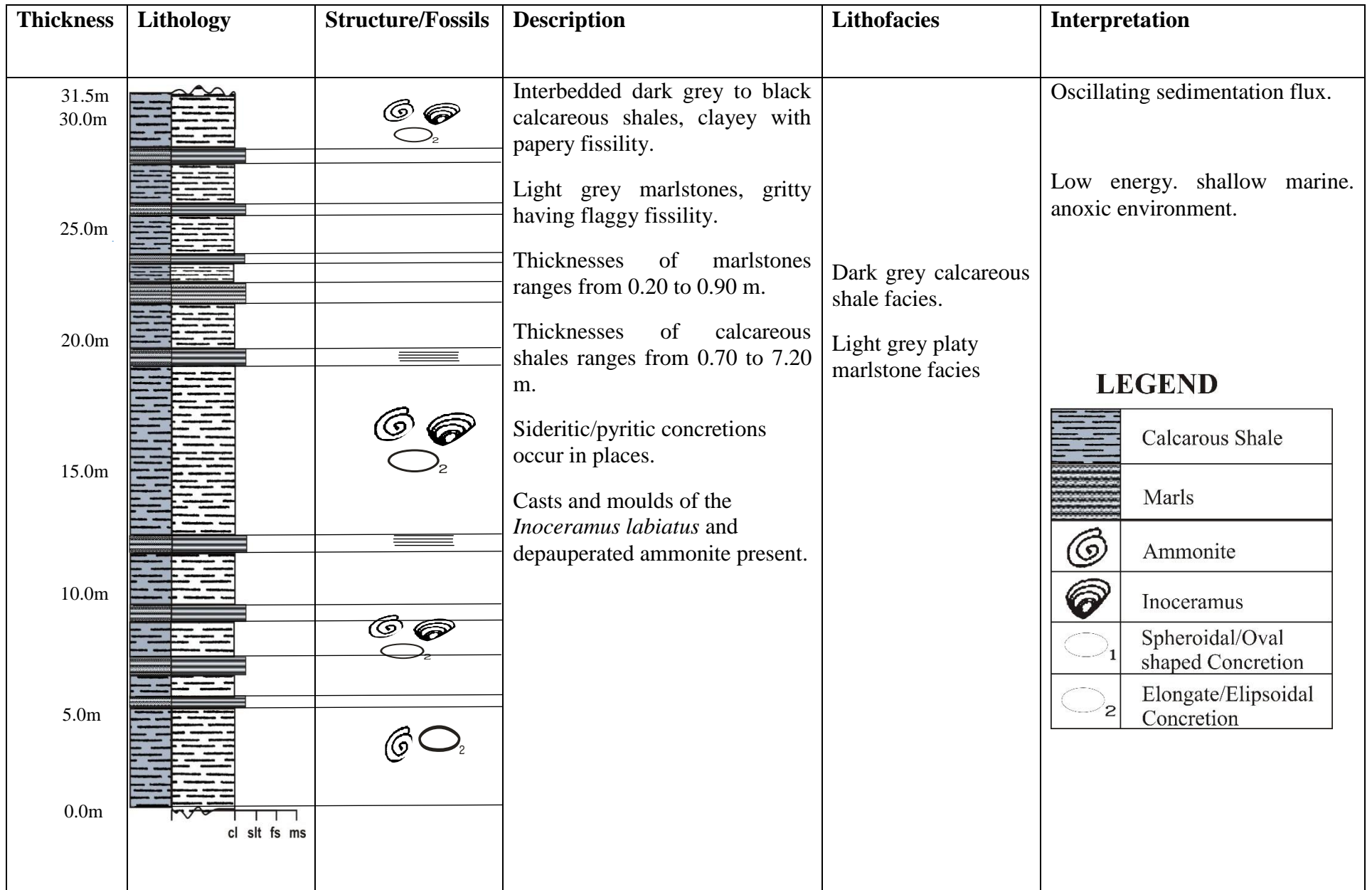


Figure 4.25: Lithologic log of OT 8 Section along Nnavu River Channel

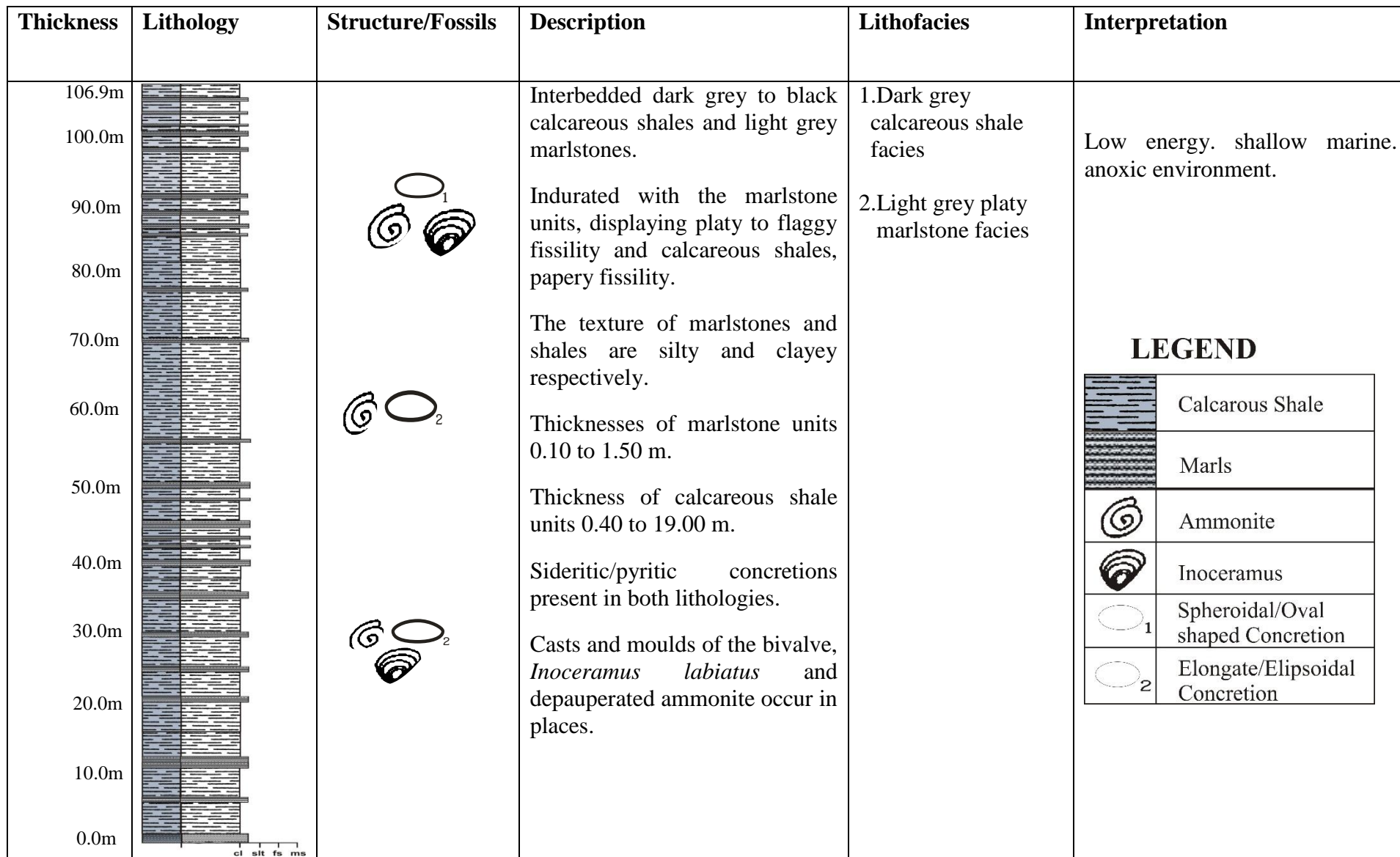


Figure 4.26: Composite Lithologic Log of River Nmavu Outcrop Section



### 4.3.3 Ezzaegu Section

The exposure occurs beneath the Ebonyi River bridge between Ezzaegu and Agba communities in Ebonyi at coordinate of Latitude  $6^{\circ}15'20''$  N and Longitude  $7^{\circ}49'25''$  E. The exposure on both banks of the river occur for about 300m (Figure 4.27 a). The exposure is about 10.00m thick and consist of calcareous shales alternating with marlstones. The marlstones are fissile showing platy fissility. The calcareous shales show papery fissility varying from 0.50-1.00 mm in thickness. The marlstones are light grey in colour. The shales are dark grey in colour. Ellipsoidal sideritic concretions are common in the rocks. The concretions reveal calcite efflorescent crystals within their internal structure (Figure 4.27 b). The calcareous shales vary in thickness from 0.90 to 1.00 m while marlstones are approximately 0.40 m. Macrofossils and bioturbations are absent. Casts of *Inoceramus Labiatus* and diminutive ammonites are present. Figure 4.28 is the lithologic log of the exposed section. Figure 4.29 is the composite lithologic log of the exposed sections of the Lokpanta Shale in the study area.



Figure 4.27 a: A marlstone bed between two calcareous Shale units as exposed at Ezzaegu



Figure 4.27b: Calcite efflorescent crystals on a concretion at the exposure at 76 Ezzaegu



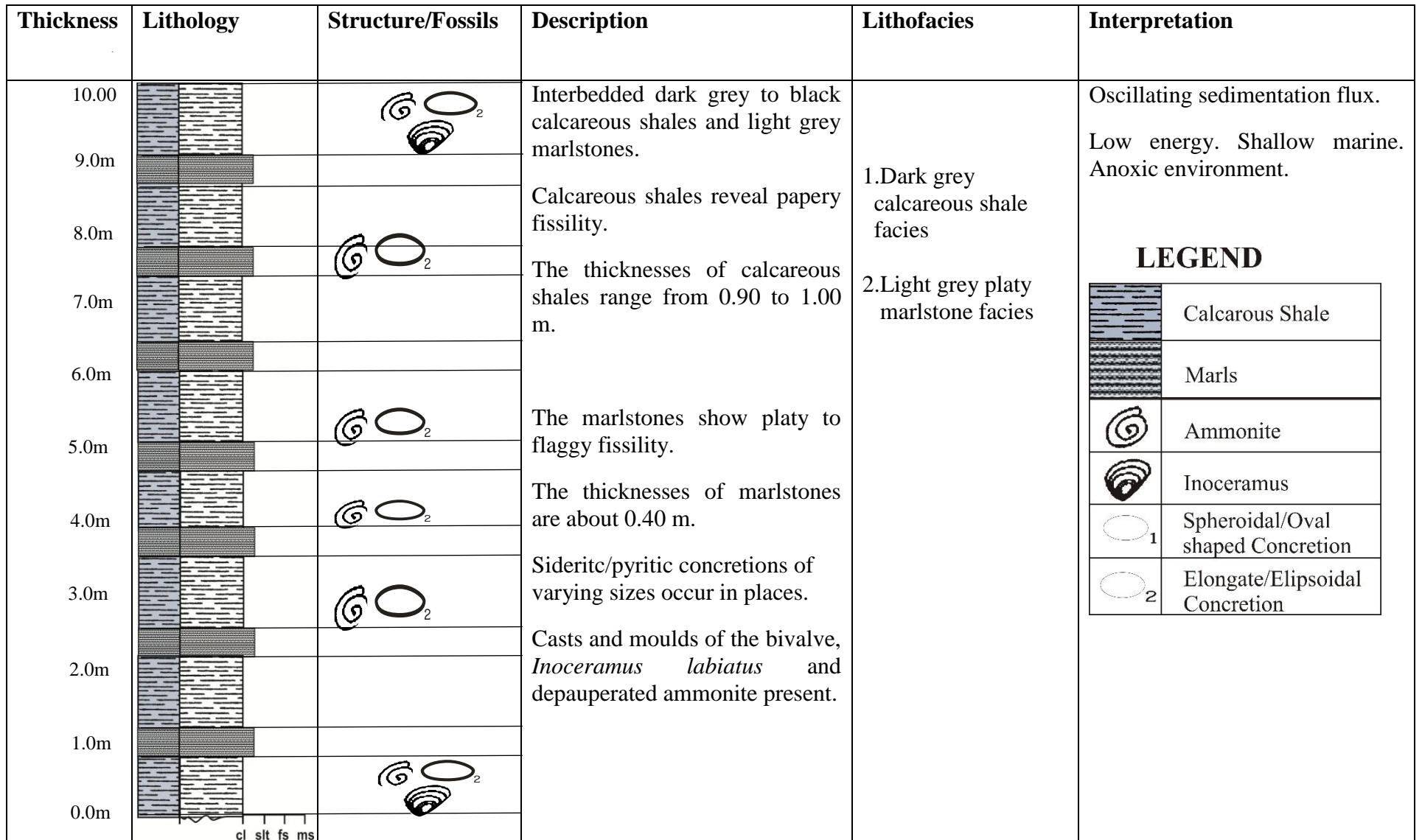


Figure 4.28: Lithologic log of Ezzaegu Section

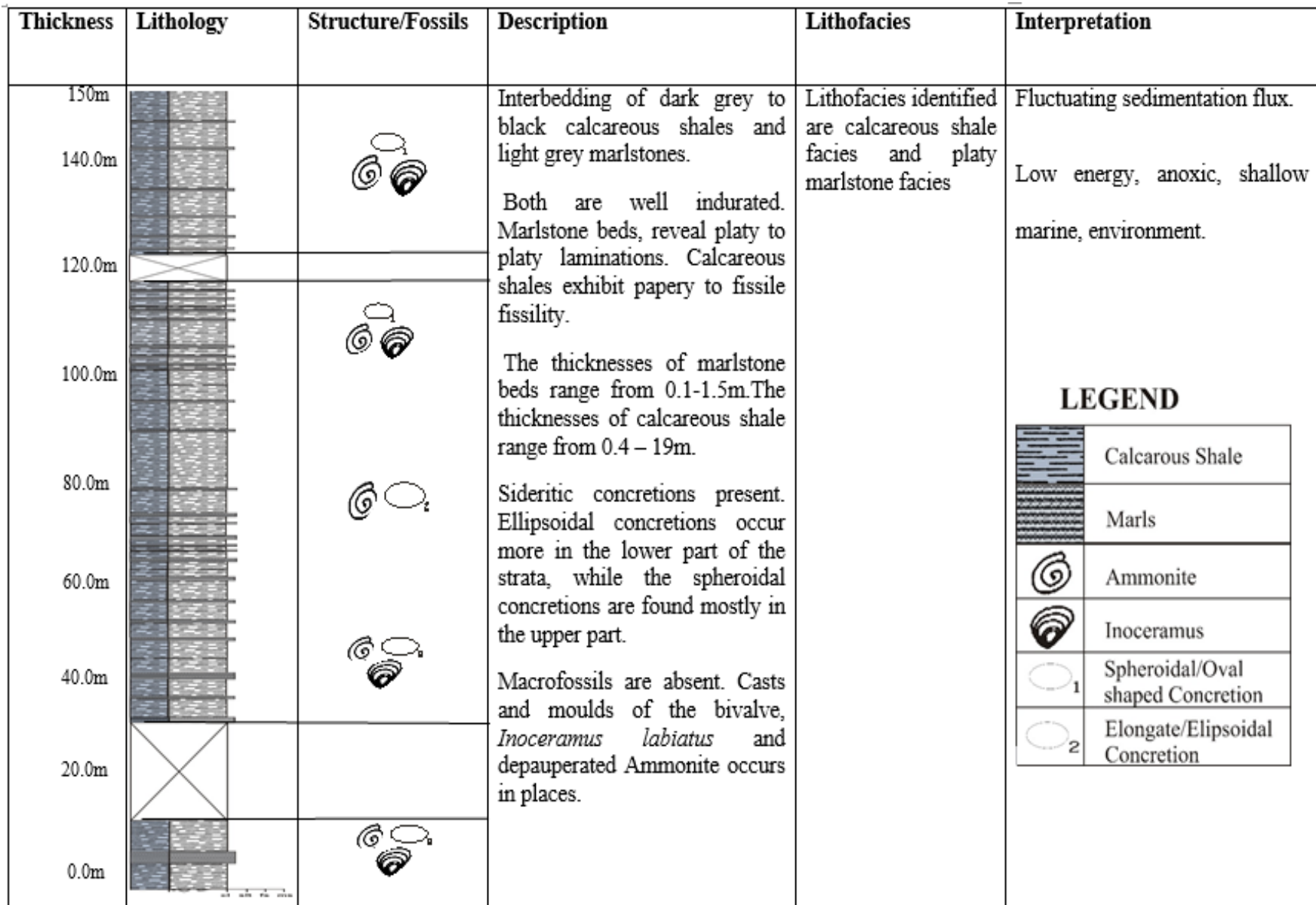


Figure 4.29: Composite lithologic log of the Lokpanta Shale of the study area

#### **4.3.4 Lithofacies of the Lokpanta Shale**

From the field studies of the exposures of the Lokpanta Shale, two lithofacies were identified. They are the dark grey calcareous shale facies and light grey platy marlstone facies.

The lithofacies were recognized using the critical descriptive lithologic and sedimentologic characteristics of the rocks. These include different textural attributes, stratal thicknesses, and sedimentary structures including vertical lithologic variation and patterns. Lithofacies analysis is based on detailed outcrop descriptions, which provide the basis to decipher relationship(s) and propose depositional model for the deposits (Miall, 2000). Each lithofacies represents an individual depositional event (Collinson, 1969; Reading and Levell, 1996).

The characteristics and sedimentary structures, which occur in the dark grey calcareous shale facies, are;

- 1) Papery fissility (0.5 mm)
- 2) Sideritic/pyritic concretions
- 3) Depauperate ammonites casts and moulds
- 4) Inoceramid casts and moulds

Based on the field observations; the dark grey calcareous facies is interpreted as transgressive deposit and represent deposition by low energy, shallow (inner neritic) marine and anoxic environment.

This deduction is supported from similar works of various authors who asserted that dark colour of the stratum, thin laminations, high biogenic activity of Inoceramids, presence of

stunted ammonites as well as the sideritic/pyritic concretions indicate low energy, anoxic shallow marine environment (Cooks and Corboy, 2003; Essien and Bassey, 2012; Njoh and Taku, 2016)

The light grey marlstone facies shows the following characteristic physical, chemical and biogenic structures;

- 1) Platy to flaggy fissility (5 to 10 mm)
- 2) Sideritic/pyritic concretions
- 3) Depauperate ammonites casts and moulds
- 4) Inoceramid casts and moulds

The light grey platy marlstones facies is interpreted as transgressive deposits. It represents deposition in a low energy, shallow (middle neritic) marine and anoxic environment.

The deduction of the depositional environment is consistent with several workers who alluded that the dark grey shales were deposited in a deeper setting and when the sea level shallows, the marlstones (more carbonate bearing rocks) are deposited (Tucker and Wright, 1990; Cooks and Corboy, 2003; Nichols, 2009; Essien and Bassey, 2012; Njoh and Taku, 2016). The lithological differences in the Lokpanta Shale suggest slight sea level fluctuations that caused variation in terrigenous clastic inputs (Nichols, 2009). This is true for coasts that were characterized by successive rise and fall in sea level (Njoh and Taku, 2016).

These two lithofacies can be grouped into one lithofacies Association and lithofacies succession, **Anoxic Shallow Marine Association**. A lithofacies succession is a lithofacies

association in which lithofacies occur in a particular order or pattern (Reading and Levell, 1996). The Lokpanta Shale shows repetition of a series of processes as response to regular changes in the conditions of environment of deposition. The localities of the occurrence of these two lithofacies are Lokpaukwu, Lekwesi, Ndeaboh, Isiogbo, Agba and Ezzaegu areas.

#### 4.4 X-Ray Diffraction Results

The results (Figures 4.30a– 4.34b) based on the individual intensity peaks of all the carbonates, clay and detrital mineral identified the dominant mineral as quartz (50.50 – 77.00%). The main carbonate mineral is calcite, with composition ranging from 16.00– 36.00%, averaging 25.40%. Kaolinite is the main clay mineral with composition ranging from 7.00–19.20%, averging 13.64%. Table 4.1 show the results of the analysis.

Table 4.1: Mineral Assemblage and Composition (%) obtained from X-Ray Diffraction Analysis

<b>SAMPLE NO.</b>	<b>ROCK TYPE</b>	<b>CALCITE (%)</b>	<b>KAOLINITE (%)</b>	<b>QUARTZ (%)</b>
EZZ 1	CALC SHALE	36.00	12.00	52.00
EZZ 2	CALC SHALE	30.30	19.20	50.50
EZZ 3	CALC SHALE	24.00	17.00	59.00
EXLK 3	CALC SHALE	21.00	14.00	65.00
EXLK 5	CALC SHALE	16.00	7.00	77.00
<b>AVERAGE %</b>		<b>25.40</b>	<b>13.64</b>	<b>60.70</b>

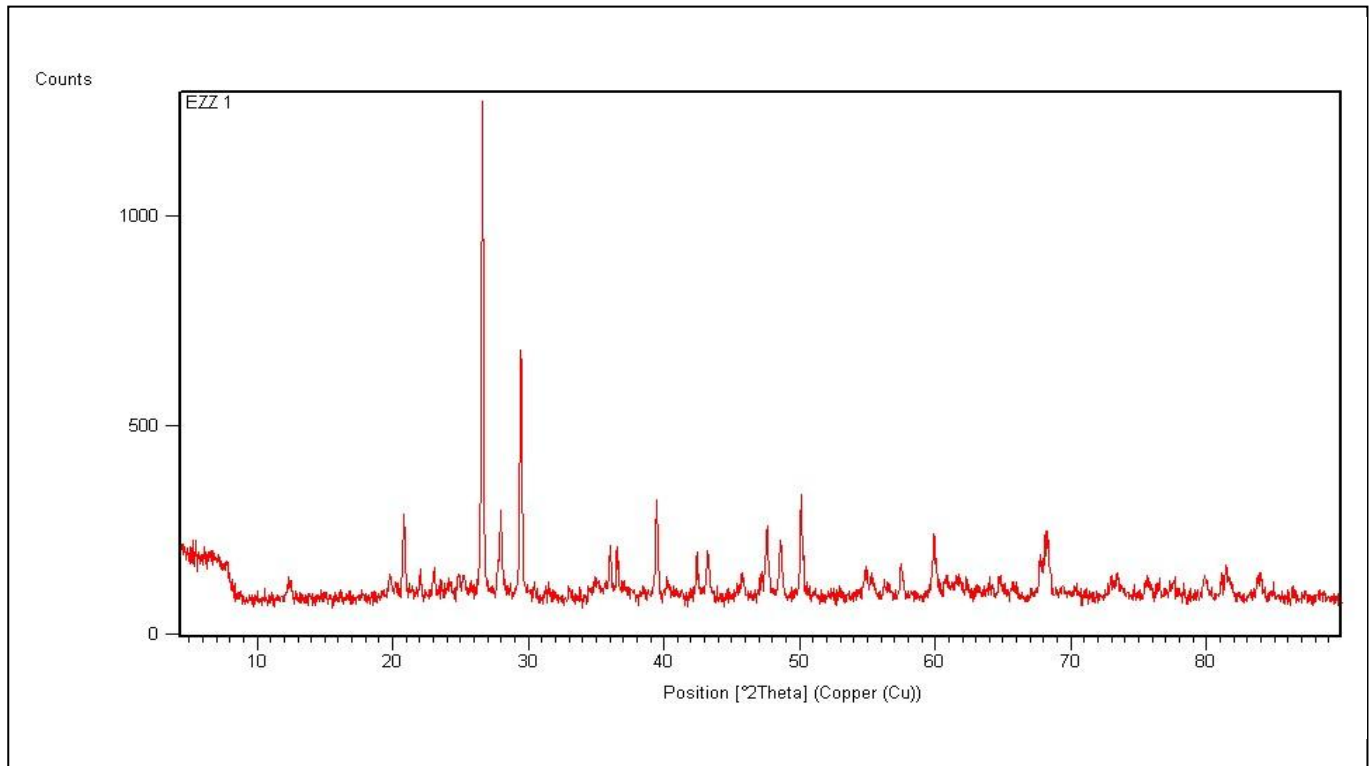


Figure 4.30a: X-ray Diffractogram of EZZ 1 rock sample

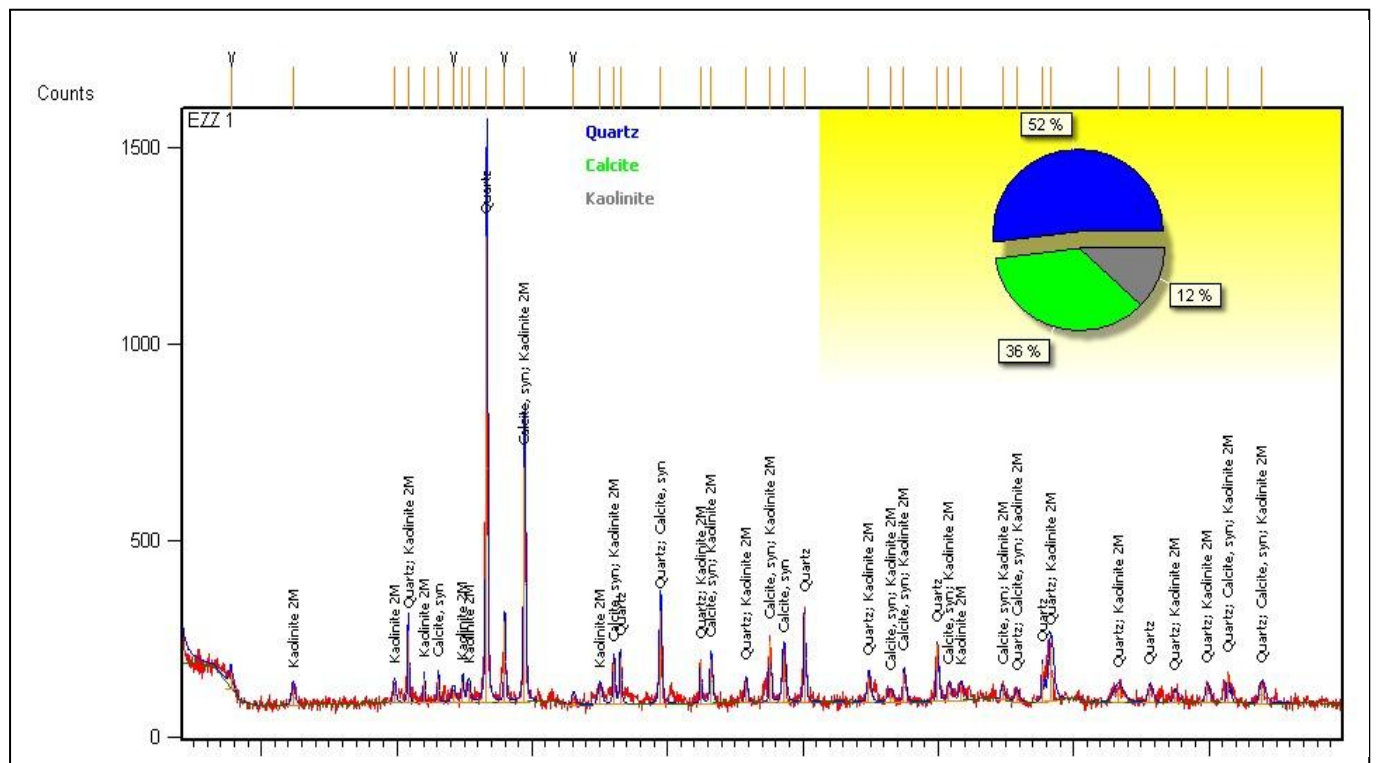


Figure 4.30 b: Minerals composition from the X-ray diffraction analysis of EZZ 1 83

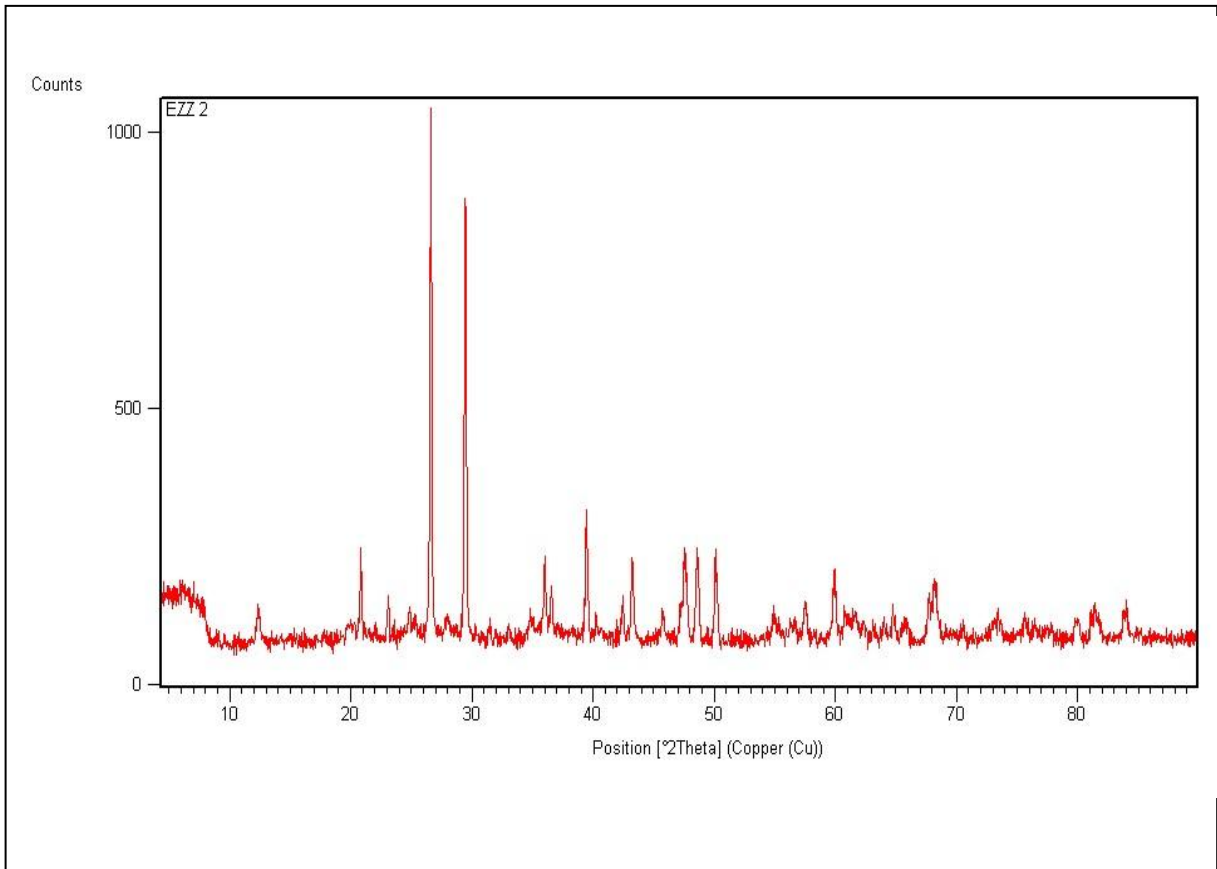


Figure 4.31 a: X-ray Diffractogram of EZZ 2 rock sample

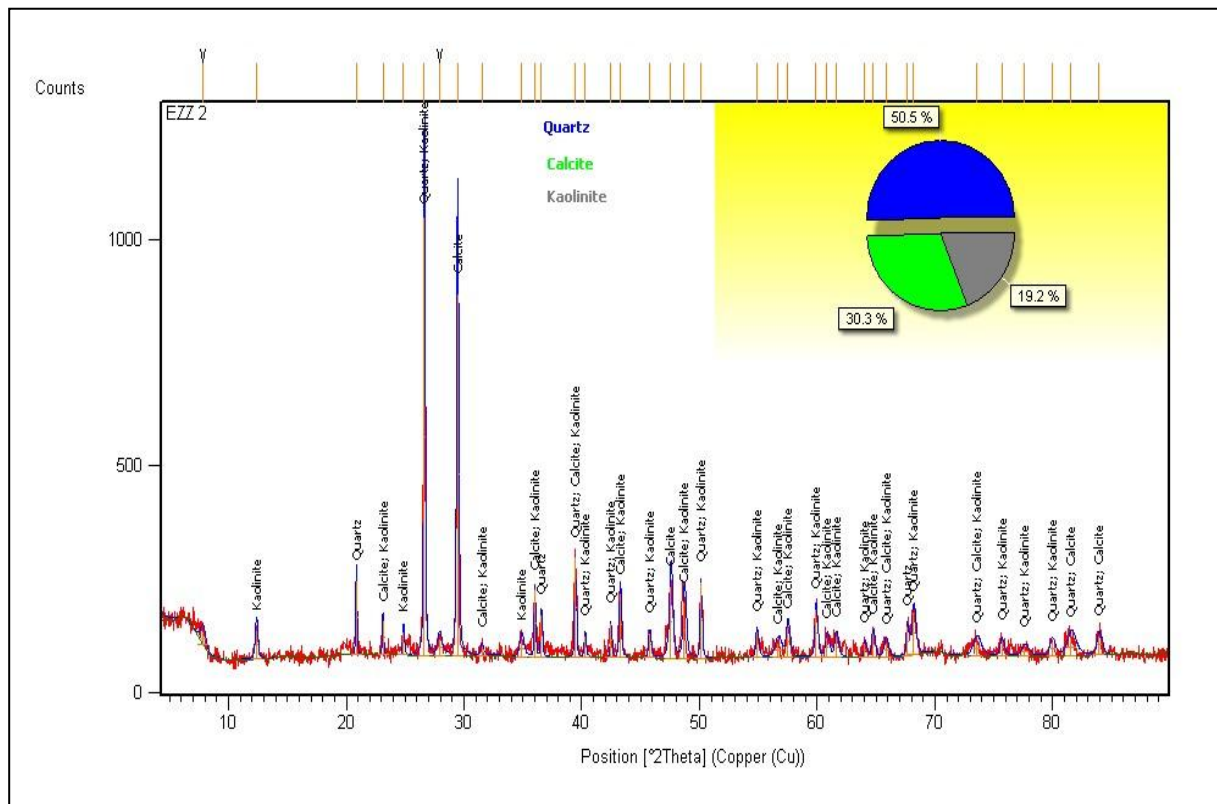


Figure 4.31 b: Minerals composition from the X-ray diffraction analysis of EZZ 2 rock sample



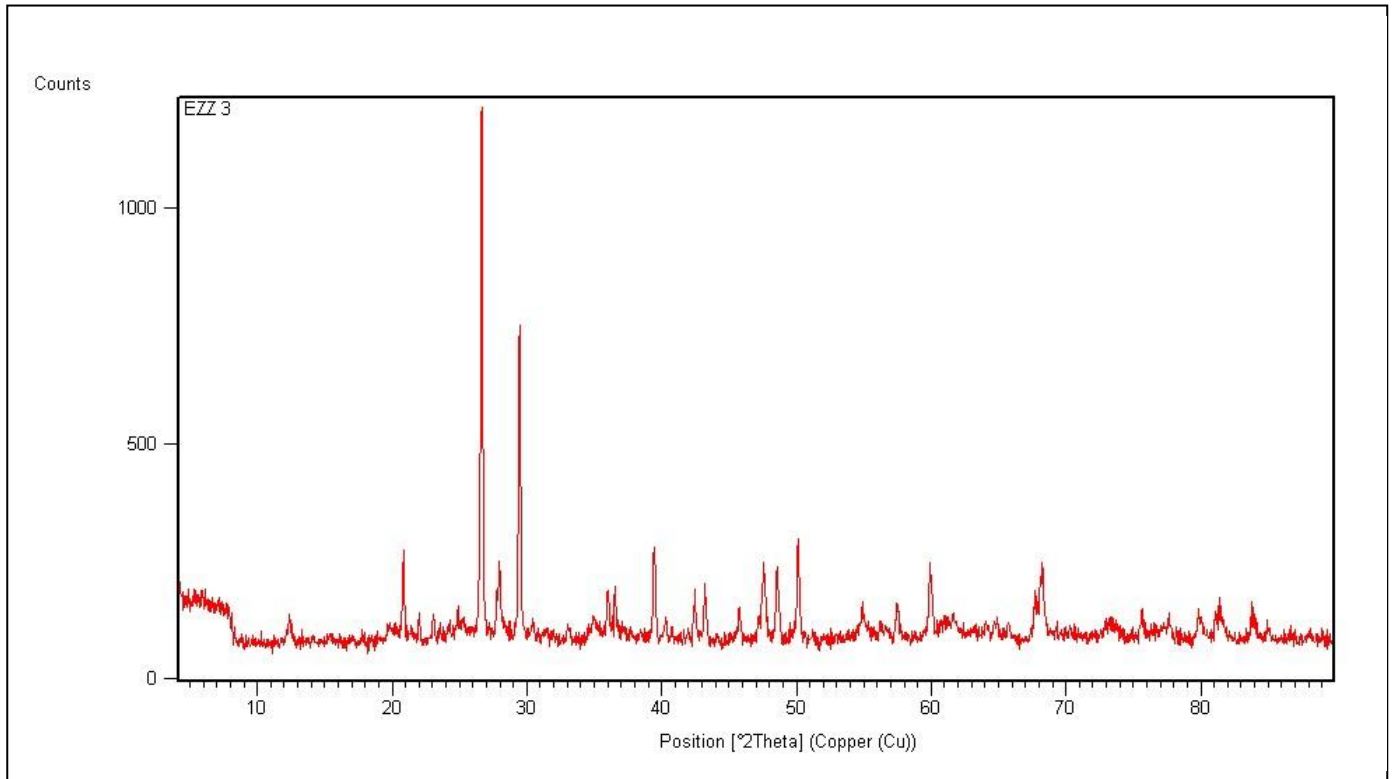


Figure 4.32 a: X-ray Diffractogram of EZZ 3 rock sample

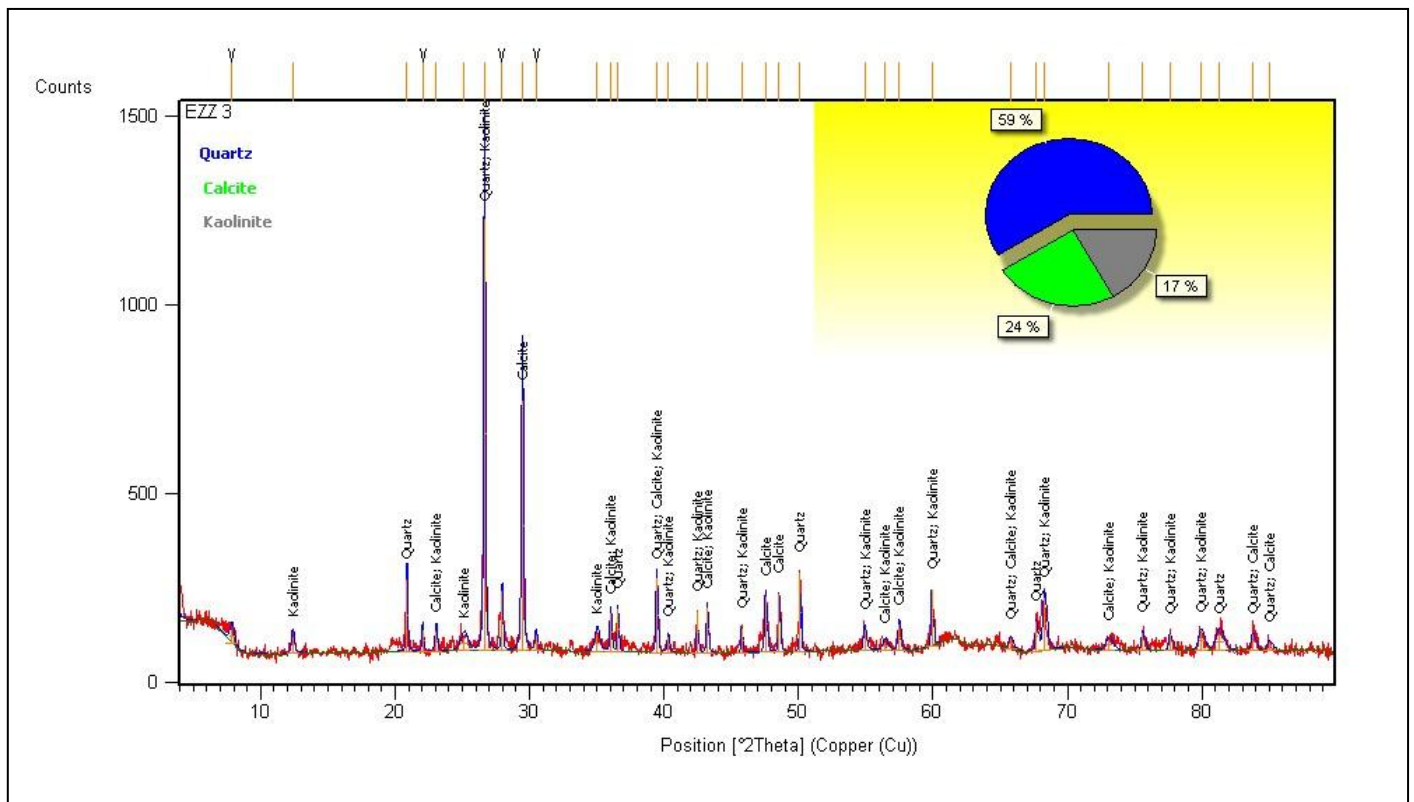


Figure 4.32 b: Minerals composition from the X-ray diffraction analysis of EZZ 3 rock

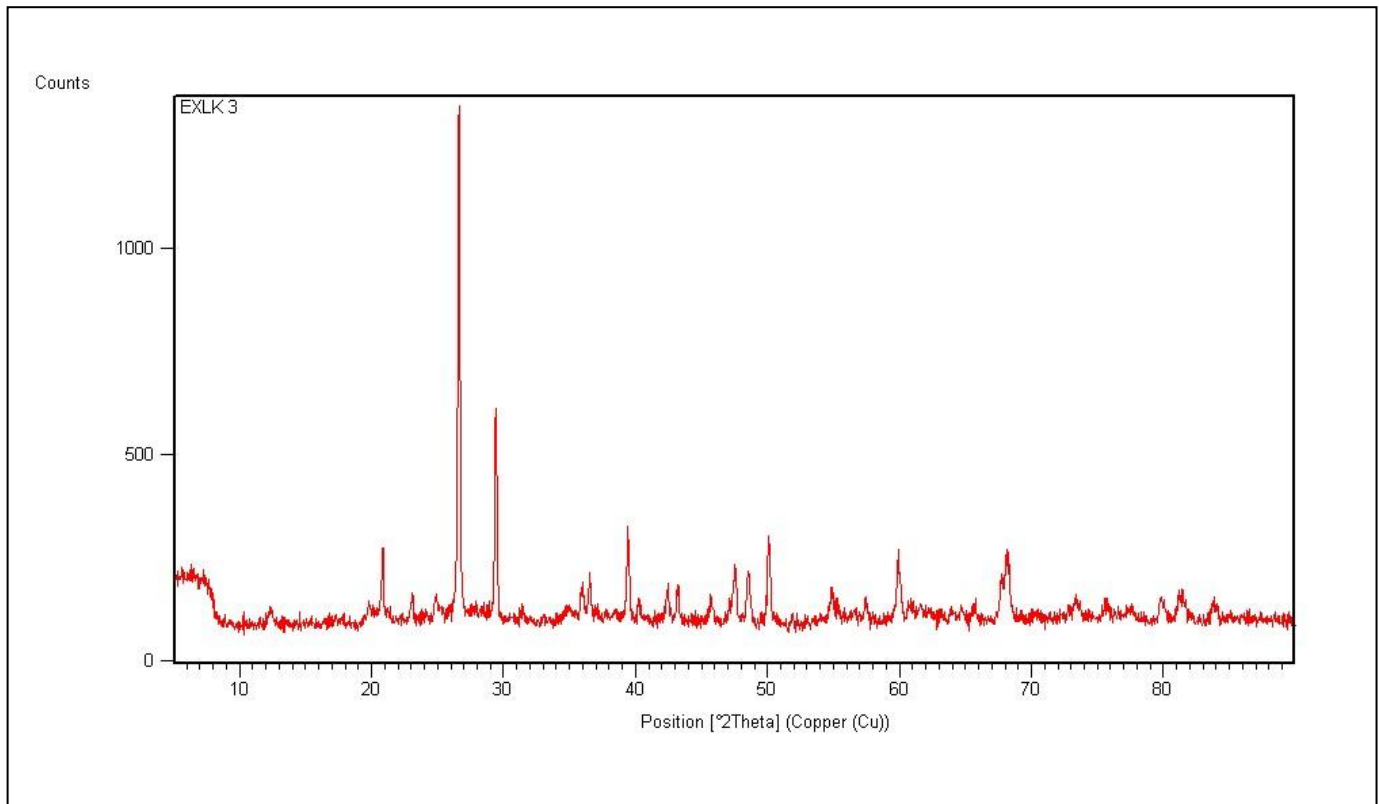


Figure 4.33 a: X-ray Diffractogram of EXLK 3 rock sample

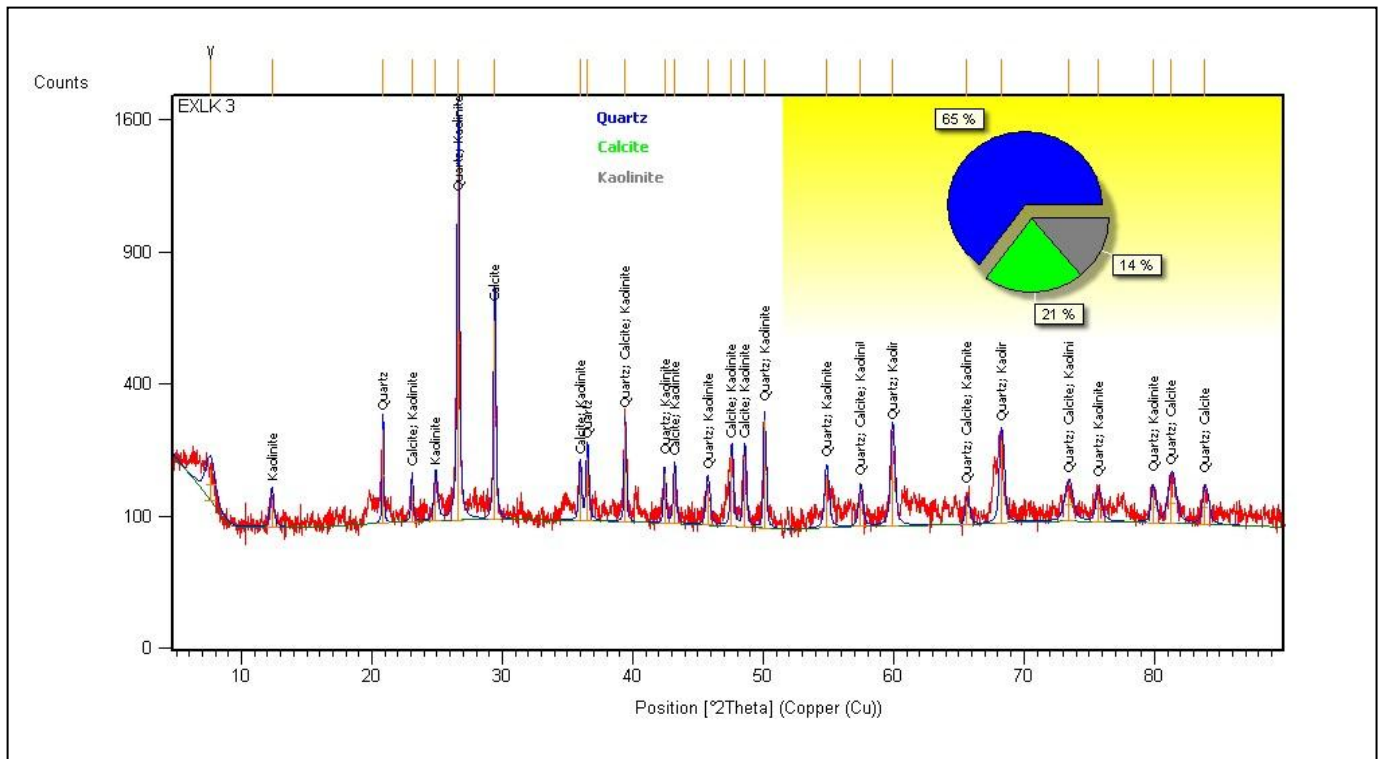


Figure 4.33 b: Minerals composition from X-ray diffraction analysis of EXLK 3 rock

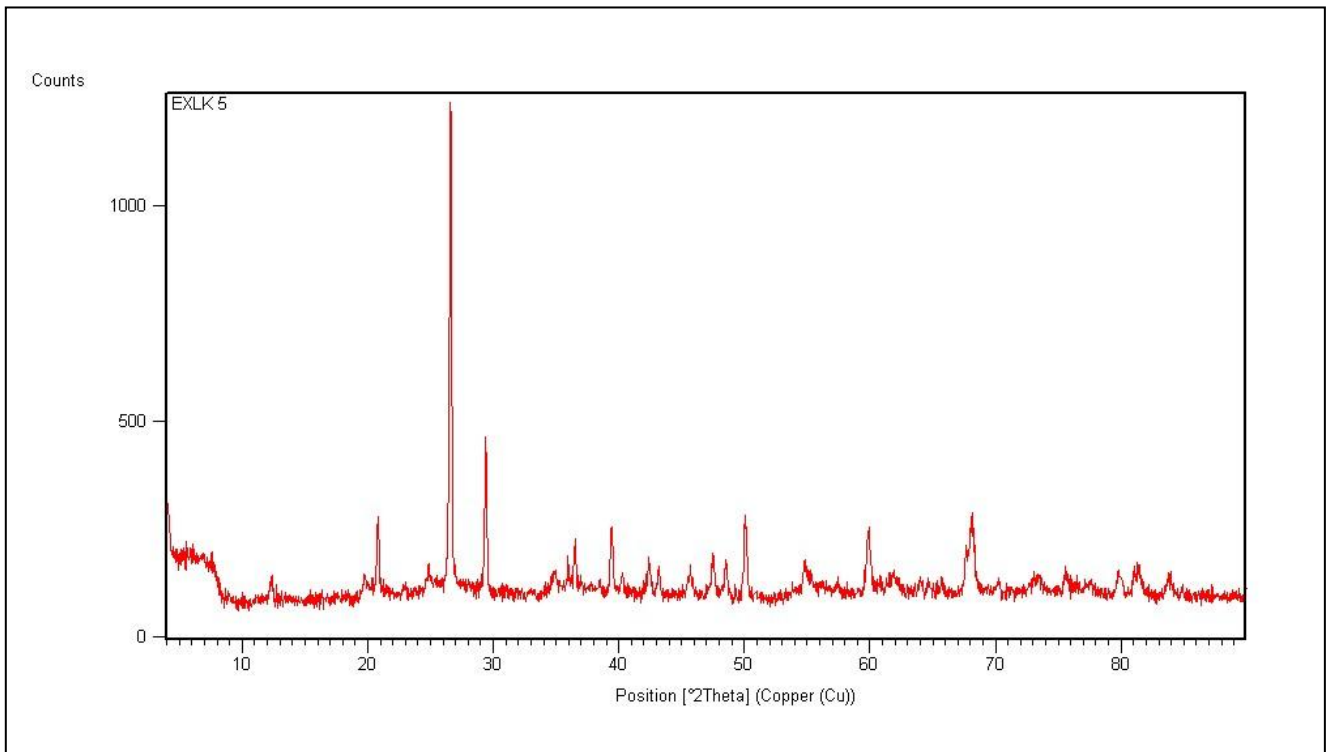


Figure 4.34 a: X-ray Diffractogram of EXLK 5 rock sample

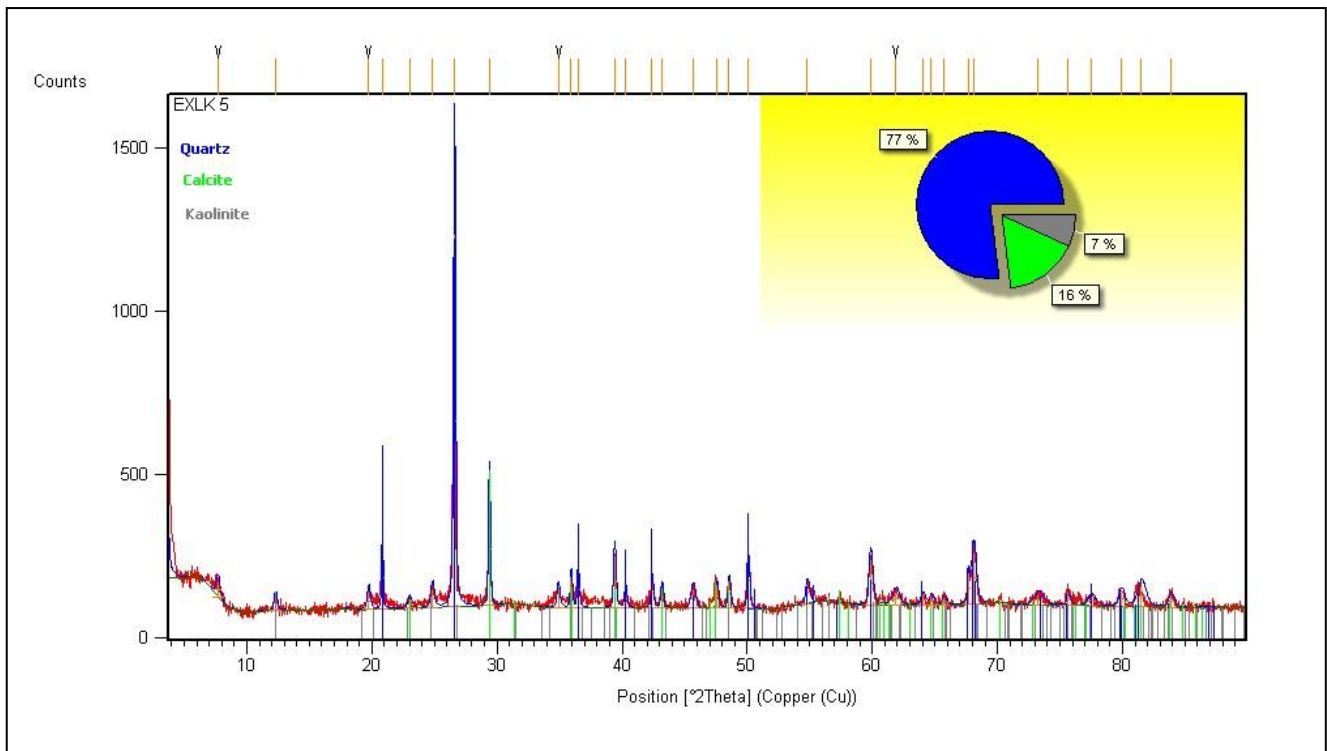


Figure 4.34 b: Minerals composition from X-ray diffraction analysis of EXLK 5 rock sample

## 4.5 X-Ray Fluorescence Results

Tables 4.2 and 4.3 show the results obtained from X-ray fluorescence analysis, with major elemental oxides (in percentage) and trace elements (in ppm). The oxides analysed for include  $\text{SiO}_2$ ,  $\text{Al}_2\text{O}_3$ ,  $\text{MgO}$ ,  $\text{CaO}$ ,  $\text{Fe}_2\text{O}_3$  (total Fe),  $\text{Na}_2\text{O}$ ,  $\text{K}_2\text{O}$ ,  $\text{SO}_3$ ,  $\text{MnO}$  and  $\text{TiO}_2$  (Table 4.2). The trace elements analyzed for include Sc, V, Cr, Co, Ni, Cu, Zn, Sr, Y, Zr, Ba and Pb (Table 4.3).

The  $\text{SiO}_2$  values for the marlstones range from 19.00-39.68%, averaging 29.11% and for the calcareous shales, 25.69-58.80%, averaging 47.16 %. The  $\text{Al}_2\text{O}_3$  values of marlstones range from 3.75-6.13 %, averaging 3.04% and for calcareous shales, 5.77-15.30 %, averaging 12.05 %. The  $\text{CaO}$  values of the marlstones range from 36.08 to 52.57 % averaging 43.28 %, and for the calcareous shales 5.17 to 21.16 %, averaging 15.75 %. The  $\text{Fe}_2\text{O}_3$  values of the marlstones and calcareous shales range from 1.75 to 7.59 % and 3.73 to 7.33 %, averaging 5.05 % and 4.88 % respectively. The  $\text{MgO}$  values of the marlstones range from 1.38 to 1.85 %, averaging 1.62 % and for the calcareous shales, 1.37 to 2.43 % with an average of 2.06 %. The values of  $\text{K}_2\text{O}$  of the marlstones and calcareous shales range from 0.37-5.38 % and 0.94-7.89 %, averaging 3.01 % and 2.80 % respectively. The  $\text{SO}_3$  values of the marlstones and calcareous shales range from 0.06-0.98 % and 0.40-1.88 %, averaging 0.47 % and 0.90 % respectively. The values of  $\text{MnO}$  of the marlstones and calcareous shales range from 0.11-0.13 % and 0.02-0.09 %, averaging 0.12 % and 0.04 % respectively. The values of  $\text{TiO}_2$  of the marlstones and calcareous shales range from 0.46 to 1.00 % and 1.03 to 1.43 %, averaging 0.72 % and 1.18 % respectively. Table 4.4 shows the various oxide ratios, Mineralogical Index of Alteration (MIA), where  $(\text{MIA} = 2 \times (\text{CIA}-50))$  and Chemical Index of Alteration

(CIA) where  $(CIA = [Al_2O_3 / (Al_2O_3 + CaO^* + Na_2O + K_2O)] \times 100)$  calculated from the result of the analyses. The ratio of  $Al_2O_3/MgO$  ranges from 3.21 to 6.99 and 2.03 to 3.84, averaging 5.69 and 3.20 for the calcareous shales and marlstones respectively. The ratios of  $MgO/K_2O$  range from 0.20 to 2.45, 0.31 to 3.73, averaging 1.50 and 1.54 for the calcareous shales and marlstones respectively. The ratios of  $SiO_2/Al_2O_3$  range from 2.99 to 6.37 and 3.58 to 7.64, averaging 4.14 and 5.90 for the calcareous shales and marlstones respectively. The ratios  $Al_2O_3/TiO_2$  for the calcareous shales range from 4.24 to 14.85, averaging 10.70 and for marlstones, 5.43 to 11.52 with an average of 7.69. The ratios of  $Na_2O/K_2O$  for the calcareous shales range from 0.01 to 0.10, averaging 0.05 and for marlstones, 0.02 - 0.57 with an average of 0.20. The ratios of  $K_2O/Al_2O_3$  range from 0.06 to 1.02 and 0.06 to 0.88, averaging 0.35 and 0.60 for the calcareous shales and marlstones respectively. The ratios of  $Al_2O_3/K_2O$  for the calcareous shales range from 0.97-16.28 averaging 9.37 and for marlstones, 1.14 - 14.32, averaging 5.54. The values of the Chemical Index of Alteration (CIA) vary widely from 48.60 to 93.18 %, averaging 74.70 % for the rocks analysed. The values of the Mineralogical Index of Alteration (MIA) vary widely from -1.60 to 86.36 %, average 49.40 % for the rocks.

Table 4.2: Major elemental oxides from X-ray Fluorescence analysis in weight Percents

<b>SAMPLE NO.</b>	<b>LK 5(1)</b>	<b>LK5(4)</b>	<b>LK8(7)</b>	<b>LK8(18)</b>	<b>EZZ1</b>	<b>EZZ2</b>	<b>EZZ3</b>	<b>EKLX2</b>	<b>EXLK3</b>	<b>EXLK5</b>	<b>AVERAGE</b>
<b>ROCK TYPE</b>	<b>SHALE</b>	<b>MARL</b>	<b>SHALE</b>	<b>MARL</b>	<b>SHALE</b>	<b>SHALE</b>	<b>SHALE</b>	<b>MARL</b>	<b>SHALE</b>	<b>SHALE</b>	<b>Wt %</b>
SiO <sub>2</sub> (Wt %)	48.95	28.66	25.69	39.68	49.10	45.80	50.60	19.00	51.20	58.80	41.75
Al <sub>2</sub> O <sub>3</sub> (Wt %)	7.68	3.75	5.77	6.13	14.60	15.30	14.40	5.30	14.13	12.50	9.96
CaO (Wt %)	21.16	52.57	48.68	36.08	9.73	11.30	6.41	41.19	7.82	5.17	24.01
Fe <sub>2</sub> O <sub>3</sub> (Wt %)	7.33	7.59	6.71	5.82	3.73	4.20	4.60	1.75	3.87	3.75	4.94
MgO (Wt %)	1.37	1.85	1.80	1.65	2.37	2.30	2.06	1.38	2.09	2.43	1.93
K <sub>2</sub> O (Wt %)	7.89	3.27	5.86	5.38	1.02	0.94	1.03	0.37	1.26	1.59	2.86
Na <sub>2</sub> O (Wt %)	0.11	0.06	0.05	0.08	0.05	0.09	0.07	0.21	0.08	0.09	0.09
SO <sub>3</sub> (Wt %)	1.88	0.38	1.54	0.98	0.70	0.50	0.80	0.06	0.40	0.50	0.77
MnO (Wt %)	0.09	0.13	0.09	0.13	0.02	0.04	0.02	0.11	0.02	0.02	0.07
TiO <sub>2</sub> (Wt %)	1.43	0.69	1.36	1.00	1.07	1.03	1.05	0.46	1.11	1.21	1.04
LOSS@1000 <sup>0</sup> C	2.11%	1.05%	2.45%	3.07%	17.61%	18.50	18.96%	30.17%	18.02%	13.94%	
TOTAL (Wt %)	100	100	100	100	100	100	100	100	100	100	

Table 4.3: Trace elements from X-Ray Fluorescence Analysis in parts per million

<b>SAMPLE NO</b>	<b>LK5(1)</b>	<b>LK5(4)</b>	<b>LK8(7)</b>	<b>LK8(18)</b>	<b>EZZ1</b>	<b>EZZ2</b>	<b>EZZ3</b>	<b>EXLK2</b>	<b>EXLK3</b>	<b>EXLK5</b>
<b>ROCK TYPE</b>	<b>SHALE</b>	<b>MARL</b>	<b>SHALE</b>	<b>MARL</b>	<b>SHALE</b>	<b>SHALE</b>	<b>SHALE</b>	<b>MARL</b>	<b>SHALE</b>	<b>SHALE</b>
Sc (PPM)	5.01	7.12	3.33	8.05	8.11	3.32	7.22	5.41	12.22	10.18
V (PPM)	300.15	130.23	220.12	390.10	156.18	197.25	160.44	130.33	251.20	254.03
Cr (PPM)	30.10	10.15	30.22	50.35	40.11	134.22	45.35	22.34	80.46	180.30
Co (PPM)	6.09	10.31	5.04	10.04	2.03	13.14	3.04	14.22	5.31	3.13
Ni (PPM)	140.12	97.33	122.01	138.44	176.42	138.42	180.43	12.14	197.04	193.33
Cu (PPM)	18.44	22.31	26.44	16.41	26.21	18.22	28.20	17.32	31.13	48.21
Zn (PPM)	180.24	230.32	250.34	180.23	164.42	135.03	159.25	184.04	237.02	228.13
Rb (PPM)	20.20	25.23	27.03	43.33	33.04	32.04	38.03	9.02	67.04	73.31
Sr (PPM)	160.42	200.43	350.01	186.11	198.21	200.32	206.14	160.03	210.01	170.12
Y (PPM)	6.02	9.14	8.14	13.13	14.04	6.14	12.04	16.01	21.12	19.05
Zr (PPM)	162.22	89.04	74.24	64.20	186.33	161.11	252.14	24.14	64.32	56.24
Ba (PPM)	87.14	79.10	102.12	126.21	41.21	116.13	56.14	178.14	50.40	34.04
Pb (PPM)	8.31	12.22	6.33	9.34	4.21	12.44	13.32	7.12	5.33	4.04

Table 4.4: Oxides ratios of samples from the Lokpanta Shale

SAMPLE NO	LITHOLOGY	SiO <sub>2</sub> /Al <sub>2</sub> O <sub>3</sub>	Al <sub>2</sub> O <sub>3</sub> /MgO	MgO/K <sub>2</sub> O	Al <sub>2</sub> O <sub>3</sub> /TiO <sub>2</sub>	Na <sub>2</sub> O/ K <sub>2</sub> O	K <sub>2</sub> O/ Al <sub>2</sub> O <sub>3</sub>	Al <sub>2</sub> O <sub>3</sub> / K <sub>2</sub> O	CIA (%)	MIA (%)
LK 5(1)	SHALE	6.37	4.89	0.20	5.37	0.01	1.02	0.97	48.60	-2.80
LK 5 (4)	MARL	7.64	2.03	0.57	5.43	0.02	0.87	1.15	52.50	5.00
LK 8 (7)	SHALE	4.45	3.21	0.31	4.24	0.01	1.02	0.98	49.20	-1.60
LK 8 (18)	MARL	6.47	3.72	0.31	6.13	0.01	0.88	1.14	52.50	5.00
EZZ 1	SHALE	3.36	6.16	2.32	13.64	0.05	0.07	14.31	92.88	85.76
EZZ 2	SHALE	2.99	6.65	2.45	14.85	0.10	0.06	16.28	93.18	86.36
EZZ 3	SHALE	3.51	6.99	2.00	13.71	0.07	0.07	13.98	92.50	85.00
EXLK 2	MARL	3.58	3.84	3.73	11.52	0.57	0.06	14.32	87.02	74.04
EXLK 3	SHALE	3.62	6.76	1.66	12.73	0.06	0.09	11.21	91.00	82.00
EXLK 5	SHALE	4.70	5.14	1.53	10.33	0.06	0.13	7.86	87.60	75.20



Table 4.5 is a correlation of all the oxides obtained from the X-Ray Fluorescence (XRF) analysis against each other for paleoenvironmental interpretation. Figure 4.35 a-h show correlation plots of the major oxides and Al<sub>2</sub>O<sub>3</sub>. Figure 4.36 a-c shows positive correlation of CaO and the oxides Fe<sub>2</sub>O<sub>3</sub>, K<sub>2</sub>O and MnO.

Table 4.5: Correlation Coefficient between major oxides

	SiO <sub>2</sub>	Al <sub>2</sub> O <sub>3</sub>	Fe <sub>2</sub> O <sub>3</sub>	MgO	CaO	Na <sub>2</sub> O	K <sub>2</sub> O	TiO <sub>2</sub>	MnO
SiO <sub>2</sub>	1.00	0.78	-0.09	0.62	-0.91	-0.38	-0.13	0.57	-0.76
Al <sub>2</sub> O <sub>3</sub>		1.00	-0.47	0.78	-0.94	-0.27	-0.57	0.31	-0.95
Fe <sub>2</sub> O <sub>3</sub>			1.00	-0.27	0.45	-0.55	0.82	0.43	0.47
MgO				1.00	-0.65	-0.55	-0.57	0.20	-0.79
CaO					1.00	0.14	0.43	-0.38	0.91
Na <sub>2</sub> O						1.00	-0.21	-0.54	0.27
K <sub>2</sub> O							1.00	0.55	0.55
TiO <sub>2</sub>								1.00	-0.37
MnO									1.00

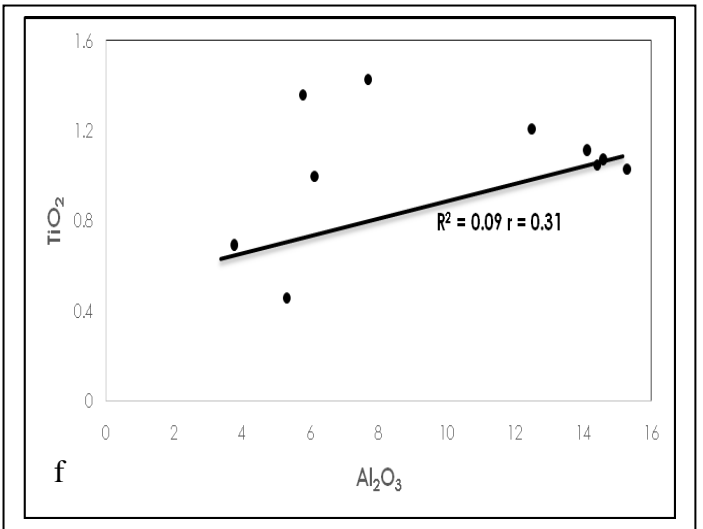
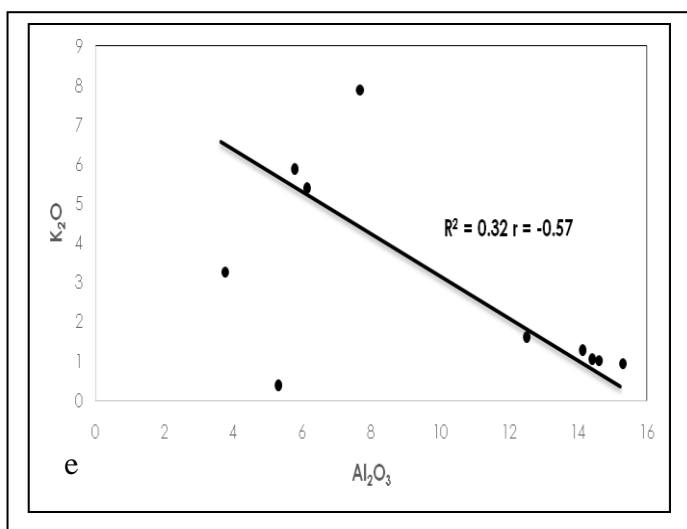
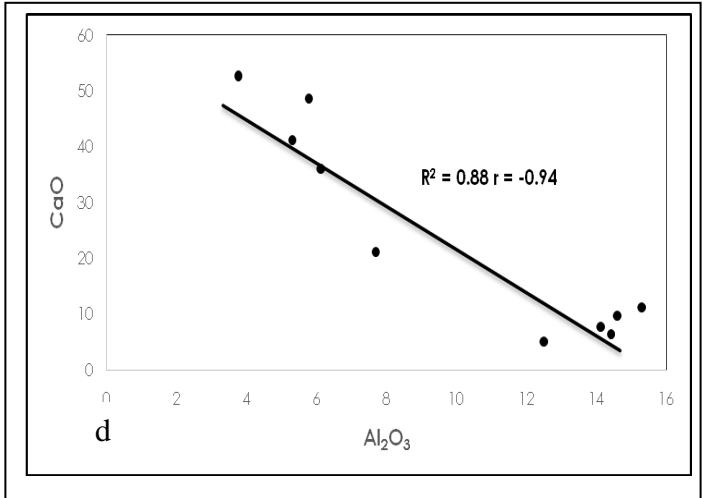
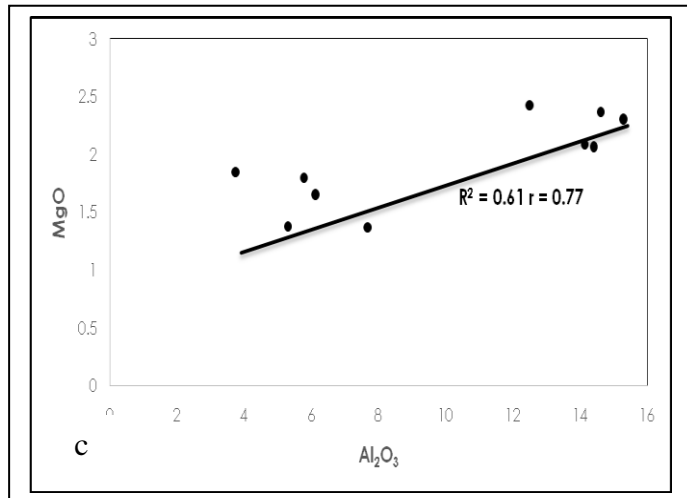
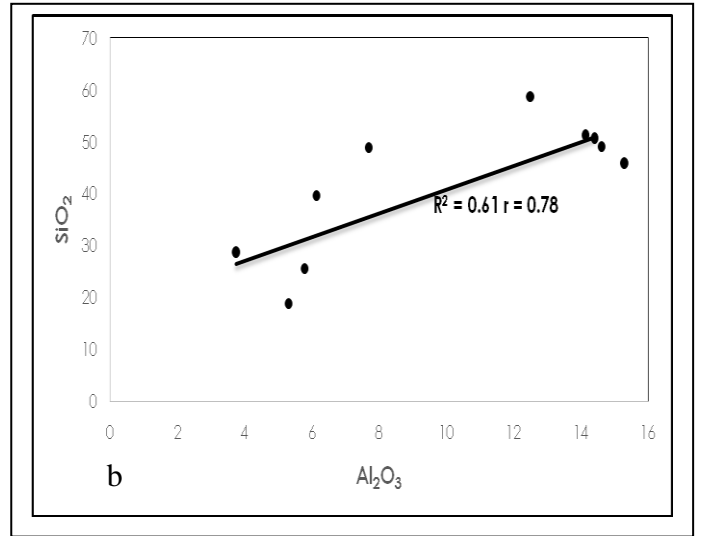
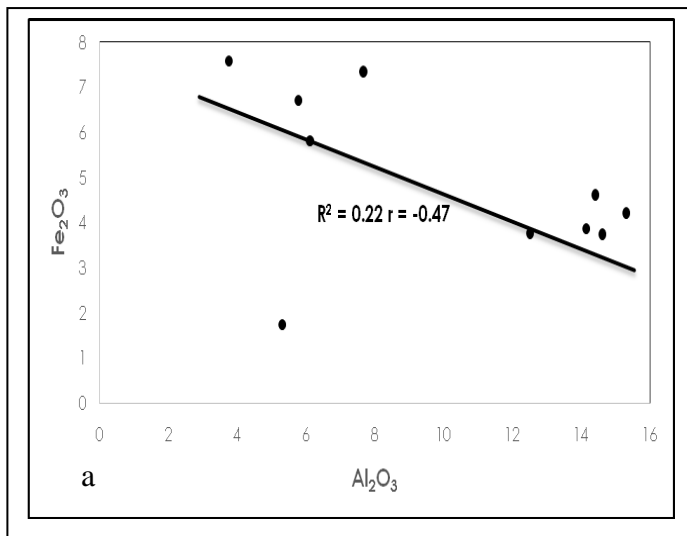


Figure 4.35 a-f: Relationship between major oxides and  $Al_2O_3$

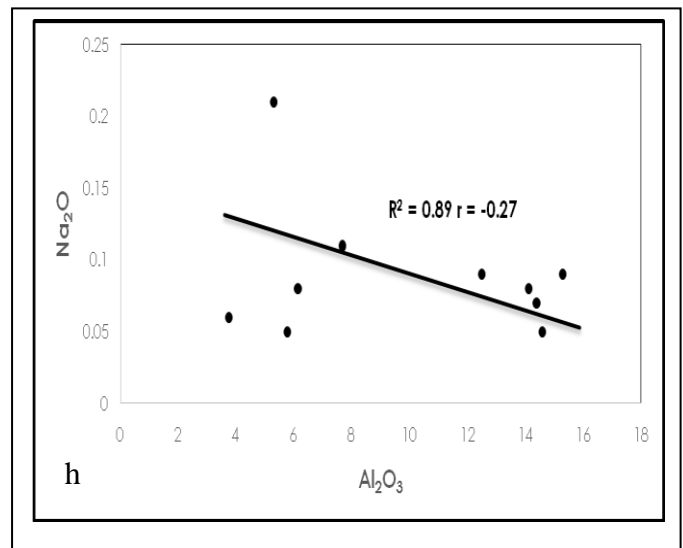
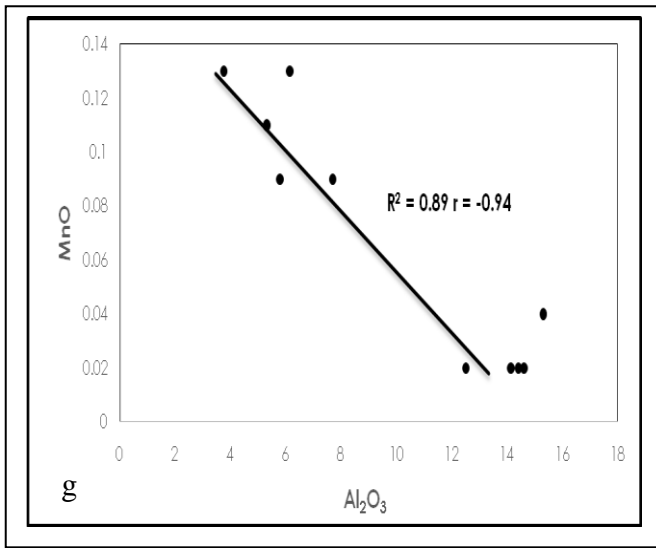


Figure 4.35 g-h: Relationship between major oxides and Al<sub>2</sub>O<sub>3</sub>

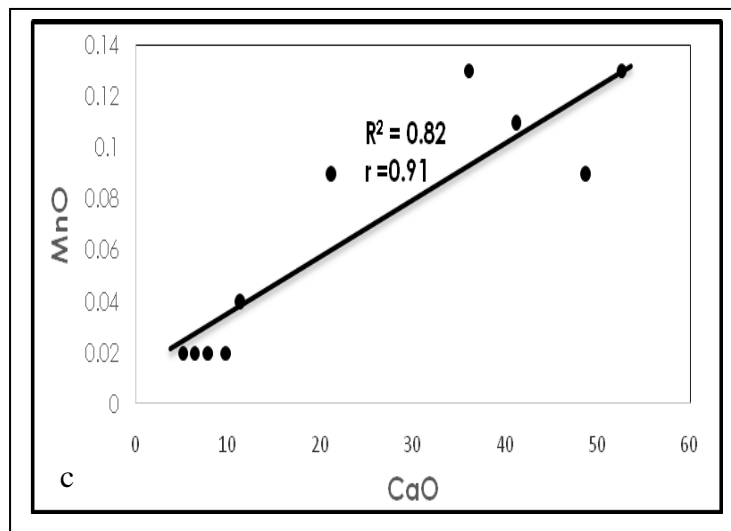
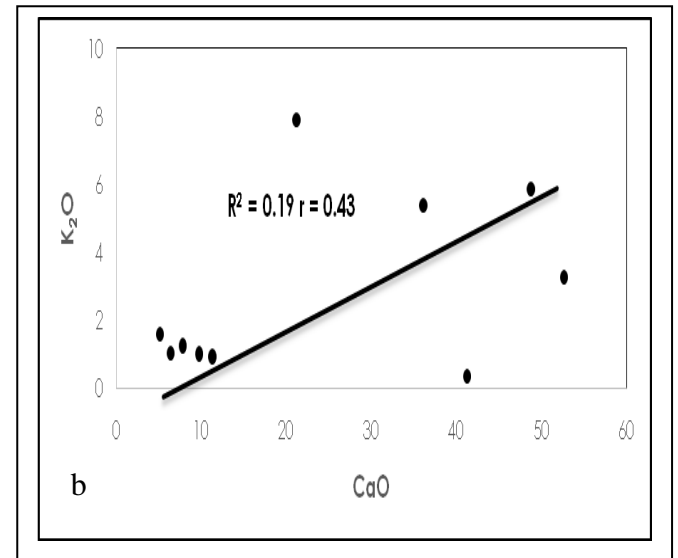
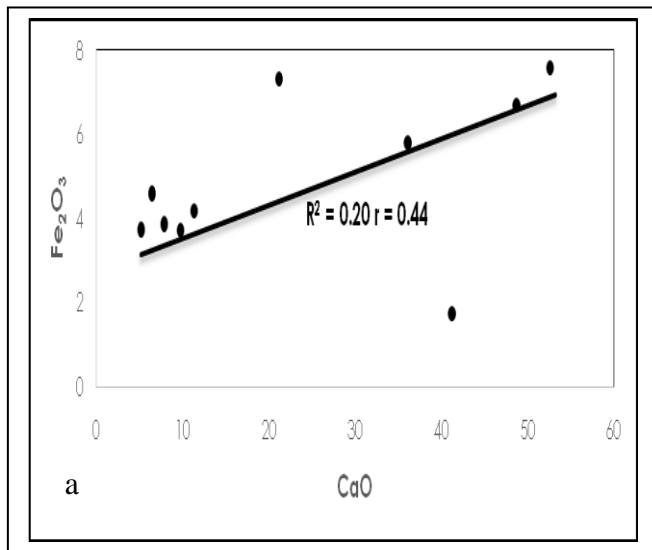


Figure 4.36 a-c: Relationship between Iron, Manganese and Potassium oxides and CaO

## 4.6 Atomic Absorption Spectrometry Results

Table 4.6 shows the results obtained from Atomic Absorption Spectrometry/Inductively Coupled Plasma Mass Spectrometry (AAS/ICP-MS) for major and trace elements composition of the rocks. The results show that Ca (calcium) has the highest composition in the rocks, followed by Al (Aluminum), Ti (Titanium), Fe (Iron) and K (Potassium) (Table 4.6). The lowest compositions were recorded by Ag (Silver), Co (Cobalt), Sn (Tin) and Mo (Molybdenum). Table 4.7 show the ratios of the elements needed for necessary interpretations. The elemental ratios,  $V/(V+Ni)$ ,  $V/Cr$  and  $Ni/Co$ , are useful for paleoredox interpretations. The elemental ratio,  $Sr/Ba$  is a parameter for paleosalinity interpretation. The ratios of  $V/(V+Ni)$  range from 0.71 to 0.93 and 0.80 to 0.93 for the calcareous shales and marlstones respectively. The ratios of  $V/Cr$  range from 6.88 to 23.41 and 10.26 to 22.95 for the calcareous shales and marlstones respectively. The ratios of  $Ni/Co$  range from 26.00 to 61.83 and 25.97 to 49.84 for the calcareous shales and marlstones respectively. The ratios of  $Sr/Ba$  range from 1.23 to 4.43 and 2.03 to 2.25 for the calcareous shales and marlstones respectively.

Table 4.6: Elemental composition of the analyzed samples from AAS analysis

SAMPLE NO	LK(5)1	LK(5)4	LK(5)13	LK(8)7	LK(8)18	EXLK2	EXLK3	EXLK5	EZZ 1	EZZ 3
LITHOLOGY	SHALE	MARL	SHALE	SHALE	MARL	MARL	SHALE	SHALE	SHALE	SHALE
Be (PPM)	1.16	0.36	0.78	0.88	0.36	0.69	1.61	1.71	1.88	1.17
Li (PPM)	202.66	196.96	138.43	167.39	170.43	160.95	192.22	206.69	279.78	161.25
Bi (PPM)	0.88	0.60	1.61	0.74	0.39	0.44	0.88	2.34	1.31	1.06
Ga (PPM)	9.72	2.72	8.82	10.52	5.33	4.56	15.78	15.82	10.96	10.11
Zr (PPM)	49.15	21.53	41.43	37.07	48.77	32.47	77.36	88.60	146.98	56.82
In (PPM)	1.24	0.65	0.32	0.13	1.03	0.00	0.00	0.40	0.00	0.00
Zn (PPM)	145.22	17.01	634.74	803.46	691.57	264.19	685.89	234.27	44.85	40.38
Pb(PPM)	22.71	10.55	18.90	27.41	10.76	15.01	30.41	31.01	27.80	26.18
Ca (PPM)	30483.08	18408.72	32617.56	31072.43	27362.55	31901.29	25223.28	25123.47	46836.20	39629.33
K (PPM)	10465.92	2310.32	8531.28	10902.22	6067.00	3679.40	11174.35	9771.72	10606.69	9590.03
Mg (PPM)	1816.78	1292.07	1856.94	1715.51	1475.11	1146.07	1538.87	1433.09	1869.31	1335.19
Ag (PPM)	0.88	0.00	0.00	0.05	0.24	0.00	0.01	0.79	0.31	0.01
Al (PPM)	2821.29	2069.33	2573.57	2549.79	3198.59	2971.38	3486.92	4792.72	6398.94	4432.25
As (PPM)	1.58	2.16	8.27	5.14	8.49	1.56	4.91	7.26	5.20	3.34
Ba (PPM)	40.62	23.81	85.63	132.26	80.84	41.29	124.95	98.56	77.26	157.18
Cd (PPM)	2.70	0.21	5.80	21.46	15.05	3.86	8.36	4.40	0.41	0.29
Co (PPM)	0.84	0.56	0.91	0.87	1.17	0.86	2.25	0.00	1.65	1.25
Cr (PPM)	123.90	11.06	46.53	72.03	34.89	27.04	82.73	110.17	55.01	47.91

Table 4.6 (contd): Elemental composition of the analyzed samples from AAS analysis

	34.68	6.45	24.99	54.64	33.79	11.62	31.80	33.40	16.62	15.96
Cu (PPM)										
Fe (PPM)	13850.03	8949.42	10535.04	13404.85	7569.00	10091.29	15621.58	17386.32	16272.57	15080.30
Mn (PPM)	280.59	373.91	132.02	148.92	178.18	352.03	151.54	126.28	176.73	161.02
	2.49	10.21	19.92	22.48	24.79	5.04	21.81	12.37	23.01	19.16
Mo (PPM)										
	46.00	16.43	47.19	52.03	58.31	22.33	58.49	61.83	68.44	72.59
Ni (PPM)										
	4.42	0.00	2.00	20.94	8.03	3.15	3.16	6.58	1.67	1.01
Se (PPM)										
Sn (PPM)	4.09	2.79	2.42	2.90	2.37	1.42	2.47	3.06	3.11	2.61
	179.85	49.65	167.24	203.12	181.79	83.70	162.09	132.30	243.96	193.27
Sr (PPM)										
	2431.74	627.49	2034.92	2438.68	1703.76	1202.71	3074.17	3412.07	3029.13	2640.13
Ti (PPM)										
	0.00	0.00	0.32	0.00	0.00	0.23	0.19	0.12	0.83	0.68
Ti (PPM)										
	238.63	66.15	577.68	657.80	775.59	224.53	744.36	569.94	190.15	179.72
V (PPM)										
	41.69	19.76	45.71	50.52	3.28	27.18	29.13	23.17	54.68	54.31
Rb (PPM)										

Table 4.7: Elemental ratios of the analyzed samples from AAS analysis

<b>Sample No</b>	<b>Lithology</b>	<b>V/V+Ni</b>	<b>V/Cr</b>	<b>Ni/Co</b>	<b>Sr/Ba</b>
LK(5)1	SHALE	0.84	6.88	54.76	4.43
LK(5)4	MARL	0.80	10.26	29.34	2.09
LK(5)13	SHALE	0.92	23.12	51.86	1.95
LK(8)7	SHALE	0.93	12.04	59.80	1.54
LK(8)18	MARL	0.93	22.95	49.84	2.25
EX LK 2	MARL	0.91	19.32	25.97	2.03
EX LK 3	SHALE	0.93	23.41	26.00	1.30
EX LK 5	SHALE	0.90	17.06	61.83	1.34
EZZ 1	SHALE	0.74	11.44	41.48	3.16
EZZ 3	SHALE	0.71	11.26	58.07	1.23

## 4.7 Palynological Results

Figures 4.37 and Table 4.8 show the results obtained from palynological and kerogen (palynodebris) analyses.

The samples yielded a very low abundance and low diversity of miospores. Microfloral assemblage recovered from the samples are *Longapertites marginatus*, *Ephedripites spp*, *Triorites spp*, *fungal spores*, miospores (*Psilatricolporites*, *Verrucatosporites*, *Polypodiaceoisporites*, *Leotriletes*, *Sphaeromorph spp*, *Leoisphaeridia spp* and *Laevigatosporites sp*).

Most of the palynomorphs recovered are non-age diagnostic and long ranging except the pollens *Ephedripites spp*, *Triorites spp* and *Longapertites marginatus* which are diagnostic Cretaceous miospores.

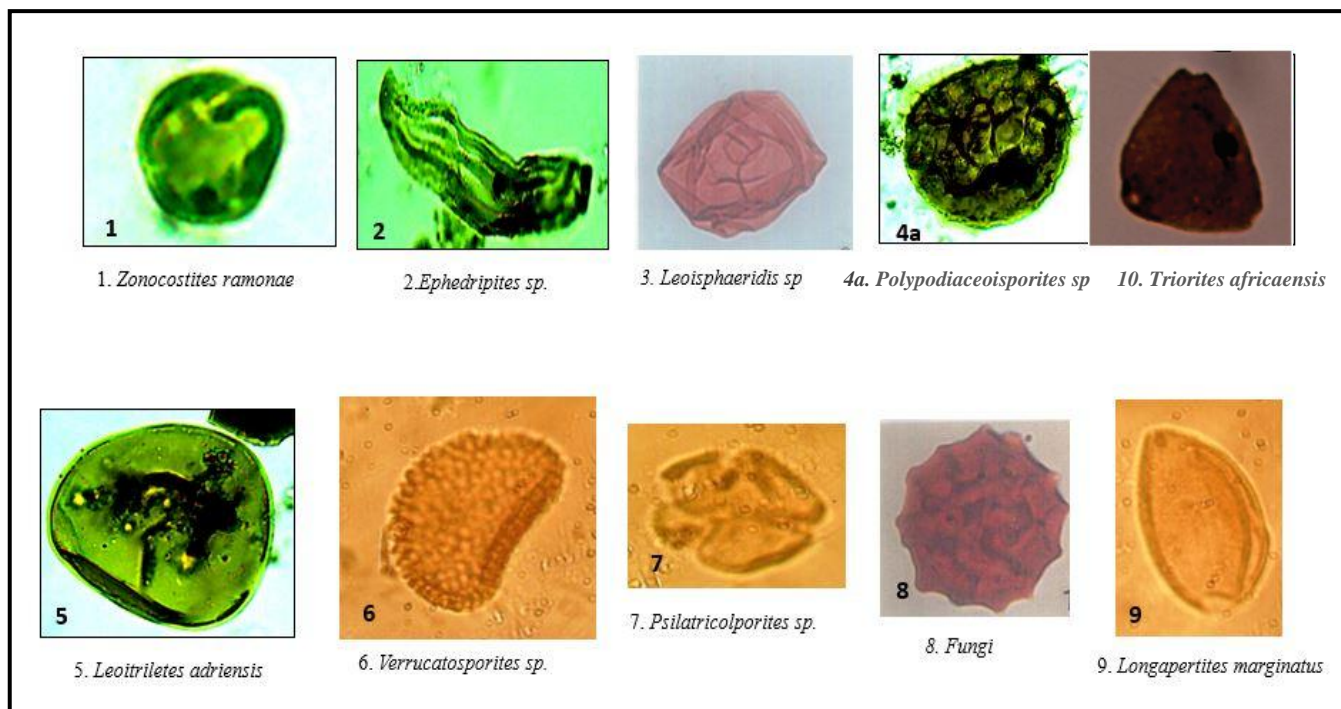


Figure 4.37: Photomicrographs of some of the palynomorphs recovered (*Magnification*  $\times 400$ ) 100



Table 4.8: Palynological results of the Lokpanta Shale

SAMPLE	PALYNOMORPHS	COUNT	AGE
<b>EXLK 2</b>	<i>Laevigatosporites sp.</i>	4	<i>Ephedripites sp.</i> and <i>Triorites afrikaensis</i> suggest Cenomanian-Turonian age for the rock. (Jan Du Chene, 1978, Petters, 1980 and Amoke, 2009)
	<i>Leotriletes adriensis</i>	1	
	<i>Verrucatosporites spp</i>	1	
	<i>Retidiporites magdalenensis</i>	1	
	<i>Ephedripites sp.</i>	1	
	<i>Triorites afrikaensis</i>	2	
<b>ELK 3</b>	<i>Psilatricolporites sp.</i>	2	Not diagnostic of age
	<i>Psilatricolporites sp.</i>	1	
	Fungal spore/hyphae	2	
<b>EXLK 5</b>	<i>Ephedripites sp</i>	2	<i>Ephedripites sp.</i> and <i>Triorites afrikaensis</i> suggest Cenomanian-Turonian age for the rock.( Jan Du Chene, 1978, Petters, 1980 and Amoke, 2009)
	<i>Triorites afrikaensis</i>	2	
	<i>Longapertites marginatus</i>	1	
<b>LK (5) 1</b>	<i>Leoisphaeridia sp.</i>	2	Not diagnostic of age
	<i>Leotriletes adriensis</i>	1	
	<i>Indeterminate pollen.</i>	1	
	<i>Verrucatosporites sp.</i>	2	
<b>LK (5) 4</b>	<i>Laevigatosporites sp.</i>	4	Not diagnostic of age
	<i>Polypodiaceoisporites sp.</i>	1	
	<i>Leotriletes adriensis</i>	4	
	<i>Psilatricolporites sp.</i>	2	
	<i>Longapertites marginatus</i>	1	
<b>LK (8) 7</b>	<i>Laevigatosporites sp.</i>	3	Not diagnostic of age
	<i>Verrucatosporites sp.</i>	1	
	<i>Leotriletes adriensis</i>	1	
	Fungal spore/hyphae	4	
<b>LK (8) 18</b>	<i>Laevigatosporites sp.</i>	2	
	<i>Psilatricolporites sp.</i>	8	
<b>EZZ 1</b>	<i>Ephedripites sp</i>	2	<i>Ephedripites sp.</i> and <i>Triorites</i>

	<i>Triorites afrikaensis</i>	1	<i>afrikaensis</i> suggest Cenomanian-Turonian age for the rock. (Jan Du Chene, 1978, Petters, 1980 and Amoke, 2009)
	<i>Longapertites maginatus</i>	2	
<b>EZZ 2</b>	Fungal spore/hyphae	1	Not diagnostic of age
<b>EZZ 3</b>	<i>Psilatricolporites sp.</i>	2	
	<i>Psilatricolporites sp. (cupo)</i>	2	
	<i>Laevigatosporites sp.</i>	3	
	Fungal spore/hyphae	1	
	<i>Verrucatosporites sp.</i>	2	

The palynodebris are classified into five divisions namely; PM 1, PM 2, PM 3, PM 4 and SOM.

**PM-1:** (Palynomaceral – 1) is dark brown, structureless and irregular in shape with dense appearance. It is a gel-like substance and resinous cortex material (Van der Zwan, 1990).

**PM-2:** (Palynomaceral –2) is brown to orange irregularly shaped material. It is less dense and includes structured plant material like leaf, stem, small rootlet debris and algal detritus (Van der Zwan, 1990).

**PM-3:** (Palynomaceral – 3) is pale irregularly-shaped structured plant material occasionally bearing stomata with guard cells. It is mainly composed of material of cuticular origin (Whitaker, 1984; Boulter and Riddick, 1986; Van der Zwan, 1990).

**PM-4:** (Palynomaceral – 4) is black equidimensional, blade or needle-shaped structureless plant material. It includes humic gels and charcoal (Whitaker, 1984; Boulter and Riddick, 1986; Van der Zwan, 1990).

**(S.O.M):** Structureless Organic Matter is composed of structureless plant material of granular appearance, composed largely of bacterially reworked biomass preserved under anoxic conditions. It is a term used to define all amorphous material (amorphous organic material (AOM)) with no structuring or evidence of tissue. It could appear yellow and gel-like or grey (Oboh, 1992; Traverse, 2008).

Figure 4.38 and Table 4.9 show the quantification of the palynomacerals (PM) and structureless Organic Matter (SOM) in the analysed rocks.

Generally, palynodebris vary in size from small to large and could be poorly to well sorted. The palynomaceral 1 (PM-1) contents in the samples analysed are high, varying from 58.50 to 75.00%. They are generally small (30  $\mu\text{m}$ ) to medium (50  $\mu\text{m}$ ) in size, though, few large (150  $\mu\text{m}$ ) particles were recorded (Table 4.10). Palynomaceral 2 (PM-2) percentages vary from 2.50 to 9.50%. The particle sizes range from small (20  $\mu\text{m}$ ) to medium (50  $\mu\text{m}$ ) (Table 4.10). Palynomaceral 3 (PM-3) percentages vary from 1.00 to 2.00%. They are generally small (30  $\mu\text{m}$ ) to medium (50  $\mu\text{m}$ ) in size. Rare occurrence of large (150 $\mu\text{m}$ ) particle sizes was noted (Table 4.10). Palynomaceral 4 (PM-4) percentages range from 20.50 to 32.50%. The sizes are generally small (30  $\mu\text{m}$ ), though, few medium (50 $\mu\text{m}$ ) particles were recorded. Structureless Organic Matter (SOM) occurs in most of the samples in low percentages varying from 1.00 to 3.50%.

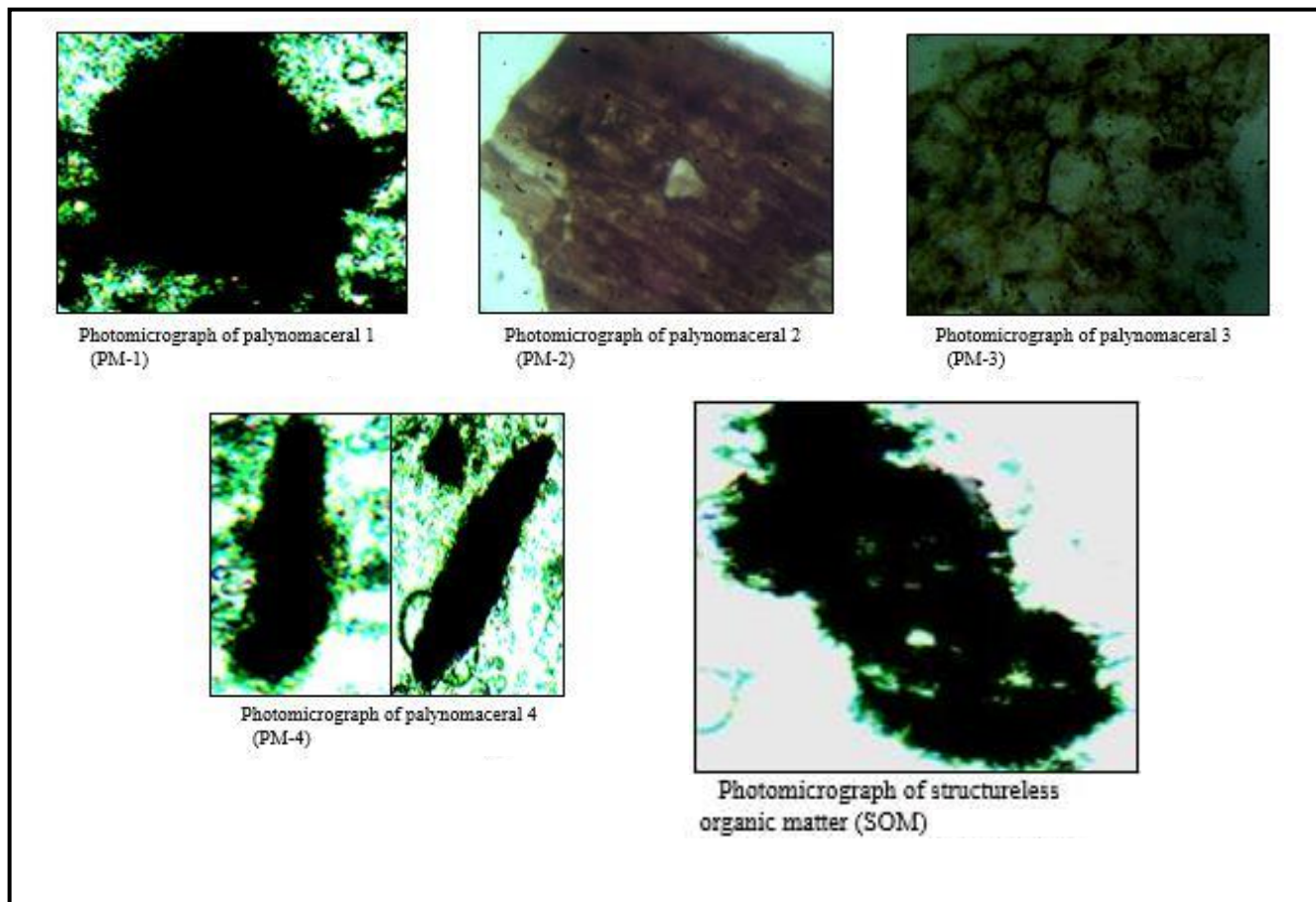


Figure 4.38: Photomicrographs of palynomacerals and structureless organic matter (*Magnification*  $\times 400$ )

Table 4.9: Palynomacerals and their compositional percentages for the Lokpanta Shale

SAMPLE NO.	LK 5 (1) (%)	LK 5 (4) (%)	LK 8 (7) (%)	LK 8(18) (%)	EZZ 1 (%)	EZZ 2 (%)	EZZ 3 (%)	EKLX 2 (%)	EXLK 3 (%)	EXLK 5 (%)	PARTICLE SIZE DISTRIBUTION
PM-1	75.00	72.50	69.00	70.00	58.50	63.00	61.50	59.00	61.50	66.00	Small (30 μm) to medium (50 μm), rare large (150 μm) particles
PM-2	2.50	4.50	7.50	5.00	4.50	5.50	3.50	9.50	3.50	2.50	Small (30 μm) to medium (50 μm) particles
PM-3	1.00	1.00	1.00	1.50	2.00	1.50	2.00	2.00	1.50	1.00	Small (30 μm) to medium (50 μm), rare large (150 μm) particles
PM-4	20.5	22.00	22.50	22.50	32.50	28.50	31.00	29.50	31.00	27.00	Predominantly small (30 μm), subordinate medium (50 μm) particles
SOM	1.00	-	-	1.00	2.50	1.50	2.00	-	2.50	3.50	-

## 4.8 Rock-Eval Pyrolysis Results

Table 4.10 shows the results of Rock Eval pyrolysis carried out on ten (10) rock samples of the Lokpanta Shale.

The Total Organic Carbon (TOC) percentages in the rocks range from 0.83 to 4.56 wt% (Av. 2.75 wt%). The Total Organic Matter (TOM) percentages range from 1.01 to 4.98 wt% (Av. 3.68 wt%). The content of the free hydrocarbons,  $S_1$  ranges from 0.15 to 2.91 mgHC/g (Av. 1.29 mgHC/g). The remaining hydrocarbon generated;  $S_2$  varies from 2.06 to 21.42 mgHC/g (Av. 10.69 mgHC/g). The amount of carbon (IV) oxide,  $S_3$  evolved during the process varies from 0.32 to 0.99 mgHC/g (Av. 0.59 mgHC/g). The ratios,  $S_2/S_3$  vary widely from 3.90 to 49.40 (Av. 21.47) (Table 4.10). The maximum temperature at which  $S_2$  was generated ( $T_{max}$ ) range from 430 to 459°C (Av. 437.4 °C). The values for the equivalent vitrinite reflectance ( $R_o$  eq.) was calculated from the  $T_{max}$  using the formula:  $[(0.018 \times T_{max}) - 7.16]$  (Jarvie *et al.*, 2001). The equivalent vitrinite reflectance varies from 0.58 to 1.10% (Av. 0.71%). Hydrogen index (HI) ranges from 186 to 487 mgHC/g TOC (Av. 328.30 mgHC/gTOC). The Oxygen Index (OI) ranges from 8.00 to 59.00 mgCO<sub>2</sub>/g TOC with average of 26.40 mgCO<sub>2</sub>/g TOC). The Genetic Potential (GP) values range from 2.34 to 24.33 mgHC/g (Av. 11.98 mgHC/g). The pyrolyzable Carbon (PC) ranges from 0.19 to 2.02 wt%. The Hydrocarbon Production Index (PI) ranges from 0.04 to 0.20 (Av. 0.11).

Table 4.10: Results of Rock-Eval pyrolysis of the Lokpanta Shale

SAMPLE NO.	ROCK TYPE	TOC wt%	TOM wt%	S <sub>1</sub> mgHC/g	S <sub>2</sub> mgHC/g	S <sub>3</sub> mgHC/g	T <sub>max</sub> (° C)	HI mgHC/gTOC	OI mgCO <sub>2</sub> /gTOC	S <sub>2</sub> /S <sub>3</sub>	GP mgHC/g	PC wt%	PI	Ro(eq.) %
LK(5)1	SHALE	2.08	2.54	0.15	3.85	0.99	435	186	48	3.9	4.00	0.33	0.04	0.67
LK(5)4	MARL	0.83	1.01	0.28	2.06	0.49	433	247	59	4.2	2.34	0.19	0.12	0.634
LK(5)13	SHALE	2.78	3.39	1.61	12.25	0.42	435	441	15	29.2	13.86	1.15	0.12	0.67
LK(8)7	SHALE	3.48	4.25	0.92	11.86	0.94	430	341	27	12.6	12.78	1.06	0.07	0.58
LK(8)18	MARL	4.56	5.56	2.91	21.42	0.57	433	470	12	37.6	24.33	2.02	0.12	0.634
EX LK 2	MARL	1.21	1.48	0.17	2.92	0.63	434	242	52	4.6	3.09	0.26	0.06	0.652
EX LK 3	SHALE	3.95	4.82	1.93	19.25	0.39	430	487	10	49.4	21.18	1.76	0.09	0.58
EX LK 5	SHALE	4.08	4.98	1.18	17.73	0.50	432	435	12	35.5	18.91	1.57	0.06	0.616
EZZ 1	SHALE	3.18	3.88	1.51	6.72	0.67	453	211	21	10.0	8.23	0.68	0.18	0.994
EZZ 3	SHALE	3.98	4.86	2.24	8.85	0.32	459	223	8	27.7	11.09	0.92	0.20	1.102

The plot of  $s_2$  (remaining hydrocarbon potential) against TOC (total organic content) shows that the kerogen type II and II-III (Figure 4.39).

The plot of HI (Hydrogen Index) against OI (Oxygen Index) on the modified Van Krevelen diagram shows that the rocks contain type I and II kerogen, with predominance of type II (Figure 4.40).

The plot of Hydrogen Index (HI) against  $T_{max}$  ( $^{\circ}C$ ) shows type II and II-III kerogen that are immature to marginally mature (Figure 4.41). The deeper part of the strata plotted in the type II kerogen domain in the mature (oil window and condensate-wet gas) zone.

The plot of Production Index (PI) against  $T_{max}$  ( $^{\circ}C$ ) shows that most of the rocks are immature to marginally mature and within low and high-level conversion rate. The deepest part of the strata contains mature source rock within oil window and condensate-wet gas zone (Figure 4.42).



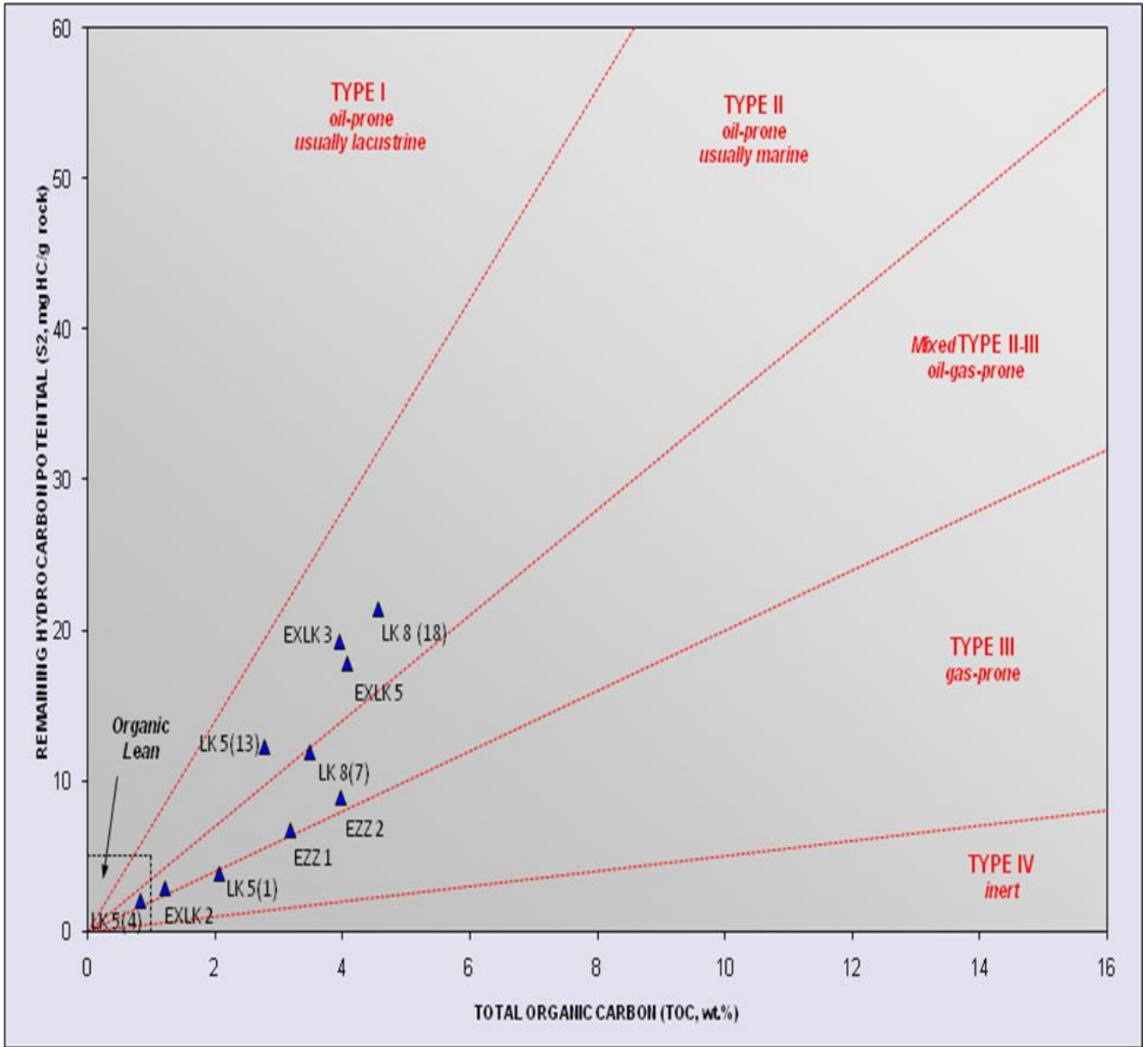


Figure 4.39: The plot of  $s_2$  against TOC of the Lokpanta Shale

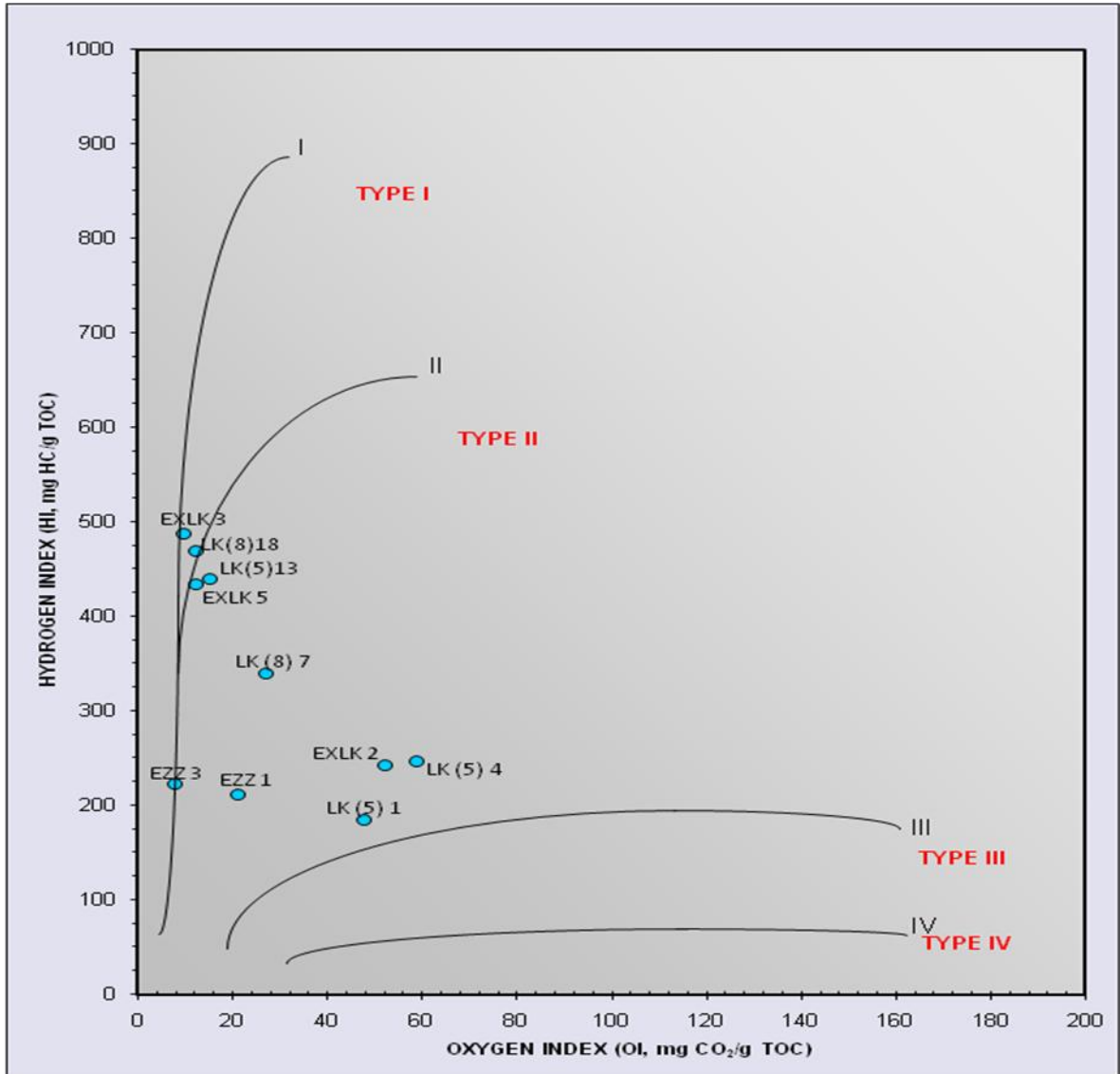


Figure 4.40: HI against OI plots on the modified Van Krevelen diagram of the Lokpanata Shale

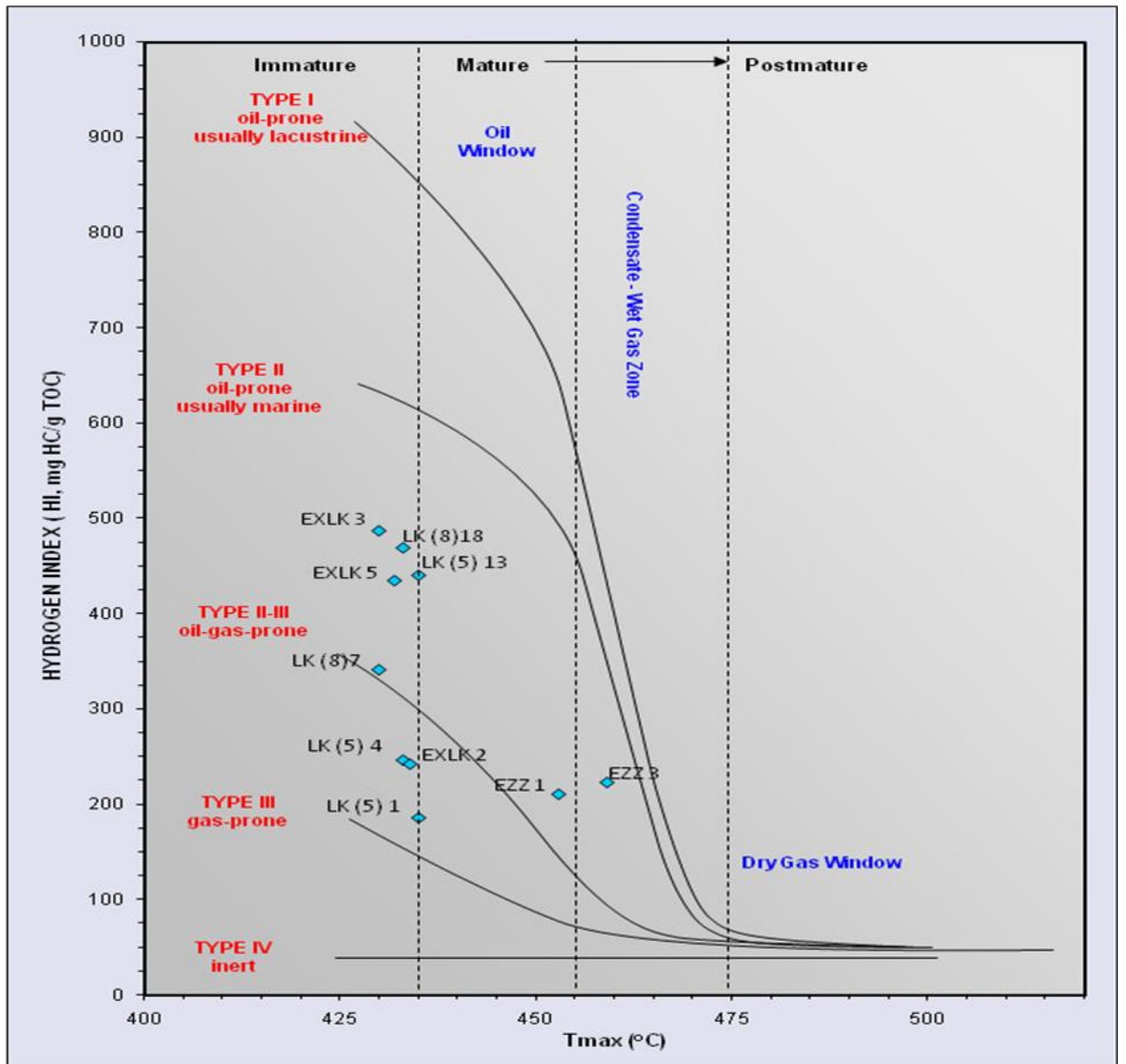


Figure 4.41: Plot of Hydrogen Index (HI) against  $T_{max}$  ( $^{\circ}$ C) for the Lokpanta Shale

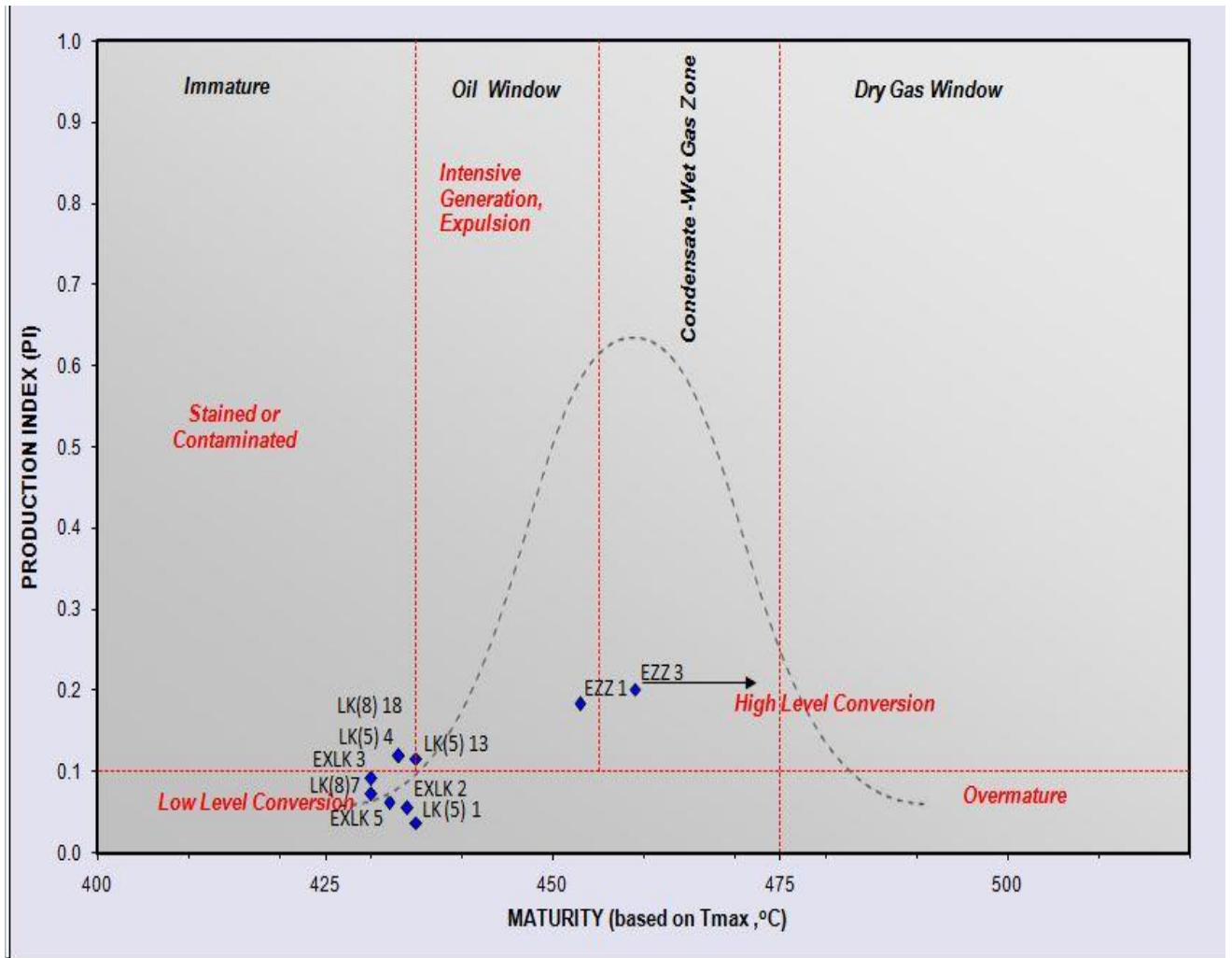


Figure 4.42: The plot of Production Index (PI) against  $T_{max}$  (°C) of the Lokpanta Shale

## 4.9 Petrographic Results

Petrographic study of ten polished thin sections of the marls from the outcrops (OT 1-8) of the Lokpanta Shale reveals varying abundance and morphology of their constituent minerals and fossils (Figures 4.43-4.52). This was done to determine mineralogy, textures, and composition of the rocks in order to interpret their provenance, maturity and palaeoclimate indices. The prepared thin sections were examined with the aid of transmitted light under the flat stage of the petrographic microscope using point count method according to Ingersoll *et al.* (1984) and Osae *et al.* (2006). Photomicrographs were taken and features of the mineral grains were observed based on the optical properties of the minerals. Mineralogical composition and diagenetic features of these carbonaceous rocks were identified. The texture of the samples is heterogenous comprising of both poorly sorted, medium grained allochems (framework) and a fine grained micritic groundmass. The allochems or bioclasts (skeletal fragments) which are foraminera tests and bivalve shells of *Inoceramus labiatus* occur as euhedral to anhedral grains within a micritic groundmass. Spar (calcite) occurs in all the photomicrographs in varying proportions ranging from 5 to 20% (Table 4.11). The skeletal composition is calcitic and mainly composed of planktonic foraminiferal tests (mostly *hedbergellids* and *heterohelicids*) and shells of the bivalve, *Inoceramus labiatus*. The percentage abundance of the allochems range from 25%-65% while micrite range from 25%-65% (Table 4.11). Thus, the fabric of the sections is mud-supported with micrite filling the pore space between the allochems or bioclasts. The micritic groundmass, comprising of microcrystalline calcite, quartz and clay mineral which has been identified as kaolinite. The micritic groundmass has parallel laminations (laminae) with preferred orientation which is suggestive of variations in composition.

Generally, tests of *heterohelicids* and *hedbergellids* foraminera are also aligned parallel to the laminations (Figures 4.43-4.51). The shape of allochems range from sub-angular to rounded with grain sizes ranging from 5-100 $\mu$ m in diameter. The grain size of the particles in the micritic groundmass range from 1-2 $\mu$ m in diameter.

Calcite observed in the photomicrographs occurred in three forms namely; a) skeletal fragments which are of high relief and are euhedral to anhedral in shape. b) recrystallized calcite grains which are the neomorphic spar of low relief filling dissolved micrite and even obscuring the groundmass (eg Figure 4.46 b). c) as part of the micrite, microcrystalline calcite.

In addition, iron oxide occurs in the thin sections as dark stains on the *Inoceramus labiatus* seams (eg Figure 4.43). Diagenetic fabric observed include neomorphism of some the skeletal fragments and micritic groundmass, preferred orientation and laminations of the groundmass. Stylolitic seams which are pervasive product of pressure solution are present (Figure 4.45, 4.46 and 4.50). Microinterparticulate porosity exists between the micrite grains of the sections.



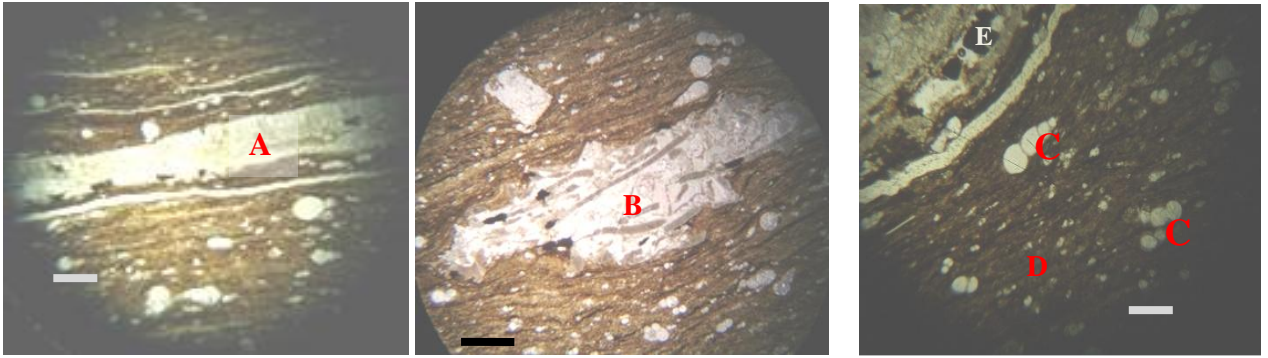


Figure 4.43: Photomicrograph of OT.1.1 (A) shells of *Inoceramus labiatus* (B) Neomorphic spar (C) Planktic foraminiferal tests (D) Micrite (microcrystalline calcite and kaolinite) (E) Iron oxide appearing as dark stains on the skeletal fragments (Bar scale = 2 mm Magnification:  $\times 50$ )

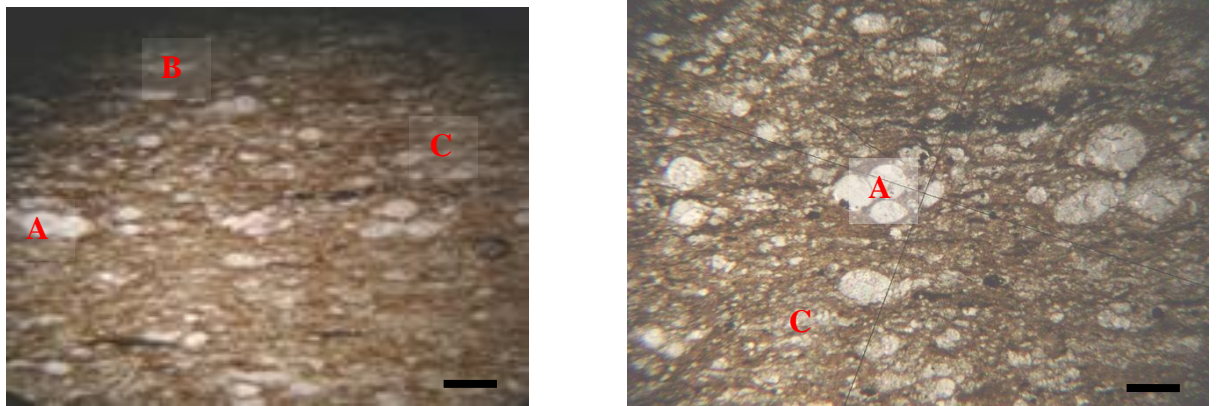


Figure 4.44: Photomicrograph of OT.3.1 (A) Planktic foraminiferal tests (B) Micrite (microcrystalline calcite and kaolinite) (c) Neomorphic spar (Bar scale = 2 mm Magnification:  $\times 50$ )

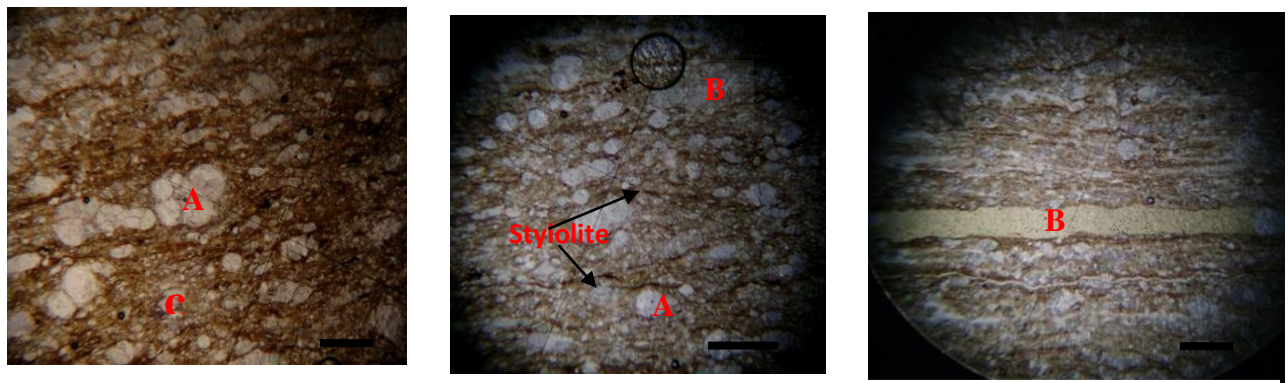


Figure 4.45: Photomicrograph of OT.4.1 showing (A) Planktic foraminiferal tests (B) Neomorphic spar (C) Micrite (microcrystalline calcite and kaolinite) (Bar scale = 2 mm Magnification:  $\times 50$  Resolution: (150 dpi))



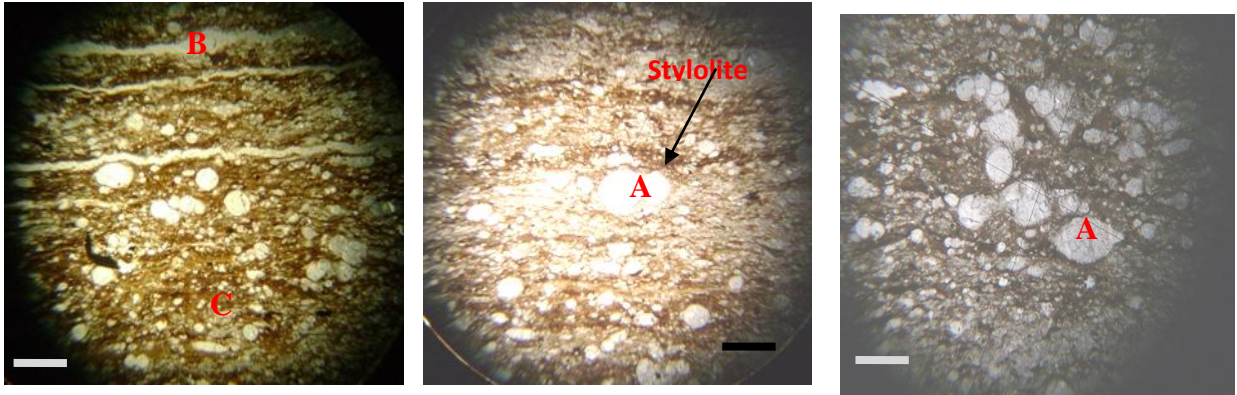


Figure 4.46: Photomicrograph of OT.5.1 showing (A) Planktic foraminiferal tests (B) Neomorphic spar (C) Micrite (microcrystalline calcite and kaolinite) (Bar scale = 2 mm Magnification:  $\times 50$  Resolution: (150 dpi))

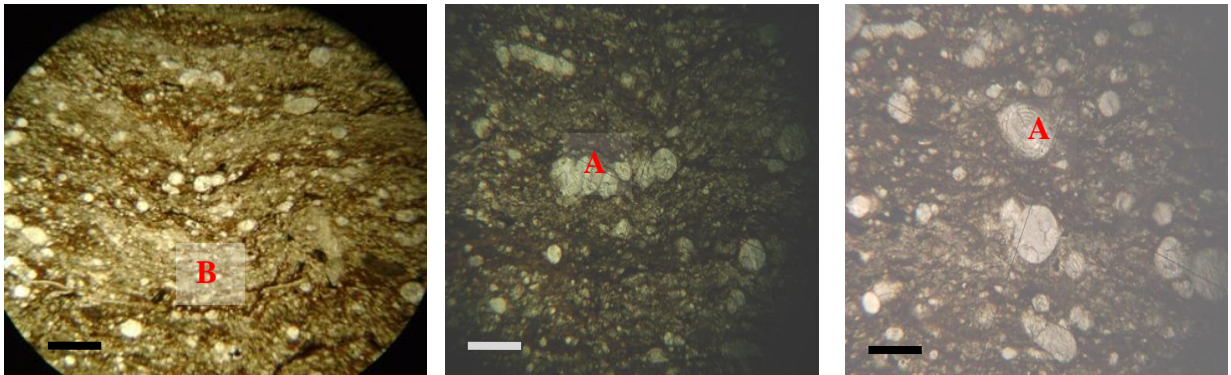


Figure 4.47: Photomicrograph of OT.5.2 showing (A) Planktic foraminiferal tests (B) Micrite (microcrystalline calcite and kaolinite) (Bar scale = 2 mm Magnification:  $\times 50$  Resolution: (150 dpi))



Figure 4.48: Photomicrograph of OT.5.3 showing (A) Planktic foraminiferal tests (B) Micrite (microcrystalline calcite and kaolinite) Bar scale = 2 mm Magnification:  $\times 50$  Resolution:

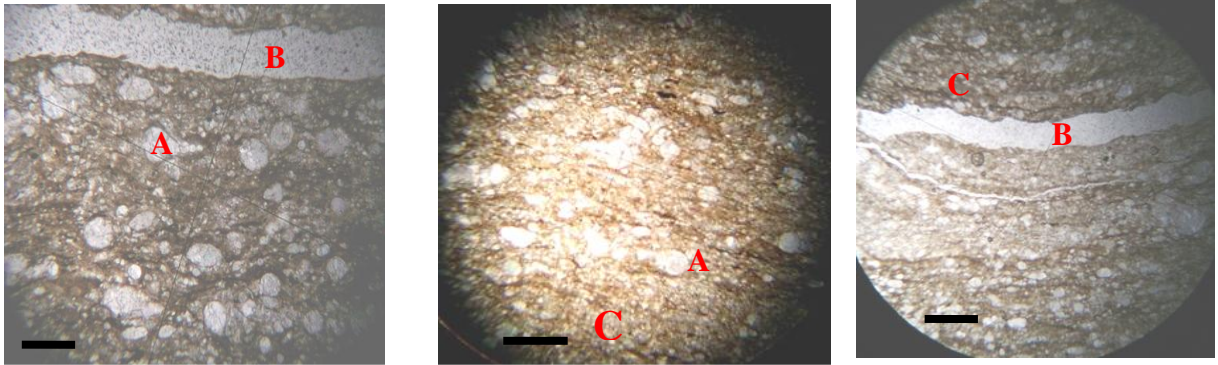


Figure 4.49: Photomicrograph of OT.5.4 (A) Planktic foraminiferal tests (B) Neomorphic spar (C) Micrite (microcrystalline calcite and kaolinite) (Bar scale = 2 mm Magnification:  $\times 50$  Resolution: (150 dpi))

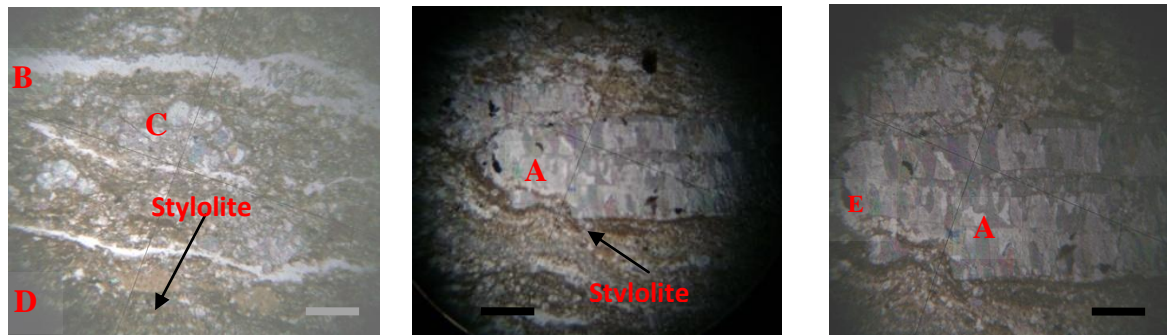


Figure 4.50: Photomicrograph of OT.5.5 (A) shells of *Inoceramus labiatus* (B) Neomorphic spar (C) Planktic foraminiferal tests (D) Micrite (microcrystalline calcite and kaolinite) (E) Iron oxide appearing as dark stains on the skeletal fragments (Bar scale = 2 mm Magnification:  $\times 50$  Resolution: (150 dpi))



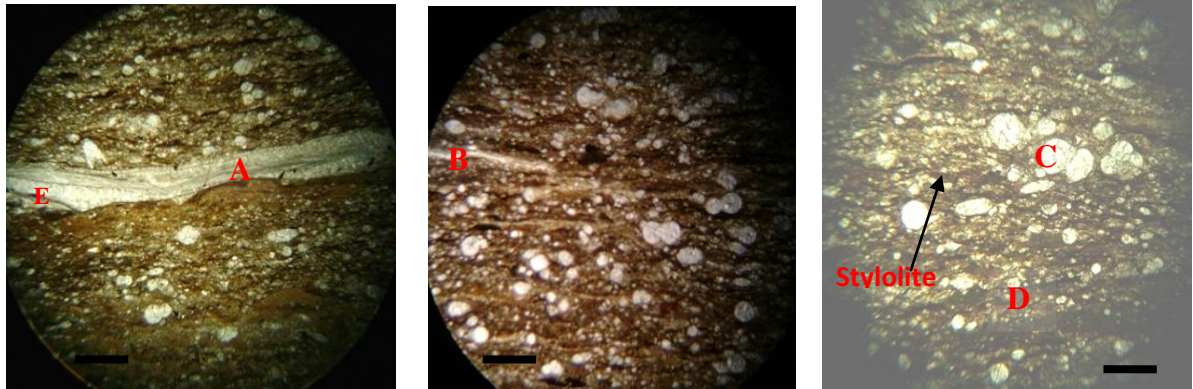


Figure 4.51: Photomicrograph of OT.8.2 (A) shells of *Inoceramus labiatus* (B) Neomorphic spar (C) Planktic foraminiferal tests (D) Micrite (microcrystalline calcite and kaolinite) (E) Iron oxide appearing as dark stains on the skeletal fragments (Bar scale = 2 mm Magnification:  $\times 50$  Resolution: (150 dpi))

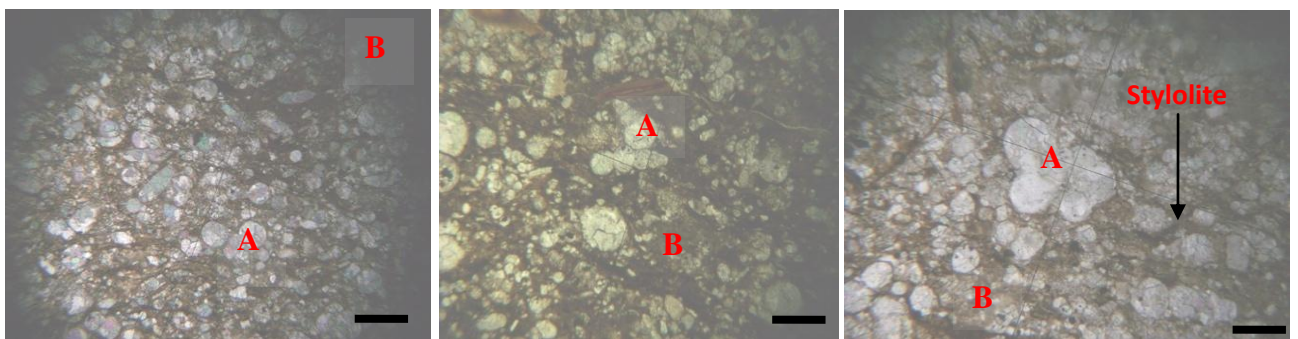


Figure 4.52: Photomicrograph of OT.8.4 (A) Planktic foraminiferal tests (B) Micrite (microcrystalline calcite and kaolinite) (Bar scale = 2 mm Magnification:  $\times 50$  Resolution: (150 dpi))

Table 4.11: Petrographic attributes of selected samples of the carbonaceous rocks

SAMPLE NO.	ALLOCHEM (%)	MICRITE (%)	SPAR	DIAGENETIC FEATURES
OT 1.1 (Figure 4.42)	Tests of <i>hedbergellids</i> , <i>heterohelicids</i> . <i>Inoceramus labiatus</i> bivalve. Mud supported. Calcite grains are euhedral to subhedral 30 %	Clay (Kaolinite), quartz and calcite mineral laminae 50%	20%	Neomorphism of micrite to spar, presence of iron oxide, microinterparticule porosity
OT 3.1 (Figure 4.43)	Tests of <i>hedbergellids</i> , <i>heterohelicids</i> . Mud supported. Calcite grains are euhedral to anhedral 25%	Clay (Kaolinite), quartz and calcite mineral laminae 60%	15%	Neomorphism of micrite to spar, microinterparticule porosity
OT 4.1 (Figure 4.44)	Tests of <i>hedbergellids</i> , <i>heterohelicids</i> . Mud supported. Calcite grains are euhedral to subhedral 35%	Clay (Kaolinite), quartz and calcite mineral laminae 50%	15%	Neomorphism of micrite to spar, stylolites, microinterparticule porosity
OT 5.1 (Figure 4.45)	Tests of <i>hedbergellids</i> , <i>heterohelicids</i> . Mud supported. Calcite grains are euhedral to subhedral 40%	Clay (Kaolinite), quartz and calcite mineral laminae 50%	10%	Neomorphism of micrite to spar, stylolites, microinterparticule porosity
OT 5.2 (Figure 4.46)	Tests of <i>hedbergellids</i> , <i>heterohelicids</i> . Mud supported. Calcite grains are euhedral to subhedral 40%	Clay (Kaolinite), quartz and calcite mineral laminae 55%	5%	Neomorphism of micrite to spar, microinterparticule porosity
OT 5.3 (Figure 4.47)	Tests of <i>hedbergellids</i> , <i>heterohelicids</i> . Mud supported. Calcite grains are euhedral to anhedral 25%	Clay (Kaolinite), quartz and calcite mineral laminae 65%	10%	Neomorphism of micrite to spar, stylolites, microinterparticule porosity
OT5.4 (Figure 4.48)	Tests of <i>hedbergellids</i> , <i>heterohelicids</i> . Mud supported. Calcite grains are euhedral to subhedral 30%	Clay (Kaolinite), quartz and calcite mineral laminae 50%	20%	Neomorphism of micrite to spar, microinterparticule porosity

OT 5.5 (Figure 4.49)	Tests of <i>hedbergellids</i> , <i>heterohelicids</i> . <i>Inoceramus labiatus</i> bivalve. Mud supported. Calcite grains are euhedral to anhedral 45%	Clay (Kaolinite), quartz and calcite mineral laminae 35%	20%	Neomorphism of micrite to spar, presence of iron oxide, stylolites, microinterparticule porosity
OT 8.2 (Figure 4.50)	Tests of <i>hedbergellids</i> , <i>heterohelicids</i> . <i>Inoceramus labiatus</i> bivalve. Mud supported. Calcite grains are euhedral to anhedral 35%	Clay (Kaolinite), quartz and calcite mineral laminae 55%	10%	Neomorphism of micrite to spar, presence of iron oxide, stylolites, microinterparticule porosity
OT 8.4 (Figure 4.51)	Tests of <i>hedbergellids</i> , <i>heterohelicids</i> <i>Bolivina</i> . Mud supported. Calcite grains are euhedral to anhedral 65%	Clay (Kaolinite), quartz and calcite mineral laminae 25%	10%	Neomorphism of micrite to spar, stylolites, microinterparticule porosity

#### 4.10 Discussion of Results: Paleoenvironment of Deposition of the Lokpanta Shale

Lithofacies description of the Lokpanta Shale reveal the rhythmic alternation of the marlstones and calcareous shales (see Figures 4.15, 4.20, 4.24, 4.26 and 4.28). This indicates variations in sediment flux and frequent oscillations of the bottom water conditions during the deposition. The dark colour, calcareous nature of the facies, the thin laminations, the presence of sideritic/pyritic concretions, the lack of burrows and the dominantly planktic foraminiferal assemblage, are indicative of a quiet water, anoxic shallow marine environment (Cooks and Corboy, 2003; Essien and Bassey, 2012; Njoh and Taku, 2016).

Ehinola *et al.* (2003) also inferred shallow marine shelf environment of deposition based on the presence of *Heterohelix* and *Hedbergella* tests. The abundance of the calcareous planktic and rare benthic foraminiferal content as observed from the thin sections (Figures 4.43-4.52) suggest a shallow marine environment. Tucker and Wright (1990) stated that presence of abundant calcareous foraminifera (high biogenic productivity) in rocks is indicative of shallow marine deposition.

This depositional setting is consistent with epicontinental sea condition, which prevailed in the Benue Trough during the Cenomanian-Turonian period (Ekweozor and Petters, 1982; Ehinola *et al.*, 2003 and Ekweozor, 2005).

Macrobenthic bivalves such as *Inoceramus labiatus* present as a monospecific bivalve assemblage occur in large abundance in the calcareous shales and marlstones. Their occurrence may suggest a possibly stressed and anoxic bottom water environment (Hallam, 1982). The presence of depauperate ammonites further support a stressed anoxic shallow marine depositional setting.

The presence of kaolinite in the rocks from x-ray diffraction result indicates nearness to shoreline (shallow marine). The mineral is known to concentrate in many near-shore sediments and decrease in abundance with distance from shoreline (Parham, 1966). Robert and Kennett (1994) reported that increased kaolinite contents in marine sediments resulted either from increased runoff, which could be caused by sea level fall.

The lithofacies identified in the Lokpanta Shale are 1) Dark grey calcareous shale facies and 2) Light grey platy marlstone facies. The two (2) lithofacies have been grouped into a lithofacies association and lithofacies succession due their repetitive nature. The lithofacies association/succession is the **Anoxic Shallow Marine Association**. This lithofacies association represents low energy, repetitive sedimentation flux, shallow marine setting. The depositional setting is therefore anoxic, inner - middle shelf setting.

The major oxides were compared to the average shale worldwide (Pettijohn, 1957), NASC (North American Shale Composite) (Gromet *et al.*, 1984) PAAS (Post Archaean Australian Shale) (Taylor and McLennan, 1985). The SiO<sub>2</sub> values from this present study range from 19.00 – 58.80 % (averaging 41.75 %) (see Table 4.2). Its average value is lower than those of the average for shales worldwide, NASC and PAAS (58.10 %, 64.82 % and 62.08 % respectively). This depletion can be attributed to the enrichment of the other major oxide such as CaO, which suggests a marine character for the depositional environment of the rocks.

The Al<sub>2</sub>O<sub>3</sub> values range from 3.75 – 15.30 % (averaging 9.96 %). Its average value is lower than those of the average for shales worldwide, NASC and PAAS (15.4 %, 17.05 % and 18.90 % respectively). This depletion can also be attributed to the enrichment of CaO, which

indicates marine character. The  $\text{Al}_2\text{O}_3$  content is attributed to terrestrial input to the depositional environment (Sari and Koca, 2012).

The CaO values range from 5.17 – 48.68 % (averaging 24.01 %). Its average value is higher than those of the average for shales worldwide, worldwide, NASC and PAAS (3.10 %, 3.51 % and 1.30 % respectively). This enrichment strongly implies marine character for the depositional environment. The combined average value of  $\text{SiO}_2$ ,  $\text{Al}_2\text{O}_3$  and CaO for the Lokpanta Shale is 75.72%.

The ratio of  $\text{SiO}_2/\text{Al}_2\text{O}_3$  ranges from 2.99-7.64, averaging 4.67 (see Table 4.4). This value is higher than the average for shales worldwide, NASC and PAAS, which are 3.77, 3.88 and 3.28 respectively. The average value of the ratio indicates high silica to alumina content (El-wekeil and Abou El-Anwar, 2013; Popoola *et al.*, 2014). This high  $\text{SiO}_2/\text{Al}_2\text{O}_3$  ratio coupled with the negative correlation of  $\text{SiO}_2$  against  $\text{Na}_2\text{O}$  and  $\text{K}_2\text{O}$  (see Table 4.5) indicates high siliceous content and therefore a tendency towards terrestrial conditions.

The value of  $\text{Al}_2\text{O}_3/\text{MgO}$  ratio in the rocks range from 3.21- 6.99 (averaging 4.94). This is low compared to average ratio for shales worldwide, NASC and PAAS which are 6.41, 6.04 and 8.59 respectively, and indicates high alumina content and terrestrial input to the environment of deposition.

The values of the  $\text{Na}_2\text{O}/\text{K}_2\text{O}$  ratio range from 0.01-0.57 (average 0.10). This average is lower than those for the average shale worldwide (0.40), NASC (0.31) and for PAAS (0.32). This ratio, coupled with the negative correlation between  $\text{SiO}_2$  and  $\text{Na}_2\text{O}$ ,  $\text{K}_2\text{O}$  (see Table 4.5) strongly indicate that silica content is incorporated in the quartz component of the rock (see Table 4.1). Madukwe and Bassey (2015) stated that ratio of  $\text{Na}_2\text{O}/\text{K}_2\text{O}$  less than unity (1)



indicates incorporation of these elemental oxides to the clay component of the rock, thus suggesting marine input in the depositional environment.

The values of  $\text{Fe}_2\text{O}_3$  in the rock vary from 1.75 to 7.59 % (average 4.94 %). The average  $\text{Fe}_2\text{O}_3$  content is higher than those of the average shale worldwide and PAAS (4.02 % and 0.11 % respectively) but lower than for NASC (5.70 %). The relative depletion of the  $\text{Fe}_2\text{O}_3$  content and positive correlation of  $\text{Fe}_2\text{O}_3$  and CaO content of the rocks indicate they were deposited in an oxygen reducing marine environment. Sari and Koca (2012) stated that any oxide with a positive correlation with CaO indicate marine character for the depositional environment.

The values of  $\text{SO}_3$  in the rock range from 0.06-1.88 % (average 0.77 %). The average value of  $\text{SO}_3$  in the rock is higher than those of average shale worldwide, NASC and PAAS as it was not detected in all. The enrichment of  $\text{SO}_3$  in the rock implies a reducing (anoxic) depositional environment. Raiswell (1976) and Ehinola *et al.* (2010) stated that the presence of sulphate or sulphide bearing minerals in strata suggests an anoxic depositional environment.

The concentrations of  $\text{SiO}_2$ ,  $\text{Al}_2\text{O}_3$  and  $\text{TiO}_2$  are indicators of terrestrial input or character. However, high concentration of CaO is an indicator of marine input or character (Sari and Koca, 2012; Hossein *et al.*, 2012, Oni *et al.*, 2014). Strong and moderate positive correlations of MgO with  $\text{SiO}_2$ , will indicate that the rock is of terrestrial input or character. Likewise, strong and moderate positive correlations of  $\text{Fe}_2\text{O}_3$ ,  $\text{K}_2\text{O}$ ,  $\text{Na}_2\text{O}$  and MnO with CaO, will infer marine input or character.

$\text{Al}_2\text{O}_3$  present in the rocks has a strong positive correlation with  $\text{SiO}_2$  and  $\text{MgO}$ ,  $\text{TiO}_2$  (Table 4.5 and Figures 4.35b, c and f). This indicates that  $\text{SiO}_2$ ,  $\text{Al}_2\text{O}_3$ ,  $\text{MgO}$  and  $\text{TiO}_2$  are of terrestrial character.

However, there are strong negative correlations between  $\text{Al}_2\text{O}_3$  and major oxides,  $\text{CaO}$  (-0.94),  $\text{MnO}$  (-0.95),  $\text{K}_2\text{O}$  (-0.57) and  $\text{Fe}_2\text{O}_3$  (-0.47) which indicates opposing depositional characteristics, marine depositional setting (Table 4.5, Figures 4.35 a, d, e and g).

Furthermore, the strong positive correlations between  $\text{CaO}$  and  $\text{MnO}$  (0.91), mild positive correlation with  $\text{Fe}_2\text{O}_3$  and  $\text{K}_2\text{O}$  and slight correlation with  $\text{Na}_2\text{O}$  indicates marine depositional setting. (Table 4.5, Figures 4.36 a, b and c).

The concentrations of  $\text{Al}_2\text{O}_3$ ,  $\text{Fe}_2\text{O}_3$ ,  $\text{MgO}$ ,  $\text{MnO}$ ,  $\text{K}_2\text{O}$  and  $\text{TiO}_2$  are very low apart from  $\text{SiO}_2$  but the concentrations of  $\text{CaO}$  are generally high (Table 4.2). This implies that there are terrigenous inputs in a marine setting. The foregoing strengthens the inference that the carbonaceous rocks were deposited in a shallow marine shelfal environment.

The strontium (Sr) content of the rock ranges from 49.65 to 243.96 ppm, (see Table 4.6) with an average of 159.70 ppm. The amount of “Sr” present in the carbonaceous rocks has direct relation with the amount of clay since clay minerals have properties of absorption of (Sr) Strontium. Sr content greater than 100 ppm is indicative of marine environment (Degens, 1958; Westphal and Munnecke, 2003; Elricke and Hinnov, 2007 and Hossein *et al.*, 2012). The range of values of the Sr content of the rock indicates marine depositional environment.

Microfloral assemblage (see Figure 4.37) from the rock exhibited low abundance and diversity of miospores such as *Longapertites marginatus*, *Fungi*, *Psilatricolporites*,

*Verrucatosporites Polypodiaceoisporites, Leoitriletes, Sphaeromorph acritarch,*  
*Leoisphaeridia spp and Laevigatosporites.* The pollens were *Ephedripites regularis*  
and *Triorites spp.*

The predominance of these land-derived palynomorphs suggests sediment deposition was in a proximal transitional environment (Schrank, 1994). Whitaker (1984) uses the term 'palynomaceral' to refer to these coal maceral categories of organic particles. According to Batten and Stead (2005), palynofacies are "associations of palynological matter (PM) in sediments, considered primarily in terms of the reasons for their association, which is usually geological, but may be connected to the biological origin of the particles".

Palynomaceral is the term used to refer to all organic material, including both structured and unstructured fragments, that can be found in palynological preparations, excluding what are traditionally thought of as palynomorphs (organicwalled microfossils, such as pollen, spores, dinoflagellate cysts and acritarchs) (Tschudy, 1961). Palynodebris is another term which refer to palynomacerals (Manum, 1976; Habib, 1979; Tyson, 1984; Boulter & Riddick 1986; Pocock *et al.*, 1988; Mudie, 1989; van Bergren *et al.*, 1990).

Whitaker *et al.* (1992) and Batten (1996) recognized four palynomacerals with respect to buoyancy sizes and the distribution trends of palynomorphs in paleoenvironments. The composition of the palynomaceral assemblage can inform us about sediment source, transport and depositional processes (Batten 1996; Tyson and Follows 2000).

Palynomaceral size, shape, density and buoyancy influence how they are transported and deposited. PM-4 is more buoyant than PM-1, PM-2 and PM-3, and can be transported over longer distances (van der Zwan & van Veen 1978; Richelot & Streel 1985; van der Zwan 1990). The authors stated that buoyancy was related to sizes. PM-1, PM-2, PM-3 and PM-4 are primarily terrestrially derived, and their abundance and buoyancy are predicted to decrease with increasing distance from shore and water depth. Abundances of these four categories are expected to increase with increasing sedimentation rate, as sedimentation rates are usually higher near shore.

SOM is predicted to increase with increasing water depth and distance from shore and shelf/slope break, where burial of marine organic matter outweighs delivery and deposition of terrestrial organic matter. SOM which are yellow or gel-like suggest continental depositional environment while if the colour is grey, suggest marine depositional environment (Oboh, 1992). In general, amorphous material is best recovered in settings where the preservation potential is high (Tyson, 1993; Carvalho *et al.*, 2006).

Nearshore rocks show much higher abundances of PM-1 and PM-2, while offshore rocks show much higher abundances of PM-4 and SOM (Thomas *et al.*, 2015). Counts of PM-1, PM-2 and PM-3 increase with increasing sedimentation rate and shallower water depths.

(Palynomaceral 1, 2, 3 and 4) as well as Structureless Organic Matter (S.O.M) of the Lokpanta Shale were counted and quantified based on their percentages, sizes, buoyancy and distribution trends (Tables 4.9 and 4.12). PM-1, PM-2, PM-3, PM-4 and SOM values range from 59.00-75.00 %, 2.50-9.50 %, 1.00-2.00 %, 20.50-32.50 % and 1.00-3.50 % respectively.

Generally, all of the palynomacerals are of small to medium particle sizes. PM-1 and PM-4 have the highest abundance of the palynomacerals. The abundance of these palynomacerals, coupled with the particle sizes strongly suggest shallow (inner-middle shelf) marine environments. The presence of Structureless Organic Matter (SOM), greater than 1 % that shows slight enrichment, also suggest shallow marine setting. Figure 4.53 shows a paleodepositional model for the Lokpanta Shale.

Table 4.12: Palynomacerals and Their Compositional Percentages of the Lokpanta Shale

Kerogen Type	Range Of Values (%)	Particle Sizes	Paleoenvironmental Indications
PM-1	59.00 – 75.00	Small and medium	SHALLOW MARINE
PM-2	2.50 - 9.50	Small and medium	
PM-3	1.00-2.00	Small and medium	INNER-MIDDLE SHELF
PM-4	20.50 - 32.50	Predominantly small with subordinate medium particles	
SOM	1.00 - 3.50	--	

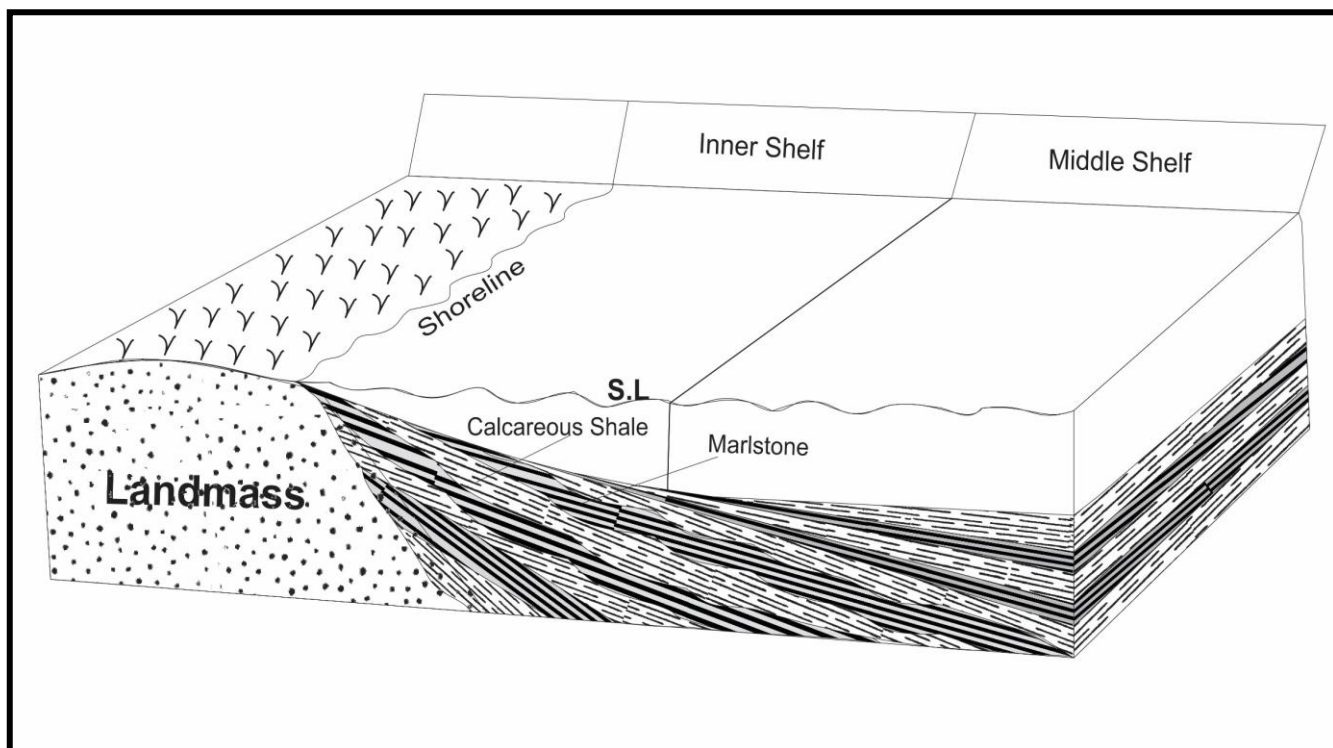


Figure 4.53: Block Paleodepositional model of the Lokpanta Shale

#### 4.11 Diagenesis

Two phases of diagenesis can be distinguished from the concretions in the Lokpanta Shale. This is evaluated using the shapes of the concretions, euhedral calcite grains, anhedral and sparry calcite attributes in the rocks representing early stage and late stage. Two types of concretions based on shapes occur: - spheroidal and ellipsoidal concretions (Raiswell, 1976). The Ezzaegu outcrop is dominated by ellipsoidal concretions while the spheroidal concretions dominate the Nmavu River and Lokpanta exposures. The ellipsoidal concretions indicate more compaction, less porosity and permeability while the spheroidal concretions indicate less compaction, more porosity and permeability. The early phase of diagenesis is characterized by relatively high  $\text{CaCO}_3$  content and the concretions are spheroidal in shape. This stage is related to the sulphate reduction zone in the sediment column. It is also characterized by high mud porosity, allowing the migration of carbonate-precipitating fluids in all directions (Raiswell, 1976). The late diagenetic phase is related to the zone of fermentation characterized by anisotropy imposed by compaction, causing the migration of fluids to become more parallel than normal to the bedding planes (Raiswell, 1976). The concretions will change shape from spheroidal to ellipsoidal (Figure 4.54) as the diagenetic changes in the rock progresses to the late stage of diagenesis. There is lower porosity and permeability at this later growth phase (Hallam, 1982).

The euhedral calcite grains noted in the photomicrographs (Figures 4.43-4.52) were probably formed as a result of recrystallization. Their formation may be due to passage of carbonate-rich water, which have sufficient time to precipitate out of solution along bedding planes as temperature and pressure increases. This can be inferred as late diagenesis (Raiswell, 1976; Agagu 1985). Likewise, anhedral calcite grains and sparry calcite are attributed to presence of



carbonate-rich water with insufficient time to percolate and a much more reduced temperature and pressure regimes. This is early diagenesis (Raiswell, 1976; Agagu, 1985). The induration of the rocks and the thin planar laminations are further evidence of the degree of compaction and dewatering which has taken place in the rocks.

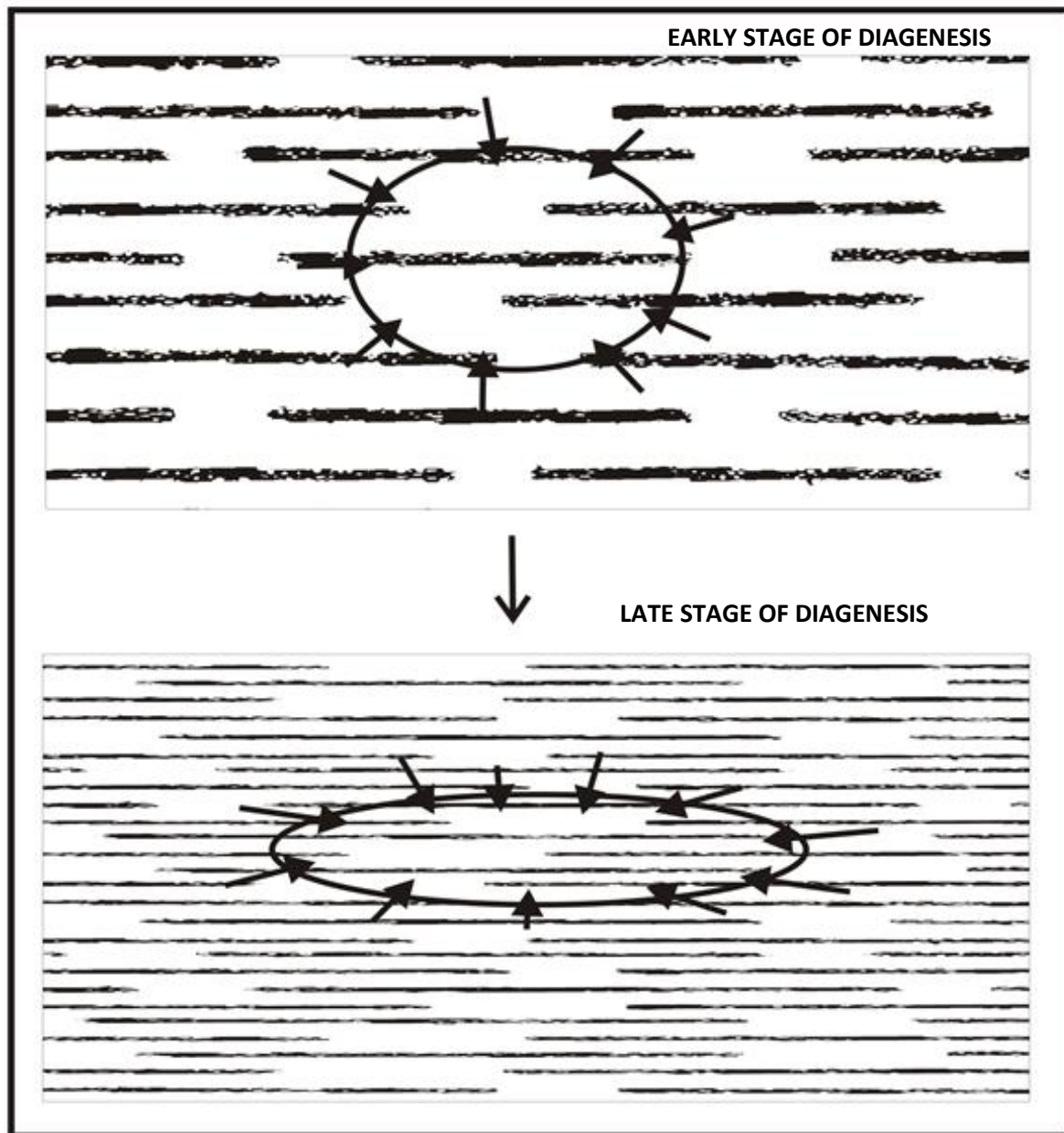


Figure 4.54: Early and Late stage of diagenesis and concretional growth. (after Raiswell, 1976)

#### 4.12 Age Determination

The dating of the Formation has been done using the fossil content- pollens, palynomorphs and foraminifera. The dominant palynomorphs in the rocks are *Ephedripites regularis* and *Triorites sp.* These indicate a Cretaceous age, especially Cenomanian-Turonian age (Jan Du Chene, 1978; Petters, 1980). *Triorites africanensis* has been used to mark the top of the Cenomanian age in West Africa (Jan Du Chene, 1978 and Petters, 1980). Amoke (2009) recovered a rich microfloral of *Hexaporotricolpites spp*, *Cretaceaepollenites sp*, *Ephedripites multicostatus*, *Ephedripites regularis*, *Ephedripites ambiguous*, *Araucariacites australis*, *Triorites sp*, *Monocolpites marginatus*, *Monosulcites sp*, *Cingulatisporites ornatus*, *Cyathidites australis*, *Spiniferites spp*, *Dinogymnium spp*, *Subtilisphaera spp*, *Gonyaulacysta spp*, *Tasmanites spp*, *Cleistosphaeridium spp* among others.

The foraminifera assemblage in the rocks include *Globigerinelloides caseyi*, *Heterohelix moremani*, *Eouvigerina gracilis* (Figures 4.43 - 4.52). These foraminifera were used to date the Lokpanta Shale as Cenomanian-Turonian (Amoke, 2009). He also recovered foraminiferal faunas such as *Hedbergella delrioensis*, *Hedbergella gorbachikae*, *Heterohelix moremani*, *Heterohelix globulosa*, *Globigerinelloides caseyi*, *Rugoglobigerina rugosa*, *Haplophragmoides sp.*, *Gavelinella sp.*, *Eponides morani* and *Bolivina sp.* An association of *Heterohelix moremani* and *Eouvigerina gracilis* was used to date rocks of Cenomanian age in the Gulf Coast of the United States and Brazil (Darmonian, 1975).

Ehinola *et al.* (2010) proposed a Lower Turonian age for the Lokpanta Shale based on mostly planktonic and very few benthonic foraminifera in the shale. The planktonic forms include *Heterohelix*, *Hedbergella*, *Wittheinella*, *Globotruncana* and *Pseudotextularia* while the

benthonic foraminifera are *Ammobaculites*, *Lenticulina*, *Gabonita*, *Dentalina*, *Gavelina*, *Pirebulimina* and *Eouvigerina*. *Heterohelix globulosa* predominates among others such as *Heterohelix reussi*, *H. pulchra* and *H. moremani*. *Hedbergella delrioensis* and *Hedbergella planispiral* dominate the genus *Hedbergella*. *Heterohelix moremani* ranges from Albian to Turonian in the US Gulf Coast (Pessagno, 1967) and in the Atlantic coastal plain of New Jersey (Petters, 1978) while in Libya, it is restricted to the late Cenomanian (Barr, 1972).

*Hedbergella delrioensis* and *Dorothia oxycona* were described from Cenomanian sediments in the Ituk-2 well (Fayose, 1979).

Petters (1980) dated the Eze-Aku Shale in Calabar Flank as Cenomanian-Turonian age based on microfauna comprising mostly *Ammobaculites* and few specimens of *Heterohelix moremani*, *H. reussi* and *Hedbergella delrioensis*. The marl bands contain a richer foraminiferal assemblage with *Heterohelix moremani*, *H. pulchra*, *Guembelitra harrisi*, *Hedbergella amabilis*, *H. delrioensis*, *H. planispira* and *Praebulimina fang*.

Iwobi (1991) established the Cenomanian stage in the Lower part of the Nkalagu Formation based on the co-occurrence of *Rotalipora balernaensis* and *Globigerinelloides caseyi*.

Bellier (1998) recorded the occurrence of *Whiteinella sp.*, *Ticinella sp.*, *Heterohelix moremani*, *Gavelinella sp.*, *Hedbergella gorbachikae*, *Hedbergella delrioensis*, *Bolivina sp.*, and *Bolivina anambra* while studying the Cenomanian-Santonian Cretaceous wells of Eastern Equatorial Atlantic.

While studying the foraminiferal assemblage and stable Isotopic change across the Cenomanian-Turonian boundary in the subtropical north Atlantic, Huber *et al.* (1999) also

recorded the occurrence of *Hedbergella delrioensis*, *Heterohelix globulosa*, *Hedbergella planispira* etc in the rocks of the area.

From the review and based on the occurrence of foraminifera such as *Globigerinelloides caseyi*, *Heterohelix moremani*, *Eouvirgerina gracilis*, it is proposed that the Lokpanta Shale is Late Cenomanian-Turonian in age

### **4.13 Paleogeography**

#### **4.13.1 Provenance and Paleoclimate**

Clay minerals are used in paleoclimate interpretation (Churchman, 2000; Islam *et al.*, 2002; Ghandour *et al.*, 2003 and Odoma *et al.*, 2013). Climatic conditions, hydraulic sorting and relative sea-level changes seem to be the major controlling factors for the clay mineral assemblage in shales (Ghandour *et al.*, 2003). Clay minerals susceptibility varies due to its structural and chemical compositions. The clay mineral identified in the shales and marlstones of the Lokpanta Shale is mainly kaolinite (Table 4.1, Figures 4.30 - 4.34 (a and b)).

Kaolinite is formed under specific environmental and chemical conditions that can help to interpret depositional/climatic conditions (Ghandour *et al.*, 2003 and Odoma *et al.*, 2013). Clay minerals in sediments can be useful indicators of paleoclimatic conditions and provenance, particularly when the sedimentary basins are small (Von Eynatten and Gaupp 1999). According to Churchman (2000), the two-layer/three-layer clay mineral ratio is mainly controlled by climate. Warm and humid conditions are typical for kaolinite formation (Chamley, 1989; Hallam *et al.*, 1991; Islam *et al.*, 2002; Ghandour *et al.*, 2003 and Odoma *et al.*, 2013).

The presence of kaolinite indicates warm, humid tropical climate for the source area where the sediments were derived. It further indicates that the rocks were deposited in marginal marine setting due to its hydraulic sorting (Ghandour *et al.*, 2003).

$\text{Al}_2\text{O}_3/\text{K}_2\text{O}$  ratio has been used to suggest precipitation (rainfall) rates (Aplin, 1993). If  $\text{Al}_2\text{O}_3/\text{K}_2\text{O}$  ratio is less than 1.00, then precipitation (rainfall) is low.  $\text{Al}_2\text{O}_3/\text{K}_2\text{O}$  ratio higher than 1.00, suggest high precipitation (rainfall). The ratio for the Lokpanta Shale vary from 0.97 to 16.28 (Average 8.22) (Table 4.4). This indicates that the precipitation (rainfall) was high.

The  $\text{Al}_2\text{O}_3/\text{TiO}_2$  ratio serves as a climate indicator for the provenance area (Maslov *et al.*, 2003). If  $\text{Al}_2\text{O}_3/\text{TiO}_2$  ratio is less than 20, then the climate is humid but if it is greater than 30, it is an arid climate. The values of  $\text{Al}_2\text{O}_3/\text{TiO}_2$  ratio from the Lokpanta Shale vary from 4.24 to 14.85 (average 9.80) (Table 4.4). This suggests that the climate was humid.

Provenance analysis reconstructs the source region, size and setting of the source region, climate and relief in the source region, the specific types of sedimentary rocks and the distance and transport direction travelled by the sediments (Pettijohn *et al.* 1987; Von Eynatten and Gaupp 1999).

The formation of kaolinite is favoured by acidic conditions, and highly leached environments. Table 4.1 and Figures 4.30 - 4.34 (a and b) present the clay type and other mineralogical constituents in the rocks and their distribution in the Lokpanta Shale. Kaolinite percentages range from 7.00-19.20 % (averaging 13.64 %). Its presence may be interpreted as due to

climate changes, depositional condition, erosional rate and the composition of the initial provenance rocks (Bruce, 1984; Odoma *et al.*, 2013).

The presence of kaolinite is favoured by weathering or hydrothermal alteration of aluminosilicate minerals (Bruce, 1984 and Odoma *et al.*, 2013). Rocks rich in feldspar commonly weather to kaolinite (Ghandour *et al.*, 2003). In order for kaolinite to form, Na, K, Ca, Mg, and Fe must initially be leached away by weathering or alteration process. This leaching is favoured by acidic conditions (low pH). Granitic rocks, because they are rich in feldspar, are common source for kaolinite (Odoma *et al.*, 2013). Thus, the provenance of the rocks can be inferred to be from a granitic domain.

Amajor (1987) used  $\text{Al}_2\text{O}_3$  vs.  $\text{TiO}_2$  plot to discriminate source rock of sedimentary rocks. A plot of  $\text{Al}_2\text{O}_3$ - $\text{TiO}_2$  for the Lokpanta Shale shows that the rocks were derived from mixed domain of granites and basalt (Figure 4.55 a). Hayashi *et al.* (1997) gave a range of  $\text{Al}_2\text{O}_3/\text{TiO}_2$  for sediments derived from different igneous rocks. The ratio for mafic magmatic rocks is 3-8 %, intermediate rocks, 8-21 % and felsic rocks, 21-70 %. The Lokpanta Shale has ratios ranging from 4.24 to 14.85 % (Table 4.13), suggesting that the rocks were derived from mafic magmatic (basic) to intermediate igneous rocks. The  $\text{TiO}_2$  bearing mineral phase may have been derived from felsic and basic rocks.

Since most elements are easily redistributed as a result of weathering and alteration, they must be carefully used in source determination. Plots of trace element against major oxides have been used as source indicators (Mader and Neubauer, 2004; Gabo *et al.*, 2009). Floyd and Leveridge (1987) used  $\text{K}_2\text{O}$  vs. Rb plot to discriminate sediments which are derived from

rocks of acidic to intermediate and basic rock composition in the Devonian Gramscatho basin. A  $K_2O$  vs Rb plot for the Lokpanta Shale reveals all the shales were derived from rocks of the acidic and intermediate rock composition (Figure 4.55 b).

Strong correlation between Chromium (Cr) and Nickel (Ni) and high concentrations of both elements have been used by several authors to determine sources of the sedimentary rocks (Hiscott 1984; Garver *et al.*, 1994, 1996). High Cr and Ni concentrations in shales reflect their incorporation into clay particles during weathering of chromite and other Cr- and Ti-bearing minerals in the mafic/ultramafic rocks (Garver *et al.*, 1996). Weak correlation between Cr and Ni indicates that the rocks containing these elements are of felsic composition (Garver *et al.*, 1996). The Cr content of the rocks ranges from 11.06 to 123.90 ppm (averaging 61.12 ppm) and the Ni content, from 16.43 to 72.59 ppm (averaging 50.36 ppm). The plot of Cr and Ni contents of the Lokpanta Shale reveal lower enrichment of Ni with respect to Cr (Figure 4.56). Cr vs Ni plot shows weak but positive correlations ( $r=0.41$ ) (Figure 4.57). These indicate that the sediments were derived from granitic or felsic terrain, following Garver *et al.* (1996).

The Lokpanta Shale was therefore sourced from granitic/intermediate rocks, in wet humid climate. The most probable direction of granitic/intermediate provenance is from east of the basin (Abakaliki Anticlinorium) due to its composition of the rocks and proximity of the study area. Figure 4.58 shows a paleogeographic sketch map for the Cenomanian-Turonian indicating the provenance area of the Lokpanta Shale.

Table 4.13: Al<sub>2</sub>O<sub>3</sub>/TiO<sub>2</sub> ratio of the Lokpanta Shale and their critical values

Sample No.	Al <sub>2</sub> O <sub>3</sub> / TiO <sub>2</sub>
LK 5 (1)	5.37
LK 5 (4)	5.43
LK 8(7)	4.24
LK 8 (18)	6.13
EZZ 1	13.64
EZZ 2	14.85
EZZ 3	13.71
EXLK2	11.52
EXLK 3	12.73
EXLK 5	10.33
MAFIC MAGMATIC*	3.00-8.00
INTERMEDIATE*	8.00-21.00
FELSIC*	21.00-70.00

\*Range of Al<sub>2</sub>O<sub>3</sub>/TiO<sub>2</sub> values for different igneous rock composition (after Hayashi *et al.*, 1997)



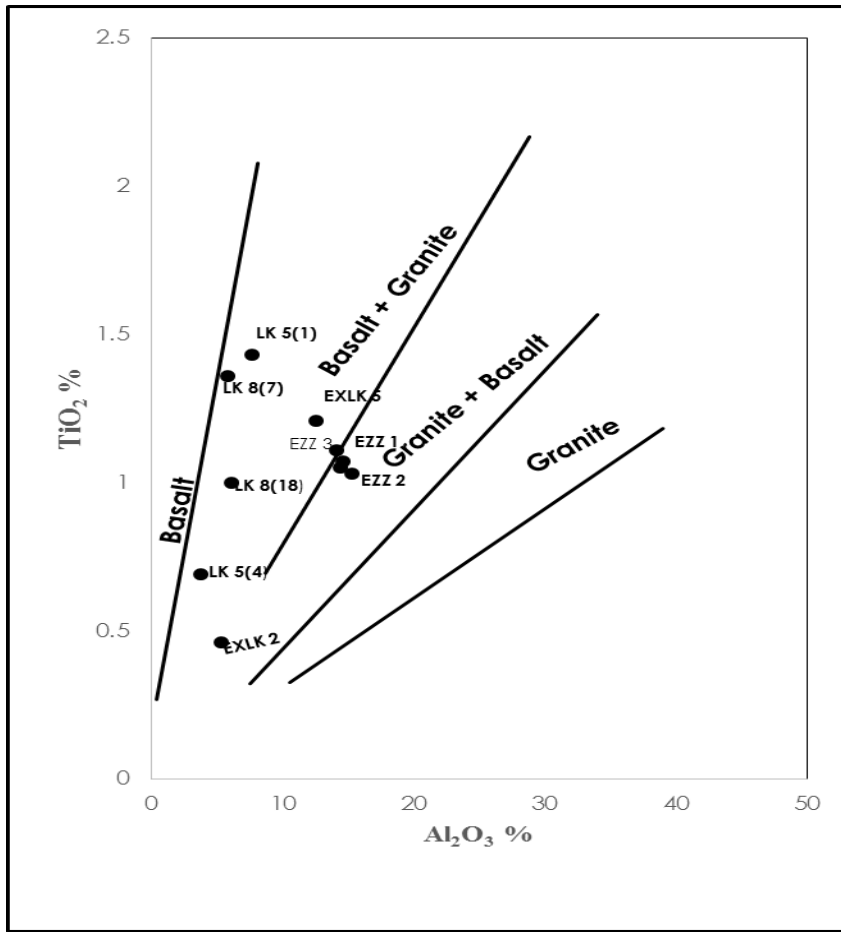


Figure 4.55a:  $\text{TiO}_2$  versus  $\text{Al}_2\text{O}_3$  diagram for the Lokpanta Shale

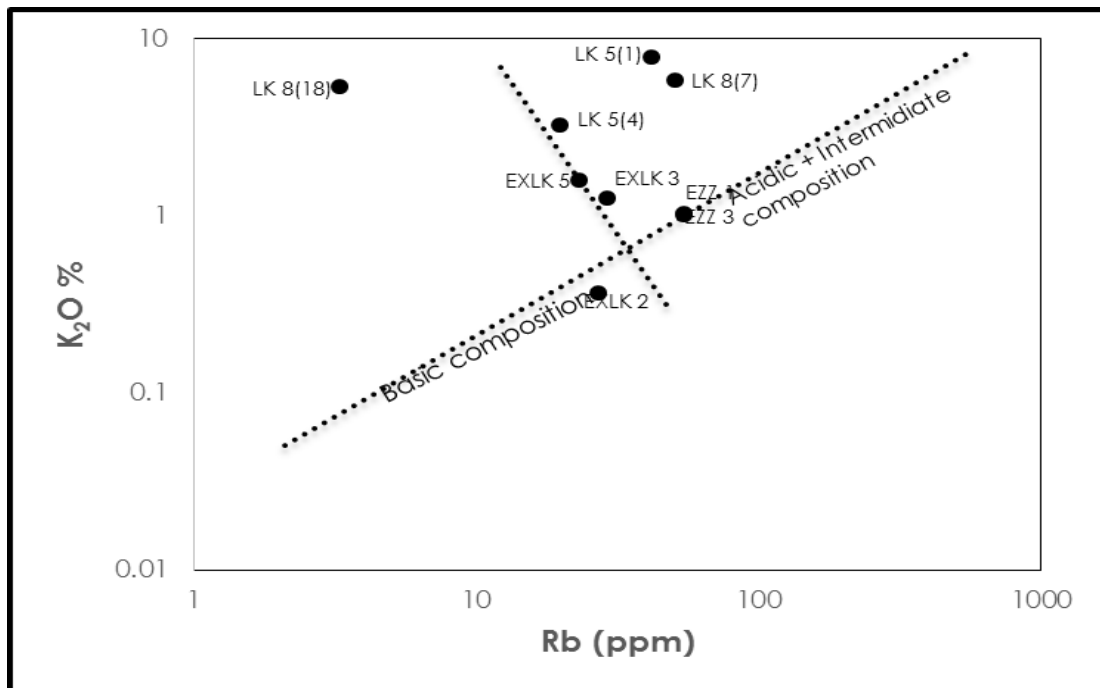


Figure 4.55b:  $\text{K}_2\text{O}$  vs Rb diagram showing the rocks are granitic/intermediate

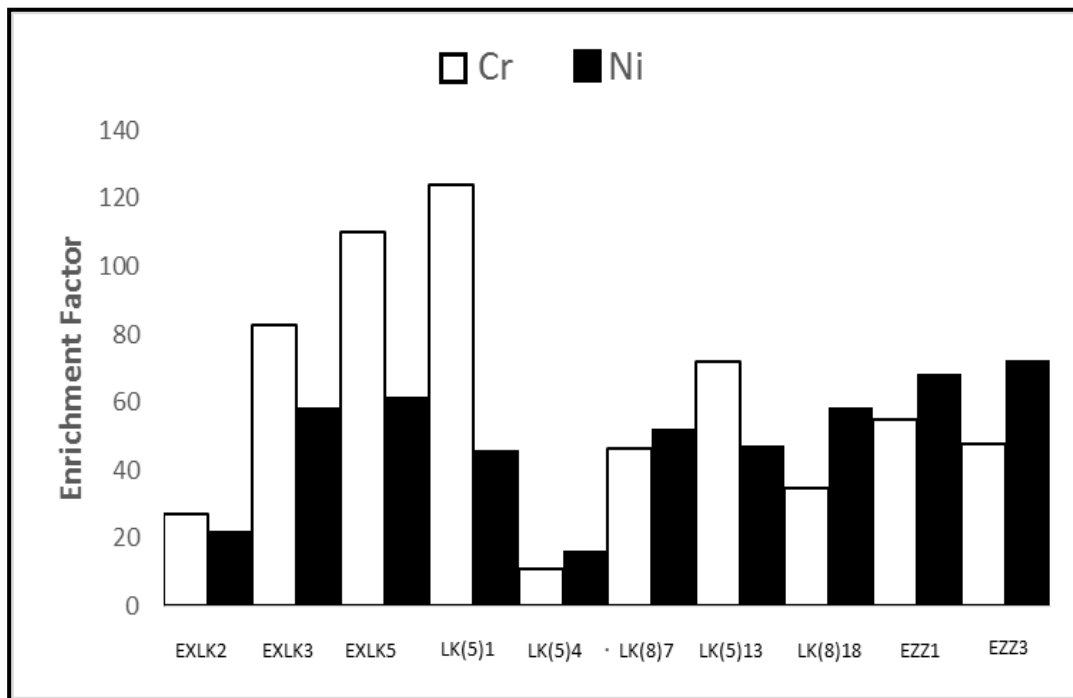


Figure 4.56: Cr and Ni enrichment factors showing Cr enrichment relative to Ni in the rocks

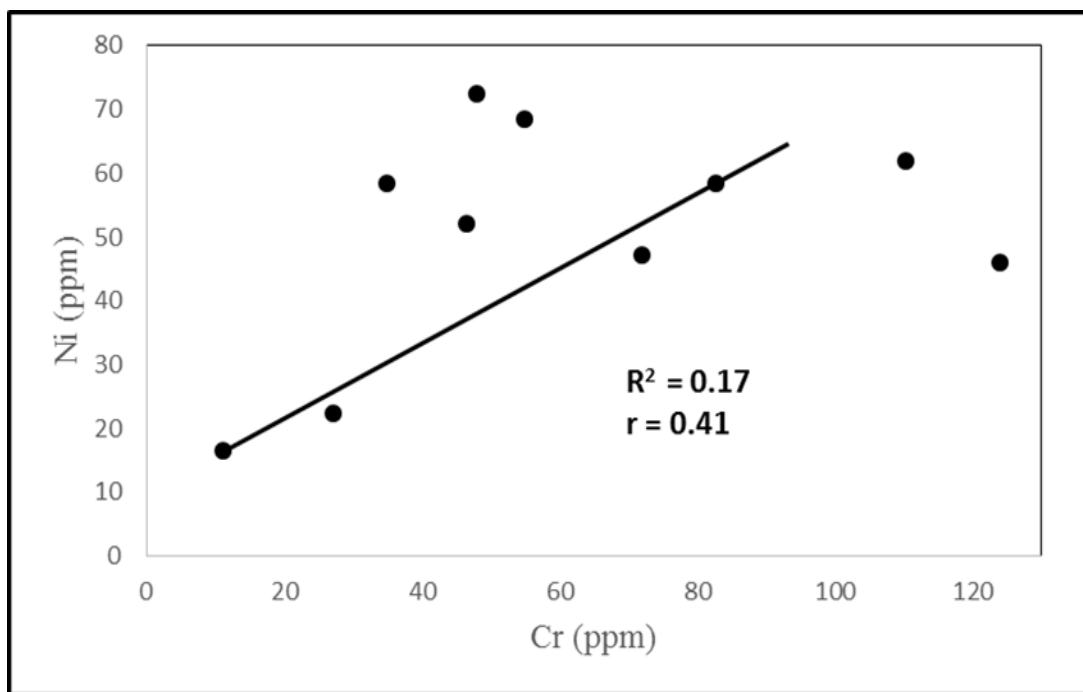


Figure 4.57: Correlation of Cr and Ni contents of the rock showing weak but positive

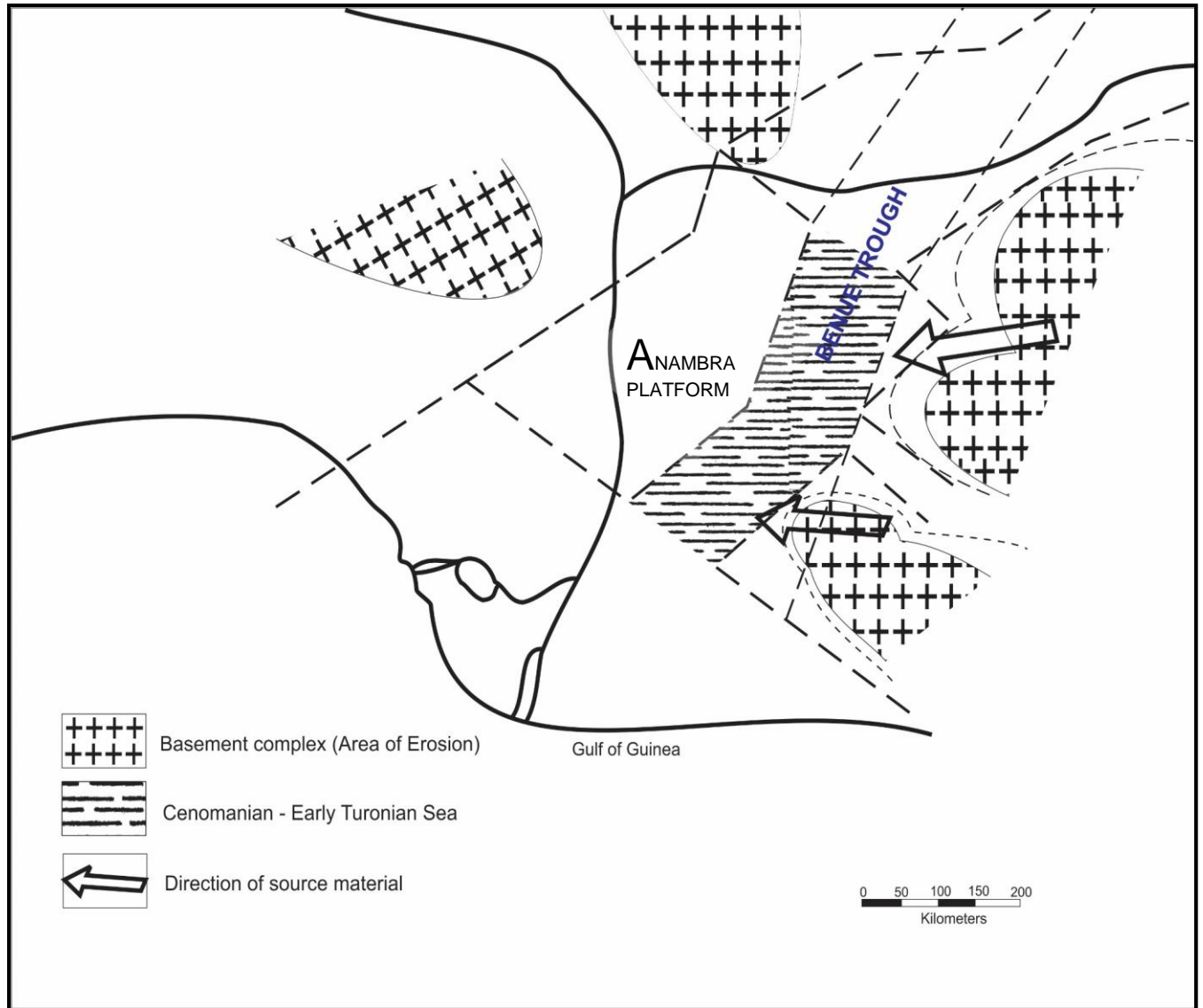


Figure 4.58: Paleogeographic Model of the Cenomanian – early Turonian Time.

#### 4.13.2 Paleoweathering

Weathering is described as a complex interaction of physical, chemical and biotic processes which alter and disintegrate the rocks at the surface or close to the surface of the earth (Selby, 1993). Chemical weathering of rocks is one of the major processes that modify the earth's surface and is one of the vital processes in the geochemical cycling of elements (Berg, 1932). The rate and nature of chemical weathering vary widely and are controlled by many variables such as parent rock type, topography, climate and biological activity (Islam *et al.*, 2002). Chemical weathering indices are commonly used in recent and old weathering profile studies (Kirschbaum *et al.*, 2005; Goldberg and Munir Humayun, 2010). Weathering index and chemical alteration index are used to measure the degree of weathering of the terrestrial land from which sediments are derived (Kronberg and Nesbitt, 1981 and Nesbitt and Young, 1982).

The degree of compositional maturity of shales is estimated from weathering index following Kronberg and Nesbitt (1981). In the erosion index plot of  $(\text{Na}_2\text{O}+\text{K}_2\text{O})/(\text{Al}_2\text{O}_3+\text{Na}_2\text{O}+\text{K}_2\text{O})$  vs  $(\text{SiO}_2+\text{Na}_2\text{O}+\text{K}_2\text{O})/(\text{SiO}_2+\text{Al}_2\text{O}_3+\text{Na}_2\text{O}+\text{K}_2\text{O})$ , it is shown that the rock samples from the Ezzaegu (EZZ) and Lokpanta Junction (EXLK) areas plotted in the Kaolinite Field while the rock samples from the Nmavu River channel (LK) plotted within the K-feldspar Field (Figure 4.59). The  $\text{K}_2\text{O}/\text{Al}_2\text{O}_3$  ratio of rocks can be used as an indicator of the original composition of ancient rocks. Cox *et al.* (1995) showed that  $\text{K}_2\text{O}/\text{Al}_2\text{O}_3$  ratios for clay minerals and feldspars differ. For clay minerals, the ratio is 0.00 to 0.30, and for feldspars, 0.30 to 0.90. The rocks under study has  $\text{K}_2\text{O}/\text{Al}_2\text{O}_3$  ratios from 0.06 – 1.02 (averaging 0.43) (see Table 4.4). These indicate the presence of clay mineral and feldspar within the lower limit of their ranges

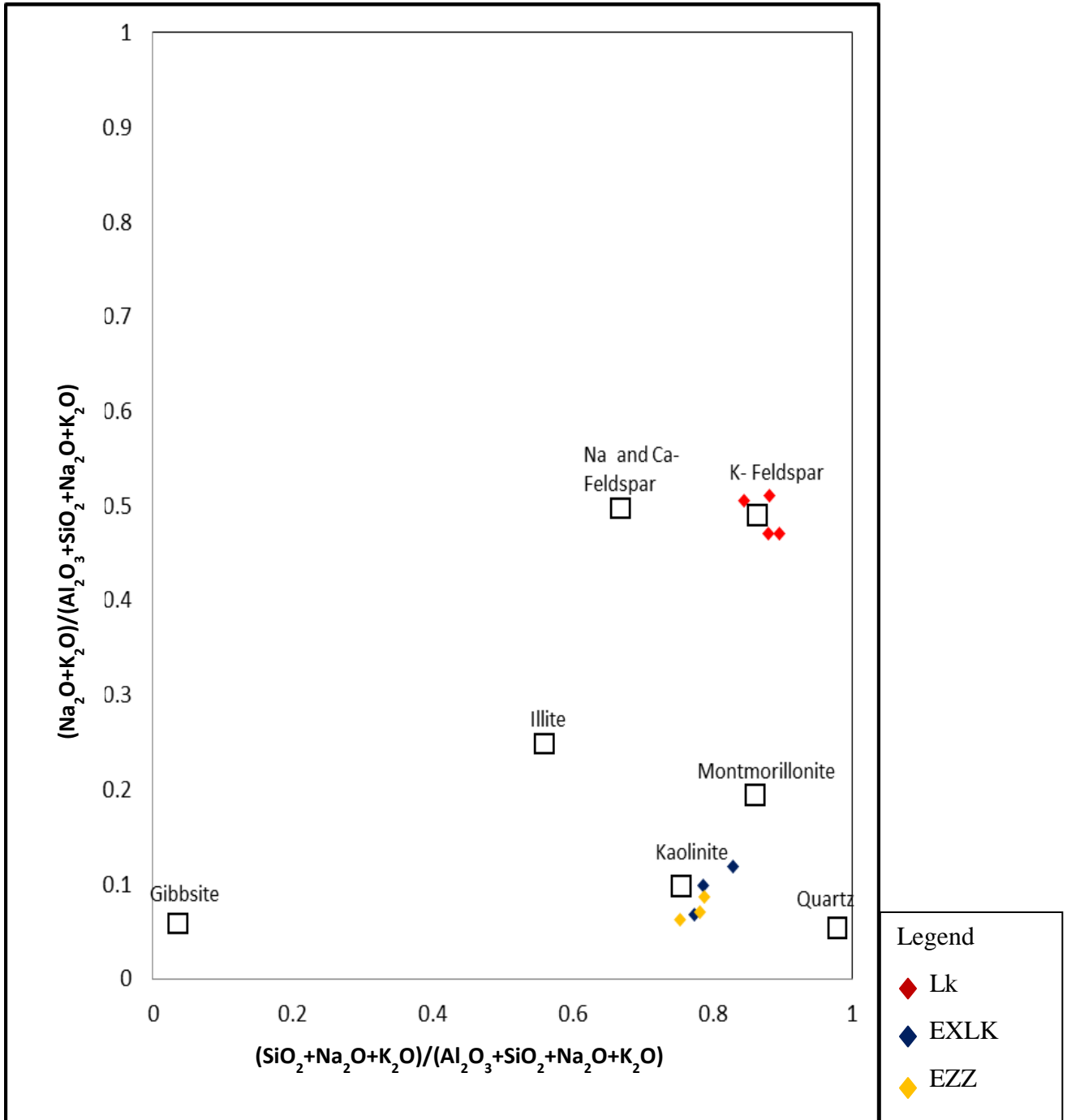


Figure 4.59: Plot of Weathering Index of the Lokpanta Shale showing degree of weathering of the source area of the rocks.

(Kaolinite and Orthoclase). This agrees with the erosion index plot as the rock samples plotted within the Kaolinite and K-feldspar (Orthoclase) domains.

Fedo *et al.* (1995) and Mishra and Sen (2012) stated that the presence of kaolinite implies that the chemical weathering in the source area was active, having a gentle topography with humid and warm climatic condition. Alternatively, the authors stated that the presence of feldspars indicate a source area possessing a high topography, inactive chemical weathering with arid to semi-arid climatic condition. According to Adeigbe and Jimoh (2013), the presence of clay minerals in rocks suggest they are texturally mature while the presence of feldspars infers textural immaturity. This is the most plausible case for the Lokpanta Shale.

Thus, the presence of kaolinite, a weathering product of potassium feldspar, indicates that the chemical weathering of the source area of the rocks within the Ezzaegu and Lokpanta Junction areas was active and intense. It also indicates the source area has gentle topography with humid and warm tropical climate. These sections of the stratigraphic unit are geochemically and texturally mature. The K-feldspars found in the samples from the Nmavu River Channel, indicate that the chemical weathering of source area was very weak and or inactive. It may further indicate that the source area possesses an active topography, with arid climatic condition. The Lokpanta shale may have alternating climatic and weathering conditions. This assertion is not the most plausible case for the Lokpanta Shale. This portion of the stratigraphic unit can be termed geochemically and texturally immature due to the primary mineral(s); feldspars, being present. Madukwe and Bassey (2015) suggested the difference in degree of chemical weathering may be due to sediment sorting, fractionation or sediment supply from the pre-existing rocks. The difference in the degree of chemical weathering of the source area of the Lokpanta Shale may be due to these factors.

The chemical composition of the various weathering products depends largely upon the rock types and degree of weathering (Singh *et al.*, 2005). The degree of weathering of rocks can be demonstrated by the well-established concepts on mobility of various elements during weathering and thus can be used to assess the state of chemical weathering (Singh *et al.*, 2005). The preferential removal of Ca, Na and K by solution during weathering processes (Nesbitt *et al.*, 1980) due to their high mobility means that the abundance of these elements with respect to less easily removed elements can be used as a measure of the extent of chemical weathering in provenance area. In feldspars, aluminum (Al) is the least mobile element, Nesbitt and Young (1982) proposed a chemical index of alteration (CIA) where:  $CIA = [Al_2O_3 / (Al_2O_3 + CaO^* + Na_2O + K_2O)] \times 100$ . Where CaO\* represents CaO associated with the silicate fraction of the rock sample.

The CaO\* concentration was calculated based on the following: (a) if the concentration of CaO was less than or equal to the concentration of Na<sub>2</sub>O in the sample, then CaO\*=CaO (b) if the CaO concentration was higher than the Na<sub>2</sub>O concentration, then it is assumed that the CaO\*= Na<sub>2</sub>O (Bock *et al.*, 1998; Újvári *et al.*, 2008 and Liua *et al.*, 2013).

The CIA enables the intensity of weathering in source areas to be estimated. It may be used to compare the relative proportions of chemically weathered material present in a rock sample. CIA value of 0-50 indicates very weak chemical weathering, CIA of 50-60 indicates weak chemical weathering degree, while CIA of 60-80 indicates moderate degree of weathering and CIA of 80-100 indicates intensive weathering (Nesbitt and Young, 1982).

In the investigated rocks, the calculated CIA values range from 87.03 – 93.20 for the Ezzaegu (EZZ) and Lokpanta Junction (EXLK) outcrop samples and 48.60-52.50 for the Nmavu River

channel (LK) samples (Figure 4.60). These indicate that the source area of the Lokpanta Shale experienced very weak to intense weathering. Nyakairu and Koeberl (2001) showed that intense weathering depletes feldspars in source area and increase of clay minerals. This also agrees with the erosion index plot (Figure 4.59). Weakly to very weakly weathered source area indicates presence of feldspars in the rocks (Nyakairu and Koeberl, 2001). The variation in the intensity of weathering index shown in Figure 4.60 may indicate alternating climatic conditions during the depositional history of the Lokpanta Shale. This may not be plausible.

Also, intense weathering of the source area suggests a prolonged transport across the basin margin while weak weathering infers a proximity to basin margin (Asiedu *et al.*, 2005). Thus, the variation in the intensity of weathering (Figure 4.59) leads to the inference of differing distances of the sediments derived from the source area from the basin margin.

The Mineralogical Index of Alteration (MIA) is another weathering parameter proposed by Voicu *et al.* (1997). The Mineralogical Index of Alteration (MIA) indicates the degree of weathering for the source area, independent of the depth of sampling. According to Voicu *et al.*, (1997)  $MIA = 2 \times (CIA - 50)$ . The ranges of MIA values indicate incipient 0 – 20 %, weak 20 – 40 %, moderate 40 – 60 %, and intense to extreme 60 - 100% weathering. 100% MIA means complete weathering of a primary material into its equivalent weathered product (Voicu and Bardoux, 2002).

The MIA for the studied rock samples ranges from -2.80 – 5.00 % for the Nmavu River channel samples (LK), 74.04 - 86.36% for the Ezzaegu (EZZ) and Lokpanta Junction (EXLK) samples (Figure 4.61). These values indicate incipient weathering of the source area (LK)



samples and extreme weathering of the source area (EXLK and EZZ) samples. The Nmavu River (LK) samples plotted in the incipient weathering domain, which implies that the primary mineral(s) from the source area were not weathered. The Lokpanta Junction samples (EXLK) and Ezzaegu samples (EZZ) plotted in the intense to extreme weathering domain, which strongly indicate complete weathering of the primary mineral(s) of the source area into its equivalent weathered product. The variation in the intensity of weathering index shown in Figure 4.61 may indicate alternating climatic conditions during the depositional history of the Lokpanta Shale. This interpretation agrees with the other plots for chemical weathering in this study.

In addition, intense weathering of the source area suggests a prolonged transport across the basin margin while weak weathering infers a proximity to basin margin (Asiedu *et al.*, 2005). Thus, the variation in the intensity of weathering (Figure 4.61) leads to the inference of differing distances of the sediments derived from the source area from the basin margin.

The wide value range of weathering indices might be due to sediment sorting, fractionation, variation in the climatic conditions, tectonics or sediment supply from the pre-existing rocks in the source area (Fedo *et al.*, 1995; Voicu and Bardoux, 2002; Ghandour *et al.*, 2003; Madukwe *et al.*, 2015). This is the case for both CIA and MIA for the Lokpanta Shale

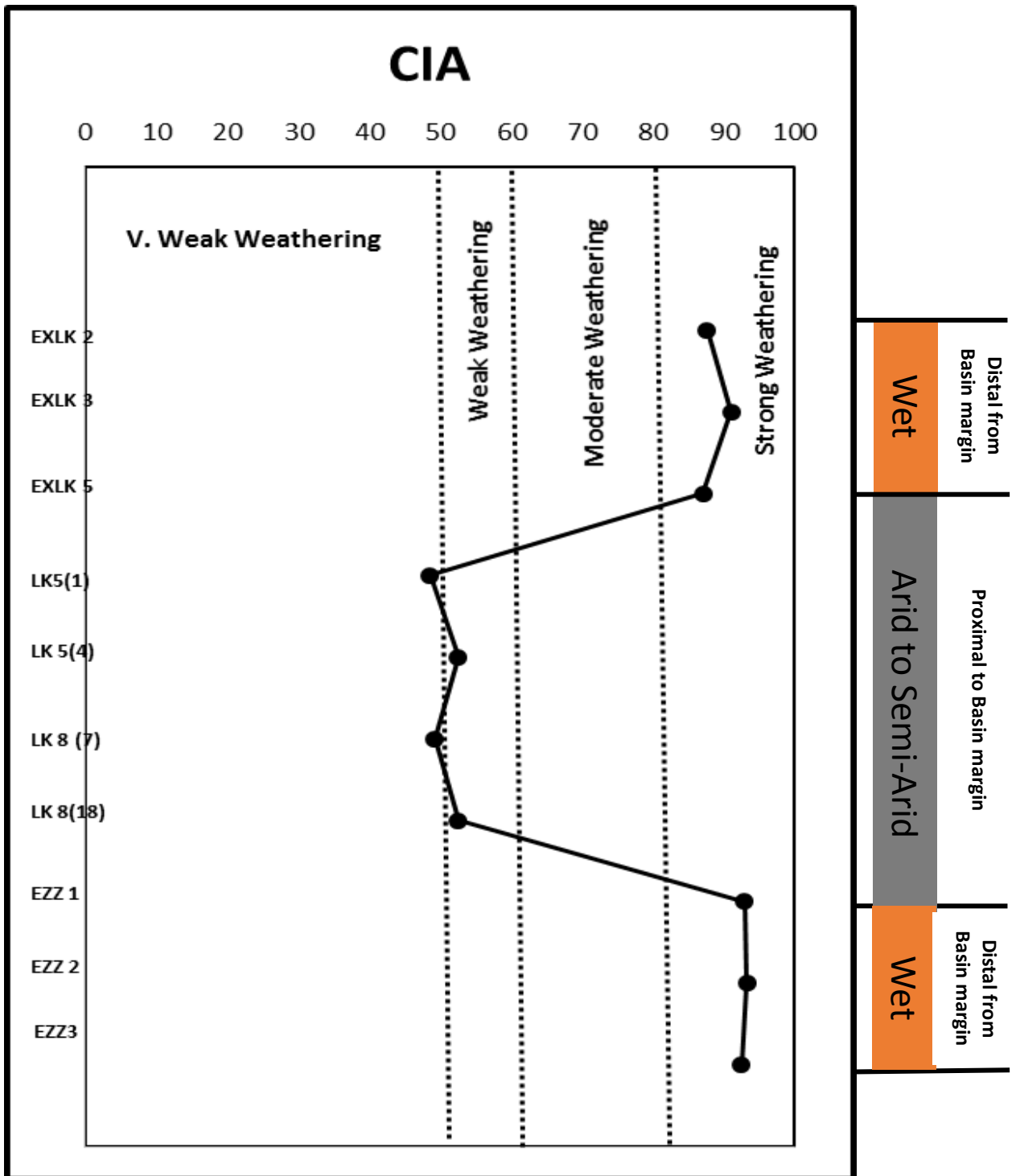


Figure 4.60: Chemical Index of Alteration of the source area

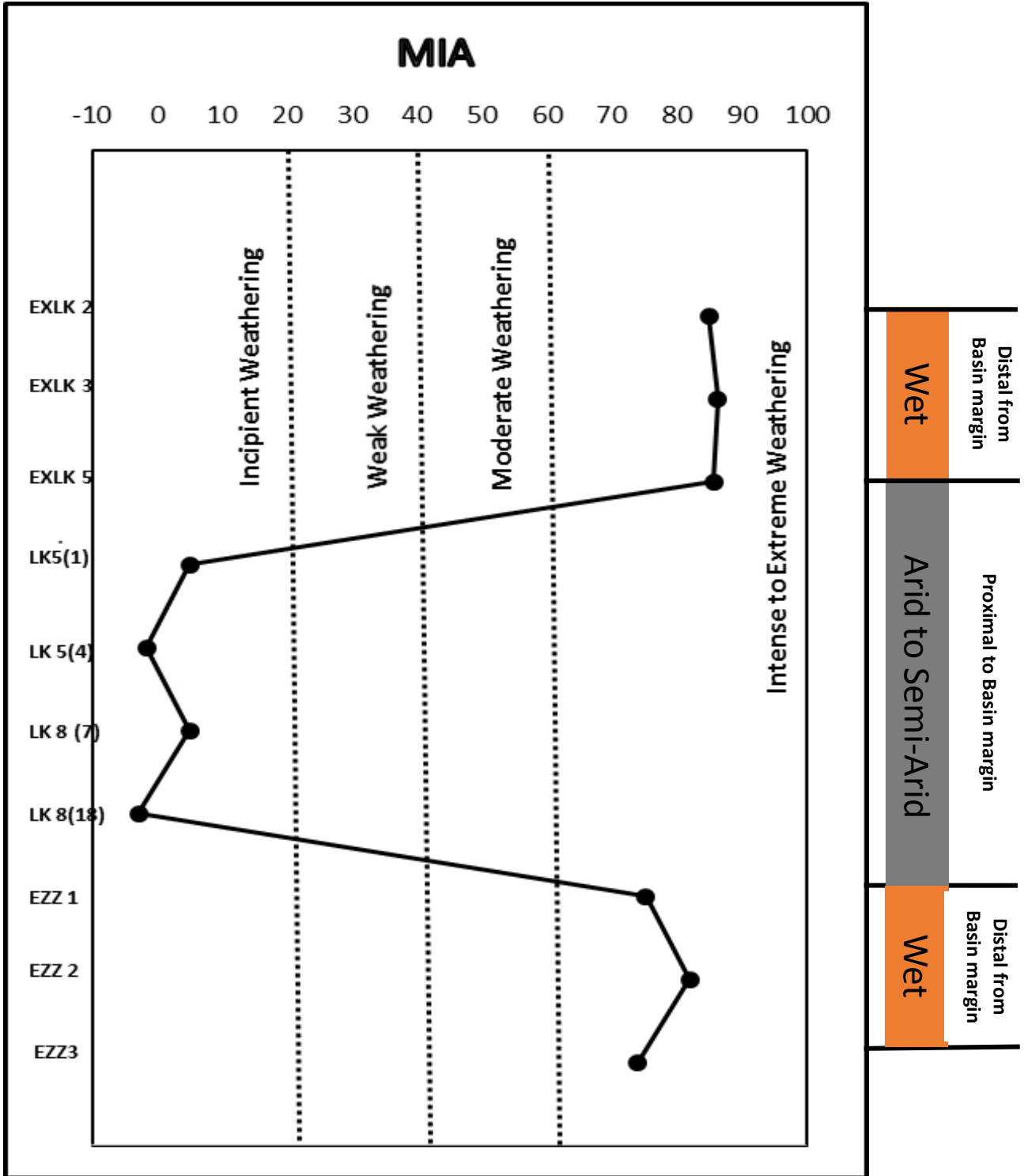


Figure 4.61: Plot of Mineralogical Index of Alteration of the source area

### 4.13.3 Plate Tectonic Setting

Knowledge of the plate tectonic setting of a basin is important for the exploration of petroleum and other resources as well as for paleogeography. Bhatia, (1983) and Roser and Korsh (1986) uses major elemental oxides from sedimentary rocks to infer plate tectonic setting. It is believed that plate tectonics processes impart distinctive geochemical signature to sediments in two separate ways. Firstly, tectonic environments have distinctive provenance characteristics and secondly they are characterized by distinctive sedimentary process (Oni *et al.*, 2014).

Bhatia (1983) proposed major element geochemical criteria to discriminate plate tectonic settings from identified well-defined siliciclastic rock suites. He assigned sedimentary basins to tectonic settings based on the major oxides as follows: (1) Oceanic arc: fore arc or back arc basins, adjacent to volcanic arcs developed on oceanic or thin continental crust; (2) Continental island arc: inter arc, fore arc, or back arc basins adjacent to a volcanic arc developed on a thick continental crust or thin continental margins; (3) Active continental margin: Andean type basin developed on or adjacent to thick continental margins and strike-slip basins also developed in this environment; (4) Passive continental margin: rifted continental margins developed on thick continental crust on the edges of continents and sedimentary basins on the trailing edge of continent.

Siliciclastic rocks from oceanic arc, continental arc, active and passive continental margins have variable composition, especially in their  $\text{Fe}_2\text{O}_3 + \text{MgO}$ ,  $\text{Al}_2\text{O}_3/\text{SiO}_2$ ,  $\text{K}_2\text{O}/\text{Na}_2\text{O}$ , and  $\text{Al}_2\text{O}_3/(\text{CaO} + \text{Na}_2\text{O})$  ratios (Bhatia, 1983; Sari and Koca, 2012; Madukwe *et al.*, 2015). Bhatia (1983) used this chemical variability to discriminate between different tectonic settings

on a series of bivariate plots. Plots of  $\text{TiO}_2$  versus  $(\text{Fe}_2\text{O}_3 + \text{MgO})$  and  $\text{Al}_2\text{O}_3/\text{SiO}_2$  versus  $(\text{Fe}_2\text{O}_3 + \text{MgO})$  are used to discriminate plate tectonic settings. The fields are oceanic island arc, continental island arc, active continental margin, and passive margins (Bhatia, 1983). Figures 4.62 a and b represent plots for Lokpanta Shale and indicates deposition in a passive margin setting. Bhatia (1983), Roser and Korsh (1986) and Oni *et al.* (2014) stated deposition in a passive margin further suggests that the rocks were derived from quartz-rich sediments in plate interiors. Madukwe and Basseyy (2015) said that deposition on passive margin creates favourable conditions for accumulation and maturation of organic matter.

Three plate tectonic settings; passive continental margin PM, active continental margin ACM, and oceanic island arc (ARC) are recognized on the  $\text{K}_2\text{O}/\text{Na}_2\text{O}$  versus  $\text{SiO}_2$ ,  $\text{Al}_2\text{O}_3/\text{SiO}_2$  versus  $\text{K}_2\text{O}/\text{Na}_2\text{O}$  discrimination plots of Roser and Korsch (1986) (Figures 4.63 a and b). The plots reveal that the sediments of Lokpanta Shale were deposited in a passive tectonic margin setting.

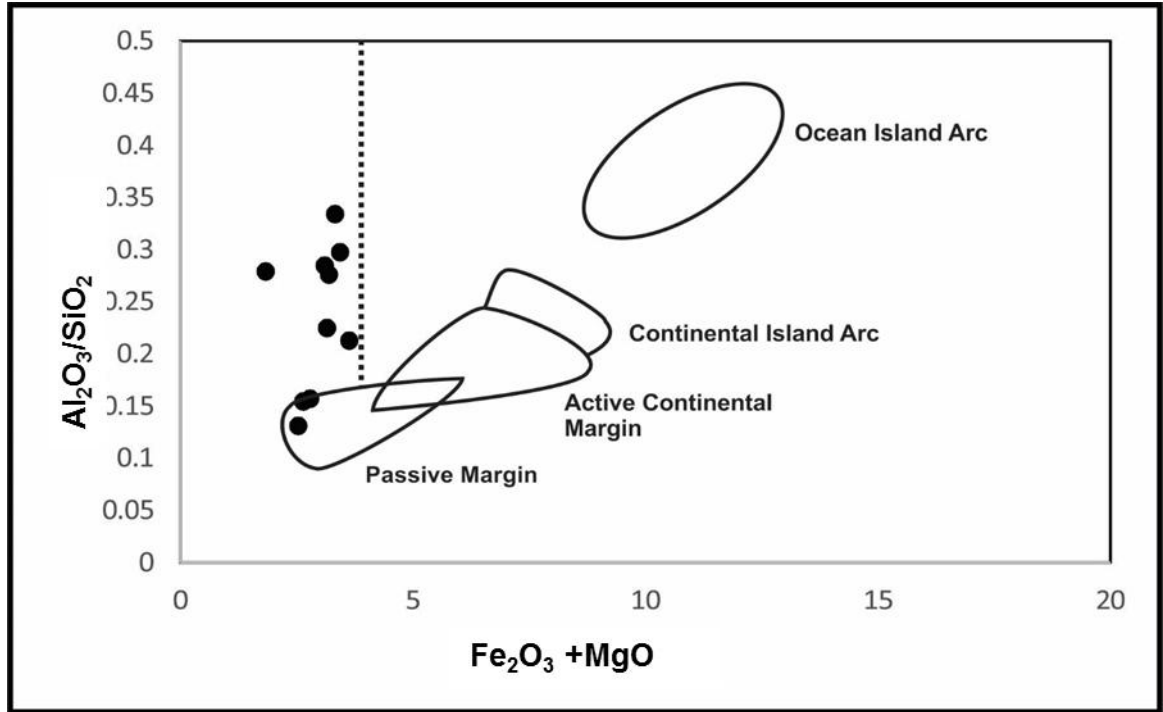


Figure 4.62 a: Discriminating tectonic settings diagram by major element compositions

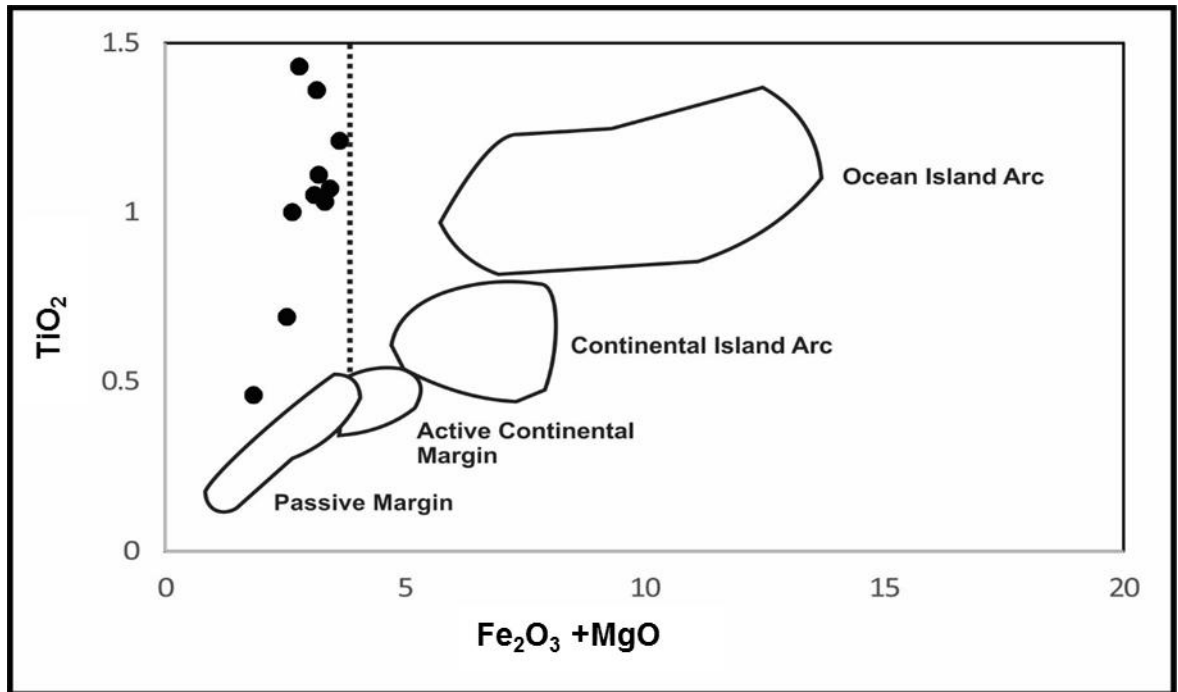


Figure 4.62 b: Discriminating tectonic settings diagram by major element compositions

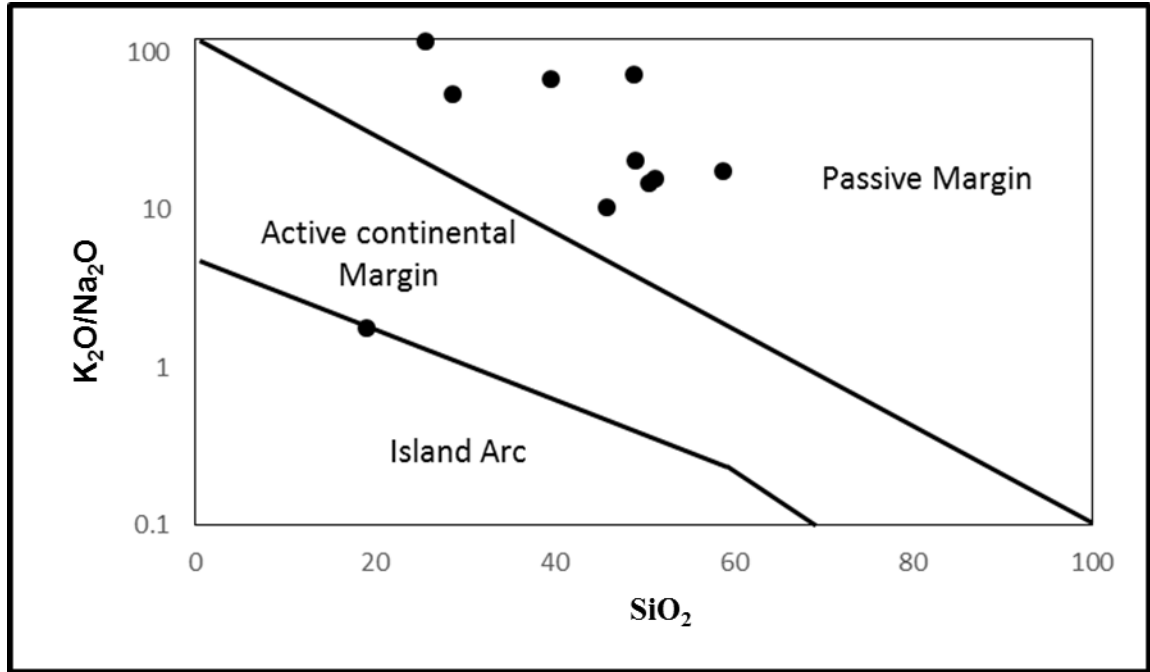


Figure 4.63a: Major and trace elemental oxides diagram for determining tectonic settings

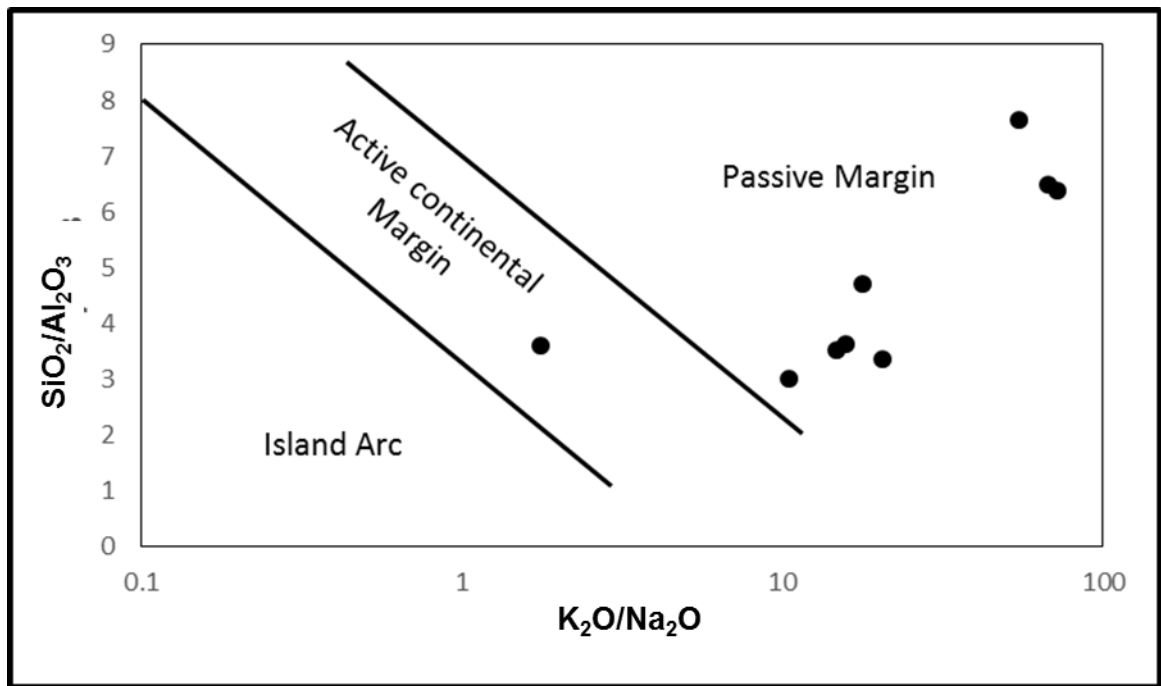


Figure 4.63b: Major and trace elemental oxides diagram for determining tectonic settings

#### **4.14 Paleooceanography**

Paleooceanography deals with the physical, chemical and biological conditions of the past water bodies at the time of the deposition of rocks (Herbert, 2003). Paleotemperature and paleosalinity are controlling factors in understanding paleooceanography (Henderson, 2002). Most carbonaceous and carbonate grains are produced biotically within a specified range of salinity, temperature, oxygen, and nutrient conditions (Nichols, 2009). Salinity and temperature plays a direct role in the production and distribution of carbonate rocks (Tucker and Wright 1990).

Paleooceanographic inferences make use of proxy methods as a way to evaluate past state and evolution of the worlds oceans (Henderson, 2002). The geochemical proxy tools include long-chain organic molecules (e.g. alkenones), stable and radioactive isotopes and trace metals (Henderson, 2002).

However, trace elements and elemental oxides of rocks have been used as proxies to give vital information about paleosalinity and paleotemperature of ancient oceans (Hossein *et al.*, 2012). The elements Ca, Mg, Fe, Mn, Sr and Na in carbonates rocks are essential to understand carbonate mineralogy, salinity and temperatures (Rao, 1996).

##### **4.14.1 Paleosalinity and Paleotemperature Evaluation**

Paleosalinity is the salinity of the global ocean or of an ocean basin at a point in geological history (Adkins *et al.*, 2002). Paleotemperature is the determination of sea surface temperature in the geologic past (De Villiers *et al.*, 1994). Some naturally occurring records



and rocks can serve as paleothermometers for determining past temperature conditions of an environment (De Villiers *et al.*, 1994).

The Lokpanta Shale has abundance of calcareous foraminifera. This infers high biogenic productivity in the ancient sea where the rocks were deposited. The areas where there is a high biogenic productivity in the sea is referred to as the carbonate factory (Tucker and Wright, 1990). For carbonate production to be sustained, the optimum temperature range should be 20 to 25<sup>0</sup>C in saline water (Tucker and Wright, 1990). Thus, qualitatively, the paleotemperature at the time of deposition of the rocks can be inferred to be in the range of 20 to 25<sup>0</sup>C.

Elements and elemental ratios can be used to determine of paleotemperature and salinity conditions of ancient seas. Strontium (Sr) content in the rocks has been used to discriminate between fresh and salt water environment (Degens, 1958 and Hossein *et al*, 2012). Several trace elements in rocks including Sr, B, Ga, V, Li, Ni and Rb has been used as paleosalinity indicators especially for shales (Degens, 1958, Potter *et al.*, 1963, Dominik, 1985 and Schreier, 1988). Studies have shown that high concentrations of Sr, B, and Rb occur in marine shales, whereas high concentrations of Zr, Ti, Al, Ga, Li, Co and Cr are terrestrial indicators. Hence, B, Rb, Sr Ga in studied rocks can be used to determine marine depositional environment.

Strontium (Sr) contents less than or equals to 100 ppm in rocks would suggest fresh water environment while Sr contents higher than 100 ppm would suggest salt water environment (Degens, 1958 and Hossein *et al*, 2012). Sr contents in the rock of Lokpanta Shale range from

49.65 to 243.96 ppm with an average of 159.70ppm (see Table 4.7). This strongly suggests that the shales were deposited in a very saline (hypersaline) marine environment.

Gallium (Ga) contents of 8-16 ppm in rock would suggest salt water environment while Ga content higher than 17 ppm suggest fresh water environment (Degens *et al.*, 1957 and Tourtelot, 1964). Ga contents in the rock studied range from 2.72 to 15.82 ppm with average of 9.43ppm (see Table 4.7). This also strongly suggests that the rocks were deposited in saline (hypersaline) marine environment.

It has been noted that Sr/Ba ratio can be used to distinguish fresh water from salt water environment (Hossein *et al.*, 2012). If the ratio is greater than 1, the environment is salt water while a ratio of less than 1 suggest fresh water environment. The ratio of Sr/Ba in the Lokpanta Shale vary from 1.23-4.43, averaging 2.13. This is further evidence that the rock was deposited in a saline (hypersaline) marine environment.

The correlation between  $Al_2O_3$  and  $TiO_2$  for the analysed rock reveals a correlation coefficient of 0.31 (Table 4.5 and Figure 4.35 f). This slightly weak but positive correlation indicates a good bond with the alkaline oxide. This can be used as a paleosalinity indicator (Hossein *et al.*, 2012) and further strengthens the assertion that the rocks were deposited in a saline (marine) environment.

#### **4.14.2 Paleoproductivity**

Many trace elements are present in seawater in either insoluble form or adsorbed onto particles. Removal of dissolved trace elements from the water column to the sediments results from either biotic or abiotic processes (Tribovillard *et al.*, 2006).

Biotic processes comprise the uptake of trace elements that serve as minor or micronutrients for plankton (mainly phytoplankton). Abiotic processes are relatively limited in oxic environments, but in suboxic environments, some enrichment may occur through diffusion of dissolved trace elements from the water column across the sediment–water interface or through remobilization and repartitioning along redox gradients within the sediments (Tribovillard *et al.*, 2006). Trace elements may also be efficiently concentrated through the redox cycling of manganese and iron (Algeo and Maynard, 2004).

Abiotic processes are particularly efficient under reducing conditions, including adsorption of metallic ions or ionic species onto organic or mineral substrates, formation of organometallic complexes, and precipitation of (iron-) sulphides and/or insoluble oxyhydroxides (Algeo, 2004). In theory, this variety of processes results in trace-element enrichments that mirror the specific conditions prevailing by the time of deposition and early diagenesis (Tribovillard *et al.*, 2004a). Consequently, trace-element abundances in sediments and sedimentary rocks allow us to reconstruct paleodepositional conditions (Werne *et al.*, 2003; Lyons *et al.*, 2003; Riboulleau *et al.*, 2003; Sageman *et al.*, 2003; Rimmer, 2004; Rimmer *et al.*, 2004; Algeo and Maynard, 2004; Algeo, 2004; Nameroff *et al.*, 2004; Tribovillard *et al.*, 2004a, 2005; Riquier *et al.*, 2005).

Oceanic anoxic events (OAE) with euxinic (i.e. sulphidic) conditions have been linked to extreme episodes of volcanic outgassing. Thus, volcanism contributes to the buildup of CO<sub>2</sub> in the atmosphere, increases global temperatures and causing an accelerated hydrological cycle that introduced nutrients to the oceans to stimulate planktonic productivity. These processes potentially act as a trigger for euxinia in restricted basins where water-column

stratification could develop. Under anoxic to euxinic conditions, oceanic phosphate is not retained in sediment and could hence be released and recycled, aiding continued high productivity (Meyer and Kump, 2008). The lack of P<sub>2</sub>O<sub>5</sub> concentration in the Lokpanta Shale is attributed to the above conditions, anoxia or euxinia of the sea.

Barium (Ba) is present in marine sediments mainly as crystals and in the form of barite (Bishop, 1988; Rutsch *et al.*, 1995). Live phytoplanktons incorporate Ba (actively or passively; i.e., metabolic uptake or adsorption) and Ba released during phytoplanktonic necromass decay may precipitate as barite in microenvironments where Ba-sulphate reaches supersaturation (Dehairs *et al.*, 1980, 1987, 1991, 1992; Dymond *et al.*, 1992; Kenison Falkner *et al.*, 1993).

Cadmium (Cd) is present in only one coordination state (Cd<sup>2+</sup>) in the water column and sediments. It has a nutrient-like behavior, which implies a relatively short residence time (Boyle, 1981, 1988; Rosenthal *et al.*, 1995, 1997; Morford and Emerson, 1999). Cadmium (Cd) is delivered to marine sediments mainly in association with organic matter (Piper and Perkins, 2004) and is released to interstitial waters during organic matter decay and authigenically enriched in sediments, probably in the form of a sulphide (Gobeil *et al.*, 1997; Morford and Emerson, 1999; Morford *et al.*, 2001). Cadmium (Cd) is enriched in both mildly and strongly reducing sediments (Calvert and Pedersen, 1993; Rosenthal *et al.*, 1995; Russell and Morford, 2001; Chaillou *et al.*, 2002).

In general, Barium (Ba) and Cadmium (Cd) are used as geochemical indicators for paleoproductivity (van Capellen and Ingall, 1994; Filipelli *et al.*, 1994). High Ba contents

indicate strong primary organic productivity. High Cd content can be attributed to high paleoproductivity. (Middleburg and Comans, 1991).

In the rocks studied, Barium (Ba) ions concentrations range from 23.81 to 157.18 ppm, with an average value of 86.19 ppm. The average value of Ba concentration in the rocks is higher than that for the average shale worldwide (not detected) but lower than those of NASC (636 ppm) and PAAS (650 ppm). The Cadmium (Cd) ions concentrations of the rocks range from 0.21 to 21.46 ppm, averaging 6.25 ppm. The average of Cd concentration in the rock is higher than those of the average shale worldwide, NASC and PAAS (not detected). Figure 4.64 a and b is a bar chart showing Ba and Cd enrichments and correlation plot of both trace elements in the rocks. The enrichment of Cd, relative depletion of Ba and weak positive correlation between Cd and Ba are all indicative of relative high productivity in the environment where the rocks were deposited.

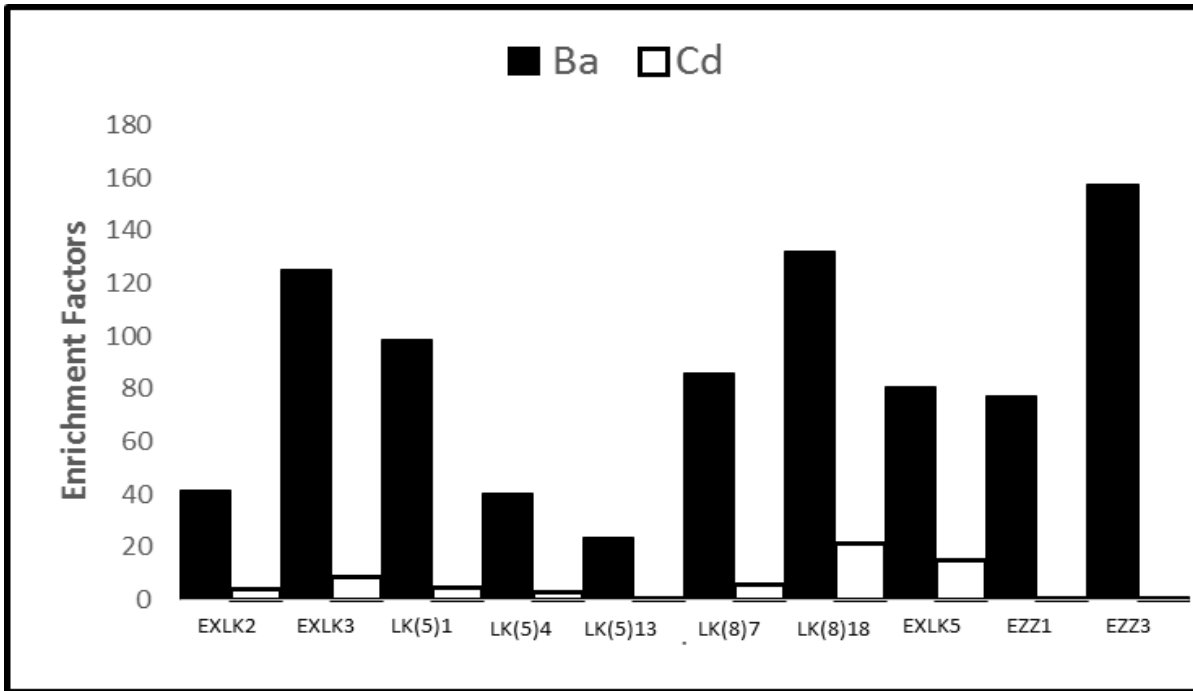


Figure 4.64 a: Cd and Ba enrichment of the Lokpanta Shale

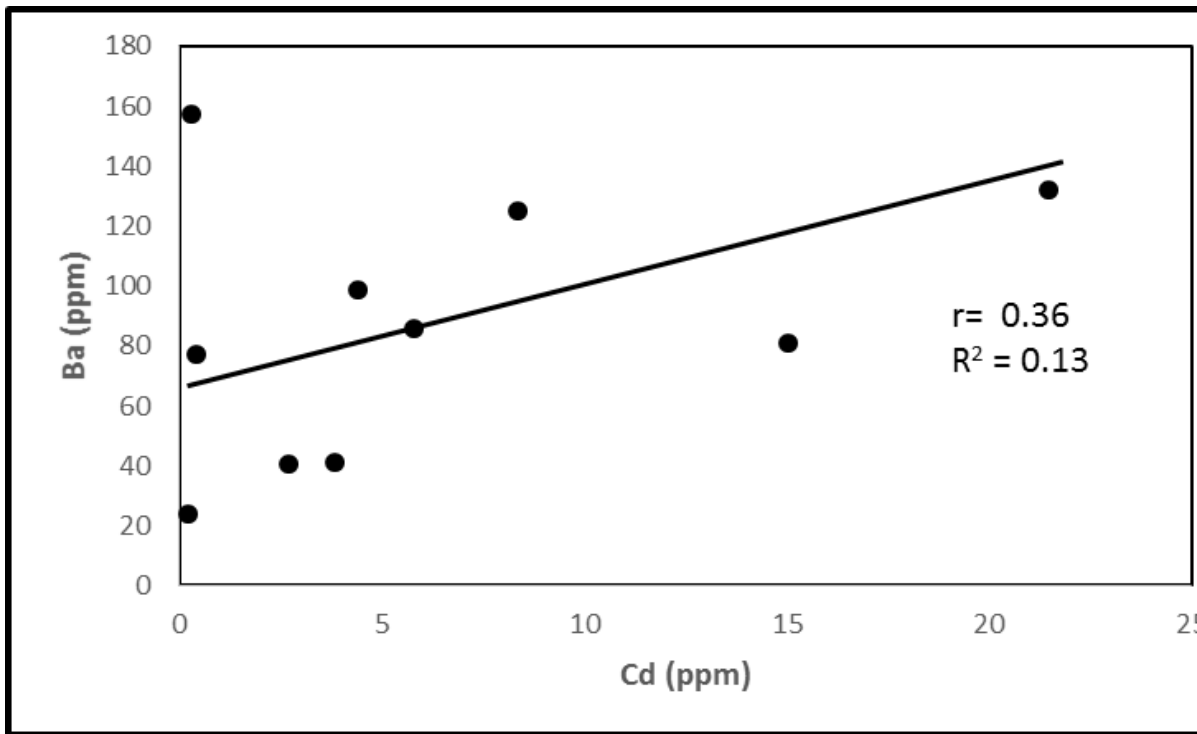


Figure 4.64 b: Correlation of Cd and Ba content of the Lokpanta Shale

### 4.14.3 Paleoredox

Certain elements, which are sensitive to redox changes in marine environment and pore waters, are used for reconstruction of redox conditions in young and ancient sedimentary basins associated with organic material deposits and sulphide occurrences in oxygen deficient media (Brumsack, 2006; Tribovillard *et al.*, 2006). Oxidation of sulphides produces a sulphate source for sulphate-reducing bacteria that facilitates anoxic conditions (Brüchert *et al.*, 2003).

As the organic matter content of rocks increases Uranium (U), Barium (Ba), Strontium (Sr), Cadmium (Cd), Molybdenum (Mo), Rubidium (Rb), Selenium (Se), Arsenic (As), Zinc (Zn), Copper (Cu), Nickel (Ni), Cobalt (Co), Chromium (Cr) and Vanadium (V) element concentrations also increase. The reasons for significant enrichment of these elements in organic-rich rocks is attributed to primary production of organic material in upper water column, sedimentation rate, redox conditions (Eh, pH) of depositional environment, H<sub>2</sub>S enrichment by sulphate-reducing bacteria, organic material preservation and precipitation of sulphide components (Sari and Koca, 2012).

Under dysoxic-anoxic and euxinic redox conditions, metals are mostly accumulated as metal sulphides. The greatest metal enrichment occurs under euxinic redox conditions which reflect complete sulphide phase (Warning and Brumsack, 2000; Arnaboldi and Meyers, 2003; Brumsack, 2006). Several trace elements such as Mo, Mn, Ni, V, U, Cr, Co have been used to evaluate paleoredox conditions (Hatch and Leventhal, 1992; Jones and Manning, 1994; Algeo and Maynard, 2004; Rimmer *et al.*, 2004).

It is believed that Ni and V are preferentially retained in tetrapyrrole structure which is preserved under anoxic conditions (Lewan and Maynard, 1982). In sediments and rocks of

reducing environment, Ni and V are retained by organic material (Lewan and Maynard, 1982). Lewan (1984) suggested that V/Ni ratio in crude oil which is not altered by diagenesis, reflects environmental conditions during its deposition. He showed that V/ (V+Ni) ratio for organics forming under euxinic conditions is greater than 0.50. According to Hatch and Leventhal (1992), V/ (V+Ni) ratios are greater than 0.84 for euxinic conditions, in the range of 0.54 – 0.82 for anoxic conditions and between 0.46 and 0.60 for oxic conditions. Vanadium (V), which is incorporated into tetrapyrrole structure under anoxic conditions may also be precipitated by adsorbing onto surface of clay minerals which most probably occurs after burial (Breit and Wanty, 1991). The V/V+Ni ratios of the Lokpanta Shale indicate anoxic and euxinic conditions during the deposition of the Lokpanta Shale (Figure 4.65 a).

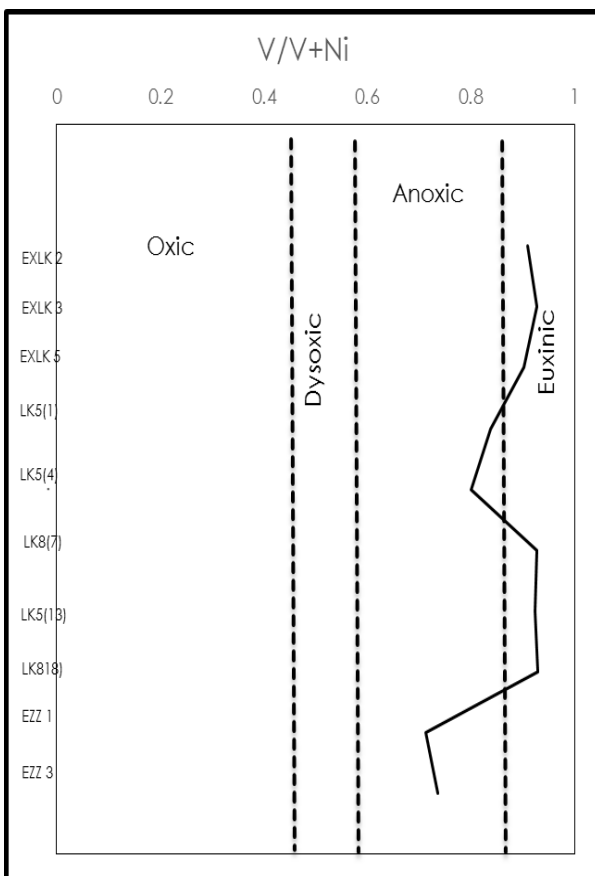
Chromium (Cr), thought to be related only to detrital fraction (Dill, 1986) is not affected by redox conditions. V/Cr ratio is suggested as an index for paleo-oxidation conditions (Dill *et al.*, 1988). Jones and Manning (1994) used V/Cr ratio to evaluate paleoenvironments of shales. High V/Cr ratios (> 4.25) are believed to reflect anoxic conditions (Jones and Manning, 1994). The V/Cr ratios of the Lokpanta Shale also indicate anoxic conditions as shown by their values (Figure 4.65 b).

Chromium (Cr) and cobalt (Co) concentrations enrichment in rock are believed to be of detrital fraction and not affect by redox conditions (Ross and Bustin, 2006). Both Ni and Co are incorporated into pyrite structure. High Ni/Co ratios are believed to be related to anoxic conditions (Jones and Manning, 1994). The Ni/Co ratios for the Lokpanta Shale suggest anoxic conditions, tending towards euxinic conditions due to their extremely high values (Figure 4.65 c). Table 4.14 shows elemental ratios and their critical values for particular environments

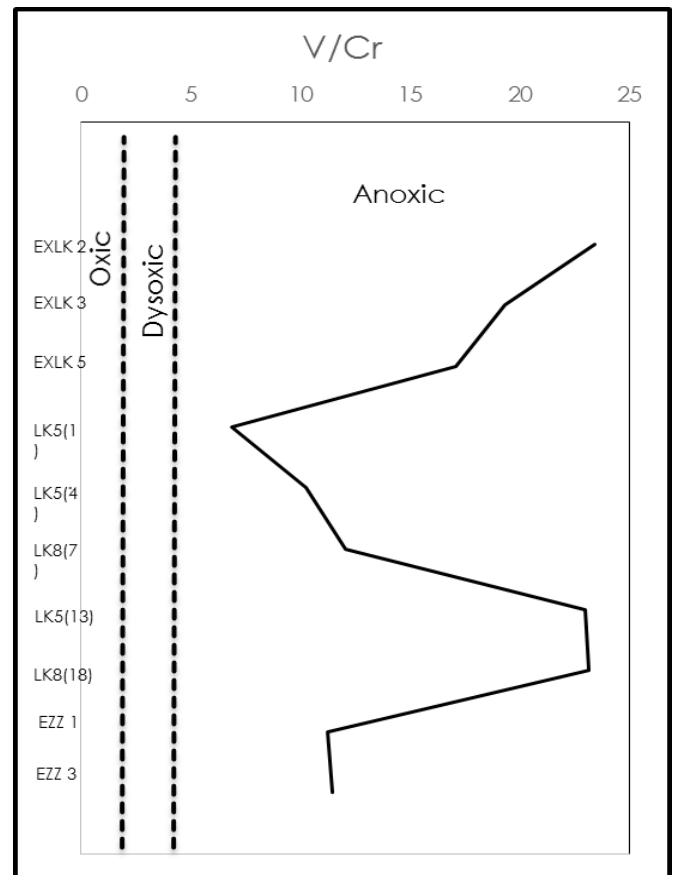


Table 4.14: Elemental ratios and critical values of Trace Elements Ni, V, Cr and Co for Paleoredox interpretation

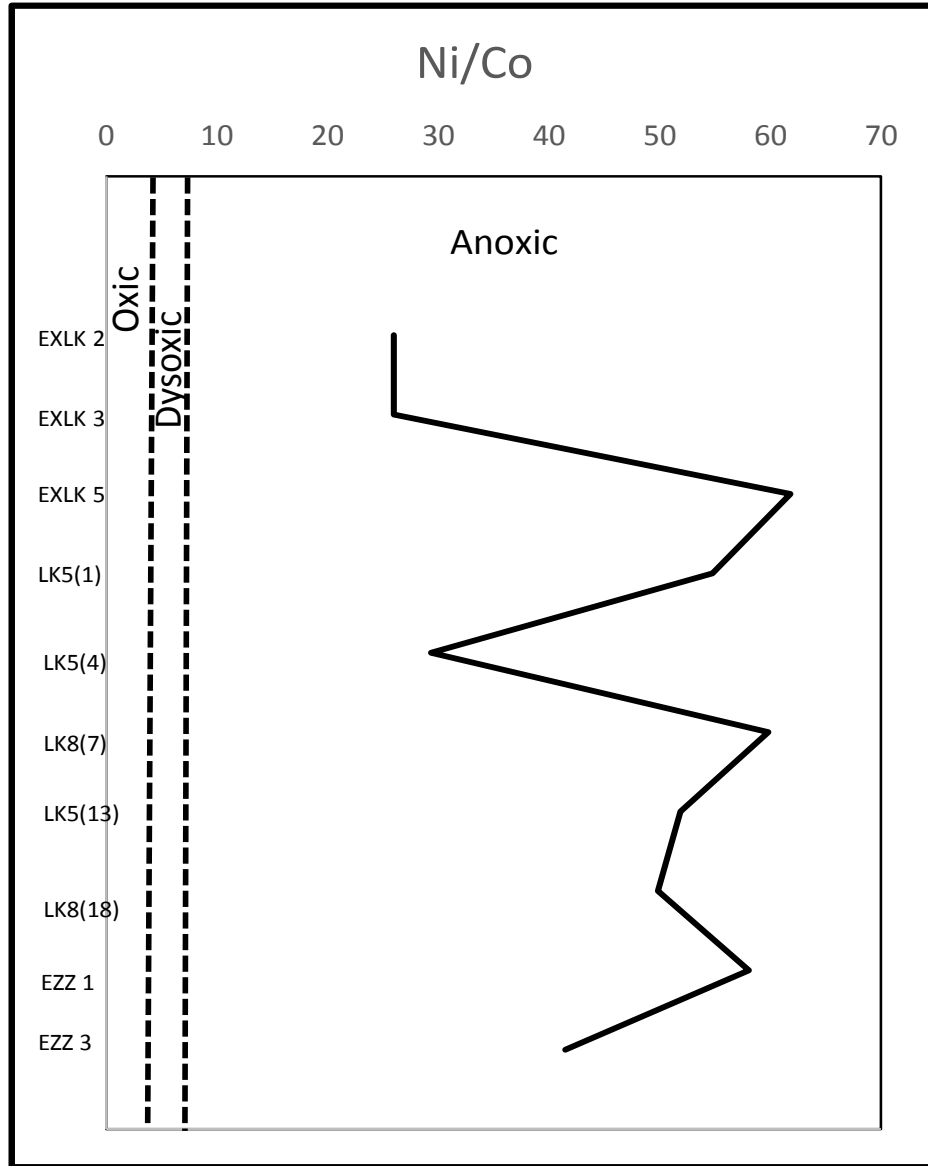
Elemental Ratios	Oxic	Dysoxic	Anoxic	Euxinic	Source	Present Study
Ni/Co	<5	5-7	>7		Jones and Manning (1994)	25.97 - 61.83
V/Cr	<2	2-4.5	>4.5		Dill <i>et al.</i> (1988)	6.88 - 23.41
V/(V+Ni)	<0.46	0.46-0.60	0.54-0.82	>0.84	Hatch and Laventhal (1992)	0.71 - 0.93



Figures 4.65 a: Paleoredox conditions of the carbonaceous rocks of the Lokpanta Shale



Figures 4.65 b: Paleoredox conditions of the carbonaceous rocks of the Lokpanta Shale



Figures 4.65 c: Paleoredox conditions of the carbonaceous rocks of the Lokpanta Shale

#### 4.14.4 Bathymetry

Paleobathymetry is the determination of ancient water depth (paleodepth). It is the paleoenvironmental interpretation most widely used in petroleum exploration because of its value in determining the depositional history of a basin (Dodd and Stanton, 1981). Benthic foraminifera are usually used for this purpose (Dodd and Stanton, 1981). As bottom dwellers, they provide information about conditions at the sea floor. Many species live within a relatively limited range of water depths in patterns normally related to water mass distribution within the basin rather than just a specific depth.

The concept of *taxonomic uniformitarianism* is utilized in paleobathymetry, which assumes most modern organisms have the same or very similar environmental restrictions as their fossil relatives (Dodd and Stanton, 1981).

Trochospiral morphotypes particularly species like *Hedbergella* and *Whiteinella* were “weeds” of the Mid- Cretaceous oceans found in great abundances in both epicontinental and open ocean settings (Leckie, 1987; 1989). These taxa are grouped as major components of the “Shallow Water Fauna” because, like the more common and widespread species today, they most probably lived in the sun-lit (photic zone) near surface waters of the mixed layer and/or upper reaches of thermocline, where trophic resources are concentrated (Leckie, 1987; 1989).

These trochospiral morphotypes especially *Hedbergella delrioensis* and *H. planispira* are the most abundant recovered foraminifera in the Lokpanta Shale (Ehinola *et al.*, 2003; Amoke, 2009). Mostly abundant are planktic foraminifera with low diversity and high abundances and sparse benthic foraminifera with low abundance and diversity. This strongly suggests that a shallow sea during the Cenomanian-Turonian times.

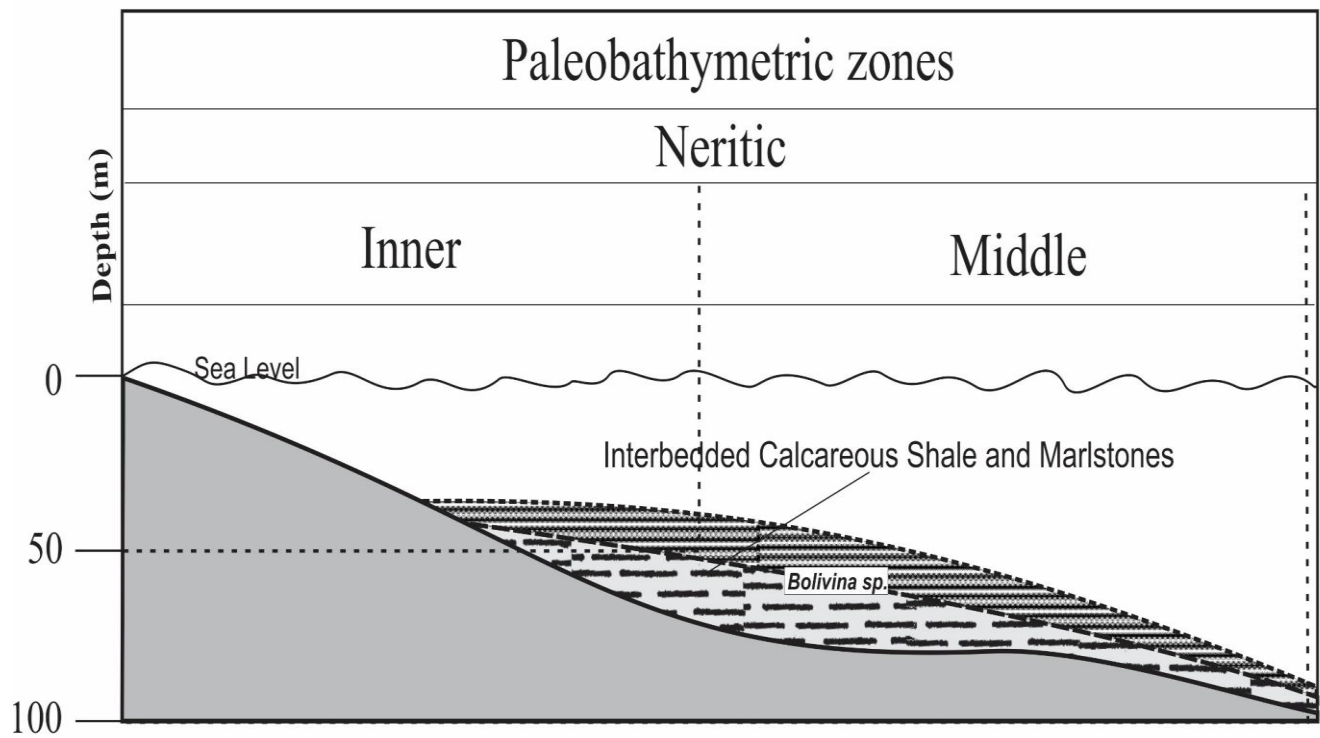
Wonders (1980) stated that the occurrence of *Heterohelix* and *Hedbergella* suggest water depth of about 50 m. Ehinola *et al.* (2003) used the presence of *Heterohelix*, *Hedbergella* and *Whiteinella* to propose a shallow marine bathymetry probably no greater than 50m depth. This is supported by the presence of *Haplophragmoides sp*, *Gavelinella sp*, *Eponides morani*, *Bolivina anambra* and *Bolivina sp* (Amoke, 2009). These foraminifera are diagnostic for the water depth range of 35-100 m especially the *Bolivina sp.* (Onyekuru *et al*, 2012).

Unlike temperature or salinity, water depth is not a true environmental parameter because it does not directly influence the morphology, distribution, or biological processes of marine organisms (Leckie, 1987; 1989). However, foraminifera have been used to estimate paleodepth because many environmental factors influencing their distribution (notably ambient light, oxygen, and temperature) change systematically with increasing water depth (Dodd and Stanton, 1981).

Demaison and Moore (1980) observed that preservation of laminations in shales and marls indicate low energy, oxygen deficient environment where there was drastic reduction in the activity of the benthonic foraminiferal communities. This is the case for the Lokpanta Shale where there is great abundance of planktonic foraminifera and very low benthonic population.

Based on the above, the Lokpanta Shale may have been deposited within the inner-mid neritic water depth. No single paleobathymetric model will account for all occurrences of Mesozoic organic-rich shales but the range of possibilities is limited (Demaison and Moore, 1980 and Hallam, 1982).

A paleobathymetric model for the Lokpanta Shale suggests epicontinental sea is so extensive and shallow, that the hydrodynamic regime will tend towards restriction of oxygen circulation (Figure 4.66).



Figures 4.66: Paleobathymetric model of the Lokpanta Shale

#### 4.15 Source Rock Evaluation

According to Obaje *et al.* (2004), at the core of any petroleum system is a good quality source rock with Total Organic Carbon (TOC) > 0.50%, Hydrogen Index (HI) >150mgHC/gTOC, Maximum Temperature ( $T_{max}$ )  $\geq 435^{\circ}\text{C}$  and Vitrinite Reflectance ( $R_o$ ) from 0.60-1.20%. Other petroleum system elements must include reservoir and sealing lithologies, established trapping structures and favorable regional migration pathways.

It is known that adequate amount of organic matter, measured as percentage total organic carbon (TOC), is one necessary pre-requisite for sediment to generate oil and gas (Cornford, 1986). The TOC is the weight percent of carbon in the potential source rock and is measured as the amount of carbon dioxide produced when acid-leached rock sample is combusted in the presence of oxygen.

The Rock-Eval pyrolysis results in this study are as presented in Table 4.10 and Figures 4.39-4.42. They show that the Total Organic Carbon (TOC) of the rocks ranges from 0.83 to 4.56 wt% (Av. 2.75 wt %). This suggests that the source rock quality is good to very good. This inference is in accord with various authors (Tissot and Welte, 1978; North, 1985; Peters and Cassa, 1994; Hunt, 1996, Killops and Killops, 2005 and McCarthy *et al.*, 2011).

The parameter  $S_1$ , represents the amount of free hydrocarbon already generated from the source rock by geospheric maturity and merely distilled out of the rock during pyrolysis. The  $S_1$  value can be used to measure the source rock generative potential. The values from the Lokpanta Shale vary from 0.15 to 2.91 mgHC/g with an average of 1.29 mgHC/g. The minimum  $S_1$  value for good source rocks is 1.00 mgHC/g dry rock (Pennsylvania State

Geological Survey, 2011). In terms of free hydrocarbons, the Lokpanta Shale has generally, very good generative potential.

The parameter  $S_2$  represents the bitumen that would be generated if burial and maturation of source rock continued to completion (Leckie *et al.*, 1988). This decreases with increasing maturation (Leckie *et al.*, 1988). This parameter corresponds to the hydrocarbons that would evolve from the rock during the second programmed heating stage of pyrolysis. It results from cracking heavy hydrocarbon and from the thermal breakdown of kerogen. The  $S_2$  values for the Lokpanta Shale range from 2.06 to 21.42 mgHC/g with average value of 10.69 mgHC/g.  $S_2$  minimum value for good source rocks is 5.00 mgHC/ dry rock (Tissot and Welte, 1978; Peters and Cassa, 1994; McCarthy *et al.*, 2011; Pennsylvania State Geological Survey, 2011). Based on the  $S_2$  values, the Lokpanta Shale is of good quality and generative potential.

The  $S_2/S_3$  ratio of the Lokpanta Shale range from 3.90 to 49.40 with an average value of 21.47. This ratio is theoretically equivalent to the ratio HI/OI and useful for describing the kerogen type and the type of hydrocarbon likely to be expelled by a rock (Weber and Green, 1981; Peters, 1986; Leckie, *et al.*, 1988; Peters & Cassa, 1994). The critical values of  $S_2/S_3$  ratio for Types I, II, II-III, III and IV are >15, 10-15, 5-10, 1-5 and <1 respectively. The values obtained for the Lokpanta Shale indicate Types I, II and II-III kerogen (see Table 4.10, Figures 4.38 and 4.39). The values of  $S_2/S_3$  ratio obtained therefore indicate oil generative capacity (Dayal *et al.*, 2013).

Hydrogen Index (HI) represents the quantity of pyrolysable organic compounds from  $S_2$  relative to Total Organic Carbon (TOC) in the rock (Snowdon, 1989). Peters and Cassa (1994) and McCarthy *et al.* (2011) classified source rocks with HI values of 50-200, 200-300

and 300-600 as gas, mixed oil & gas and oil prone rocks respectively. HI has a direct relationship with elemental H/C; it is proportional to the amount of hydrogen in the kerogen and thus indicates the potential of the rock to generate oil (Peters and Cassa, 1994). The hydrogen index (HI) values of the Lokpanta Shale vary widely from 186.00 to 487.00 mgHC/g TOC (Av. 328.30mgHC/gTOC). The values obtained indicate a source rock that is predominantly oil with associated gas prone.

Genetic Potential (GP) is the summation of free hydrocarbon ( $S_1$ ) and hydrocarbon generation through thermal cracking ( $S_2$ ) i.e.  $S_1+S_2$  (Peter & Moldowan, 1993). A good source rock should have GP of at least 2.00 mgHC/g (Tissot and Welte, 1984, Dymann *et al.*, 1996 and McCarthy *et al.*, 2011). The genetic potential (GP) of the Lokpanta Shale range from 2.34 to 24.33 mgHC/g, having an average value of 11.98 mgHC/g. Therefore, these exceptionally high values of GP strongly indicate good to excellent source rock quality.

The production index (PI) also known as transformation ratio is a maturation parameter. It is the ratio of already generated hydrocarbons to potential hydrocarbon from the source rock (Miles, 1989). Its upper and lower limits indicate the early mature to late mature boundaries respectively (Peters and Cassa, 1994), provided there is no migration into or out of the rock being studied (Leckie, *et al.*, 1988). Peters and Cassa (1994) stated that the critical range of values for PI are 0.00 - 0.10, 0.10 - 0.15, 0.25-0.40 and >0.40 which is indicative of immature, early maturity, peak maturity and late maturity respectively. The hydrocarbon production index (PI) values for the Lokpanta Shale range from 0.04 - 0.20. These values are indicative of immature to peak maturity for the shale.



$T_{\max}$  is the temperature at which the pyrolytic yield of hydrocarbons from a rock reaches its maximum. It is kerogen-dependent and affected by mineral matrix, organic contamination and migration (Clementz, 1979; Epistalie *et al.*, 1980; Horsfield and Douglas, 1980; Peters, 1986).  $T_{\max}$  values for the Lokpanta Shale range from 430 to 459°C. In terms of thermal maturity, the rocks can be said to range from the onset of maturity (oil generation) to fully mature, almost tending to the onset of gas generation (see Table 4.10).

Vitrinite reflectance is a measure of the amount of light reflected by vitrinite present in the organic component of the rock. It is used as a maturity indicator but dependent on kerogen type (Peter and Moldowan 1993). This parameter is based on the change in the reflectance of polished vitrinite particles with increasing time and temperature. Increase in reflectance is caused by the progressive aromatization of the kerogen with accompanying loss of hydrogen in the form of hydrocarbon gases. The end product of the process is graphite (Miles, 1989). Equivalent vitrinite reflectance ( $R_o$  eq.) can be calculated from  $T_{\max}$  obtained from pyrolysis using the formula  $R_o \text{ eq} = 0.0180 \times (T_{\max}) - 7.16$  (Jarvie *et al.*, 2001). The equivalent vitrinite reflectance ( $R_o$  eq.) for the Lokpanta Shale ranges from 0.58-1.10 %, with an average of 0.71 %. This indicates that the shale is marginally mature to mature in the condensate-gas window.

The plot of remaining hydrocarbon potential ( $S_2$ ) versus total organic carbon (TOC) (see Figure 4.39) revealed that the shale plotted in Type II and II-III kerogen domains. This indicates that the shale is predominantly oil and gas prone, deposited in transition zone of marine and terrestrial settings from a mixture of planktons, algae and higher plants.

The Van Krevelen diagram of HI versus OI for the Lokpanta Shale constrained the plots between Types I and II kerogen domains indicating also that the shale is oil and gas prone (see Figure 4.40).

The plot of HI versus  $T_{\max}$  ( $^{\circ}\text{C}$ ) revealed that the Lokpanta Shale plotted in Type II, II-III kerogen domains, suggesting that the organic matter have the potential to produce both oil and gas. Figure 4.41 shows that the shale entered the maturity window, generating hydrocarbons.

The plot of Production Index (PI) versus  $T_{\max}$  ( $^{\circ}\text{C}$ ) revealed that the shale is marginally mature to mature, having high conversion rate. Figure 4.42 shows that the shale is marginally mature to mature and already generating hydrocarbons as earlier mentioned from previous plots.

Generally, the trend of maturity shows that the Ezzaegu samples are sufficiently mature. The River Nmavu samples are immature to marginally mature, while the Express Road (Lokpanta Junction) samples are immature in terms of hydrocarbon generation. Figure 4.67 shows the maturity trend with stratigraphy and the critical parameters with which maturity is assessed.

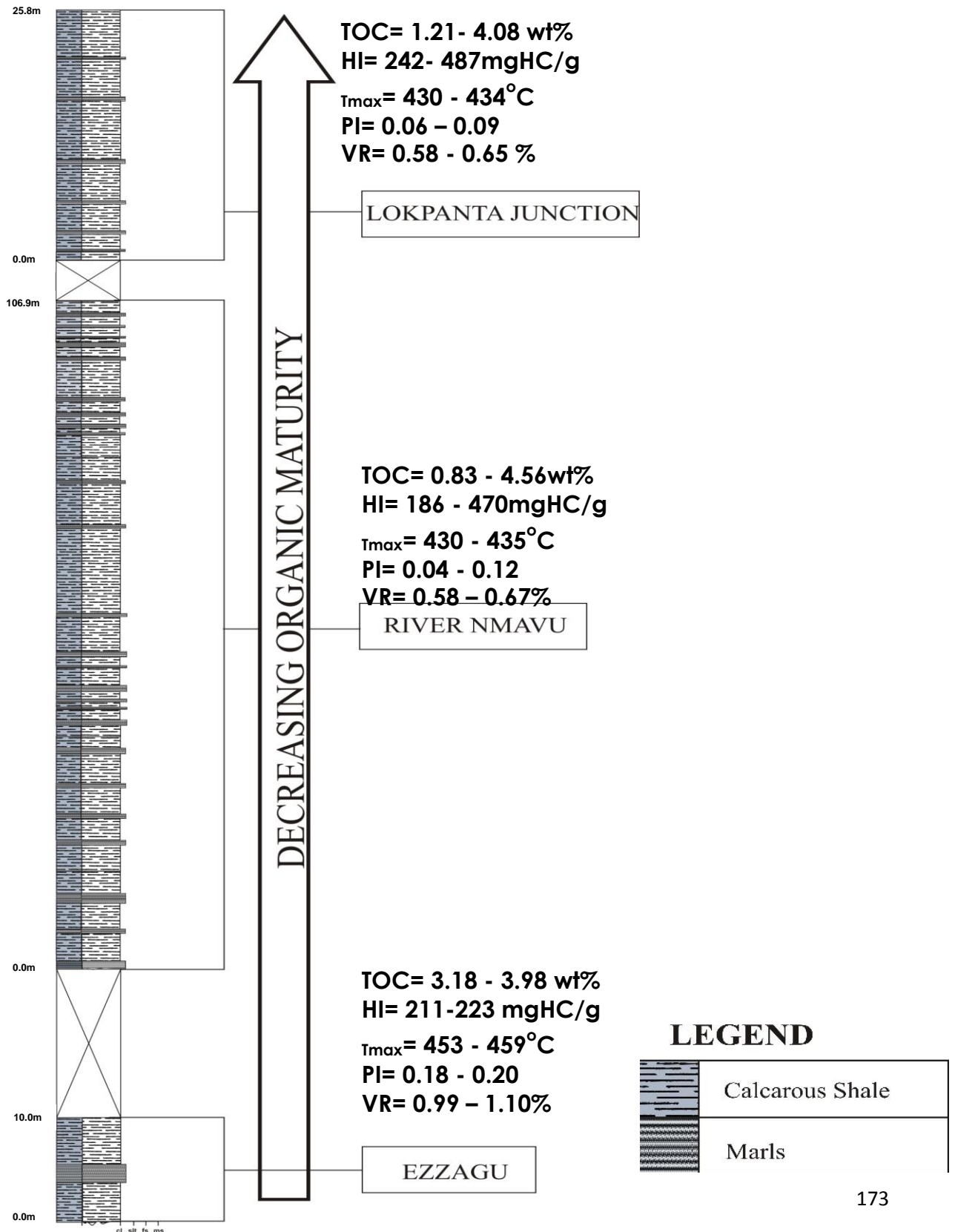


Figure 4.67: Maturity trend in the Lokpanta Shale studied

#### 4.16 Gas Shale Potential

The primary aim of this section is to examine the geochemical and geological characteristics of these carbonaceous rocks to determine its viability as a shale gas reservoir. Geochemical analyses play an essential role in determining critical parameters of appropriate gas shale reservoirs by identifying organic richness, genetic potential and thermal maturity as well as thickness of strata (Alexander *et al.*, 2011). The atypical reservoir of interest to this work is the Lokpanta Shale, a succession of interbedded calcareous shales and marlstones.

Conceptually, for any shale gas play, the most important need is to find organic-rich, gas-prone shale (Rokosh *et al.*, 2009 and Alexander *et al.*, 2011). The word ‘shale’ is used in the sense of a geological formation rather than a lithology. Shale gas reservoirs can show marked variations in rock type from claystones, marlstones and mudstones to sandstone and carbonate lithological ‘sweet spots’ (Bust *et al.*, 2013). In all cases, a thorough understanding of the fundamental geochemical and geological attributes of ‘shale’ is essential for resource assessment, development and environmental stewardship (Rokosh *et al.*, 2009). Four properties that are important characteristics in each shale gas play are the:

- 1) Maturity of the organic matter;
- 2) TOC content of the strata; and
- 3) Permeability of the reservoir.
- 4)  $R_o$  Vitrinite Reflectance (0.8 – 1.5) %, more preferably 1.1 – 1.5%.

Secondary characteristics of gas shale include:

- a) Natural fracture
- b) Clay Mineralogy

c) Thickness of the strata

These characteristics are discussed in the following subsections.

#### **4.16.1 Organic Richness**

Organic richness is the ability of hydrocarbons to be generated (Peter and Moldowan, 1993). Since petroleum is a generative product of organic matter disseminated in the source rock, the quantity of the petroleum should be correlatable with the organic richness of the source rock (Dow, 1977; Welte *et al.*, 1981; Tissot & Welte, 1984). Parameters used in determining organic richness are total organic carbon content (TOC), genetic potential (GP), hydrocarbons generated before pyrolysis ( $S_1$ ), remaining hydrocarbon potential ( $S_2$ ) and hydrogen index (HI). Table 4.10 shows the Rock-Eval pyrolysis result of the Lokpanta Shale.

Total organic carbon (TOC) is the acquired amount of organic matter, measured as percentage. It is a necessary pre-requisite for rocks to generate oil and gas (Cornford, 1986). The total carbon in a shale includes both inorganic and organic carbon (Alexander *et al.*, 2011). The TOC governs the resource potential of a shale. Rocks with higher TOC values are organically richer. The critical range of values of TOC are 0.00 - 0.50 wt%, 0.50 - 1.00 wt%, 1.00 – 2.00 wt%, 2.00 – 5.00 wt% and > 5.00 wt% indicating null, poor, fair, good and very good respectively (Alexander *et al.*, 2011; Boyer *et al.*, 2011; Geel *et al.*, 2013). The Total Organic Carbon (TOC) of the Lokpanta Shale ranges from 0.83 to 4.56 wt% (Av. 2.75 wt %) (Table 4.10). This suggests that the source rock quality is good to very good and meets the prerequisite for the good gas shale potential.

The free hydrocarbons ( $S_1$ ) is the amount of hydrocarbon in the source rock already generated by geospheric maturity and merely distilled out of the rock during pyrolysis (Peters, 1986).

The critical ranges of values of  $S_1$  are 0.00 - 0.50 mgHC/g, 0.50 - 1.00 mgHC/g, 1.00 – 2.00 mgHC/g, 2.00 – 4.00 mgHC/g and > 4.00 mgHC/g indicating poor, fair, good, very good and excellent respectively (Peters and Cassa, 1994; Alexander *et al.*, 2011; Boyer *et al.*, 2011; Geel *et al.*, 2013). The  $S_1$  values for the Lokpanta Shale vary from 0.15 to 2.91 mgHC/g with average value of 1.29 mgHC/g (Table 4.10). This is indicative of a good gas shale potential for the shale.

The remaining hydrocarbon potential ( $S_2$ ) represents the bitumen that would be generated if burial and maturation continued to completion and decreases with increasing maturation (Leckie *et al.*, 1988). The critical ranges of values of  $S_2$  are 0.00 - 2.50 mgHC/g, 2.50 - 5.00 mgHC/g, 5.00 – 10.00 mgHC/g, 10.00 – 20.00 mgHC/g and > 20.00 mgHC/g indicating poor, fair, good, very good and excellent respectively (Peters and Cassa, 1994; Alexander *et al.*, 2011; Boyer *et al.*, 2011; Geel *et al.*, 2013). The  $S_2$  for the Lokpanta Shale ranges from 2.06 to 21.42 mgHC/g with average value of 10.69 mgHC/g (Table 4.10). This range of values is strongly indicative of very good gas shale potential.

Hydrogen Index (HI) and genetic potential (G.P) are other parameters by which the organic richness of source rocks can be evaluated. 50 – 150 mgHC/gTOC, 150 – 300 mgHC/gTOC and > 300 mgHC/gTOC are the range of HI indicative of gas, gas and oil, oil prone rocks respectively (Peters, 1986; Peters and Cassa, 1994; Alexander *et al.*, 2011). The hydrogen index (HI) values of the Lokpanta Shale vary widely from 186.00 to 487.00 mgHC/g TOC (Av. 328.30 mgHC/gTOC) (Table 4.10). This result indicates predominantly oil with associated gas for the shale. The assessment criteria of Genetic potential (GP) are 0.00-2.00 mgHC/g, 2.00-6.00 mgHC/g and greater than 6.00 mgHC/g typifying little or no oil potential,

moderate or fair hydrocarbon generative potential, good to excellent source rock generative potential respectively (Tissot and Welte, 1984; Dymann *et al.*, 1996; Rokosh *et al.*, 2009; Boyer *et al.*, 2011 and Alexander *et al.*, 2011). The genetic potential (GP) of the Lokpanta Shale ranges from 2.34 to 24.33 mgHC/g, having an average of 11.98 mgHC/g (Table 4.10). The rocks are of good to excellent source rock quality and gas shale potential.

#### **4.16.2 Kerogen Type**

Organisms contribute to the organic matter present in petroleum source rocks. Since these organisms differ in their contents of lignin, carbohydrates, lipids, protein, resin, the preserved organic matter exhibits parallel diversity. Sedimentary, diagenetic, catagenetic and metagenetic processes modifies the original constituents further. The diversity influences the convertibility of kerogen to petroleum; some being oil-prone or gas-prone, while others are not convertible to petroleum (Dow, 1977). Quality organic materials must be present for a geologic unit to be considered a potential source rock (Pennsylvania State geology survey, 2011). The crossplots used here for the evaluation of the type of organic matter are HI versus OI,  $S_2$  versus TOC, HI versus  $T_{max}$  and  $S_2/S_3$ .

The  $S_2/S_3$  ratio represents a measure of the amount of hydrocarbons which can be generated from a rock relative to the amount of organic  $CO_2$  released during temperature programming up to 390° C.  $S_2/S_3$  ratios are considerably lower for Type III kerogen than for Type II and Type I because terrestrially derived organic matter contains substantially more oxygen than the marine derived types of organic matter (Weber and Green, 1981; Peters, 1986 and Dayal *et al.*, 2013). The  $S_2/S_3$  ratio of the Lokpanta Shale ranges from 3.90 to 49.40 with an average of 21.47 (Table 4.10). This indicates Types I, II and II-III kerogen having oil and gas

generative potential (see Table 4.10, Figures 4.39 and 4.40). Thus, the kerogen type of the Lokpanta Shale indicates good gas shale potential.

Crossplots of HI versus OI,  $S_2$  versus TOC, HI versus  $T_{max}$  for the shale revealed that they possess predominantly Type II and Type II-III with a subordinate Type I kerogen (Figures 4.39-4.41). These kerogen types indicate that the rock is capable of generating both oil and gas. This is good for shale gas play (Peters and Cassa, 1994; Dayal *et al.*, 2013).

### **4.16.3 Thermal Maturity**

Maturation is the process of chemical change in sedimentary organic matter, induced by burial, resulting in increasing temperature and pressure over geological time (Miles, 1989). Thermal maturity is a function of depositional history (Alexander *et al.*, 2011). Heroux, *et al.* (1979) presented a comprehensive review of the non-biomarker geochemical parameters used for the determination of the maturity level of organic matter. The maturation parameters employed for this study include Production Index (PI),  $T_{max}$ , Vitrinite Reflectance ( $VR_o$ ), the crossplots of HI versus  $T_{max}$  and PI versus  $T_{max}$ .

The PI is a maturation parameter derived from pyrolysis and it is the ratio of already generated hydrocarbons to potential hydrocarbon (Miles, 1989). It is calculated as the ratio  $S_1/S_1+S_2$ . It increases with maturity and indicates the presence of epigenetic hydrocarbons. Colloquially, its upper and lower limits indicate the oil “birth” and “death” (Hunt, 1996; Tissot & Welte, 1984; Peters, 1986) or the early mature to late mature boundaries respectively (Peters and Cassa, 1994), provided there is no migration into or out of the rock under investigation (Leckie, *et al.*, 1988). The PI is affected by mineral matrix and by migration



(Clementz, 1979; Epistalie *et al.*, 1980; Horsfield and Douglas, 1980 and Dembicki *et al.*, 1983). Production Index (PI) for the Lokpanta Shale ranges from 0.04 - 0.20 (see Table 4.10). This is indicative of range of maturity from immature to peak maturity for the shale. It shows that the shale has begun generating hydrocarbons and as such possess good gas shale potential.

$T_{\max}$  is the temperature at which the pyrolytic yield of hydrocarbons from a rock reaches its maximum. It is the temperature at which hydrocarbons are released from kerogen and reveals a proxy of thermal maturity.  $T_{\max}$  lower than 435°C indicate immature organic material, between 435 °C and 455°C is considered mature organic matter and over 470°C represents the wet gas zone or over mature organic matter (Peters and Cassa, 1994; Alexander *et al.*, 2011; McCarthy *et al.*, 2011).  $T_{\max}$  for the Lokpanta Shale ranges from 430 to 459°C (Table 4.10). The shale ranges from immature to mature, almost tending to the onset of gas generation.

Vitrinite reflectance is a visual or optical measurement of maturity which is kerogen dependent (Peters and Moldowan, 1993). The measurement of vitrinite reflectance ( $R_o$ ) was originally developed to rank coal maturity (Alexander *et al.*, 2011). The higher the percentage of reflectance of the maceral or vitrinite, the higher its thermal maturity (Jarvie *et al.*, 2001). The thermal oil window is defined as the thermal maturity zone where liquid hydrocarbons are the dominant product, although there is always associated gas formed in the oil window too (0.60 %-1.00  $R_o$ ). The thermal condensate-wet gas window is defined as the zone where light liquids and gas are the predominant products and is near the boundary where any retained oil is cracked to lighter liquids and gas (1.0-1.4 %  $R_o$ ). The thermal dry gas

window is defined as the zone where methane begins to dominate the products that are generated ( $>1.4 \%R_o$ ) (Jarvie *et al.*, 2001).

Initially, oil and condensate were considered negative indicators for gas shale development. However, there has been some success producing oil and condensate from shale and lower  $R_o$  values can be considered a positive indicator in these cases (Alexander *et al.*, 2011). It is known that vitrinite reflectance values of 0.8-1.5% is good for shale gas play, with the best being equal or greater than 1.5% (Alexander *et al.*, 2011).

The equivalent vitrinite reflectance ( $R_o$  eq.) values for the Lokpanta Shale range from 0.58-1.10%, with an average of 0.71% (Table 4.10). This range of values suggest marginal thermal maturity to full maturity, even into condensate-gas window. This further suggests the shale has sufficient maturity for shale gas play.

The plots of PI versus  $T_{max}$  and HI versus  $T_{max}$  support the maturity status of the rocks. Both plots reveal that the rocks are immature to mature, within the condensate- wet gas zone (see Figures 4.41-4.42).

Thus, the Lokpanta Shale is suitable for shale gas play based on its organic richness, kerogen type and thermal maturity.

#### **4.16.4 Clay Mineralogy**

Shales can have complex mixtures of minerals and their relative concentrations have the potential to make or break a potential gas shale play (Alexander *et al.*, 2011). Clay type can be used to predict sensitivity of the shales to fracturing fluids and to understand the fracturing characteristics of the Formation (Alexander *et al.*, 2011). When in contact with water, some

clays begin to swell, which inhibits gas production and creates numerous operational issues. Smectite is the most common swelling clay (Alexander *et al.*, 2011). Also, clay type is an indicator of rocks that are ductile and thus, do not fracture easily (Alexander *et al.*, 2011). Ductile shales are more likely to embed proppant than brittle shales. Propants are propping agents such as silica sand or other particles which are pumped into a Formation during a hydraulic fracturing operation to keep fractures open and retain the induced permeability. Other shale types may be brittle and are more easily fractured. The presence of illite is preferred for hydraulic fracturing because it is often indicative of brittle rocks that are not reactive with water while the presence of smectite usually indicates ductile clay (Jarvie *et al.*, 2001; Boyer *et al.*, 2011 and Alexander *et al.*, 2011).

The clay mineral composition of the Lokpanta Shale is dominantly kaolinite (Table 4.1). This is good for shale gas play as it does not absorb water that closes the pores. It fractures easily too thus, enhancing natural fracturing (Alexander *et al.*, 2011).

#### **4.16.5 Summary of Gas Shale Assessment**

Finally, the geochemical properties of the Lokpanta Shale revealed that the kerogen types are the Type II and Type II-III. The maturity ranges from immature to mature, with the Ezzaegu outcrop being the best to produce gas, having entered the condensate-wet gas zone (Figures 4.41 and 4.42).  $T_{max}$  values of 453-459<sup>0</sup>C show that the rocks at the Ezzaegu area are on the verge of entering the dry gas zone (see Table 4.10). These geochemical properties are strongly supported by the high TOC content, which makes the shale a good source rock for hydrocarbon generation and shale gas exploitation.

The thicknesses of the formation obtained varied with the thickest in the Nnavu River channel exceeding over a 100 m. The estimated thickness of the Formation (150 m) indicates that it is adequate as a gas shale reservoir and potential source for a shale gas play. Table 4.15 is a summary of the gas shale assessment parameters and potential for the Lokpanta Shale.

Table 4.15: Summary of Gas Shale Assessment

OUTCROPS	TOC (Wt%)	ORGANIC MATTER	T <sub>MAX</sub> (°C)	HI (MgHC/g)	PI	VR (%)	CLAY MINERAL	MATURITY	THICKNESS
LOKPANTA (NMAVU RIVER AREA)	0.83-4.56	Type II, II/II	430-435 (Av.433.2)	186-470	0.04 -0.12	0.58 – 0.67	Kaolinite	Marginally mature	106.90 m
LOKPANTA JUNCTION AREA	1.21-4.08	Type II	430-434 (Av.432)	242-487	0.06 – 0.09	0.69 – 0.65	Kaolinite	Immature	25.80 m
EZZAEGU AREA	3.18 -3.98	Type II	453 – 459 (Av.456)	211 -223	0.18 – 0.20	0.99 – 1.10	Kaolinite	Mature	10.00 m

# CHAPTER FIVE

## SUMMARY, CONCLUSION AND RECOMMENDATIONS

### 5.1 Summary

This work has examined the sedimentology, paleogeography, paleoceanography, source rock and gas shale potential of the Lokpanta Shale of the Eze-Aku Group. The shale is exposed on the western limb of the Abakaliki Anticlinorium in the Southern Benue Trough. The methods employed in this study include field and laboratory methods. The field methods employed geological field mapping, Lithofacies description and sample collection. Laboratory methods included thin section petrography, palynological biostratigraphy, Rock-Eval pyrolysis, XRD (X-Ray Diffraction), XRF (X-Ray Fluorescence) and AAS (Atomic Absorption Spectrometry).

The two lithofacies identified are the dark grey calcareous shale and light grey platy marlstone lithofacies, grouped into **Anoxic Shallow Marine Lithofacies Association**. Lithostratigraphic mapping identified five geological units comprising the Asu River Group, Lokpanta Shale, Eze-Aku Shale, Amasiri Sandstone (Eze-Aku Group), Awgu Formation and Nkporo Group. The Lokpanta Formation which is the focus of this study comprises of interbedded calcareous shales and marlstones with sideritic/pyritic concretions. Its type locality is the the Lokpanta – Onoli Awgu area. The type section (stratotype) is described along the Nmavu River channel. The Formation is traceable laterally to Ezzaegu area and has been identified as far as the Calabar Flank.

Lithofacies characteristics integrated with biostratigraphic characteristics such as presence of depauperate ammonites, mostly planktic foraminifera with rare benthics and moulds of *Inoceramus labiatus* microfossils indicate that the Formation was deposited in an anoxic, shallow, inner -middle shelfal paleoenvironment. Palynological evidence also indicates the rocks are Cenomanian-Turonian for Formation. Petrographic study revealed that the marlstones are biomicritic with abundant bivalves. Tests of *hedbergellids*, *heterohelicids* and some benthics foraminiferal constitute the allochems while micrite at various stages of neomorphism constitute the void fillers.

X-ray diffraction results revealed that calcite, kaolinite and quartz are the dominant minerals in the rocks. Elemental oxide and elemental analyses showed dominance of  $\text{SiO}_2$ ,  $\text{Al}_2\text{O}_3$  and CaO and trace elements such as Cr, V, Ni, Co, Sr and Ba are paleoenvironmental proxies. Plots of  $\text{TiO}_2$  vs  $\text{Al}_2\text{O}_3$ ,  $\text{K}_2\text{O}$  vs Rb as well as positive correlation between Cr and Ni; high  $\text{Al}_2\text{O}_3/\text{K}_2\text{O}$  ratios and presence of kaolinite indicate granitic to intermediate rock provenance in wet and warm tropical climatic regimes.

Plots of oxides vs  $\text{Al}_2\text{O}_3$  and CaO reveal sediment supply was from both terrestrial and marine sources. Crossplots of elemental oxides of  $\text{Al}_2\text{O}_3/\text{SiO}_2$  vs  $\text{Fe}_2\text{O}_3 + \text{MgO}$ ,  $\text{TiO}_2$  vs  $\text{Fe}_2\text{O}_3 + \text{MgO}$ ,  $\text{SiO}_2/\text{Al}_2\text{O}_3$  vs  $\text{K}_2\text{O}/\text{Na}_2\text{O}$  and  $\text{K}_2\text{O}/\text{Na}_2\text{O}$  vs  $\text{SiO}_2$  indicate a passive margin tectonic provenance for the sediments. Chemical Index of Alteration (CIA) and Mineralogical; Index of Alteration (MIA) show that provenance/source area rocks are strongly to very weakly weathered.

Elemental ratios such as Sr/Ba, V/V+Ni, Ni/Co, V/Cr reveal euxinic-anoxic paleoredox, oceanographic conditions and hypersalinity for the Cenomanian-Turonian Sea. Furthermore,

Cd and Ba composition (ppm) show that paleoproductivity of the ancient sea was high. The high productivity of the ancient sea indicates a paleotemperature range from 20-25<sup>0</sup>C.

The presence of mostly planktic and rare benthic foraminifera as well as the land derived palynomorphs strongly suggest variable bathymetry from 35-100m for the ancient sea during the Cenomanian - Turonian times.

Hydrocarbon source rock properties evaluation show Total Organic Carbon (TOC) contents varying from 0.83 to 4.56 wt%; genetic potential (G.P) from 2.34-24.33 mgHC/g;  $s_1$  from 0.15 to 2.91 mgHC/g and  $s_2$  from 2.06-21.42 mgHC/g. These are all indicative of very good to excellent source rock and hydrocarbon generative potential. Types of organic matter and kerogen are predominantly Type II and subordinate Type II-III kerogen. The rocks vary from marginally mature to mature and capable of hydrocarbon (oil and gas) generation. The shale outcrops in Ezzaegu area appears as the oldest stratigraphically. They are organically the most mature, and within the oil window/condensate-wet zone, with high conversion rate.

## **5.2 Conclusion**

In conclusion, a formal lithostratigraphic unit, the Lokpanta Shale has been proposed. It is one of the component formations of the Eze-Aku Group in Abakaliki Anticlinorium, Southeastern Nigeria. The Formation is Cenomanian-Turonian in age.

The sediments were deposited in anoxic, inner-middle shelfal paleoenvironment. The paleogeographic setting was a passive continental margin with warm tropical climate. The continental block, east of the study area was composed of granitic to intermediate basement rocks which provided the detritus to the Late Cenomanian – Turonian ocean.



The environment of deposition for the Formation was anoxic and varied from inner-middle shelf bathymetry (35 – 100 m). Paleooceanographic conditions of the environment of deposition of the Formation indicate that paleosalinity and paleotemperatures (20 - 25<sup>0</sup>C) were high enough to precipitate calcium carbonate (CaCO<sub>3</sub>). The gas shale and source rock potential of the Lokpanta Shale appear to be promising.

### **5.3 Recommendations**

In light of this study, the following recommendations are proffered:

1. The Lokpanta Shale should be added to the Nigerian stratigraphic lexicon as a formation of the Eze- Aku Group and validated by the Nigerian Geological Survey Agency, which has the statutory right by law to formalize stratigraphic units.
2. Its gas shale potential should be exploited, as this formation is the only shale that has been studied for that purpose in Nigeria. This can be done using extensive geochemical and petrophysical log analyses to ascertain parameters such as TOC, Gas volume and capacity (GIP), mineralogy, nano-permeability, micro-porosity, kerogen typing, thermal maturity and hydrocarbon saturation. Evaluation of geomechanical properties of the shaly reservoir to aid the exploitation of the potential shale gas play.

### **5.4 Contribution to Knowledge**

Outlined here are the contributions of this work to the body of knowledge. They are:

1. The production of a detailed geologic map of the study area (part of the western limb of the

Abakaliki Anticlinorium), breaking up the Eze-Aku Group into three formations instead of two.

2. The new formation is the **Lokpanta Shale** with type locality and stratotype described along the Nmavu River Channel.
3. The assignment of age to the new Formation (Cenomanian-Turonian).
4. The reconstruction of the paleodepositional, paleogeographic and paleobathymetric models for the Southern Benue Trough in the Cenomanian-Turonian times.
5. The evaluation of the source rock properties and preliminary assessment of its gas shale potential.

## REFERENCES

- Abubakar, M.B. (2014). Petroleum Potentials of the Nigerian Benue Trough and Anambra Basin: A Regional Synthesis. *Natural Resources*. 5, 25-58.
- Adeigbe, O.C. and Jimoh, Y.A. (2013). Geochemical Fingerprints; Implication for Provenance, Tectonic and Depositional Setting of Lower Benue Trough, Sequence, Southern Nigeria. *Journal of Environment and Earth Science*. 3 (10): 115-140.
- Adkins, J.F., McIntyre, K., and Schrag, D.P. (2002). The Salinity, Temperature, and delta <sup>18</sup>O of the Glacial Deep Ocean. *Science*. 298 (5599): 1769–1773.
- Agagu, O.A., (1985). A geological guide to bituminous sediments in Southwestern Nigeria. Unpublished Report. Department of Geology, University of Ibadan.
- Agagu, O. K. and Adighije, C. I. (1983). Tectonic and Sedimentation Framework of the Lower Benue Trough, Southeastern Nigeria. *Journal of African Earth Sciences*.1, 267 - 274.
- Agagu, O.K., Fayose, E.A., Petters, S.W. (1985). Stratigraphy and Sedimentation in the Senonian, Anambra Basin of Eastern Nigeria. *Nigeria Journal of Mining and Geology*. 22 (2): 30 – 33.
- Agumanu, A. E. (1993). Sedimentology of the Owelli Sandstone (Campanian-Maastrichtian), Southern Benue Trough, Nigeria. *Journal of Mineralogy and Geology*. 29 (2): 21-35.
- Akande, S.O., Ogunmoyero, I.B., Petersen, H.I. and Nytoft, H.P. (2007). Source Rock Potential of the Lower Maastrichtian Mamu Formation, S.E Nigeria. *Journal of Petroleum Geology*. 30, 303-324.
- Akande, S.O., Ojo, O.J., Egenhoff, S.O., Obaje, N.G. and Erdtmann, B.D. (2011). Stratigraphic Evolution and Petroleum Sediments in the Lower and Middle Benue Trough, Nigeria: Insights from New Source Rock Facies Evaluation. *Petroleum Technology Development Journal*. 1, 1-12.

- Ajakaiye, D. E. (1981). Geophysical Investigations in the Benue Trough – A review. *Earth Evolution Science*. 2, 110 – 125.
- Algeo, T.J. (2004). Can Marine Anoxic Events Draw Down the Trace Element Inventory of Seawater? *Geology*. 32, 1057–1060.
- Algeo, T.J. and Maynard, J.B. (2004). Trace–Element Behavior and Redox Facies in Core Shales of Upper Pennsylvanian Kansas-Type Cyclothems. *Chem. Geol.* 206, 289 – 318.
- Alexander, T., Baikly, J., Bowyer, C., Clark, B., Jochen, V., Calvez, J., Lewis, R., Thaeler, J and Toelle, B. (2011). Shale Gas Revolution. *Oilfield Review*. 23 (3): 40-55.
- Altun, N. E.; Hiçyilmaz, C.; Hwang, J.-Y.; Suat Bağcı, A. and Kök, M. V. (2006). Oil shales in the World and Turkey; Reserves, Current Situation and Future Prospects: A Review" (Pdf). *Oil Shale. A Scientific-Technical Journal*. Estonian Academy Publishers. 23 (3): 211–227. ISSN 0208-189X. Retrieved 16 June 2007
- Amajor, L.C., (1985). The Cenomanian Hiatus in the Southern Benue Trough, Nigeria. *Geological Magazine*. 122, 39-50.
- Amajor, L.C. (1987). Major and Trace Elements Geochemistry of Albian and Turonian Shales from the Southern Benue Trough, Nigeria. *Journal of African Earth Science*. 6, 461-633.
- Amajor, L.C. (1992). “Storm Induced Turbidity-like Deposits: An example from the Turonian Eze-Aku Formation at Nkalagu, South Eastern Nigeria”. *Journal of Mining and Geology*. 28 (1): 7-17.
- Amoke, I. (2009). Biostratigraphy of Cenomanian-Turonian Sediments of the Abakaliki Basin and the Calabar Flank, Southeastern Nigeria. Unpublished M.Sc. thesis. University of Nigeria, Nsukka.
- Anyiam, O.A. and Onuoha, K.M. (2014). A Study of Hydrocarbon Generation and Expulsion of the Nkporo Shales in Anambra Basin, Nigeria. *Arabian Journal of Geosciences*. 7 (9): 3779-3790.

- Aplin, A. C. (1993). The Composition of Authigenic Clay Minerals in Recent Sediments: Links to the Supply of Unstable Reactants. *In: Manning, D. A. C., Hall, P. L. and Hughes, C. R. (Eds.), Geochemistry of Clay-Pore Fluid Interactions. Chapman and Hall.* 81–106.
- Arnaboldi, M. and Meyers, P.A. (2003). Geochemical Evidence for Paleoclimatic Variations during Deposition of Two Pliocene Sapropels from the Vrica Section, Calabria. *Palaeogeography, Palaeoclimatology, Palaeoecology.* 190, 257–271.
- Arua, I. and Rao, V.R. (1978). Ammonite Evidence for the Age of Nkalagu Limestone, Anambra State, Nigeria. *Journal of Mining and Geology.* 15, 47-50.
- Asiedu, D.K., Hegner, E., Rocholl, A and Atta-Peters, D. (2005). Provenance of Late Ordovician to early Cretaceous Sedimentary Rocks from Southern Ghana as Inferred from Nd isotopes and trace elements. *Journal of African Earth Science.* 41, 316-328.
- Banerjee, I. (1980). Subtidal Bar Model for the Eze-Aku Sandstone, Nigeria. *Sedimentary Geology.* 2 (4): 291 – 309.
- Banerjee, I. (1981) Storm Lag and Related Facies of the Bioclastic Limestones of the Eze-Aku Formation (Turonian), Nigeria. *Sedimentary Geology.* 30, 133 – 147.
- Banikowski, J. E. and Hand, B.M. (1987). Radon in Onondaga County: Preliminary Report Prepared for Onondaga County Department of Health. *In: Gundersen, L.C.S. and Wanty, R.B. (Eds.), 1992. Field Studies of Radon in Rocks, Soils and Water. (CRC Press) 216.*
- Barr, F.T. (1972). Cretaceous Biostratigraphy and Planktonic Foraminifera of Libya. *Micropaleontology.* 18, 1-46.
- Batten, D.J. (1996). Chapter 26A. Palynofacies and paleoenvironmental interpretation, *In: Jansonius, J. and McGregor, D.C. (Eds.), Palynology: Principles and Applications, American Association of Stratigraphic Palynologists Foundation.* 1011-1064.

- Batten, D.J. and Stead, D.T. (2005). Palynofacies Analysis and its Stratigraphic Application, *In: Applied Stratigraphy*, Koutsoukos, and E.A.M (Eds.) Springer Dordrecht, Netherlands. 203-226
- Bellier, J. (1998). Cretaceous Planktonic Foraminifers, Eastern Equatorial Atlantic. *In: Mascle, J., Lohmann, G. P. and Moullade, M (Eds.). Proceedings of the Ocean Drilling Program, Scientific Results.* 159, 335-343.
- Benkhelil, J. (1982). Benue Trough and Benue Chain. *Geological Magazine.* 119, 155 – 168.
- Benkhelil, J. (1986). Structure et Evolution geodynamique du basin intracontinental de la Bénoué (Nigeria). These de Doctorat d'Etat, University of Nice. 226.
- Benkhelil, J. (1987). Structural Frame and Deformations in the Benue Trough of Nigeria. *Bull.Centres Rech. Explor – Prod. Elf Aquitaine.* 11, 160 – 170.
- Benkhelil, J. (1989). The Evolution of the Cretaceous Benue Trough, Nigeria. *Journal of African Earth Sciences.* 8, 251 – 282.
- Benkhelil, J., and Guiraud, M. (1980). La Bénoué (Nigeria): une chaine intracontinentale de style atlasique. *C. R. Acad. Sci., Paris.* 290, 1517 – 1520.
- Benkhelil, J., and Robineau, B. (1983). Fosse de la Bénoué est – il un rift? *Bull. Centers Rech. Explor. Prod. Elf Aquitaine.* 7, 315 – 321.
- Berg, G. (1932). Das Vorkommen der chemischen Elementen auf der Erde. Johann Ambrosius Barth, Leipzig. 240.
- Bhatia, M.R. (1983). Plate Tectonics and Geochemical Composition of Sandstones. *Journal of Geology.* 91, 611–627.
- Bishop, J.K.B. (1988). The Barite-Opal-Organic Carbon Association in Oceanic Particulate Matter. *Nature.* 332, 341–343.

- Bock, B., McLennan, S.M. and Hanson, G. N. (1998). Geochemistry and Provenance of the Middle Ordovician Austin Glen Member (Normanskill Formation) and the Taconian Orogeny in New England. *Journal of Sedimentology*. 45, 635–655.
- Boulter, M. C and Riddick, A. (1986). Classification and analysis of palynodebris from the Palaeocene sediments of the Forties Field. *Sedimentology*. 33, 871-876.
- Boyle, E.A. (1981). Cadmium, Zinc, Copper and Barium in Foraminifera Tests. *Earth Planet. Sci. Lett.* 53, 11–35.
- Boyle, E.A. (1988). Cadmium: Chemical Tracer of Deep Water Paleooceanography. *Paleoceanography*. 3, 471–489.
- Boyer, C., Clark, B., Jochen, V. and Lewis, R. (2011). Shale Gas: A Global Resource. *Oil Review*. 23 (3): 28-39.
- Breit, G.N. and Wanty, R.B. (1991). Vanadium Accumulation in Carbonaceous Rocks: A Review of Geochemical Controls during Deposition and Diagenesis. *Chem. Geol.* 91, 83-97.
- Bruce, C.H. (1984). Smectite dehydration- Its Relation to Structural Development and Hydrocarbon Accumulation in Northern Gulf of Mexico Basin. *AAPG Bull.* 68, 673-683.
- Brüchert, V.R., Jorgensen, B.B., Neumann, K., Richmann, D., Schlösser, M. and Schulz, H. (2003). Regulation of Bacterial Sulphate Reduction and Hydrogen Sulphide Fluxes in the Central Namibian Coastal Upwelling Zone. *Geochimica et Cosmochimica Acta*. 67, 4505–4518.
- Brumsack, H. J. (2006). The Trace Metal Content of Recent Organic Carbon-Rich Sediments: Implications for Cretaceous Black Shale Formation. *Palaeogeography, Palaeoclimatology, Palaeoecology*. 232, 344–361.
- Bullin, K. and Krouskop, P. (2008). Composition Variety Complicates Processing Plans for US Shale Gas. A Presentation at the Forum, Gas Processors Association-Houston Chapter. 1-9.

- Burke, K.C.B., Dessaugie, T. F. J., and Whiteman A.J. (1970). The opening of the Gulf of Guinea and the Geological History of the Benue Depression and Niger Delta. *Nature, Phys. Sci.* 233 (38): 51-55.
- Burke, K.C., Desavaugie, T.F.J., and Whiteman, A.J. (1972). Geology History of the Benue Valley and Adjacent Areas. *In: Desavaugie, T.F.J. and Whiteman, A.J. (Eds.) African Geology.* University of Ibadan Press, Nigeria. 47-67.
- Bust, V.K., Majid, A.A., Oletu, J.U. and Worthington, P.F. (2013). The Petrophysics of Shale Gas Reservoirs: Technical Challenges and Pragmatic Solutions. *Petroleum Geoscience.* 19, 91-103. doi: 10.1144/petgeo. 2012-031.
- Calvert, S.E. and Pedersen, T.F. (1996). Sedimentary Geochemistry of Manganese: Implications for the Environment of Formation of Manganiferous Black Shales. *Econ. Geol.* 91, 36-47.
- Carvalho MA, Filho JGM, Menezes TR. (2006). Paleoenvironmental Reconstruction Based on Palynofacies Analysis of the Aptian - Albian Succession of the Sergipe Basin, Northeastern Brazil. *Marine Micropaleont.* 59, 56-81.
- Chaillou, G., Anschutz, P., Lavaux, G., Schäfer, J. and Blanc, G. (2002). The distribution of Mo, U, and Cd in Relation to Major Redox Species in Muddy Sediments of the Bay of Biscay. *Mar. Chem.* 80, 41-59.
- Chamley, H. (1989). Clay Sedimentology. Springer Verlag, Berlin. 623.
- Churchman, G.J. (2000). The alteration and formation of soil minerals by weathering. *In: Summer, M.E. (Ed.), Handbook of soil Science.* CRC Press, New York. 1, F3-27.
- Clementz, D.M. (1979). Effect of oil and bitumen saturation on source rock pyrolysis. *AAPG Bull.* 63, 2227-2232.
- Collinson, J.D. (1969). The Sedimentology of the Grindslow Shales and the Kinderscout Grit: A deltaic complex in the Namurian of Northern England. *Journal of Sedimentary Petrology.* 39, 194 - 221.



- Conford, C. (1986). Source Rocks and Hydrocarbons of the North, Sea. *In*: K.W. Glannic (Ed.), Introduction to the Petroleum Geology of the North Sea. Oxford, U.K.197-236.
- Cooks, E.H. and Corboy, J.J. (2003). Great Basin Paleozoic Carbonate Platform: Facies, Facies Transitions, Depositional Models, Platform Architecture, Sequence Stratigraphy, and Predictive Mineral Host Models. Field Trip Guidebook—Metallogeny of the Great Basin Project, 17-22 August 2003, USGS, Open-File Report. 2004-1078.
- Corredor, F., Shaw, J.H. and Bilotti, F. (2005). Structural Styles in the Deep-water Field and Thrust Belts for the Niger Delta. *AAPG Bull.* 89, 753-780.
- Cox, R., Lowe, D. R., Cullers, R. L. (1995). The Influence of Sediment Recycling and Basement Composition on Evolution of Mudrock Chemistry in the Southwestern United States. *Geochimica et Cosmochimica Acta.* 59 (14): 2919-2940.
- Cratchley, C. R. and Jones, J. P. (1965). An Interpretation of the Geology and Gravity Anomalies of the Benue Valley, Nigeria. Overseas Geological Survey and Geophysical Paper. 1, 1 – 26.
- Darmonian, S. A. (1975). Planktonic Foraminiferal from the Upper Cretaceous of Southeastern Iraq: Biostratigraphy and Systematic of the *Heterohelicidae*. *Micropaleontology.* 21 (22): 185-214.
- Dayal, A.M., Mani, D., Mishra, S, and Patil, D.J. (2013). Shale Gas Prospects of the CamBay Basin, Western India. *GEOHORIZONS.* 26-31.
- Degens, E.T. (1958). Geochemical Investigations toward Determining Facies of the Ruhr- and Saar Carboniferous. *Glickauf.* 94 (15/16): 513-520.
- Degens, E.T., Williams, E.G., Keith, M.L., (1957). Environmental Studies of Carboniferous Sediments Part 1: Geochemical Criteria for Differentiating Marine from Fresh Water Shales. *AAPG Bull.* 41 (11): 2427 - 2455.

- Dehairs, F., Chesselet, R. and Jedwab, J. (1980). Discrete Suspended Particles of Barite and Barium Cycle in the Open Ocean. *Earth Planet. Sci. Lett.* 49, 528–550.
- Dehairs, F., Lambert, C.E., Chesselet, R. and Risler, N. (1987). The Biological Production of Marine Suspended Barite and the Barium Cycle in the Western Mediterranean Sea. *Biogeochemistry*. 4, 119–139.
- Dehairs, F., Stoobants, N. and Goeyens, L. (1991). Suspended Barite as a Tracer of Biological Activity in the Southern Ocean. *Mar. Chem.* 35, 399–410.
- Dehairs, F., Baeyens, W. and Goeyens, L. (1992). Accumulation of Suspended Barite at Mesopelagic Depths and Export Production in the Southern Ocean. *Science*. 258, 1332–1335.
- Demaison, G.J and Moore, G.T. (1980). Anoxic Environment and Oil Bed Genesis: *AAPG Bull.* 137, 1179-1209.
- Dembicki, H., Horsfield, B., and Ho, T.T.Y. (1983). Source Rock Evaluation by Pyrolysis - Gas Chromatography. *AAPG Bull.* 67, 1094-1103.
- De Villiers, S., Shen, G. T., and Nelson, B. K.. (1994). The Sr/Ca temperature relationship in coralline aragonite—influence of variability in (Sr/Ca) seawater and skeletal growth-parameters. *Geochim. Cosmochim. Acta.* 58, 197–208.
- Dill, H. (1986). Metallogenesis of Early Paleozoic Graptolite Shales from the Graefenthal Horst (Northern Bavaria-Federal Republic of Germany). *Econ. Geol.* 81, 889–903.
- Dill, H., Teschner, M. and Wehner, H. (1988). Petrography, Inorganic and Organic Geochemistry of Lower Permian Carbonaceous Fan Sequences (Brandschiefer Series)-Federal Republic of Germany: Constraints to their Paleogeography and Assessment of their Source Rock Potential. *Chem. Geol.* 67, 307–325.
- Dodd, J. R. and Stanton, R. J. (1981). *Paleoecology, Concepts and Applications*: New York, John Wiley. 559.

- Dominik, W. (1985). Stratigraphie und Sedimentologie (Geochemie, Schwer mineral analyse) der Oberkreide von Bahariya und ihre Korrelation zum Dakhla Becken (Western Desert, Ägypten), Berliner Geowiss. Berlin Abh. (A) 62:173.
- Dow, W. G. (1977). Kerogen Studies and Geological Interpretations. *Journal of Geochemical Exploration*. 79-99.
- Durham, L.S. (2008). Appalachian Basin's Marcellus – the new target. *Explorer*. AAPG. 7, 2-4.
- Dymann, T. S., Palacos, J. G., Tysdal, R. G., Perry, W. J. and Pawlewicz, M. J. (1996). Source Rock Potential of Middle Cretaceous Rocks in Southwestern Montana: *AAPG Bull.* 80, 1177-1184.
- Dymond, J., Suess, E. and Lyle, M. (1992). Barium in Deep –Sea Sediment: A Geochemical Proxy for Paleproductivity. *Paleoceanography*. 7, 163-181.
- Dyni, J.R. (2003). Geology and Resources of Some World Oil Shale Deposits. *USGA Oil Shale*. 20 (3): 235. [http://pubs.usgs.gov/sir/2005/5294/pdf/sir5294\\_508.pdf](http://pubs.usgs.gov/sir/2005/5294/pdf/sir5294_508.pdf)
- Dyni, J. R. (2006). Geology and resources of some world oil shale deposits. Scientific Investigations Report 2005–5294 (Pdf). United States Department of the Interior, United States Geological Survey. Retrieved 9 July 2007.
- Ede, T.A.D.U. (2009). Stratigraphy and Depositional Model of a Petroleum Source Rock Facies, Eze-Aku Group, Abakaliki Basin, Southeastern Nigeria. Unpublished M.Sc. thesis. University of Nigeria, Nsukka.
- Egboka, B.C.E., (1993). Water Resources Problem in the Enugu Area of Enugu State. *Nigerian Journal of Mining Geology*. 20, 1 – 6.
- Egboka, B. C. E., and Okpoko, E. I. (1984). Gully Erosion in the Agulu-Nanka Region of Anambra State, Nigeria: Challenges in African Hydrology and Water Resources. *Proceedings of the Harare Symposium, IAHS Publ.* 144, 335–347.

- Ehinola, O.A. (2010). Biostratigraphy and Depositional Environment of the Oil Shale Deposit in the Oil Shale Deposit in the Abakaliki Anticlinorium, Southeastern Nigeria. *Oil Shale*. 27 (2): 99-125.
- Ehinola, O.A., C.E. Bassey, and C.M. Ekweozor, (2003). Preliminary Studies on the Lithostratigraphy and Depositional Environment of the Oil Shale Deposits of Abakaliki Anticlinorium, Southeastern Nigeria. *Journal of Mining and Geology*. 39 (2): 85-94.
- Ehinola, O.A., Shengfei, Q., and Onibonoje, A.A. (2010). The Paleoenvironmental Significance of Pyritic Nodules from Lokpanta Oil Shale Interval in the Petroleum System of Lower Benue Trough, Nigeria. *Petroleum and Coal*. 110-122.
- EIA website. <http://www.eia.gov/analysis/studies/worldshalegas/> accessed on 24<sup>th</sup> April, 2011.
- Ekweozor, C.M. (2001). Type locality of Lokpanta Oil Shale: Abstract volume, Nigeria Mining and Geoscience Society (NMGS) Conference, Port Harcourt.
- Ekweozor, C.M. (2004). Insight into Origin of Giant Hydrocarbon Fields of Deep/Ultra-deep Offshore, Niger Delta from Geochemistry of Cretaceous Carbonaceous Sediments from Southeastern Nigeria. Abstract Volume, 6<sup>th</sup> International Conference on Petroleum Geochemistry and Exploration in the Afro-Asian Region, Beijing, China. 25-26.
- Ekweozor, C.M., (2005). Searching for Petroleum in the Anambra Basin, Nigeria, *In* C.O. Okogbue, (Ed.) Hydrocarbon Potentials of the Anambra Basin. Geology, Geochemistry and Geohistory Perspectives. Great AP Express Publ., Nsukka. 83-110.
- Ekweozor, C.M. and Unomah, G.I. (1990). First Discovery of Oil Shale in the Benue Trough, Nigeria. *Fuel*. 69, 502-508.
- Elricka, M. and Hinnov, L.A., 2007. Millennial-scale paleoclimate Cycles Recorded in Widespread Palaeozoic deeper Water Rhythmites of North America. *Palaeogeography, Palaeoclimatology, Palaeoecology*. 243, 348-372.

- El-Wekeil, S.S. and Abou El-Anwar, E.A. (2013). Petrology, Geochemistry and Sedimentation History of Lower Carboniferous Shales in Gebel Abu Durba, Southwestern Sinai, Egypt. *Journal of Applied Sciences Research*. 9 (8): 4781-4798.
- Ernst and Young, (2011). Shale Gas in Europe: Revolution or Evolution? 9<sup>th</sup> International Oil and Gas Conference and Exhibition, New Dehli, India. 1-16.
- Espitalie, J., Madec, M. and Tissot, B. (1980). Role of Mineral Matrix in Kerogen Pyrolysis: Influences on Petroleum Generation and Migration. *AAPG Bull.* 64, 59-66.
- Essien, U.N. and Bassey, D.E. (2012) Lithostratigraphy, Microfacies Succession, Sequence Stratigraphy and Depositional Environments of the New Netim Formation, Calabar Flank, South Eastern Nigeria. *International Journal of Basic and Applied Science*. 12, 6-19.
- Farrington, J.L., (1952). A Preliminary Description of the Nigerian Lead-Zinc Field: *Econ. Geol.* 47, 583-608.
- Falconer, J.D., (1911). The Geology and Geography of Northern Nigeria: Macmillan Publ., London.
- Fayose, E. A. (1979). Cretaceous Microfauna from Ituk-2 well Calabar, Cross River State of Nigeria. *Bulletin de L'Institute Fondamental d'Afrique Noire*. T. 40 serie A (40), 469-479.
- Fayose, E.A and De Klasz, I. (1976). Microfossils of the Eze-Aku Formation (Turonian) at Nkalagu Quarry, Eastern Nigeria. *Journal of Mining and Geology*. 13 (2): 51-61.
- Fedo, C.M., Nesbitt, H.W., and Young, G.M. (1995). Unraveling the Effects of Potassium Metasomatism in Sedimentary Rocks and Paleosoils, with Implications for Paleoweathering Conditions and Provenance. *Geology*. 23, 921-924.
- Filipelli, G.M., Delaney, M.L., Garrison, R.E., Omarzai, S.K. and Behl, R.J. (1994). Phosphorus Accumulation Rates in a Miocene Low Oxygen Basins: The Monterey Formation (Pismo Basin), California. *Mar. Geol.* 116, 419-430.

- Floyd, P.A. and Leveridge, B.E., (1987). Tectonic Environment of the Devonian Gramscatho Basin, South Cornwell: Framework Mode and Geochemical Evidence from Turbidite Sandstones. *Journal of the Geological Society London*.144, 531–542.
- Frantz, J.H. and Jochen, V. (2005). Shale Gas - When Your Gas Reservoir is Unconventional so is our Solution. Schlumberger White Paper.
- Gabo, J.A.S., Dimalanta, C.B., Asio, M.G., Queano, K.L., Yumul Jr., G.P. and Imai, A. (2009). Geology and Geochemistry of the Clastic Sequences from Northwestern Panay (Philippines): Implications for Provenance and Geotectonic Setting. *Tectonophysics*. 479, 111-119.
- Garver, J.I., Royce, P.R. and Scott, T.J. (1994). The presence of Ophiolites in Tectonic Highlands as Determined by Chromium and Nickel Anomalies in Synorogenic Shales: Two Examples from North America. *Russian Geology and Geophysics*. 35, 1-8.
- Garver, J.I., Royce, P.R. and Smick, T.A. (1996). Chromium and Nickel in Shale of the Taconic Foreland: A Case Study for the Provenance of Fine-Grained Sediments with an Ultramafic Source. *Journal of Sedimentary Research*. 66, 100-106.
- Geel, C., Schulz, H., Booth, P., deWit, M. and Brian Horsfield, B. (2013). Shale gas characteristics of Permian black shales in South Africa: Results from Recent Drilling in the Ecca Group (Eastern Cape). European Geosciences Union General Assembly, 2013. EGU Division Energy, Resources & the Environment, ERE. *Energy Procedia*. 40, 256 – 265.
- Ghandour, I. M., Masuda, H. and Maejima, W. (2003). Mineralogical and Chemical Characteristics of Bojocan-Bathonian Shales, G. Al-Maghara, North Sinai, Egypt: Climate and Environment Significance. *Geochemical Journal*. 1, 87-108.
- Gobeil, C., MacDonald, R.W. and Sundby, B. (1997). Diagenetic Separation of Cadmium and Manganese in Suboxic Continental Margin Sediments. *Geochim. Cosmochim. Acta*. 61, 4647–4654.

- Goldberg, K. and Munir Humayun, M., (2010). The applicability of the Chemical Index of Alteration as a paleoclimatic indicator: An example from the Permian of the Paraná Basin, Brazil. *Palaeogeography, Palaeoclimatology, Palaeoecology*. 293, 175-183.
- Gorin, G.E. and Feist-Burkhardt, S. (1990). Organic facies of Lower to Middle Jurassic sediments in the Jura Mountains, Switzerland. *Review of Paleobotany and Palynology*. 65, 349-355.
- Grant, N.K. (1971). South Atlantic, Benue Trough and Gulf of Guinea Cretaceous Triple Junction: *Bull. Geol. Soc. Am.* 2, 2295-2298.
- Gromet, L.P., Dymek, R.F., Haskin, L.A. and Korotev, R.L. (1984). The "North American Shale Composite. "Ist Compilations, Major and Trace Element Characteristics. - *Geochim. Cosmochim. Acta*, London. 48, 2469-2482.
- Habib, D. (1979). Sedimentology of palynomorphs and palynodebris in Cretaceous Carbonaceous Facies South of Vigo Seamount. *Init Rep Deep Sea Drill Prog.* 47, 451-467.
- Hallam, A. (1982). Mesozoic Marine Organic-rich Shales. *In*: Brooks, J.R.V. and Fleet, A.J. (Eds.), *Marine Petroleum Source Rocks*. Blackwell Oxford.
- Hallam, A., Grose, J. A. and Ruffell, A. H. (1991). Paleoclimatic significance of changes in clay mineralogy across the Jurassic-Cretaceous boundary in England and France. *Palaeogeography, Palaeoclimatology, Palaeoecology*. 81, 173–187.
- Hatch, J.R. and Leventhal, J.S., (1992). Relationship between inferred redox potential of the depositional environment and geochemistry of the Upper Pennsylvanian (Missourian) Stark Shale Member of the Dennis Limestone, Wabaunsee County, Kansas, U.S.A. *Chem. Geol.* 99, 65–82.
- Hayashi, Ken-I., Fujisawa, H., Holland, H.D., and Ohmoto, H., (1997). Geochemistry of sedimentary rocks from northeastern Labrador, Canada. *Geochim. Cosmochim. Acta* 61. 4115–4137.

- Henderson, G.M. (2002). New oceanic proxies for paleoclimate. *Earth and Planetary Sci. Lettrs.* 203, 1–13.
- Herbert, T.D. (2003). Alkenone Paleotemperature Determinations. *In: H. Elderfield and K.JK. Turekian, (Eds.), Treatise in Marine Geochemistry.* Amsterdam: Elsevier. 391–432.
- Heroux, Y., Chagnon, A. and Bertrand, R. (1979). Compilation and Correlation of Major Thermal Maturation Indicators. *AAPG Bull.* 63 (12): 2128-2144.
- Hill, D.G., Lombardi, T.E. and Martin, J.P. (2004). Fractured Shale Gas Potential in New York. *Northeastern Geology and Environmental Sciences.* 26, 57-78.
- Hiscott, R.N., (1984). Ophiolitic Source Rocks for Taconic-age Flysch: Trace Element Evidence. *Geological Society of America Bull.* 95, 1261-1267.
- Hoque, M. (1977). Petrographic differentiation of tectonically controlled Cretaceous sedimentary cycles, Southeastern Nigeria.
- Hoque, M. (1984). Pyroclastics from the Lower Benue Trough of Nigeria and their Tectonic Implications. *Journal African Earth Science.* 2 (4), 1-358.
- Hoque, M. and Nwajide, C.S. (1984). Tectono – sedimentological evolution of an elongate intracratonic basin (aulacogen): the case of the Benue Trough of Nigeria. *Nigeria Journal of Mining and Geology.* 21, 19 – 26
- Horsfield, B. and Douglas, A.G. (1980). Influence of mineral on pyrolysis of kerogens. *Geochem. Cosmichim. Acta.* 44, 1119-1131.
- Hosseini, T., Ahmad, M., Bahman, S. and Reza, K.M. (2012). Chemical Variation during Pabdeh Formation Deposition, Zagros Basin: Gurpi-Pabdeh- Asmari Boundaries determination and Paleoenvironmental Condition. *Journal of Geological Geosciences.* 1(1): 1-8. doi:10.4172/jgg.1000102.
- Huber, B. T., Leckie, M. R., Norris, R. D; Bralower, T. J and Cobase, E. (1999). Foraminiferal Assemblage and Stable Isotopic Change across the Cenomanian-Turonian



- Boundary in the Subtropical North Atlantic. *Journal of Foraminiferal Research*. 29 (4): 392-417.
- Hunt, J.M. (1996). Petroleum Geochemistry and Geology, 2nd Ed.. W.H. Freeman and Company, New York. 332.
- Hust, D. (2008). County is Next Frontier for Gas Exploration. *Sullivan County Democrat*. 11-18. <http://www.scdemocrat.com/news/01January/18/news.html>.
- Hutton, A. C. (1994). Organic Petrography and Oil Shales (Pdf). *Energieia*. [University of Kentucky](http://www.uky.edu/~geology). 5 (5). Retrieved 19 December 2012.
- Igwe, E.O. and Okoro, A.U. (2016). Field and lithostratigraphic Studies of the Eze-Aku Group in the Afikpo Synclinorium, Southern Benue Trough, Nigeria. *Journal of African Earth Sciences*. 3, 1-13. Journal homepage: [www.elsevier.com](http://www.elsevier.com). <http://dx.doi.org/10.1016/j.jafrearsci.2016.03.016>.
- Iloeje, N.P. (1981). New Geography of Nigeria. (New revised edition), Longman Nigeria Ltd. 200.
- Inyang, P. E. B. (1978). The Climatic Regions. *In: Ofomata, G. E. K. (Ed.). The Nsukka Environment*. Ethiope Publ., Benin. 17 – 24.
- Ingersoll, R.V., Bullard, T.F., Ford, R.L., Grimm, J.P., Pickle, J. D. and Sares, S.W. (1984). The Effect of Grain size on Detrital Modes: A Test of the Gazzi-Dickinson Point-Counting Method. *Journal of Sedimentary Petrology*. 54 (1): 0103-0116.
- Islam, M.R., Stuart, R., Risto, A. and Vesa, P. (2002). Mineralogical Changes During Intense Chemical weathering of Sedimentary Rocks in Bangladesh. *Journal of Asian Earth sciences*. 20, 889-901.
- Iwobi, O. C. (1991). Foraminiferal Ages in the Southern Benue Trough, Nigeria. *NAPE Bull*. 6, 39-47.
- Jan. Du Chene, R. E., Onyike, M. S. and Sowami, M. A. (1978). Some New Eocene Pollen of the Ogwashi- Asaba Formation, SE, Nigeria, *Reviste Espand. Micropaleontology*. 10 (2): 285-322.

- Jarvie, D. M., Claxton, B. L., Henk, F. and Breyer, J.T. (2001). Oil and Shale Gas from the Barnett Shale, Ft. Worth Basin, Texas. *AAPG Bull.* 85 (13): (Supplement) A100.
- Jones, B. and Manning, D.A.C., (1994). Comparison of Geological Indices used for the Interpretation of Palaeoredox Conditions in Ancient Mudstones. *Chem. Geol.* 111, 111-129.
- Kenison Falkner, K., Klinkhammer, G.P., Bowers, T.S., Todd, J.F., Lewis, B.L., Landing, W.M. and Edmond, J.M. (1993). The Behavior of Barium in Anoxic Marine Waters. *Geochim. Cosmochim. Acta.* 57, 537–554.
- Kirschbaum, A., Martinez, E., Pettinari, G. and Herrero, S., (2005). Weathering Profiles in Granites, Sierra Notre (Cordoba, Argentina). *Journal of South American Earth Sciences.* 19, 479–493.
- Killops, S.D and Killops, V.J. (2005). Introduction to Organic Geochemistry, 2nd Ed.. Blackwell Publ., USA. 400.
- Kogbe, C.A., (1989). Paleogeographic History of Nigeria from Albian Times. *In: C.A. Kogbe, (Ed.). Geology of Nigeria. Elizabethan Publ. Co. Lagos.* 257-275.
- Kogbe, C.A., (1989b.) The Cretaceous and Paleogene Sediments of Southern Nigeria. *In: C.A. Kogbe (Ed.). Geology of Nigeria. Elizabethan Publ. Co. Lagos.* 325-334
- Kronberg, B. I. and Nesbitt, H. W., (1981). Quantification of Weathering, Soil Geochemistry and Soil Fertility. *Journal of Soil Science.* 32, 453-459.
- Kuuskraa, V., Van Leeuwen, T and Wallace, M. (2011). Improving Domestic Energy Security and Lowering CO<sub>2</sub> Emissions with “Next Generation” CO<sub>2</sub>-Enhanced Oil Recovery (CO<sub>2</sub>-EOR): doe/netl-2011/1504, 89.
- Langford, F.F, and Blanc-Valleron, M.M. (1990). Interpreting Rock-Eval Pyrolysis Data Using Graphs of Pyrolzable Hydrocarbons vs. Total Organic Carbon. *AAPG Bull.* 74, 799-804.

- Lechtenböhrer, S., Altmann, M., Capito, S., Matra, Z., Weindorf, W. and Zittel, W. (2011). Impacts of Shale Gas and Shale Oil Extraction on the Environment and on Human Health. ENVI. Directorate General for Internal Policies, Policy Department A: Economic and Scientific Policy. European Parliament. 1-88.
- Leckie, R.M., (1987). Paleocology of mid-Cretaceous Planktonic Foraminifera: A comparison of Open Ocean and Epicontinental sea assemblages: *Micropaleontology*. 33, 164-176.
- Leckie, R.M. (1989). A Paleooceanographic Model for the Early Evolutionary History of Planktic Foraminifera: *Palaeogeography, Palaeoclimatology, Palaeoecology*. 73, 107-138.
- Leckie, D.A., Kalkrueth, W.D. and Snowdon, L.R. (1988). Source Rock Potential and Thermal Maturity of Lower Cretaceous Strata: Monk Pass Area, British Columbia. *AAPG Bull.* 72 (7): 820-838.
- Lewan, M.D. (1984). Factors Controlling the Proportionality of Vanadium and Nickel in Crude Oils. *Geochimica et Cosmochimica Acta*. 48, 2231–2238.
- Lewan, M.D. and Maynard, J.B. (1982). Factors controlling Enrichment of Vanadium and Nickel in the Bitumen of Organic Sedimentary Rocks. *Geochimica et Cosmochimica Acta*. 46, 2547–2560.
- Liua, B., Wangb, Y., Sua, X. and Zheng, H. (2013). Elemental Geochemistry of Northern Slope Sediments from the South China Sea: Implications for Provenance and Source Area Weathering since Early Miocene, *Chemie der Erde*. 5, 1-30.
- Lyons, T.W., Werne, J.P., Hollander, D.J., and Murray, R.W. (2003). Contrasting Sulhur Geochemistry and Fe/Al and Oceanography. *In: Izdar, E. and Murray, J.W. (Eds.). NATO ASI Series. Kluwer. 343-359.*
- Mader, D. and Neubauer, F. (2004). Provenance of Palaeozoic Sandstones from the Carnic Alps (Austria): Petrographic and Geochemical Indicators. *International Journal of Earth Sciences*. 93, 262–281.

- Madukwe, H. (2014). Organic Matter Quantity, Quality and Maturity Studies of the Paleocene Ewekoro Formation, Southwestern Nigeria. *Journal of Environment and Earth Science*. 4 (23): 118-130.
- Madukwe, H.Y. and Bassey, C.E. (2015). Geochemistry of the Ogwashi-Asaba Formation, Anambra Basin, Nigeria: Implication for Provenance, Tectonic Setting, Source-Area Weathering, Classification and Maturity. *International Journal of Science and Technology*. 4 (7): 312-327.
- Madukwe, H.Y., Obasi, R.A., Fakolode, O.R. and Bassey, C.E. (2015). Provenance, Tectonic Setting and Source-Area Weathering of the Coastal Plain Sediments, South –West, Nigeria. *Scientific Research Journal (SCIRJ)*. III (II): 20-31.
- Manum, S. B. (1976). Dinocysts in Tertiary Norwegian-Greenland Sea sediments (Deep Sea Drilling Project Leg 38), with observations on palynomorphs and palynodebris in relation to environment. *Init Rep Deep Sea Drill Prog*. 38, 897-919.
- Maslov, A.V., Krupenin, M.T. and Gareev, E.Z. (2003). Lithological, Lithochemical and Geochemical Indicators of Paleoclimate: Evidence from Riphean of the Southern Urals. *Lithology and Mineral Resources*. 38 (5): 427-446.
- Maurin, J. C., Benkhelil, J. and Robeneau, E. (1986). Fault rocks of the Kaltungo Lineament, NE Nigeria, and their relationship with the Benue Trough Tectonics. *Journal of Geological Society*, London. 143, 587 – 599.
- Mayhood, K. (2008). Low Down, Rich and Stingy - Energy Companies Just Figuring out How to Coax Natural Gas from Deepest Appalachian Shale Deposits. *The Columbus Dispatch*. 2, 15-30.
- McCarthy, K., Martin, N., Palmowski, D., Peters, K. and Stankiewicz, A. (2011). Basic Petroleum Geochemistry for Source Rock Evaluation. *Oilfield Review*. 23 (2): 32-44.
- McConnel, R.B. (1949). Notes on Lead-Zinc Deposits of Nigeria and Cretaceous Stratigraphy of Benue and Cross River Valleys: Report Geological Survey of Nigeria. 752.

- Meyer, K.M. and Kump, L.R. (2008). Oceanic Euxinia in Earth History: Causes and Consequences. *Annual Review of Earth and Planetary Sciences*. 36, 251-288.
- Miall, A. D. (2000). *Principles of Sedimentary Basin Analysis*. Springer – Verlag, Berlin Heidelberg. 616.
- Middleburg, J.J. and Comans, R.N.J. (1991). Sorption of cadmium on hydroxyapatite. *Chem. Geol.* 90, 45-53.
- Miles, J.A. (1989). *Illustrated glossary of petroleum geochemistry*. Oxford Science Publ., Oxford University Press, New York. 137.
- Mishra, M. and Sen, S. (2012). Provenance, Tectonic and Source-Area Weathering of Mesoproterozoic Kaimur Group, Vindhyan Supergroup, Central India. *Geologica Acta*. 10 (3): 283-296.
- Mode, A.W. (2002). Hydrocarbon Evaluation of Campano-Maastrichtian Strata within a Sequence Stratigraphic Framework, Southeastern Anambra basin: Unpublished PhD Thesis. University of Nigeria, Nsukka. 225.
- Morford, J.D. and Emerson, S. (1999). The Geochemistry of Redox Sensitive Trace Metals in Sediments. *Geochim. Cosmochim. Acta*. 63, 1735-1750.
- Morford, J.L., Russell, A.D. and Emerson, S. (2001). Trace Metal Evidence for Changes in the Redox Environment Associated with the Transition from Terrigenous Clay to Diatomaceous Sediments, Saanich Inlet, BC. *Mar. Geol.* 174, 355–369.
- Mudie, P.J. (1989). Palynology and Dinocyst Biostratigraphy of the Late Miocene to Pleistocene, Norwegian Sea: ODP Leg 104, Sites 642 to 644. *Proc Ocean Drilling Prog, Scientific Results*. 104, 587-610.
- Murat, R.C. (1972). Stratigraphy and Paleogeography of the Cretaceous and early Tertiary in Southern Nigeria. *In: Dissauvage T.F.J and Whiteman A.J (Eds.)*. African Geology. University of Ibadan Press. 251-266.
- Murphy, M.A and Salvador, A. (1999). International Stratigraphic Guide — An abridged version. *In: Murphy, M.A and Salvador, A. (Eds.)*, International Subcommission on

Stratigraphic Classification of I.U.G.S. International Commission on Stratigraphy. Special Episodes. 22 (4).

- Nameroff, T.J., Calvert, S.E. and Murray, J.W. (2004). Glacial–interglacial Variability in the Eastern Tropical North Pacific Oxygen Minimum Zone Recorded by Redox-Sensitive Trace Metals. *Paleoceanography*. 19, PA1010. doi:10.1029/2003PA000912.
- Nesbitt, H.W. and Young, G.M. (1982). Early Proterozoic Climates and Plate Motions Inferred from Major Element Chemistry of Lutites. *Nature*. 299, 715-717.
- Nesbitt, H.W., Mackovics, G. and Price, R.C. (1980). Chemical Processes Affecting Alkalis and Alkaline Earth during Continental Weathering. *Geochim. Cosmochim. Acta*. 44, 1659-1666.
- Nichols, G. (2009). *Sedimentology and Stratigraphy*. (2nd Ed.) John Wiley and Sons, the Atrium, Southern Gate, Chichester, UK. 419.
- Nimako, D.A. (2008). *Map Reading for West Afriabout 8th Impression*. Longman Group Ltd, England. 76.
- Njoh, O.A, and Taku, A.J. (2016). Shallow Marine Cretaceous Sequences and Petroleum Geology of the Onshore Portion Rio del Rey Basin, Cameroon, Gulf of Guinea. *Open Journal of Marine Science*. 6, 177-192.
- North, F.K. (1985). *Petroleum Geology* (2nd Ed.). Allen and Unwin, Boston.
- Norton Rose Fulbright Ltd. (2013). *Shale Gas Handbook*. 120.
- Nwachukwu, S. O. (1972). The tectonic evolution of the southern portion of the Benue Trough, Nigeria. *Geological Magazine*. 109, 411-419.
- Nwajide, C. S. (1990). Sedimentation and paleogeography of the Central Benue Trough, Nigeria. *In: C. O. ofoegbu (Ed.). The Benue Trough Structure and Evolution*. Friedrich Vieweg and Sohue, Braunchloeigh/Wiesbaden. 19 – 38.
- Nwajide, C.S., (2005). Anambra Basin of Nigeria: Synoptic Basin Analysis as a Basis for Evaluating its Hydrocarbon Prospectivity. *In: C.O. Okogbue, (Ed.). Hydrocarbon*

Potentials of the Anambra Basin: Geology, Geochemistry and Geohistory Perspectives. Great AP Express Publ., Nsukka. 1-46.

Nwajide, C.S., (2013). Geology of Nigeria's Sedimentary Basins. CSS Bookshops Ltd, Lagos. 565.

Nwajide, C. S. and Reijers, T. J. A. (1996). Geology of the Southern Anambra Basin. *In*: Reijers, T. J. A. (Ed.). Selected Chapters on Geology. SPDC, Warri. 133-148.

Nyakairu, G. W. A. and Koeberl, C. (2001). Mineralogical and Chemical Composition and Distribution of Rare Earth Elements in Clay-Rich Sediments from Central Uganda. *Geochem. Journ.* 35, 13–28.

Nyong, E.E., (1995). Cretaceous Sediments in the Calabar Flank, *In*: Ekwueme, B.N., Nyong, E.E. and Petters, S.W. (Eds.). Geological Excursion Guidebook to Calabar Flank, Oban Massif and Mamfe Embayment, SE Nigeria.

Obaje, N.G., Ulu, O.K., Petters, S.W. (1999). Biostratigraphy and Geochemical Controls of Hydrocarbon Prospects in the Benue Trough and Anambra Basin, Nigeria. *NAPE Bull.* 14 (1): 18-54.

Obaje, N.G., Wehner, H., Scheeder, G., Abubakar, M. B. and Jauro, A. (2004). Hydrocarbon Propectivity of Nigeria's Inland Basins: From the Viewpoint of Organic Geochemistry and Organic Petrology. *AAPG Bull.* 87, 325-353.

Obiora, S. C. (2002). Evaluation of the Effects of Igneous Bodies on the Sedimentary Fills of the Lower Benue Rift and vice versa. Unpublished PhD Thesis. University of Nigeria, Nsukka. 289.

Oboh, F. E. (1992). Multivariate Statistical Analysis of Palynodebris from the Middle Miocene of the Niger Delta and their Environmental Significance. *Palaios.* 7, 559-573.

Odedede, O. (2011). Sedimentology and Paleoenvironment of the Gombe Sandstone and Lower Kerri – Kerri Formation around Biri Fulani, Upper Benue Trough, Northeastern Nigeria. *Nigeria Journal of Mining and Geology.* 47 (1): 1 – 17.

- Odoma, A.N, Obaje, N.G., Omade, J.I., Idakwo, S.O. and Erbacher. J. (2013). Paleoclimate Reconstruction during Mamu Formation (Cretaceous) Based on clay Mineral Distributions. *IOSR Journal of Applied Geology and Geophysics*. 1 (5): 4-46.
- Oha, I.A., Onuoha, K.M., Nwegbu, A.N. and Abba, A.U. (2016). Interpretation of high resolution aeromagnetic data over Southern Benue Trough, Southeastern Nigeria. *Journal of Earth System Science*. 3, 1-19. <https://www.researchgate.net/publication/297889831>.
- Ojoh, K. A. (1990). Cretaceous geodynamic evolution of the southern part of the Benue Trough (Nigeria) in the equatorial domain of the South Atlantic; Basin analysis and Paleo-oceanography. *Bulletin des Centres de Recherches Exploration-Production. Elf – Aquitaine*. 14, 419-442.
- Ojoh, K.A. (1992). The Southern Part of the Benue Trough (Nigeria) Cretaceous Stratigraphy, Basin Analysis, Paleo-oceanography and Geodynamic Evolution in the Equatorial Domain of the South Atlantic. *NAPE Bull*. 7, 131-152.
- Ojo, O. J., Hameed, O. A., Alade, B. (2010). The Sedimentary Lithofacies, Paleoenvironments and Hydrocarbon Source Rock Facies of the Eze-Aku Formation, Lower Benue Trough, Nigeria. *The Journal of Earth Sciences*. 4 (1): 7 – 22.
- Okeke, H.C., Orajaka, I.P., Okoro, A.U. and Onuigbo, E.N. (2014). Biomarker Evaluation of the Oil Generative Potential of Organic Matter, in the Upper Maastrichtian Strata, Anambra Basin, Southern Nigeria. *Journal of Scientific Research*. 2 (1):16-25.
- Okoro, A.U. and Igwe, E.O. (2014). Lithofacies and Depositional Environment of the Amasiri Sandstone, Southern Benue Trough, Nigeria. *Journal of African Earth Science*. 100, 179–190.
- Olade, M. A. (1975). Evolution of Nigeria's Benue Trough, (Aulacogen); a tectonic model. *Geological Magazine*. 112, 575-581.
- Olade, M. A. (1978). Early Cretaceous Basalt Volcanism and Initial Continental Rifting in Benue Trough, Nigeria. *Nature*, London. 273, 458 – 459.



- Olade, M. A. (1979). The Abakaliki Pyroclastics of the Southern Benue Trough Nigeria: Their petrology and Tectonic Significance. *Journal of Mining and Geology*. 16, 17-26.
- Oni, S.O., Olatunji, A.S. and Ehinola, O.A. (2014). Determination of Provenance and Tectonic Setting of Niger Delta Clastic Facies Using Well-Y, Onshore Delta State, Nigeria. *Journal of Geochemistry*. Article ID 960139, 1-13.
- Onuoha, K. M. (2005). A Close Look at the Petroleum Potential of the Anambra Basin: Inputs from Geophysics and Geohistory,” *In: Okogbue, C.O. (Ed.). Hydrocarbon Potentials of the Anambra Basin. Geology, Geochemistry and Geohistory Perspectives. Great AP Express Publ., Nsukka. 47-82.*
- Onyekuru, S.O., Ibelegbu, E.C., Iwuagwu, J.C., Essien, A.G. and Akaolisa, C.Z. (2012). Sequence Stratigraphic Analysis of “XB Filed”, Central Swamp Depobelt, Niger Delta Basin, Southern Nigeria. *Internal Journal of Geosciences*. 3, 237-257.
- Orajaka, I. P and Umenwaliri, S., (1989). Diagenetic Alteration of Volcaniclastic Rocks from Abakaliki Area, Southeastern Nigeria. *Journal of Mining and Geology*. 25. (1and 2): 97-102.
- Osae, S., Asiedu, D.K., Banoeng-Yakubo, B., Koeberl, C. and Dampare, S.B. (2006). Provenance and Tectonic Setting of Late Proterozoic Buem Sandstones of Southeastern Ghana: Evidence from Geochemistry and Detrital Modes. *Journal of African. Earth Science*. 44, 85- 96.
- Ots, A. (2007). Estonian oil shale properties and utilization in power plants (Pdf). *Energetika*. Lithuanian Academy of Sciences Publishers. 53 (2): 8–18. Retrieved 6 May 2011.
- Parham, W. E. (1966). Lateral Variations in Clay Mineral Assemblages in Modern and Ancient Sediments. *In: Gekker, K and Weiss, A. (Eds.). Proc. Int. Clay Conf. Jerusalem*. 1, 136 – 145.
- Pennsylvania State Department of Conservation and Natural Resources - The Pennsylvania Petroleum Source Rock Geochemistry Database (2011): Available on: [http://www.dcnr.state.pa.us/topogeo/econresource/oilandgas/marcellus/sourcerockindex/sourcerock\\_rockeal/index.html](http://www.dcnr.state.pa.us/topogeo/econresource/oilandgas/marcellus/sourcerockindex/sourcerock_rockeal/index.html).

- Pessagno, E. A. (1967). Upper Cretaceous Planktonic Foraminifera from the Western Gulf Coastal Plain of New Jersey. *Paleontographica Americana*. 5 (37): 245-445.
- Peters, K.E. (1986). Guidelines for Evaluating Petroleum Source Rocks Using Programmed Pyrolysis. *AAPG Bull.* 70, 318-329.
- Peters, K. E. and Moldowan. J. M. (1993). The Biomarker Guide, Interpreting Molecular Fossils in Petroleum and Ancient Sediments. Prentice Hall, 363.
- Peters, K.E and Cassa, MR. (1994). Applied Source Rock Geochemistry. *In: Magoon, L.B and Dow, W.G (Eds.). The Petroleum System- From Source to Trap. AAPG, Tulsa. AAPG Memoir 60. 93-120.*
- Petters, S.W. (1978). Middle Cretaceous Paleoenvironments and Biostratigraphy of the Benue Trough, Nigeria. *Geological Society of America Bull.* 89, 151-154.
- Petters, S. W. (1980). Biostratigraphy of Upper Cretaceous foraminifera of the Benue Trough, Nigeria. *Journal of Foraminiferal Research.* 10. 191-204.
- Petters, S.W. and Ekweozor, C.M. (1982). Petroleum Geology of the Benue Trough and Southeastern Chad Basin, Nigeria. *AAPG Bull.* 66, 1141-1149.
- Pettijohn, F.J. (1957). Sedimentary Rocks, 2nd Ed.. Harper & Row, New York.
- Pettijohn, F.J., Potter, P.R. and Siever, R., (1987). Sand and sandstones. Springer, New York, 2nd Ed.. 553.
- Piper, D.Z. and Perkins, R.B., (2004). A modern vs. Permian black shale—the hydrography, primary productivity, and water-column chemistry of deposition. *Chem. Geol.* 206, 177–197.
- Pocock, S.A.J., Vasanthi, G. and Venkatachala, B.S. (1988). Introduction to the Study of Particulate Organic Materials and Ecological Perspectives. *Journal of Palynology.* 2324, 167-188.

- Popoola, S. O., Appia, Y. J. and Oyatola, O. O. (2014). The Depositional Environments and Provenance Characteristics of Selected Sediments, South of Yewa River, Eastern Dahomey Basin, South Western Nigeria. *IOSR Journal of Applied Geology and Geophysics (IOSR-JAGG)*. 2 (5): 98-121.
- Potter, P.E., Shimp, N.F. and Witters, J. (1963). Trace elements in marine and freshwater argillaceous sediments. - *Geochim. Cosmochim. Acta*, London. 27, 669-694.
- Raiswell, R., (1976). The Microbiological Formation of Carbonate Concretions in the Upper Lias of N.E. England. *Chem. Geol.* 18, 227-244.
- Ramanathan, R. M. and Nair, K. M. (1984). Lower Cretaceous Foraminifera from the Gboko limestone, eastern Nigeria. *Journal of Mining and Geology*. 21(1&2), 41 – 48
- Rao, C.P. (1996). Modern Carbonates: Tropical, Temperature, Polar. Arts of Tasmania, Hobart, Tasmania, Australia. 206.
- Reading, H.G., Levell, B.K. (1996). Controls on the Sedimentary record. In: Sedimentary Environments: *In: Reading, H.G. (Ed.). Processes, Facies and Stratigraphy*. Blackwell Science, Oxford. 5 – 36.
- Reijers, T.J.A. (1996). Selected Chapters on geology: Shell Petrol. Dev. Co. (Nigeria) Publ. 197.
- Reifsnnyder, W. E. and Darnhofer, T. (1989). [\*Meteorology and agroforestry\*](#). World Agroforestry Centre. 544. [ISBN 92-9059-059-9](#).
- Reyment, R. A. (1965). Aspects of the Geology of Nigeria. Ibadan University Press. 145.
- Riboulleau, A., Baudin, F., Deconinck, J.-F., Derenne, S., Largeau, C., Tribovillard, N. (2003). Depositional Conditions and Organic Matter Preservation Pathways in an Epicontinental Environment: The Upper Jurassic Kashpir Oil Shales (Volga Basin, Russia). *Palaeogeography, Palaeoclimatology, Palaeoecology*. 197, 171–197.

- Richelot, C. and Streel, M. (1985). Transport et sédimentation du pollen par les courants aériens, fluviaux et marins à Calvi (Corse). *Pollen et Spores*. 34, 349-364.
- Rimmer, S. M. 2004. Geochemical Paleoredox Indicators in Devonian–Mississippian Black Shales. Central Appalachian Basin (USA). *Chem. Geol.* 206 (3-4): 373–391.  
doi:10.1016/j.chemgeo.2003.12.029
- Rimmer, S.M., Thompson, J.A., Goodnight, S.A. and Robl, T.L. (2004). Multiple Controls on the Preservation of Organic Matter in Devonian–Mississippian Marine Black Shales: Geochemical and Petrographic Evidence. *Palaeogeography, Palaeoclimatology, Palaeoecology*. 215, 125–154.
- Riquier, L., Tribouillard, N., Averbuch, O., Joachimski, M.M., Racki, G., Devleeschouwer, X., El Albani, A. and Riboulleau, A. (2005). Productivity and Bottom Water Redox Conditions at the Frasnian–Famennian Boundary on both sides of the Eovariscan Belt: Constraints from Trace-Element Geochemistry. In: Over, D.J., Morrow, J.R. and Wignall, P.B. (Eds.). *Understanding Late Devonian and Permian–Triassic Biotic and Climatic Events: Towards an Integrated Approach: Developments in Palaeontology and Stratigraphy*. Elsevier Publ. Co. 199–224.
- Robert, C., and Kennett, J. P. (1994). Antarctic Subtropical Humid Episode at the Paleocene–Eocene Boundary: Clay Mineral Evidence. *Geology*. 22, 211-214.
- Rokosh, C.D., Pawlowicz, H., Berhane, S.D.A. and Beaton, A.P. (2009). What is Shale Gas? An Introduction to Shale-Gas Geology in Alberta. Energy Resources Conservation Board (ERCB), Alberta Geological Survey. Open File Report. 1-26.
- Rosenthal, Y., Lam, P., Boyle, E.A. and Thomson, J. (1995). Authigenic Cadmium Enrichments in Suboxic Sediments: Precipitation and Postdepositional Mobility. *Earth Planet. Sci. Lett.* 132, 99–111.
- Rosenthal, Y., Boyle, E.A., Labeyrie, L. (1997). Last Glacial Maximum Paleochemistry and Deepwater Circulation in the Southern Ocean: Evidence from Foraminiferal Cd. *Paleoceanography*. 12, 787–796.

- Roser, B.P. and Korsch, R.J. (1986). Determination of Tectonic Setting of Sandstone-Mudstone Suites using SiO<sub>2</sub> content and K<sub>2</sub>O/Na<sub>2</sub>O Ratio. *Journal of Geology*. 94, 635–650.
- Ross, D.J.K. and Bustin, R.M. (2006). Sediment Geochemistry of the Lower Jurassic Gordondale Member, Northeastern British Columbia. *Bull. of Canadian Petroleum Geology*. 54, 337–365.
- Russell, A.D. and Morford, J.I. (2001). The Behavior of Redox-Sensitive Metals across a Laminated-Massive-Laminated Transition in Saanich Inlet, British Columbia. *Mar. Geol.* 174 (1–4): 341–354.
- Rutsch, H.-J., Mangini, A., Bonani, G., Dittrich-Hannen, B., Kubile, P. W., Suter, M. and Segl, M. 1995. Be and Ba Concentrations in Western African Sediments Trace Productivity in the Past. *Earth Planet. Sci. Lett.* 133, 129–143.
- Sageman, B.B., Murphy, A.E., Werne, J.P., Ver Straeten, C.A., Hollander, D.J., and Lyons, T.W. (2003). A Tale of Shales: The Relative Roles of Production, Decomposition, and Dilution in the Accumulation of Organic-Rich Strata, Middle-Upper Devonian, Appalachian Basin. *Chem. Geol.* 195(1-4): 229-273.
- Sanni, L. O. (2007). [\*Cassava Post-Harvest Needs Assessment Survey in Nigeria\*](#). IITA. 165. [\*ISBN 978-131-265-3\*](#).
- Sari, A. and Koca, D. (2012). An Approach to Provenance, Tectonic and Redox Conditions of Jurassic-Cretaceous Akkuyu Formation, Central Taurids, Turkey. *Minerals Res. Expl. Bull.* 144, 51-74.
- Scheidegger, A. E. and Ajakaiye, D. E. (1985). Geodynamics of Nigeria Shield Areas. *Journal of African Earth Sciences*. 3 (4): 461 – 470.
- Schrank, E. (1994). Nonmarine Cretaceous Palynology of North Kordofan, Sudan, with Notes on Fossil Salviniiales (Water Ferns): *Geol. Rundsch.* 83, 773-786.

- Schreier, C. (1988). *Geochemie und Mineralogie Oberkretazischer und alttertiärer Pelite der östlichen Wüste Ägyptens und ihre geologische Interpretation*. Berliner Geowiss, Berlin. Ab (A): 97-124.
- Selby, M.J. (1993). *Hillslope Materials and Processes*. 2nd Ed. Oxford University Press, Oxford. 480.
- Shell-BP (1957). *Geological Maps of the Lower Benue Trough, Scale 1:250,000: Geologic Survey of Nigeria, 8 Maps*.
- Shute, T. (2007). *The Next Great Gas Play*. <http://www.fool.com/investing/value/2007/12/18/the-next-great-gas-play.aspx>
- Singh, M., Sharma, M. and Tobschall, H.L. 2005. Weathering of the Ganga Alluvial Plain, Northern India: Implications from Fluvial Geochemistry of the Gomati River. *Appl. Geochem.* 20, 1-21.
- Simpson, A. (1955). The Nigerian Coal Field: The Geology of Parts of Owerri and Benue Provinces. *Nig. Geol. Surv. Bull.* 24, 1-85.
- Singh, M., Sharma, M. and Tobschall, H.L. (2005). Weathering of the Ganga alluvial plain, northern India: implications from fluvial geochemistry of the Gomati River. *Appl. Geochem.*, 20, 1-21.
- Snowdon L. R. (1989). Organic Matter Properties and Thermal Evolution. *In: Hutcheon, I. E. (Ed.). Short Course in Burial Diagenesis*. Mineralogical Association of Canada, Short Course Handbook. 15, 39-40.
- Sumi, L. (2008). Shale gas: Focus on the Marcellus Shale, The Oil and Gas Accountability Project/Earthworks. 1-25.
- Tattam, C.M. (1944). A Review of Nigerian Stratigraphy: Report of Geological Society of Nigeria. 24-46.
- Taylor, S. R. and McLennan, S. M. (1985). *The Continental Crust: its Composition and Evolution: An Examination of the Geological Record Preserved in Sedimentary Rocks*: Blackwell., Oxford, U.K. 328.

- Tissot, B. P. and Welte, D. H. (1978). *Petroleum Formation and Occurrence*. Springer Verlag, New York. 521.
- Tissot, B. P. and Welte, D. H. (1984). *Petroleum Formation and Occurrence*. Springer, Berlin. 699.
- Tourtelot, H.A., (1964). Minor Element Composition and Organic Carbon Content of Marine and Non-Marine Shales of Late Cretaceous age in Western Interior of the United States. *Geochim. Cosmochim. Acta*. 28, 1579-1604.
- Traverse, A. (2008). *Paleopalynology*. Dordrecht (Netherlands): Springer. 814.
- Tribovillard, N., Averbuch, O., Devleeschouwer, X., Racki, G. and Riboulleau, A. (2004)a. Deep-water Anoxia over the Frasnian–Famennian Boundary (La Serre, France): a tectonically-induced Oceanic Anoxic Event? *Terra Nova*. 16, 288–295.
- Tribovillard, N., Ramdani, A. and Trentesaux, A. (2005). Controls on Organic Accumulation in Late Jurassic Shales of Northwestern Europe as Inferred from Trace-Metal Geochemistry. *In*: Harris, N. (Ed.). *The Deposition of Organic-Carbon-Rich Sediments: Models, Mechanisms, and Consequences*. SEPM Spec. Publ. 82, 145–164.
- Tribovillard, N., Algeo, T.J., Lyons, T. and Riboulleau, A. (2006). Trace Metals as Paleoredox and Paleoproductivity Proxies: An update. *Chem. Geol.* 232, 12-32.
- Tschudy, R.H. (1961). Palynomorphs as Indicators of Facies Environments in Upper Cretaceous and Lower Tertiary strata, Colorado and Wyoming. *In*: Wiloth, G., Hale, L.A., Randall, A.G. and Garrison, L. (Eds.). *16th Annual Field Conference Guidebook. Symposium on Late Cretaceous Rocks, Wyoming and Adjacent Areas*. Wyoming: Wyoming Geological Association. 53-59.
- Tucker, M.E. and Wright, V.P. (1990). *Carbonate Sedimentology*. Blackwell Scientific Publ., Oxford. 482.

- Tyson, R.V. (1984). Palynofacies Investigation of Callovian (Middle Jurassic) Sediments from DSDP Site 534, Blake Bahama Basin, western Central Atlantic. *Marine Petr. Geol.* 1, 313.
- Tyson, R.V. (1993). Palynofacies Analysis. *In: Jenkins, D.J. (Ed.) Applied Micropaleontology.* Dordrecht (Netherlands): Kluwer Academic Publ. 153-191.
- Tyson, R.V, and Follows, B. (2000). Palynofacies Prediction of Distance from Sediment Source: A Case Study from the Upper Cretaceous of the Pyrenees. *Geology.* 28, 569-571.
- Újvári G., Varga A., Balogh-Brunstad, Z. (2008). Origin, Weathering, and Geochemical Composition of Loess in Southwestern Hungary. *Quaternary Research.* 69, 421–437.
- Umenweke, M.O. (1996). The Role of Vegetation in Soil and Gully Erosion in parts of Southeastern Nig. *Jour. Sci. Engr. Tech.* 3 (1): 305-313.
- Umeji, O.P. (1984). Ammonite Palaeoecology of the Eze-Aku Formation, Southeastern Nigeria. *Journal of Mining and Geology.* 21, 55 - 59.
- Umeji, A. C. (2000). Evolution of the Abakaliki and the Anambra Sedimentary Basin, Southeastern Nigeria. A Report Submitted to the Shell Development Company of Nigeria Ltd. 155.
- Umeji, O.P. (2007). Late Albian to Campanian Palynostratigraphy of Southeastern Nigerian Sedimentary Basins. Unpublished PhD thesis. University of Nigeria, Nsukka.
- Uzuakpunwa, A. B. (1974). The Abakaliki Pyroclastics, Eastern Nigeria: New Age and Tectonic Implications. *In: Nwachukwu, J.I. 1974 (Ed). Petroleum Geology of Benue Trough, Nigeria. AAPG Bull.* 69 (4): 601-615.
- Van Bergren, P.F., Janssen, N.M.M., Alferink, M. and Kerp, J.H.F. (1990). Recognition of organic matter types in standard palynological slides. *In: Fermont, W.J.J. and Weegink,*



- J.W. (Eds.) Proceedings of the International Symposium on Organic Petrology. Zeist (Netherlands): *Mededelingen Rijks Geologische Dienst*. 9-21.
- Van der Zwan, C.J. (1990). Palynostratigraphy and Palynofacies Reconstruction of the Upper Jurassic to Lowermost Cretaceous of the Draugen Field, offshore mid Norway. *Rev Palaeobot. Palyno.* 62, 157-186.
- Van der Zwan, C.J. and van Veen, P.M. (1978). The Devonian-Carboniferous Transition Sequence in Southern Ireland: Integration of Paleogeography and Palynology. *Palinologia* I:469-479.
- Van Cappellen, P. and Ingall, E.D. (1994). Benthic Phosphorus Regeneration, Net Primary Production and Ocean Anoxia: A Model of the Coupled Marine Biogeochemical Cycles of Carbon and Phosphorus. *Paleoceanography.* 9, 677-692.
- Voicu, G., Bardoux, M., Harnois, L. and Grepeau, R. (1997). Lithological and Geochemical Environment of Igneous and Sedimentary Rocks at Omai Gold Mine, Guyana, South America *Exploration and Mining Geology.* 6, 153-170.
- Voicu, G. and Bardoux, M. (2002). Geochemical Behaviour under Tropical Weathering of the Barama-Mazaruni Greenstone Belt at Omai Gold Mine, Guiana Shield. *Appl. Geochem.* 17, 321-336.
- Von Eynatten, H. and Gaupp, R. (1999). Provenance of Cretaceous Synorogenic Sandstones in the Eastern Alps: Constraints from Framework Petrography, Heavy Mineral Analysis and Mineral Chemistry. *Sed. Geol.* 124, 81-111.
- Warning, B. and Brumsack, H.J. (2000). Trace Metal Signatures of Mediterranean Sapropels. *Palaeogeography, Palaeoclimatology, Palaeoecology.* 158, 293-309.
- Weber, G. and Green J. (1981). Guide to Oil Shale. National Conference of State Legislatures. Washington D.C., USA. 21.
- Welte, D.H., Yukler, M.A., Radke, M. and Leythaeuser, D. (1981). Application of Organic Geochemistry and Quantitative Basin Analysis to Petroleum exploration. *In: Gordon, A*

and Zuckeramm, A.J (Eds.). Origin and Chemistry of Petroleum. Pergamon Press. 67-88.

Werne, J.P., Lyons, T.W., Hollander, D.J., Formolo, M.J. and Sinninghe Damsté, J.S. (2003). Reduced Sulphur in Euxinic Sediments of the Cariaco Basin: Sulphur Isotope Constraints on Organic Sulphur formation. *Chem. Geol.* 195, 159–179.

Westphal, H. and Munnecke. A. (2003). Limestone-marl alternations: a warm-water phenomenon? *Geology*. 31, 263-266.

Whitaker, M.F. (1984). The usage of palynology in Definition of Troll Field geology. Paper presented at: Offshore Northern Seas Conference and Exhibition. 6<sup>th</sup> Meeting of the Organization; Stavanger (Norway): Norks Petroleum sforening.44.

Whitaker, M. F., Glees, M. R. and Cannon, S. J. C. (1992). Palynological Review of the Brent Group, UK Sector, North Sea. 80.

Whiteman, A. J., (1982). Nigeria: Its Petroleum Geology, Resources and Potential. Grahman and Trottan, London. 394.

Wickstrom, L.H., Slucher, E.R., Baranoski, M.T., and Mullett, D.J. (2008). Geologic Assessment of the Burger Power Plant and Surrounding Vicinity for Potential Injection of Carbon Dioxide. Ohio Department of Natural Resources. Open-File Report 2008. 1, 26. <http://www.dnr.state.oh.us/Portals/10/pdf/BurgerReport.pdf>.

Wilson, R.C., and Bain A.D., (1928). The Nigerian Caulfield Sectors II. Parts of Onitsha and Owerri Provinces. *Geol. Surv. Nig. Bull.* 12, 54.

Wipf, R.A. and Party, J.M. (2006). Shale Plays—A U.S. overview. AAPG Energy Minerals Division Southwest Section Annual Meeting. May, 2006. URL<[http://emd.aapg.org/members\\_only/gas\\_shales/index.cfm](http://emd.aapg.org/members_only/gas_shales/index.cfm)> [January 19, 2009].

Wonders, A. A. H. (1980). Middle and Late Cretaceous Planktonic Foraminifera of the Western Mediterranean Area, Utrch. *Micropalaeontology*. 24, 1-157.

Wright, J.B. (1968). South Atlantic Continental Drift and the Benue Trough: *Tectonophysics*. 6, 301-310.

Wright, J. B. (1989). Review of the Origin and Evolution of the Benue Trough in Nigeria. *In*: Kogbe, C. A. (Ed.). *Geology of Nigeria*. Elizabeth Publ. Co., Lagos, 359 – 364.

Zaborski, P. M. P. (1987). Lower Turonian (Cretaceous) ammonites from Southeastern Nigeria. *Bull. British Museum and Natural History*. 41 (2): 31-66.